TWR-5672

STUDY OF SOLID ROCKET MOTOR FOR SPACE SHUTTLE BOOSTER

VOLUME II TECHNICAL

BOOK 1 OF 5

by

Thiokol / WASATCH DIVISION
A DIVISION OF THIOKOL CHEMICAL CORPORATION

prepared for

NATIONAL AERONAUTICS AND SPACE ADMINISTRATION

George C. Marshall Space Flight Center

Contract NAS 8-28430
Data Procurement Document No. 314
Data Requirement MA-02

P.O. Box 524, Brigham City, Utah 84302
801/863-3511

Thiokol / WASATCH DIVISION

15 March 1972

National Aeronautics and Space Administration
George C. Marshall Space Flight Center
Marshall Space Flight Center, Alabama 35812

Attention: Mr. J. K. MacLean

Subject: NASA Contract Number NAS8-28430
Final Report

Gentlemen:

We are transmitting herewith the Final Report for The Study of A Solid Rocket Motor for Space Shuttle Booster pursuant to Article XIV, Reports Distribution, of the subject contract. The report comprises: Volume I, Executive Summary; Volume II, Technical (Books 1 thru 5, Appendices A thru H); Volume III, Program Planning Acquisition; and Volume IV, Cost.

Because of the size of the report and to expedite the submittal, we are transmitting three (3) of the 45 copies required by the contract designated for PD-RV. The remaining copies are being transmitted under separate cover.

Very truly yours,

John Thirkill
Project Manager
Space Shuttle Program

cc: A&TS-PR-RP/J.K. MacLean (1 cy)
A&TS-MS-IL (1 cy)
A&TS-TU (1 cy)
A&TS-MS-IP (2 cys)
PD-RV/Larry Wear (45 cys)

TWR-5672

FINAL REPORT

STUDY OF SOLID ROCKET MOTOR FOR SPACE SHUTTLE BOOSTER

VOLUME II TECHNICAL

BOOK 1 OF 5

by

THIOKOL/WASATCH DIVISION
A Division of Thiokol Chemical Corporation
P.O. Box 524, Brigham City, Utah 84302

prepared for

NATIONAL AERONAUTICS AND SPACE ADMINISTRATION

15 March 1972

CONTRACT NAS 8-28430
Data Procurement Document No. 314
Data Requirement MA-02

George C. Marshall Space Flight Center
Marshall Space Flight Center, Alabama

Publications No. 0372-36175

PREFACE

This report contains the results of Thiokol Chemical Corporation's Study of Solid Rocket Motors for Space Shuttle Booster. The objective of the study was to provide data to assist National Aeronautics and Space Administration in selection of the booster for the Space Shuttle system. This objective was satisfied through definition of specific Solid Rocket Motor (SRM) stage designs, development program requirements, and production and launch program requirements, as well as the development of credible cost data for each program phase. The study was performed by Thiokol's Wasatch Division, Brigham City, Utah, for the NASA George C. Marshall Space Flight Center under Contract NAS 8-28430. The study was conducted under the direction of Mr. Daniel H. Driscoll/PD-RV-MGR NASA/MSFC. Thiokol study direction was provided by Messrs. E. R. Kearney, Corporate Director, Space Shuttle Program, and J. D. Thirkill, Program Manager, Space Shuttle SRM Booster Study, Wasatch Division.

The final report was prepared in response to Data Procurement Document 314 and Data Requirement MA-02. The report is arranged in four volumes:

Volume I - Executive Summary

Volume II - Technical

Volume III - Program Planning Acquisition

Volume IV - Cost

Data Requirement MA-02 specified that the Cost report be part of the Program Acquisition and Planning report but because of its importance and size it has been bound as a separate volume in this Final Report.

Volume II, Technical, has been further subdivided into five books as follows for ease of review and handling:

Book 1

Section 1.0 - Introduction
Section 2.0 - Propulsion System Definition
Section 3.0 - SRM Stage

Book 2

Book 3

Book 4

Book 5

Requests for further information should be directed to:

Thiokol Chemical Corporation
Wasatch Division
P. O. Box 524
Brigham City, Utah 84302

J. D. Thirkill 801 - 863-3511, Ext 3-3481

I. C. Adams 801 - 863-3511, Ext 3-3406

CONTENTS

BOOK 1

CONTENTS (Cont)

CONTENTS (Cont)

BOOK 2

CONTENTS (Cont)

CONTENTS (Cont)

CONTENTS (Cont)

BOOK 3

BOOK 4

BOOK 5

ILLUSTRATIONS

BOOK 1

ILLUSTRATIONS (Cont)

ILLUSTRATIONS (Cont)

ILLUSTRATIONS (Cont)

ILLUSTRATIONS (Cont)

ILLUSTRATIONS (Cont)

ILLUSTRATIONS (Cont)

BOOK 2

ILLUSTRATIONS (Cont)

ILLUSTRATIONS (Cont)

TABLES

BOOK 1

TABLES (Cont)

TABLES (Cont)

TABLES (Cont)

BOOK 2

TABLES (Cont)

1.0 INTRODUCTION

1.0 INTRODUCTION

The technical data developed during Thiokol Chemical Corporation's Study of Solid Rocket Motors for a Space Shuttle Booster are presented in this document, Volume II Technical. The study was conducted for the George C. Marshall Space Flight Center under Contract NAS 8-28430. The overall objective of the study was to develop data to assist the NASA in selection of the booster concept for use in the Space Shuttle system.

Detail program objectives set forth in Exhibit A, Scope of Work, of Contract NAS 8-28430 were:

1. Define solid rocket motor (SRM) designs which satisfy the performance and configuration requirements of the various vehicle/booster concepts.

2. Define the development, production and launch support programs which are required to provide these stages at rates of 60, 40, 20, and 10 launches per year in a manrated system.

3. Acquire from the vehicle contractors the interface data necessary to define those design controlling features of the SRM systems. Particular attention should be given to structural load paths and conditions, normal separation, abort (including thrust neutralization, if required), flight dynamics, acoustics, and thrust vector control.

4. Definition of areas of significant concern or uncertainty which must be satisfactorily removed to allow use of the particular concept. Such definition should include proposed means to reduce the uncertainty.

5. Estimation of costs, including assumptions of basis, for the defined SRM. Such costs will identify all hardware systems, design, development and test efforts, production efforts, launch support facilities, transportation, ground support equipment and handling equipments.

   Separate sections should address the recoverability process.

6. To fulfill the objectives stated above, consideration will be given to the baseline booster configurations of all the Phase B study contractors.

   The configurations of these contractors fall within two broad concepts of rocket assisted boost of the reusable orbiter with external hydrogen oxygen propellant tankage: series burn and parallel burn. Primary emphasis is to be placed on parallel burn. There are also two sizes of orbiters being considered. The contractor shall establish a working relationship with the Phase B contractors and provide data to them as necessary to identify and resolve vehicle problems which mutually influence vehicle and SRM designs and use.

Large SRM's have been studied frequently for space booster and ballistic missile applications during the past decade. In addition, several technological demonstration programs have been conducted under sponsorship of the NASA and USAF. These programs have encompassed 120, 156, and 260 in. motors. These study and technological programs in conjunction with current large motor production programs (120 in. Titan IIIC, Minuteman Stage I, and Poseidon Stage I) provide excellent background for the current study of SRM's for a Space Shuttle booster. Thiokol has participated directly in several of these programs and is familiar with the results of programs conducted by other members of the solid propulsion community. The results of these previous programs and study support provided the Phase B vehicle study contractors were employed by Thiokol in the conduct of this study program.

Study scope encompassed 156, 120, and 260 in. SRM's. Major emphasis was placed on the study of 156 in. SRM stages in the parallel and series configurations. Data were developed for 120 in. stages in support of vehicle study contractors. Late in the study, data also were developed for 260 in. stages for the series burn configuration.

Program acquisition planning documentation was developed in detail and is presented in Volume III. This documentation was employed to develop cost data for all stage configurations which are presented in Volume IV. Detailed cost data were developed for 156 in. parallel and series configurations for DDT & E and for the mission model launch rate (60 launches per year) and alternate launch rates (40, 25, and 10 launches per year). Summary cost data were developed for the 120 and 260 in. configurations for DDT & E and the mission model launch rate. Cost and design data were provided to all vehicle study contractors for the specific configurations identified by them. In addition, Thiokol baseline configuration design and cost data were provided.

Areas of concern and uncertainty were identified and studied. As a result, no significant problems were identified relating to the application of SRM stages for the Space Shuttle system. Manrating was considered in the design of the SRM stages and costs developed reflect additional design, development test, and production process control effort felt necessary to manrate the SRM stages. Potential environmental problems were studied thoroughly, and it was determined that no serious environmental problem exists.

SRM stage recovery was evaluated and determined to be feasible. Recovery of the SRM stages will provide significant cost savings and should be pursued during the development of the Space Shuttle system.

During the study, considerable data were developed to assist the NASA in the selection of a booster concept for the Space Shuttle system. Results of the study indicate that SRM's provide a logical, minimum technical risk, low cost approach for the Space Shuttle booster application.

2.0 PROPULSTION SYSTEM DEFINITION

2.1 INTRODUCTION

Thiokol has been actively supporting various vehicle contractors in their Space Shuttle studies for the past 2 years. During this time period, visits have been made by Thiokol personnel to most of the vehicle contractors. The vehicle contractors have been provided specific design data and design philosophy on large SRM boosters. Consequently, when this study was initiated, Thiokol was well acquainted with the Space Shuttle propulsion system and had close working relationships with the vehicle contractors. This prior knowledge of the system and these working relationships made it possible for Thiokol to very quickly establish the size of the booster stages of current interest and the characteristics which the stages must possess.

Two SRM stages were selected very early for detailed study: (1) a stage consisting of two 156 in. diameter motors each containing 1.2 million lb of propellant for use in the parallel burn configuration and (2) a stage consisting of three 156 in. diameter motors each containing 1.5 million lb of propellant for use in the series burn configuration. The selection of these stages as baselines early in the study permitted greater engineering definition and provided a more adequate basis for cost estimating. Also, having the baselines selected early permitted data to be supplied to case and nozzle vendors, thereby enabling them to provide cost estimates for the study.

To supplement the preliminary information received from the vehicle contractors, letters requesting specific information on SRM stage requirements were sent to each of the vehicle contractors. These requests were followed by visits from Thiokol personnel. As a result, the most current information available was obtained from each of the vehicle contractors. These data varied widely as each of the vehicle contractors was examining different configurations. Subsequently, data were received from six separate contractors describing 29 configurations. These data also varied widely and it was not possible to establish a composite 156 in. stage design with any more validity than the two baselines previously selected. Therefore, the two baseline 156 in. SRM stages have been used as design nominals for the 156 in. configurations throughout the study.

Data also were requested by the vehicle contractors on SRM stages utilizing four 120 in. diameter motors. Late in the study, data were requested on a stage consisting of a single 260 in. diameter motor. A preliminary design for the 120 in. motors containing 0.566 million lb of propellant was prepared and used as a baseline from which perturbations were made to respond to requests for 120 in. stage design data. Thiokol and UTC experience with the 120 in. motor was heavily relied upon to provide 120 in. motor data and philosophy.

Earlier studies were conducted by Thiokol on 260 in. motor designs. These studies were used extensively to compile the data supplied in this report on 260 in. motors.

Specific preliminary static designs were made for each 120 and 156 in. SRM requested by the vehicle contractors. These data were supplied on a mutually agreed upon schedule so that the data could be used in the vehicle contractors' final reports.

The major objective of the study effort was to develop credible costing data on various SRM stage configurations applicable to the Space Shuttle Program. The three motor configurations selected; ie, 120 in. diameter segmented, 156 in. diameter segmented, 260 in. diameter monolithic, lend themselves well to the development of cost data.

The 120 in. diameter segmented motor is currently in production so it can be costed out in the Space Shuttle stage configurations with little margin for error. Similarly, the 156 in. diameter segmented motor is within the current state of the art and can be costed with little uncertainty.

The 260 in. monolithic motor has been studied previously and three motors have been built and tested. There is little uncertainty concerning the basic SRM but the area of transportation and handling of this size motor has not been fully demonstrated.

2.2 STAGE DESIGN REQUIREMENTS

2.2.1 Performance

Each of the vehicle contractors provided Thiokol with requirements data defining the specific SRM being studied by them for the various Space Shuttle configurations being investigated.

To provide a basis for the design and costing details provided in this document, two SRM's were selected as baseline motors. The first contains 1.2 million lb of propellant and is intended for use in pairs for the parallel burn configuration. The second contains 1.5 millions lb of propellant and is intended for use as one motor of a cluster of three to be used in the series burn configuration. The two motors were selected prior to the receipt of specific data from the vehicle contractors and do not represent a finite request from any of the contractors; however, the motors are typical of those requested by each vehicle contractor.

The actual request for data on the parallel burn motor from the vehicle contractors varied in size from 1.04 to 1.37 million lb of propellant. Thus, the Thiokol baseline at 1.2 million lb is very representative of the motor size being considered. The requests for series burn configuration motors ranged from 1.6 to 1.43 million lb of propellant. The Thiokol design at 1.5 million lb represents a motor slightly larger than any requested.

This motor was intentionally selected at 1.5 million lb as it represents a motor that is near the maximum size that should be designed at the 156 in. diameter. The features on this motor, however, are typical of the requested motors.

Table 2-1 contains a summary of the data requested by each of the vehicle contractors.

2.2.2 Thrust Vector Control

The TVC requirements specified by the vehicle contractors varied widely as shown on Table 2-1 . On the parallel configuration, consideration is being given by some contractors to deleting all TVC from the two SRM's and doing all maneuvering with the control system on the orbiter. In this concept, it is not necessary to have TVC on the SRM; however, a nozzle is utilized with a permanent cant angle such that the thrust vector is directed toward the vehicle center of gravity. This concept would require prediction of thrust vector position within approximately 1/4 deg. From a motor manufacturing and assembly standpoint, this appears to be achievable.

Other concepts for the parallel burn configuration require a movable nozzle. Nozzle deflection requirements vary from 3 to 10 deg with a slew rate of 5 to 20 deg/sec. To meet these requirements a movable nozzle utilizing a flexible bearing has been designed and is discussed below.

The series configuration requires TVC in all the options presented by the prime contractors and a flexible bearing movable nozzle is shown on the 1.5 million lb propellant baseline motor for the series configuration. Also shown is a hydraulic power unit (HPU) and linear actuators for moving the nozzle. A vector angle of 5 deg with a slew rate of 5 deg/sec was selected as the baseline. The requirements from the vehicle contractors for series burn varied from 5 to 10 deg deflection with a slew rate of 5 to 20 deg/sec.

2.2.3 Abort

The ability to abort the mission in case of a malfunction in either the orbiter or solid rocket motors stage is contained in the requirements from each of the vehicle contractors. The techniques employed by the contractors varied; however, each specified that it would be necessary to terminate the thrust on the SRM's should an abort situation arise. It may also be necessary to destroy the motor case in order to make the motors completely nonpropulsive after separation from the orbiter. The abort procedure specified by the McDonnell Douglas Astronautics Co does provide abort capability and crew safety throughout the entire sequence of booster operation. These were typical of the requirements forwarded by the other vehicle contractors but somewhat more inclusive. For the purposes of this report, they have been incorporated by Thiokol with one addition suggested by other vehicle contractors (ie, the ability to hold the vehicle on pad should a malfunction be detected after SRM ignition but prior to release). The model used by Thiokol is shown on Table 2-2 . These abort modes

TABLE 2-1

SUMMARY OF DATA REQUESTED BY VARIOUS SPACE SHUTTLE CONTRACTORS

	THIOKOL BASELINES				BOEING				CHRYSLER	
MODEL					979-162	979-163	979-164	979-165	LARGE ORBITER	SMALL ORBITER
RECOVERY									NONRECOVERABLE	
PARALLEL (P) OR SERIES (S)	P	S	P	S	S	S	P	P	P	P
BOOSTER LENGTH (IN)	[illegible]	1,690	1,177	1,833						
BOOSTER DIAMETER (IN)	156	156	120	260	2/156	6/120	2/156	4/120	2/156	2/156
PAYLOAD SIZE (FT)					60 x 15	60 x 15	60 x 15	60 x 15		
PAYLOAD WEIGHT (LB)										
MISSION										
GLOW x 10^3 (LB)										
BLOW x 10^3 (LB)										
[illegible]OW x 10^3 (LB)					1,411	1,244	1,807	1,807	1,825	1,340
WEIGHT PER BOOSTER x 10^3 (LB)	1,520	1,633	630.8	4,972	1,603	665	1,394	665		
PROPELLANT WEIGHT x 10^3 (LB)	1,390	1,500	566.1	4,500	1,430	592	1,206	592	1,204	986
THRUST PER MOTOR x 10^3 (LB)	2,884	2,964	1,407	8,920	2,920	1,200	2,420	1,400	2,303	1,805
PROPELLANT TYPE	PBAN	PBAN	PBAN	PBAN	HTPB	PBAN OR HTPB	HTPB	PBAN OR HTPB		
VACUUM Isp (SEC)	270.4	266.3	270.4	267.6	271.3	268.7	271.3	266.7	270	270
MEOP (PSIA)	1,300	1,300	900	1,300					950	950
BURN TIME (SEC)	135	135	112	135	123.9	146.4	139.4	140.7	134.9	134.8
EXPANSION RATIO	10	8.5	8	10	10	9.2	10	9.2	9.8	9.8
NUMBER SEGMENTS	3	4	2	1		6				
TVC TYPE	NONE / [illegible]	MOVABLE NOZZLE	NONE	MOVABLE NOZZLE	MOVABLE NOZZLE	MOVABLE NOZZLE	MOVABLE NOZZLE	MOVABLE NOZZLE		
TVC DEFLECTION ANGLE (DEG)	0 / ±5	±5		±5	±10	±10	±6	±6	6	5
SLEW RATE (DEG/SEC)	0 / 5	5		5	[illegible]	5	5	5	20	20
NOZZLE CANT ANGLE (DEG)	NONE	NONE	NONE	NONE	NONE	NONE	NONE	NONE		
THRUST TERMINATION PORTS	NO	NO	NO	NO	YES	YES	YES	YES	YES	YES
STAGING ROCKETS	NO	NO	NO	NO	YES	NO	YES	YES		
DESTRUCT SYSTEM	NO	NO	NO	NO	N/A	N/A	N/A	N/A	YES	YES
IGNITION TYPE	HEAD END	HEAD END	HEAD END	HEAD END	HEAD END	HEAD END	HEAD END	HEAD END		
CASE MATERIAL	D6AC	D6AC	D6AC	D6AC	D6AC	D6AC	D6AC	D6AC		
DRAWING NUMBER	TUL-13404	TUL-13405	TUL-13406	TUL-13307	TUL-13450		TUL-13451		TUL-13452	

	GENERAL DYNAMICS							
MODEL	B-25	B-26	B-25	B-29	B-23A	B-27A	B-23B	B-27B
RECOVERY								
PARALLEL (P) OR SERIES (S)	S	P	S	P	S	P	S	P
BOOSTER LENGTH (IN)								
BOOSTER DIAMETER (IN)	6/120	5/120	5/120	4/120	3/156	2/156	3/156	2/156
PAYLOAD SIZE (FT)	60 x 15	60 x 15	45 x 14	45 x 14	60 x 15	60 x 15	45 x 14	45 x 14
PAYLOAD WEIGHT (LB)	40K	40K	45K	45K	40K	40K	45K	45K
MISSION	POLAR	POLAR	EAST	EAST	POLAR	POLAR	EAST	EAST
GLOW x 10^3 (LB)	5,546	5,254	4,675	4,357	5,158	4,765	4,365	4,096
BLOW x 10^3 (LB)	4,134	3,438	3,462	2,750	3,673	2,899	3,128	2,500
[illegible]OW x 10^3 (LB)	1,407	1,316	1,212	1,407	1,485	1,866	1,237	1,596
WEIGHT PER BOOSTER x 10^3 (LB)								
PROPELLANT WEIGHT x 10^3 (LB)	585	586	589	586	1,073	1,274	928	1,096
THRUST PER MOTOR x 10^3 (LB)	1,297	1,308	1,404	1,307	2,235	2,852	1,891	2,457
PROPELLANT TYPE					HTPB	HTPB	HTPB	HTPB
VACUUM Isp (SEC)		269			265	269	269	269
MEOP (PSIA)					825	825	825	825
BURN TIME (SEC)	128.[illegible]	128.35	127.3	128.3	122.96	123.13	123.5	123.5
EXPANSION RATIO					10	10	10	
NUMBER SEGMENTS	7	7	7	7	3	4	3	3
TVC TYPE					MOVABLE NOZZLE	MOVABLE NOZZLE	MOVABLE NOZZLE	MOVABLE NOZZLE
TVC DEFLECTION ANGLE (DEG)					±11		±11	
SLEW RATE (DEG/SEC)								
NOZZLE CANT ANGLE (DEG)								
THRUST TERMINATION PORTS					YES	YES	YES	YES
STAGING ROCKETS								
DESTRUCT SYSTEM								
IGNITION TYPE					AFT END	AFT END	AFT END	AFT END
CASE MATERIAL					18% Ni MARAGING STEEL GRADE "200"			
DRAWING NUMBER							TUL-13459	TUL-13453

	LMSC							
MODEL	AE-15 LARGE EXPEND.	AR-15 LARGE RECOVER.	AE-14 SMALL EXPEND.	AR-14 SMALL RECOVER.	BE-15 LARGE EXPEND.	BR-15 LARGE RECOVER.	BE-14 SMALL EXPEND.	BR-14 SMALL RECOVER.
RECOVERY								
PARALLEL (P) OR SERIES (S)	P	P	P	P	S	S	S	S
BOOSTER LENGTH (IN)								
BOOSTER DIAMETER (IN)	2/156	2/156	2/156	2/156	3/156	3/156	3/156	3/156
PAYLOAD SIZE (FT)								
PAYLOAD WEIGHT (LB)								
MISSION								
GLOW x 10^3 (LB)								
BLOW x 10^3 (LB)								
[illegible]OW x 10^3 (LB)	1,858	1,857	1,762	1,761	1,385	1,384	1,259	1,259
WEIGHT PER BOOSTER x 10^3 (LB)								
PROPELLANT WEIGHT x 10^3 (LB)	1,347	1,368	1,036	1,050	1,130	1,147	1,352	1,370
THRUST PER MOTOR x 10^3 (LB)	2,749	2,788	2,246	2,277	2,462	2,498	2,432	3,322
PROPELLANT TYPE								
VACUUM Isp (SEC)	266	266	266	266	266	266	266	256
MEOP (PSIA)	1,000	1,000	1,000	1,000	1,000	1,000	1,000	1,000
BURN TIME (SEC)	138	138	129	129	131	132	127	127
EXPANSION RATIO								
NUMBER SEGMENTS								
TVC TYPE	MOVABLE NOZZLE	MOVABLE NOZZLE	MOVABLE NOZZLE	MOVABLE NOZZLE	MOVABLE NOZZLE	MOVABLE NOZZLE	MOVABLE NOZZLE	MOVABLE NOZZLE
TVC DEFLECTION ANGLE (DEG)	±10	±10	±10	±10	±10	±10	±10	±10
SLEW RATE (DEG/SEC)	15	15	15	15	15	15	15	15
NOZZLE CANT ANGLE (DEG)	11	11	11	11	NONE	NONE	NONE	NONE
THRUST TERMINATION PORTS	YES	YES	YES	YES	YES	YES	YES	YES
STAGING ROCKETS								
DESTRUCT SYSTEM								
IGNITION TYPE								
CASE MATERIAL	D6AC	D6AC	D6AC	D6AC	D6AC	D6AC	D6AC	D6AC
DRAWING NUMBER	TUL-13454				TUL-13460			

	MARTIN				MDAC		
MODEL	SPAC-156	SPAC-120	TRAC-156	TRAC-120	SMALL PARALLEL	LARGE SERIES	LARGE PARALLEL
RECOVERY							TBD
PARALLEL (P) OR SERIES (S)	S	S	P	P	P	S	P
BOOSTER LENGTH (IN)							
BOOSTER DIAMETER (IN)	3/156	5/120	2/156	4/120	2/156	3/156	2/156
PAYLOAD SIZE (FT)					45 x 14	60 x 15	60 x 15
PAYLOAD WEIGHT (LB)					25K	65K	65K
MISSION					RESUPPLY	EAST	[illegible]
GLOW x 10^3 (LB)					3,403.2	4,523.3	4,075.5
BLOW x 10^3 (LB)	3,350	3,396	2,700	2,730	2,746.3	3,587.0	2,233.6
[illegible]OW x 10^3 (LB)					1,542.9	1,236.0	1,541.5
WEIGHT PER BOOSTER x 10^3 (LB)							
PROPELLANT WEIGHT x 10^3 (LB)	1,300	590	1,200	900	733.4	1,046.3	991.6
THRUST PER MOTOR x 10^3 (LB)					1,417	2,010	2,401.9
PROPELLANT TYPE							
VACUUM Isp (SEC)					254	254	254
MEOP (PSIA)	600 - 1,200 RANGE - ALL CASES						
BURN TIME (SEC)	130 - 180	180	140 - 150	125			125
EXPANSION RATIO							
NUMBER SEGMENTS							
TVC TYPE	MOVABLE NOZZLE	MOVABLE NOZZLE	MOVABLE NOZZLE	MOVABLE NOZZLE			NONE
TVC DEFLECTION ANGLE (DEG)	±10	±10	±5	±5			N/A
SLEW RATE (DEG/SEC)							N/A
NOZZLE CANT ANGLE (DEG)	<10	<10	<10	<10			15
THRUST TERMINATION PORTS	YES	YES	YES	YES			
STAGING ROCKETS	NONE	NONE	FORE AND AFT	FORE AND AFT			
DESTRUCT SYSTEM	YES	YES	YES	YES			NONE
IGNITION TYPE							
CASE MATERIAL							D6AC
DRAWING NUMBER	TUL-134[illegible]		TUL-134[illegible]			TUL-134[illegible]	TUL-134[illegible]

impose two requirements on the SRM's: (1) the ability to hold on pad during the full burntime at full thrust, and (2) the ability to negate positive forward thrust on the motors. Capability to meet these requirements has been provided in the motors discussed within this document. The thrust termination ports are not designed to flow for more than 5 sec.

TABLE 2-2

ABORT MODES*

- Prior to Liftoff

  Hold down until SRM burnout

- Liftoff to T = 40 sec

  Terminate SRM thrust
  Separate orbiter from HO tank and SRM'S
  Ignite abort rockets
  Glide to landing (unpowered)

- T = +40 to T = +85 to 110 sec

  Terminate SRM thrust
  Separate orbiter from HO tank and SRM'S
  Glide to landing (unpowered)

- T = +110 sec to Staging

  Terminate SRM thrust
  Jettison SRM'S
  Use orbiter main engines and fly back to landing

*Derived from data received from McDonnell Douglas Astronautics Co.

2.2.4 Stage Structures

Thiokol has designed attachment structures for both the series and parallel burn configurations. From the vehicle contractors requirements, it is apparent that the complete weight of the vehicle as it sits on the launch pad must be supported through the solid rocket motors and that the structure must be capable of holding the vehicle on pad at full orbiter and SRM thrust. To meet this requirement, aft skirt structures have been designed suitable for supporting the vehicle during assembly and prior to vehicle liftoff. Interstage attachment structures for both the series and parallel configurations assume that all SRM thrust will be transmitted to the vehicle through staging structure located at the forward end of the SRM. In the parallel configuration, attachment at the aft end of the SRM will be sufficient to prevent roll and sway but the structures do not transmit the thrust load of the motor to the vehicle at this point. The aft skirt structure, for both series and parallel configuration, has been sized to withstand the tension loads of the SRM and orbiter thrust and is designed to hold the vehicle on the pad, without thrust terminating the SRM, should an abort situation require this.

2.2.5 Staging and Separation

The vehicle contractor requirements all specify that normal motor staging will be accomplished without thrust terminating the SRM's. Two modes of staging have been specified for the parallel burn configuration. The first is that a mechanical system will be used which releases the motors at the forward attach point just prior to complete SRM burnout and allows the SRM's to drag-separate and fall away from the vehicle. At about 30 deg, a latch on the aft end releases the motors and they fall clear. The alternate concept considered is to use small solid propellant staging rockets located on both the nose cone and aft skirt of the SRM to force it away from vehicle. Thiokol analyses indicate that either approach is feasible and can be used.

2.2.6 Electromechanical Display and Avionics

Vehicle contractor requirements for performance monitoring data transferal to the orbiter were not documented in information received by Thiokol. Thiokol, however, will furnish with each stage the necessary sensors, electronics, and circuits to monitor chamber pressure, HPU pressures, and nozzle position.

A signal indicating the position (safe or arm) for the safe and arm device (S & A) in the main motors, and thrust termination (TT) devices, destruct system, staging system, recovery system (as required) will be provided for display in the oribiter.

Although not presently defined in detail it is assumed that avionics hardware will be required for additional onboard checkout, sequencing control, and data management.

3.0 SRM STAGE DESIGN

3.1 INTRODUCTION

The design for the SRM stages was influenced significantly by the need to manrate the vehicle and by the NASA guideline that a low program cost was essential. To meet these two requirements, Thiokol established the ground rules that demonstrated state of the art in both materials and design techniques would be used in all components. The technology selected for each of the major components is shown in Table 3-1.

The segmented steel case will use the same Ladish D6AC material currently being used in the Minuteman Stage 1 motor and in the 120 in. SRM for the Titan IIIC.

Two nozzle designs are presented; one for a fixed nozzle, the other a movable nozzle for TVC. Both nozzles use materials and construction techniques similar to those used in the Minuteman, Titan IIIC SRM, and Poseidon missiles. Nozzles of both types have been demonstrated on 156 in. motors. The movable nozzle TVC system uses a flexible bearing similar to those manufactured by Thiokol for use on the Poseidon. This concept is presently used in both stages of the Poseidon. Thiokol demonstrated a similar flexible bearing on a 156 in. motor firing. A bearing of this type also was manufactured and bench tested in a size suitable for 260 in. motors.

The actuators for moving the nozzle are similar to those presently used on Saturn. The HPU used to supply power to the nozzle actuators is a developed system presently flying as an emergency power unit on the Concorde aircraft.

The propellant selected is the demonstrated reliable propellant used on Stage I Minuteman. Thiokol's Wasatch Division has produced approximately 125 million lb of this propellant for Minuteman application. The propellant is extremely well characterized. It has relatively high energy, good physical properties, and has demonstrated an excellent aging capability.

The ignition system utilizes a head end mounted Pyrogen igniter similar to that used on almost all large SRM's. The propellant used in the igniter is the same as that presently being used in the Stage I Minuteman motor igniter. An S & A device similar to that used on Titan and Minuteman will provide a positive arming of the Pyrogen igniter. Redundant squibs with redundant wiring from the S & A to the Pyrogen igniter are used to assure ignition.

Thrust termination ports in the forward dome of each motor are provided to terminate thrust in the SRM, should some condition on the vehicle dictate that it is necessary to abort the flight. Thrust termination is initiated by linear shaped

TABLE 3-1

TECHNOLOGY LEVEL -- BASELINE DESIGN

	Experience	
	Operational	Demonstration
Case--Ladish D6AC steel Roll formed segments	Minuteman 120 in. Titan IIIC	
Nozzle--Standard composite plastic construction, graphite carbon cloth phenolic	Minuteman Poseidon 120 in.	156 in.
TVC--Flexible bearing	Poseidon	156 in.
APU, actuators	Apollo Concorde	
Propellant--Minuteman Stage I 125 million lb processed	Minuteman Poseidon	156 in.
Ignition--Pyrogen igniter Safe and arm Redundant squibs	Minuteman Minuteman Apollo 120 in.	156 in.
Thrust Termination--Forward ports LSC	Minuteman Poseidon Pershing 120 in.	

charges which cut through the motor case. This technique is currently in use on Stage III Minuteman, Stage 1 Poseidon, Pershing, and has been demonstrated on the 120 in. SRM for Titan IIIC.

The selection of demonstrated materials in all components has the advantage that cost and performance data can be supported by actual manufacturing experience. Where choices existed in the demonstrated technology to be used, the choice was based upon least program cost.

The design approach to manrating was to design with well established materials, use proven concepts and manufacturing techniques, include redundant features wherever necessary, and use high safety factors. Design safety factors were selected as shown on Table 3-2.

3.2 SYSTEMS ANALYSIS SUMMARY

A preliminary Systems Requirements Analysis (Appendix A) was prepared to document the system and design requirements for the SRM and associated Ground Support Equipment (GSE). The analysis was conducted in accordance with the procedure of AFSCM 375-5, "Systems Engineering Management Procedures" for expedience in preparation.

The documents of the analysis were developed and used to establish the SRM airborne equipment and GSE configurations. The analysis was based upon data from the NASA work statement (Contract No. NAS 8-28430) and from inputs and documents provided Thiokol by the various vehicle study contractors. Information was received from North American Rockwell, The Boeing Company, Lockheed Missiles & Space Co, General Dynamics, McDonnell Douglas Astronautics Co., Martin Marietta Corporation, and Chrysler Corporation. The analysis identifies all possible aspects of the SRM system including those subsystems described as alternates to the baseline system. The scope and extent of the analysis was limited due to the time available and scope of the study program. Therefore, many blank areas exist throughout the analysis. These blanks indicate areas where further systems definition is required and/or more indepth tradeoff studies need to be conducted.

The analysis identifies, to the maximum extent possible, the most practical and economic combination of airborne equipment, GSE, facilities, personnel, and technical data that best satisfy the system and design requirements. Where various solutions were available to solve a system or design requirement, a solution was selected based upon past experience to insure that the most practical solution was utilized to satisfy all requirements. The analysis approach emphasizes the philosophy of a minimal quantity of airborne equipment and GSE to accomplish multiple tasks. Traceability between all documents of the analysis has been maintained.

TABLE 3-2

DESIGN SAFETY FACTORS*

1.2	proof test (on MEOP)
1.4	ultimate (on MEOP)
2.0	nozzle ablator (on thickness)
2.0	case insulation (on thickness)
1.4	ultimate on interstage structures

*Lockheed Missiles and Space Company
Final Report, Alternate Concepts Study, Volume II, Part 3, pages 4-12.

3.2.1 Operational System Analysis

The SRM stage configurations and associated GSE, as presented in this study, were designed to satisfy all the requirements of the Operational Systems Analysis contained in Appendix A. This analysis establishes the baseline for the SRM design plus the requirements and criteria for all subsystems and components discussed as alternates to the baseline.

In addition, the analysis has established a basis for a preliminary summary of GSE, facilities, manpower quantities and skills, and procedural data required to support the SRM from manufacture through recovery.

The following assumptions were made concerning the operational sequence in order to form a basis for analysis.

1. The integrated Space Shuttle system orbiter or ground power will furnish all required excitation and stimuli to perform a complete functional check of the TVC system after SRM Space Shuttle integration.

2. Ordnance unit checkout after Space Shuttle vehicle integration will be limited to monitoring to assure safe or arm condition and connector mating integrity.

3. Ordnance S & A devices will not be installed until after the combined system tests. Simulators will be used to this point.

4. Checkout of the SRM before integration with the Space Shuttle will be accomplished to the maximum extent possible to preclude a teardown due to anomalies found during combined system tests.

5. A low pressure test of the assembled SRM will be conducted to check for leaks.

6. The support base on which the SRM stage is assembled will have capability for SRM vertical alignment.

7. The support base will be provided by the prime contractor/NASA.

8. Maximum assembly of SRM components will be accomplished prior to transfer to the Vertical Assembly Building (VAB) for SRM buildup, so far as economically practical.

9. The VAB will be used for assembly of the Space Shuttle vehicle.

10. All shipment of SRM segments to the Kennedy Space Center (KSC) will be via railroad.

11. All components coming from vendors directly to the KSC will be packaged for shipment by the vendor and shipped via common carrier.

12. A railroad extension will be provided from the existing railroad to a building (RISS Building) to be built near the Space Shuttle Vehicle Assembly building.

13. A roadway will be built from the new Receiving, Inspection, Subassembly, Storage (RISS) Building to the Space Shuttle Vehicle Assembly building which will handle approximately 400,000 lb loads.

14. Thrust termination, command destruct, thrust vector control, TVC stage separation, and recovery capability may be required.

It is recognized that complete substantiation or corrections to the assumptions can only occur following further system definition and indepth tradeoff studies.

3.2.1.1 Functional Flow Diagrams

Functional Flow Diagrams (FFD's) developed include top level FFD's with subflows to the level required to properly define a reasonable development of design requirements and criteria. The FFD's are based on the above listed assumptions. The FFD's have been prepared to reflect only those specific functions associated with the SRM stage. Functions that pertain to the Space Shuttle vehicle exclusively have been grouped into a reference function.

3.2.1.2 System Functional Analysis

Requirement Allocation Sheets (RAS's) were used to document the detailed analysis. These sheets were prepared for each block of the FFD's involving SRM stage equipment and associated GSE design constraints. The RAS's identify design requirements for the SRM stage airborne equipment, GSE, and facilities. Personnel and procedural data requirements are identified to support all operations from completion of manufacture of the SRM stage through SRM stage recovery.

The design requirements contained in the RAS's for the SRM and the SRM stage have been compiled into Section 3 of the Contract End Item Specification for the SRM and SRM stage. These are the requirements from which the design was developed.

3.2.2 Maintenance Analysis

Due to the limited scope of the study program, no maintenance engineering analysis has been performed. However, the following maintenance philosophy has been used by Thiokol in preparing designs and plans associated with this study program.

1. Maintenance will be performed at one of three locations; (1) at the site, (2) at Thiokol/Wasatch or (3) at the vendor, as applicable.

   Maintenance performed at the site will be identified as site or field level maintenance while that of the vendor or Thiokol will be identified as depot level maintenance.

2. On pad maintenance will consist of removal and installation of modules or subassemblies.

3.3 STAGE DESIGN SUMMARY

Four SRM stages were selected as baseline designs to provide data typical of that required for the various shuttle configurations. Each of the four baseline designs presented is of a complete SRM propulsion stage which will be assembled on the launch pad ready for mating with the orbiter tank. The designs are discussed in the following sections of this document.

Figure 3-1 presents one of two 156 in. motors, complete with all stage hardware, used in a 156 in. SRM stage for the parallel burn configuration. Table 3-3 is a performance summary of this one-half stage.

Figure 3-2 presents one of three 156 in. motors which are clustered to provide the SRM stage for the series burn configuration. Table 3-4 presents a performance summary for this motor.

Figure 3-3 presents one of four 120 in. SRM motors for a parallel burn configuration. Performance data for this stage is shown in Table 3-5.

Figure 3-4 and Table 3-6 present data on a 260 in. stage for a series burn configuration.

3.4 SRM STAGE DESIGNS

3.4.1 Introduction

The 156 in. SRM stage for the parallel configuration received major emphasis during the study. Consequently, it has been defined in considerably more detail than the others. Since the design concepts for all large solid rocket motors are similar, most of the design work done on the 156 in. parallel configuration is applicable to the 156 in. series, 120 in. parallel, and the 260 in. series configuration. Rather than provide redundant data on each design, the 156 in. parallel design is discussed in detail in this section; the other configurations are discussed in detail only where they differ from that described for the 156 in. parallel configuration.

3.4.2 156 In. SRM Stage Parallel Configuration

The 156 in. SRM stage for the parallel configuration is discussed in three parts: (1) the basic motor, (2) special design features, and (3) stage components. The basic motor discussion covers the case, propellant grain, insulation, liner, nozzle, ignition, and an electrical system. The special design features are optional features which can be incorporated on the basic motor. These features consist of a movable nozzle TVC system and an abort system. The stage components discussion involves the description of the nose cone, the aft skirt and the structure for attachment to the HO tank.

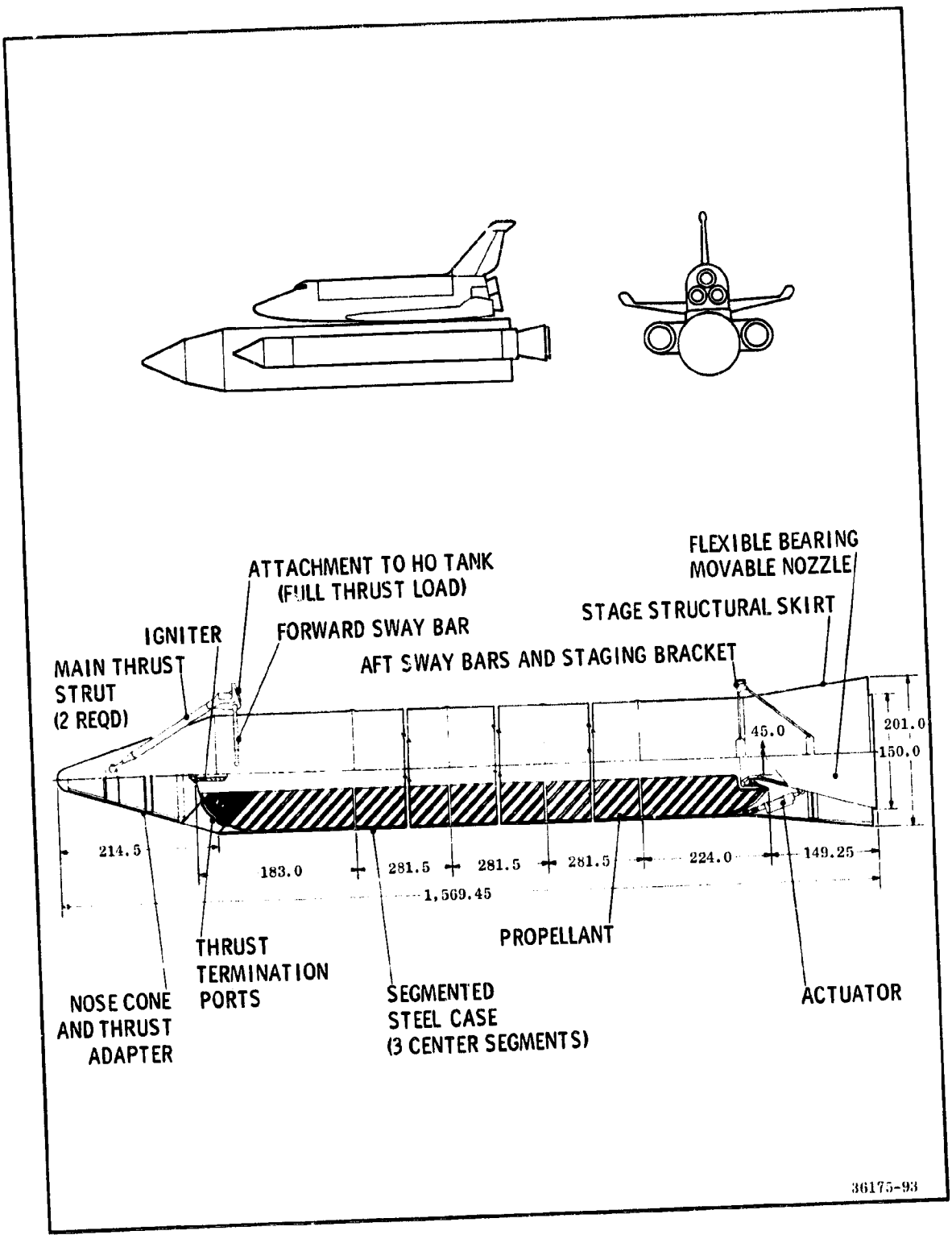

Figure 3-1. 156 In. SRM Stage for Parallel Burn Configuration

TABLE 3-3

PERFORMANCE SUMMARY
156 INCH PARALLEL BURN CONFIGURATION
(Two SRM's per Launch Vehicle)

Performance	
Average vacuum thrust (lb)	2,400,000
Burn time (sec)	135
Operating pressure (psia)	
Average	830
MEOP	1,000
Vacuum specific impulse (sec)	270.9
Weight	
Propellant (lb)	1,214,000
Total motor (lb)	1,346,000
Motor mass fraction	0.903
Total stage weight (lb)	1,372,000
Stage mass fraction	0.885

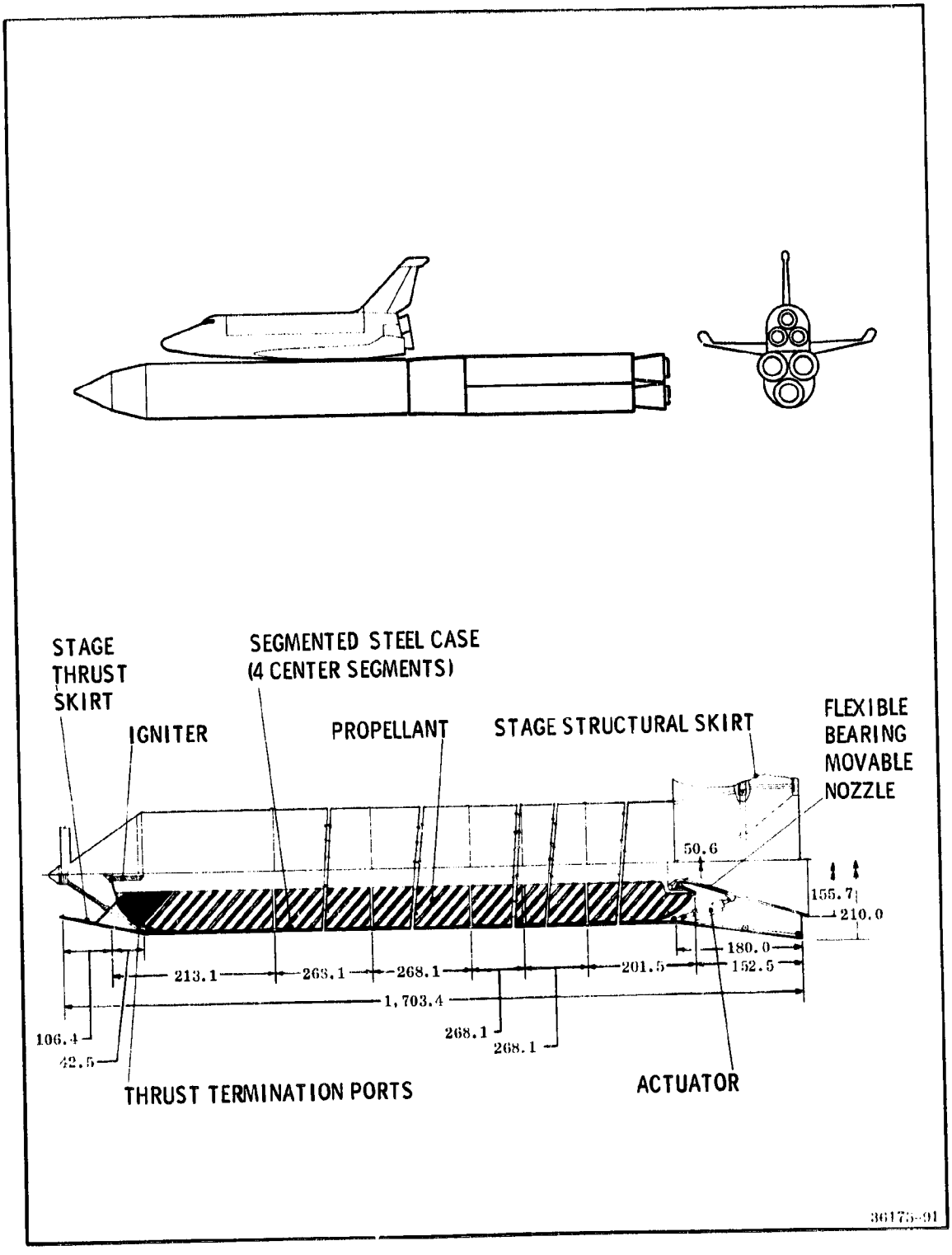

Figure 3-2. 156 In. SRM Stage for Series Burn Configuration

TABLE 3-4

PERFORMANCE SUMMARY
156 INCH SRM FOR SERIES BURN CONFIGURATION
(Three SRM's per Launch Vehicle)

Performance	
Average vacuum thrust (lb)	2,970,000
Burn time (sec)	135
Operating pressure (psia)	
Average	830
MEOP	1,000
Vacuum specific impulse (sec)	267.2
Weight	
Propellant weight (lbm)	1,500,000
Total motor weight (lbm)	1,654,000
Motor mass fraction	0.906
Total stage weight (lbm)	1,677,000
Stage mass fraction	0.894

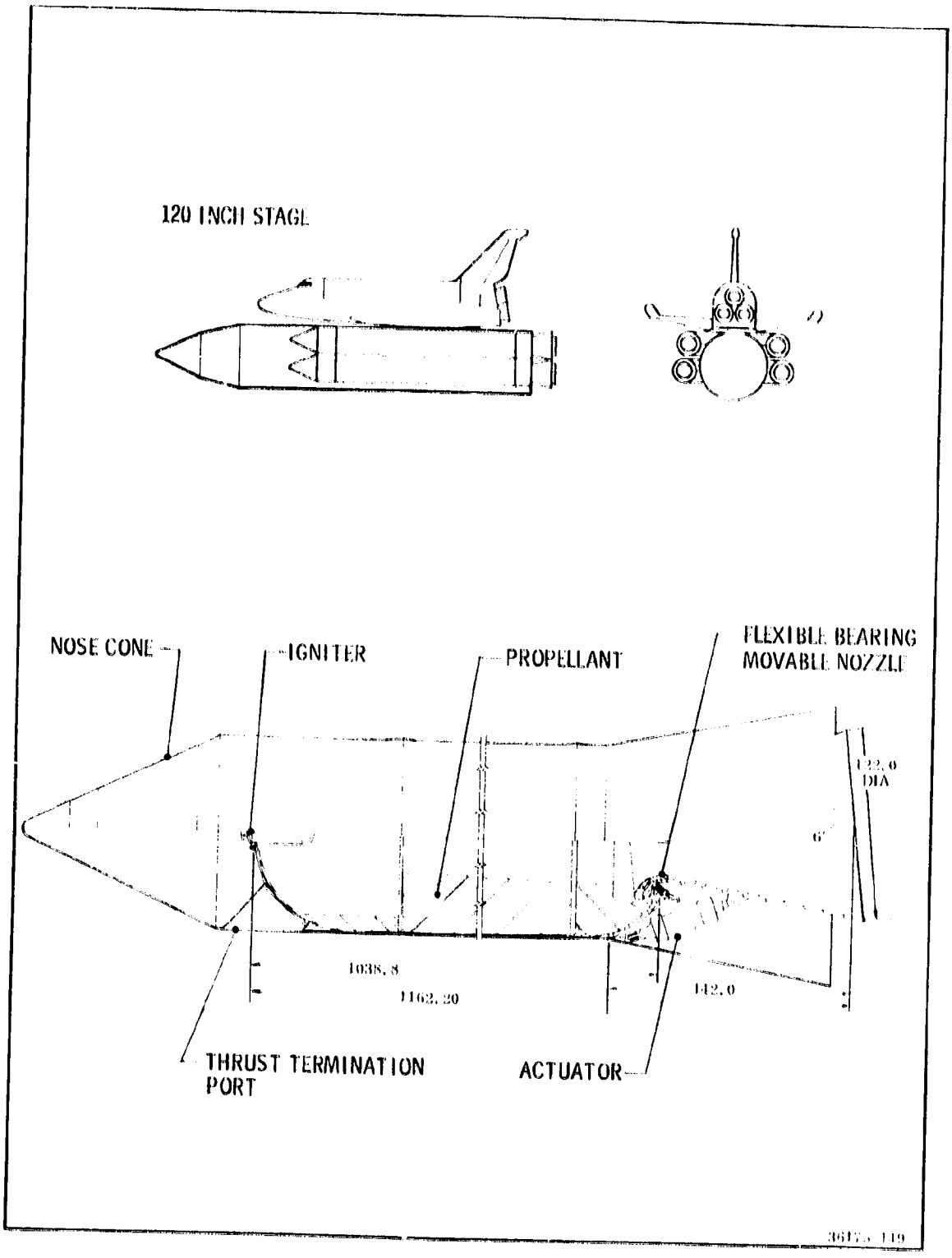

Figure 3-3. 120 In. SRM Stage for Parallel Burn Configuration

TABLE 3-5

PERFORMANCE SUMMARY
120 INCH SRM PARALLEL BURN CONFIGURATION
(Four SRM's per Launch Vehicle)

Performance	
Average vacuum thrust (lb)	1,407,000
Burn time (sec)	112
Operating pressure (psia)	
Average	665
MEOP	800
Vacuum specific impulse (sec)	270
Weight	
Propellant weight (lbm)	566,100
Total motor weight (lbm)	634,830
Motor mass fraction	0.892
Total stage weight (lbm)	642,241
Stage mass fraction	0.881

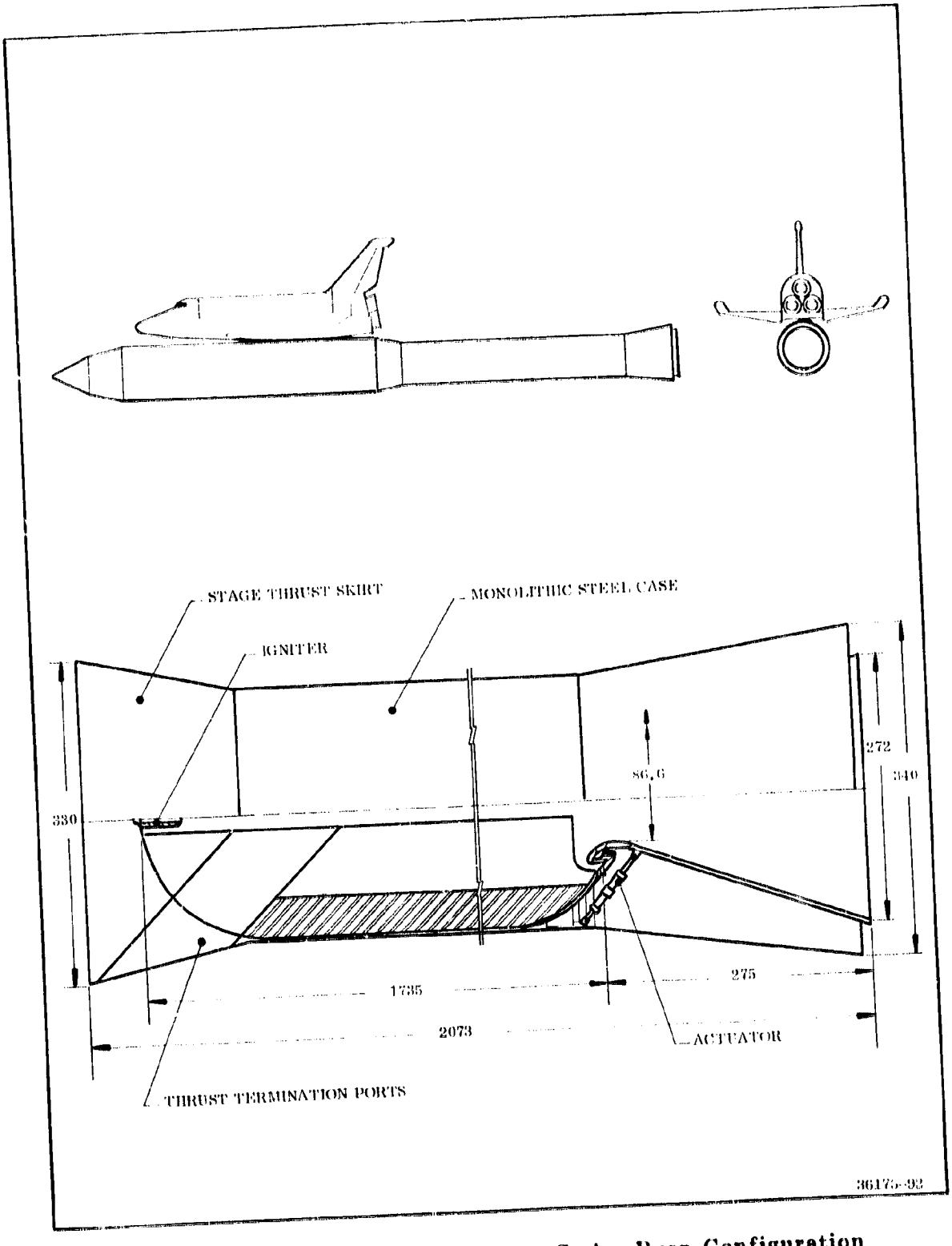

Figure 3-4. 260 In. SRM Stage for Series Burn Configuration

TABLE 3-6

PERFORMANCE SUMMARY
260 INCH SRM FOR SERIES BURN CONFIGURATION
(One SRM per Launch Vehicle)

Performance	
Average vacuum thrust (lb)	8,920,000
Burn time (sec)	135
Operating pressure (psia)	
Average	830
MEOP	1,000
Vacuum specific impulse (sec)	267.6
Weight	
Propellant weight (lbm)	4,500,000
Total motor weight (lbm)	4,972,000
Motor mass fraction	0.905
Total stage weight (lbm)	5,023,000
Stage mass fraction	0.896

A discussion on a recovery system for this SRM stage is contained in Section 5.0.

3.4.2.1 Basic Motor

The basic SRM stage is shown on Figure 3-5. The stage consists of two 156 in. SRM,nose cones and attachment structures on the forward end and skirts, and attach structures on the aft end.

The motor consists of a segmented D6AC steel case with a forward and aft segment and three center segments. The nozzle is fixed and there are no provisions for TVC. The propellant is a PBAN propellant identical to that presently used in Stage 1 Minuteman. The design details are discussed below.

FOLDOUT FRAME

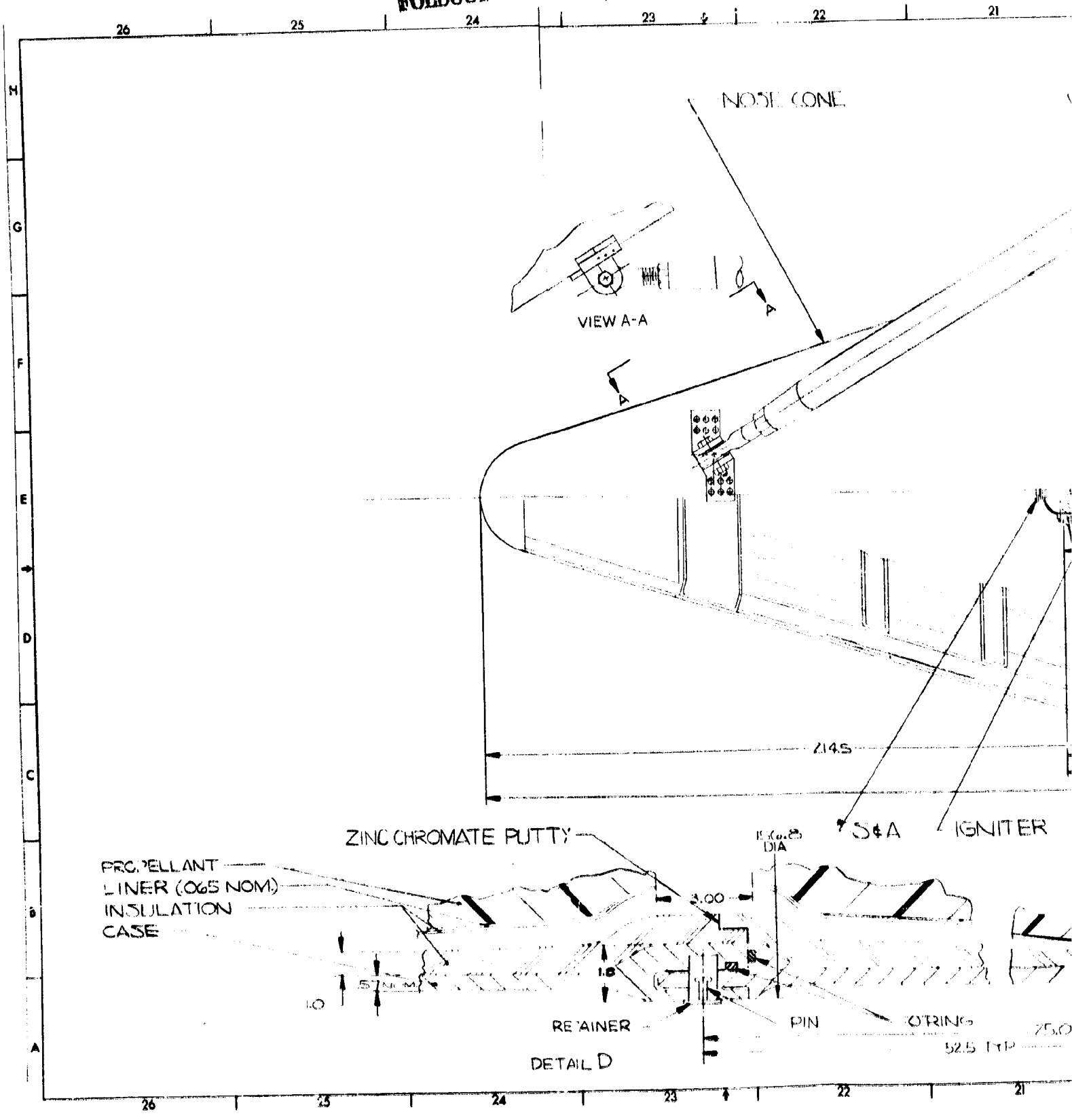

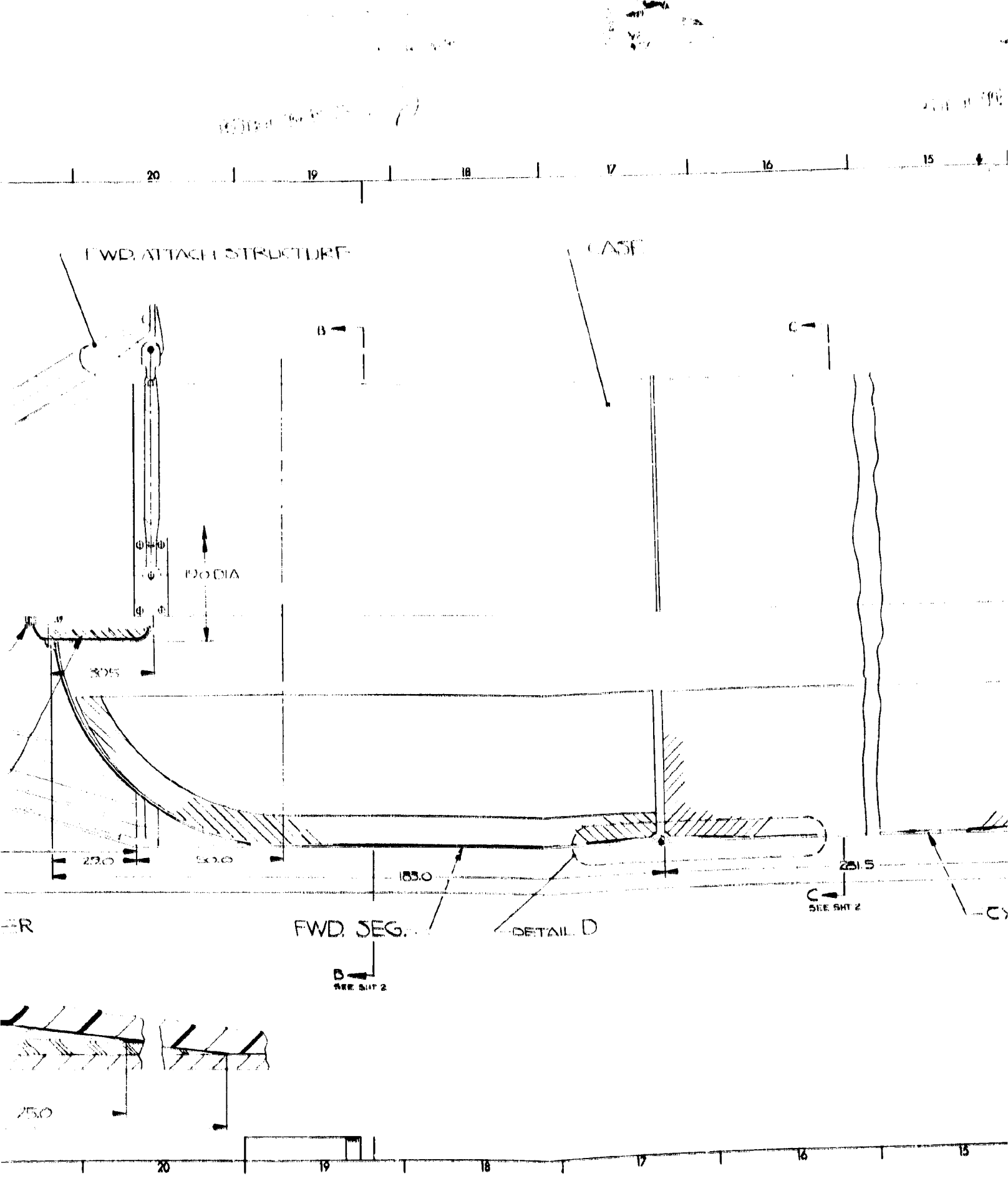
20
19
18
17
16
15
FWD ATTACH STRUCTURE
CASE
B
C
P.C.D. DIA
30.5
27.0
5 x 2.0
183.0
281.5
C
SEE SHT 2
FWD. SEG.
DETAIL D
B
SEE SHT 2
25.0
20
19
18
17
16
15

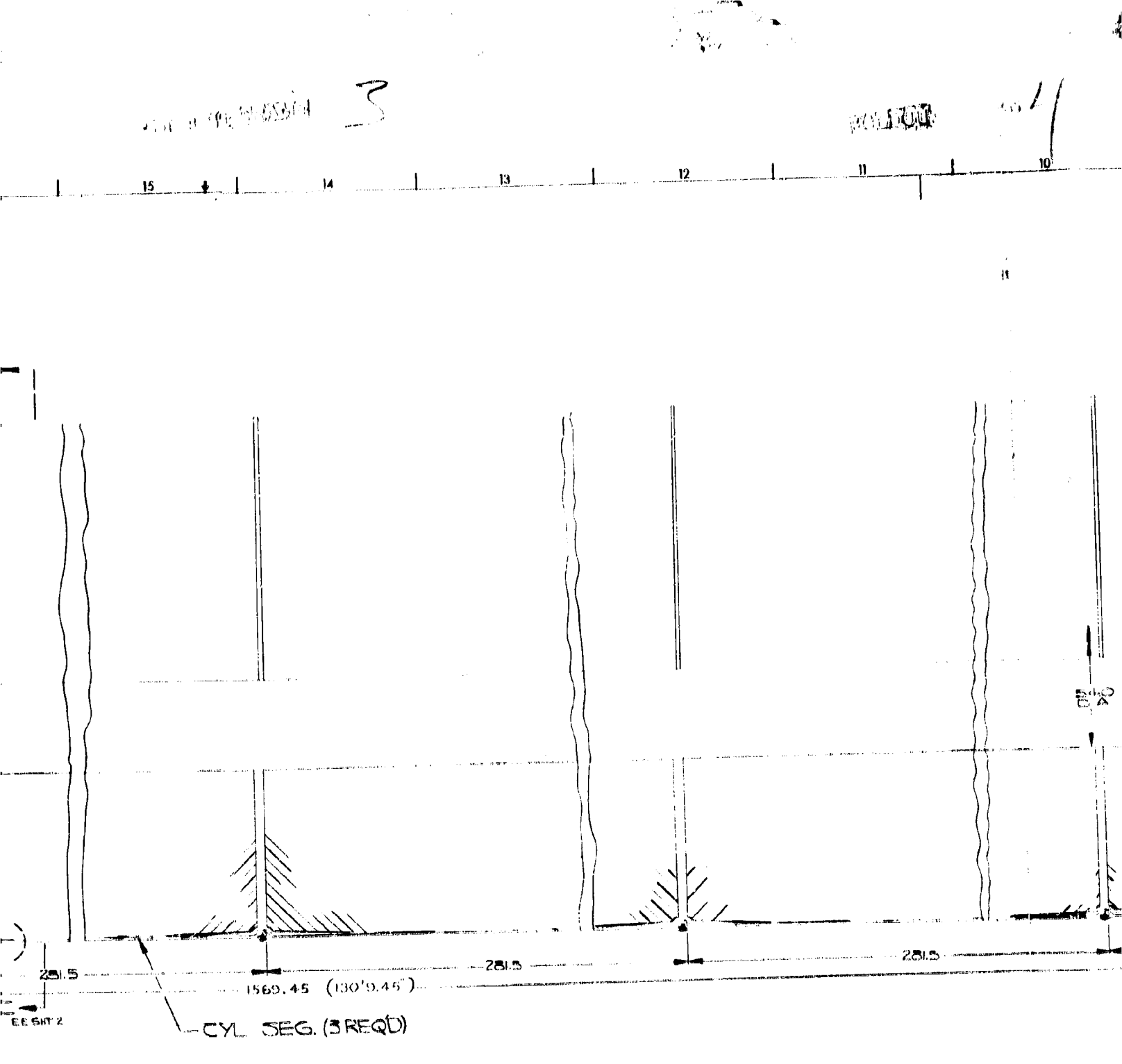
15
14
13
12
11
10
281.5
281.5
281.5
1569.45 (130'9.45")
CYL SEG. (3 REQ'D)
SEE SHT 2

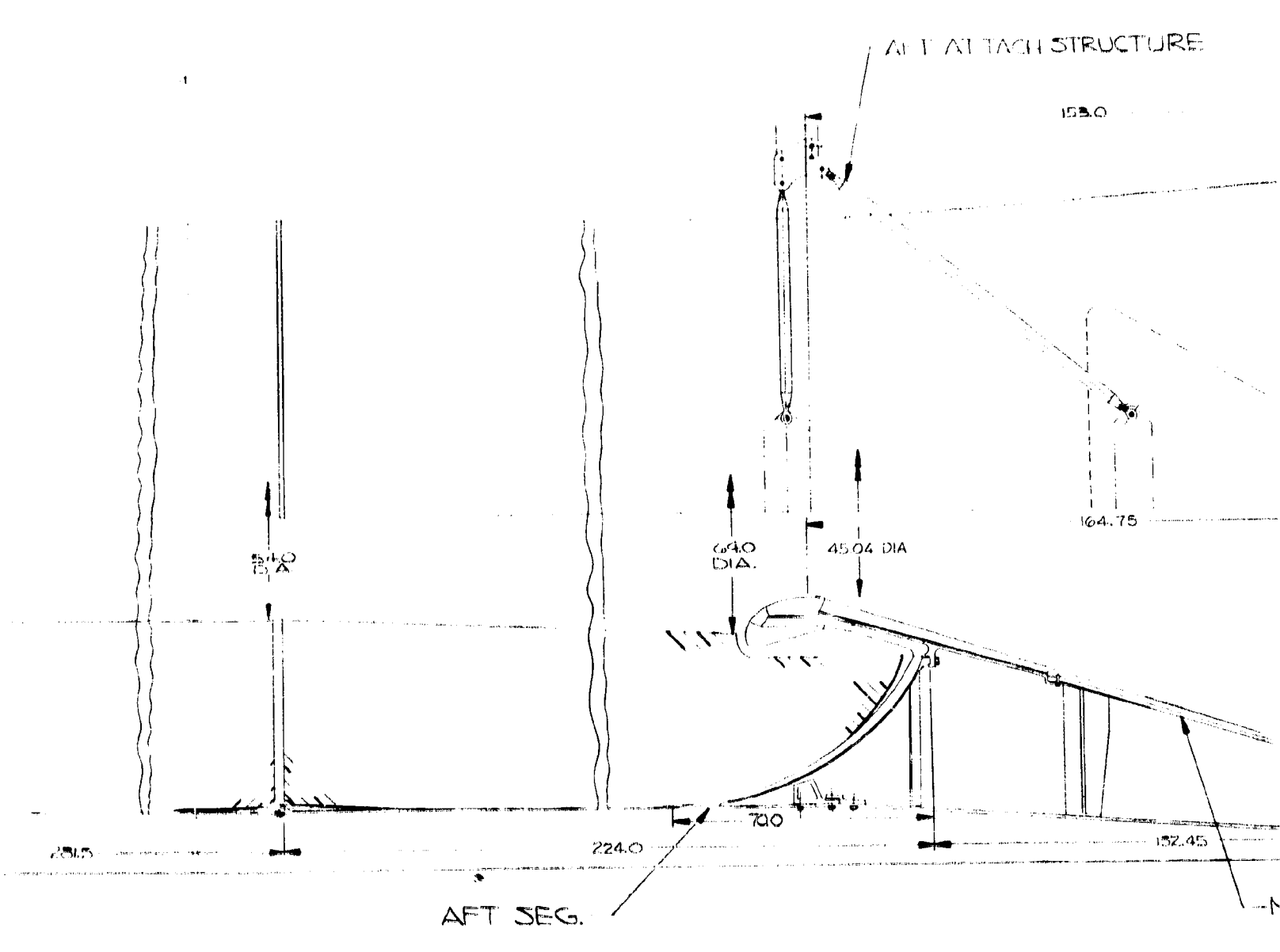
AFT ATTACH STRUCTURE
153.0
164.75
64.0 DIA.
45.04 DIA
70.0
224.0
152.45
AFT SEG.

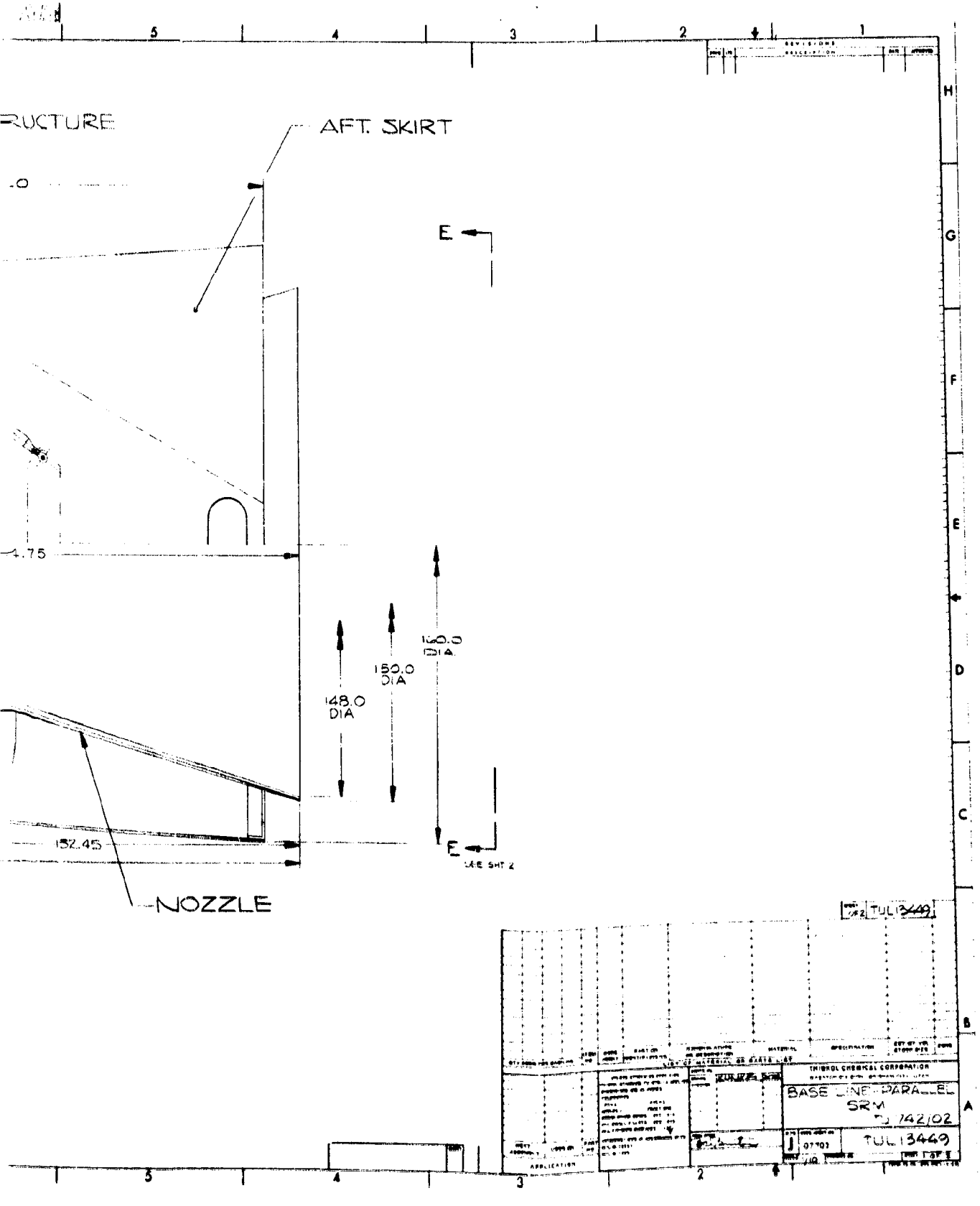
RUCTURE
AFT. SKIRT
E
E
E
4.75
148.0
DIA
150.0
DIA
160.0
DIA
152.45
NOZZLE
SEE SHT 2
TUL13449
THIOKOL CHEMICAL CORPORATION
BASE LINE PARALLEL
SRM
TUL13449

Fig. 3-2. [illegible]

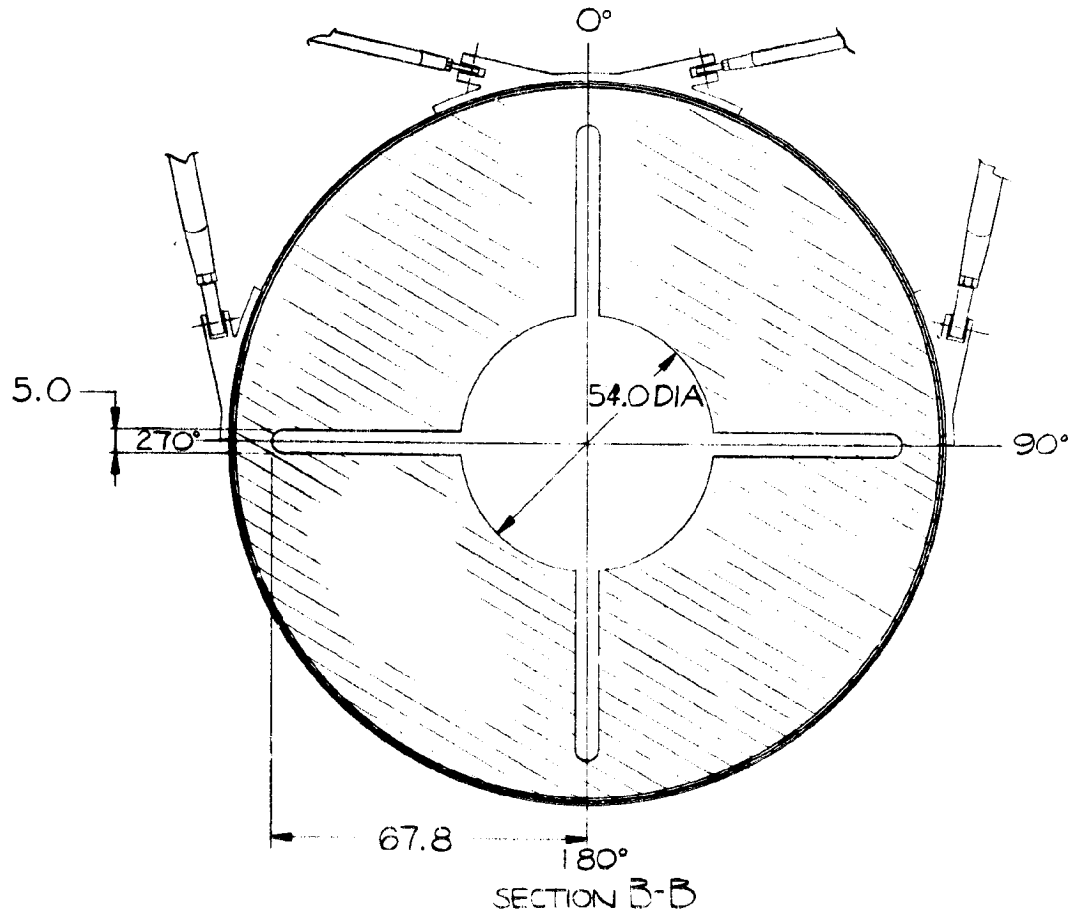

SECTION B-B

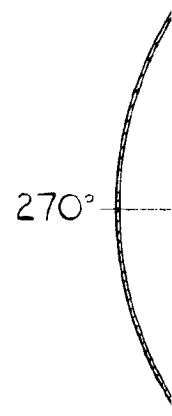

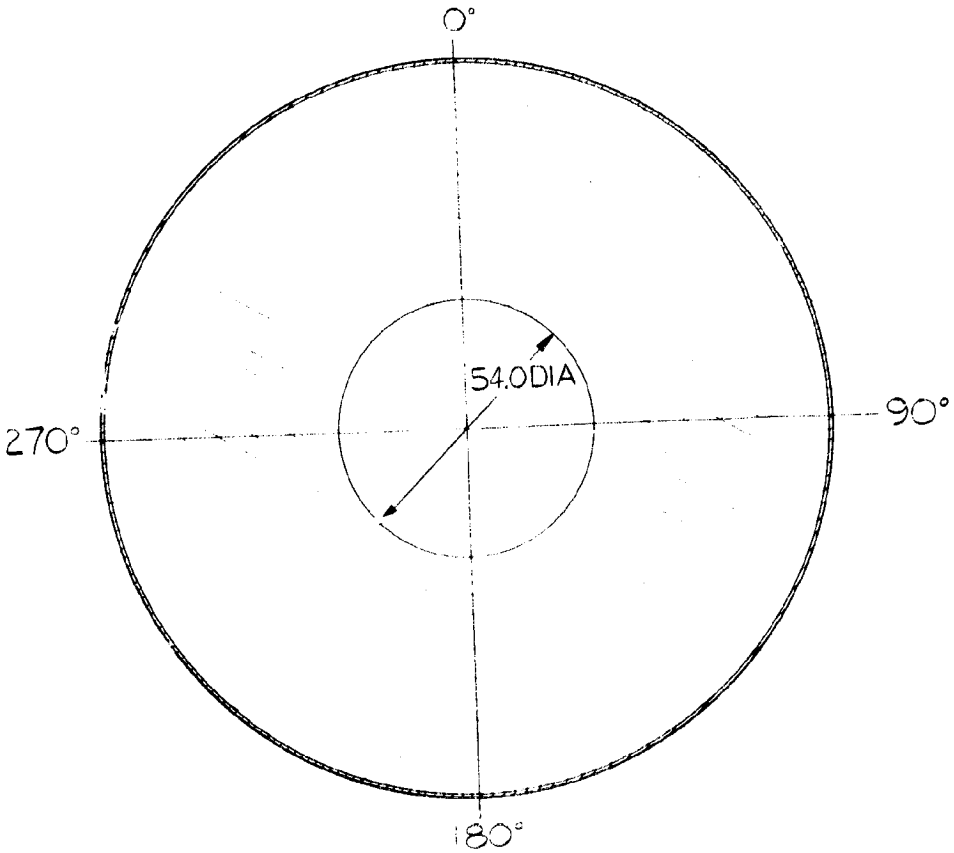

SECTION C-C

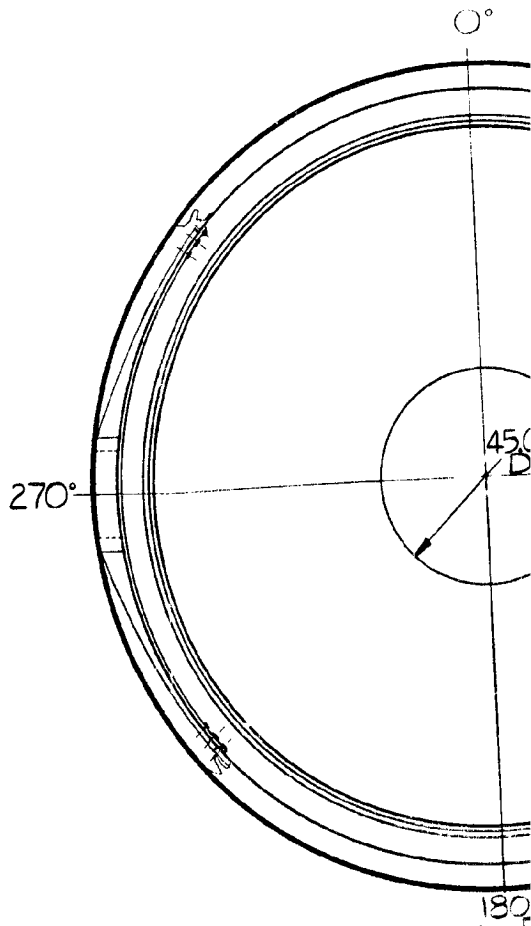

VIEW E

FOLD

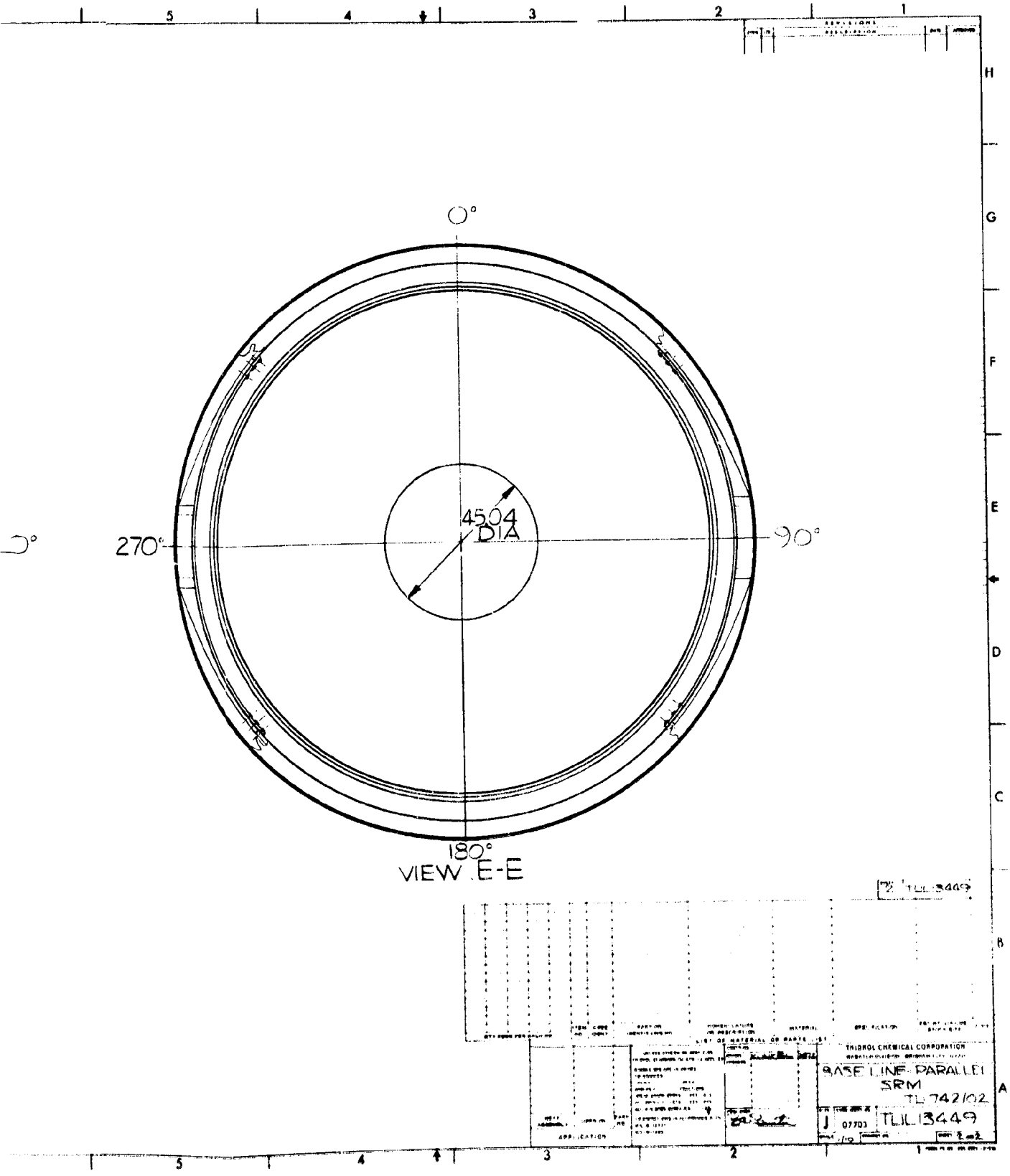
0°
270°
90°
180°
4504
DIA
VIEW E-E
TRIDROL CHEMICAL CORPORATION
BASE LINE PARALLEL
SRM
TL 742102
J
07703
TLIL13449

3.4.2.1.1 Grain Design and Performance

The propellant grain for the parallel motor baseline design consists of three cylindrical segments with a straight cylindrical perforated (CP) configuration, a forward segment with a four slot, slotted tube configuration, and an aft segment with a tapered circular port (conical) configuration. The design is presented in Figure 3-5.

The design selected has achieved success in many solid rocket motor programs including the 120 in. Air Force Titan IIIC, the Stage I Poseidon, Stage III Minuteman, the current version of the Thiokol-developed Pershing propulsion system, and 156 in. demonstration motors. The reliability of this design has been demonstrated in flight in all of the above programs with the exception of the 156 in. motor demonstrations, which consisted of static tests only.

Cost and development time savings are substantial through the use of the circular core due to the low initial core fabrication costs and ease by which design changes may be incorporated. The selection of the simple internal and end burning CP design has not compromised the ballistic performance of the design selected.

The ballistic performance of this design is summarized in Tables 3-7 and 3-8 and the thrust and pressure time characteristics are shown in Figures 3-6 and 3-7 . The main criteria used in this design were a thrust performance of at least 70 percent regressivity (final thrust/maximum thrust) and an MEOP of 1,000 psia upon which the case design is based. The resulting regressivity of this design actually exceeded the 70 percent goal, achieving a value of 0.50.

To achieve maximum loading density and provide maximum protection to end domes, the forward and aft segments incorporate propellant in their respective domes. Split flaps are provided at the ends of the dome to prevent possible propellant pull-away due to differential thermal contraction during cooldown from cure temperature. Split flaps will be provided at both ends of each main segment, and at the ends of the cylindrical sections of both forward and aft segments.

The CP design is the optimum configuration for minimizing erosive burning. The design provides initial surface area, much of which is composed of end surfaces initially shielded from high velocity gases at the time when erosive burning tends to be most critical. The rate of growth of perforation flow area is relatively slow because of the low surface area, a factor which tends to extend the period of erosive burning, thus avoiding sharp initial pressure peaks and gradients. The CP design also requires higher propellant burning rates as compared to star designs, a factor which has historically been observed to reduce the erosion burning increment of the burning rate.

The tapered port of the aft segment was provided to reduce gas velocities and thus reduce erosive burning.

TABLE 3-7

BALLISTIC PERFORMANCE SUMMARY

Type	Cylindrical port
Web fraction (%)	65.1
Chamber volume (insulated) (cu in.)	22,420,000
Void volume (cu in.)	3,230,000
Propellant volume (cu in.)	19,190,000
Volumetric loading (%)	0.856
Cross sectional loading (lb/in.)	1,020
Initial Ap/At ratio (crit point)	1.4
Weight of propellant (lbm)	1,218,000
Initial surface area (sq in.)	391,000
Average surface area (sq in.)	380,200
Maximum surface area (sq in.)	415,400
Final surface area (sq in.)	259,300
Dimensions (in.)	
Web thickness	50.47
Slot width	3.0
Diameter at headend opening	54
Nominal CP diameter	54
Diameter at nozzle cutout	80

TABLE 3-8

CALCULATED BALLISTIC PERFORMANCE
TU-742/02 PROPELLANT GRAIN
(70°F and Zero psia Ambient Pressure)

Time	
Web burning time (sec)	130
Action time (sec)	135
Pressure	
Maximum chamber (psia)	940
Average web (psia)	780
Average action time (psia)	777
Thrust	
Maximum thrust (lbf)	2,830,000
Average web (lbf)	2,468,000
Average action time (lbf)	2,455,000
Impulse	
Total impulse (lbf-sec)	331,300,000
Action time impulse (lbf-sec)	331,000,000
Vacuum delivered specific impulse (lbf-sec/lbm)	270.9
Mass flow	
Propellant weight (total) (lbm)	1,218,000
Propellant expended during action time (lbm)	1,217,000
Action time mass flow rate (lbm/sec)	9,030
Miscellaneous	
Propellant burning rate (ips) (motor avg)	0.376
Nozzle initial throat diameter (in.)	45.04
Nozzle average throat diameter (in.)	46.86
Radial erosion (ips)	0.0135

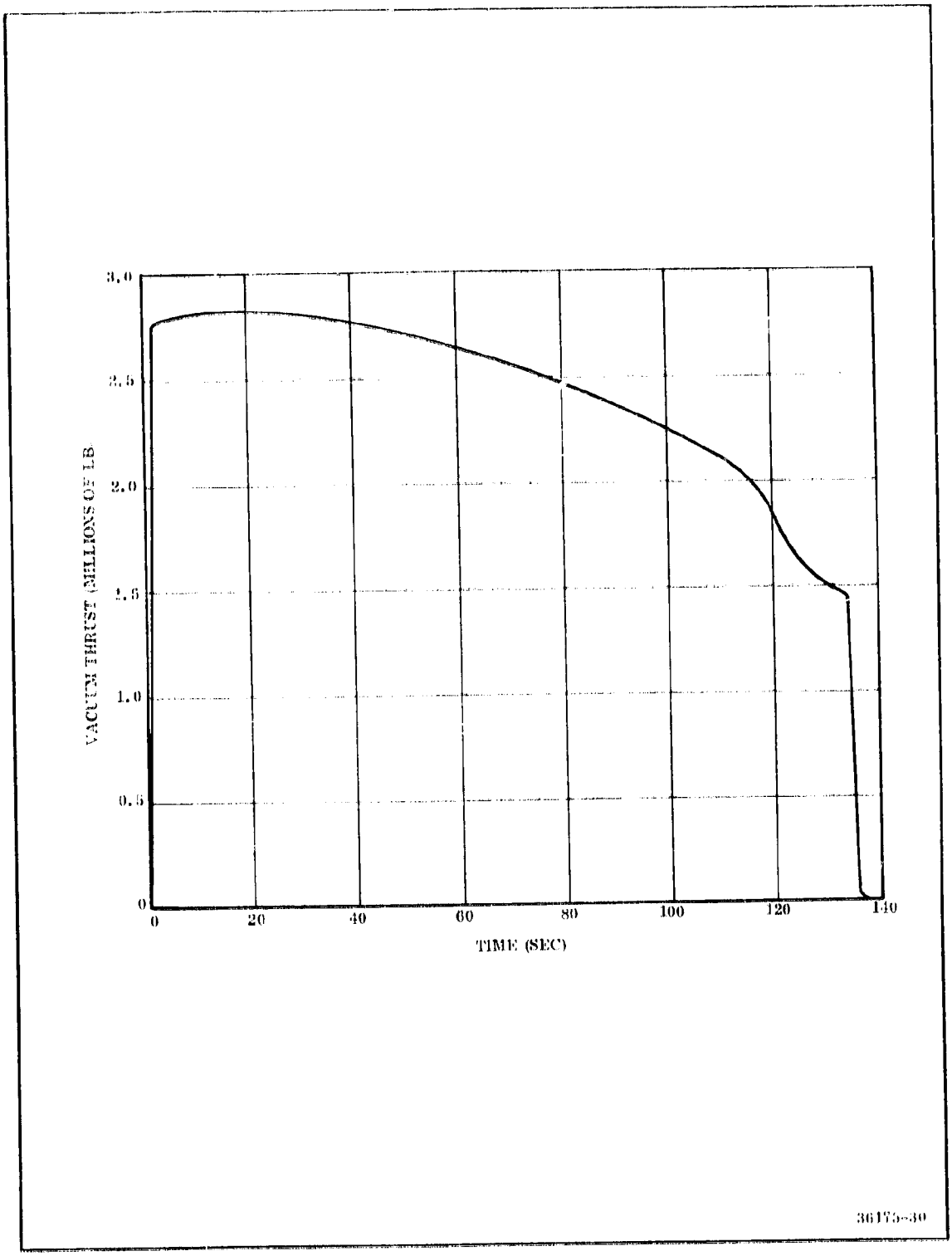

Figure 3-6. Motor Thrust vs Time Performance, Parallel Configuration

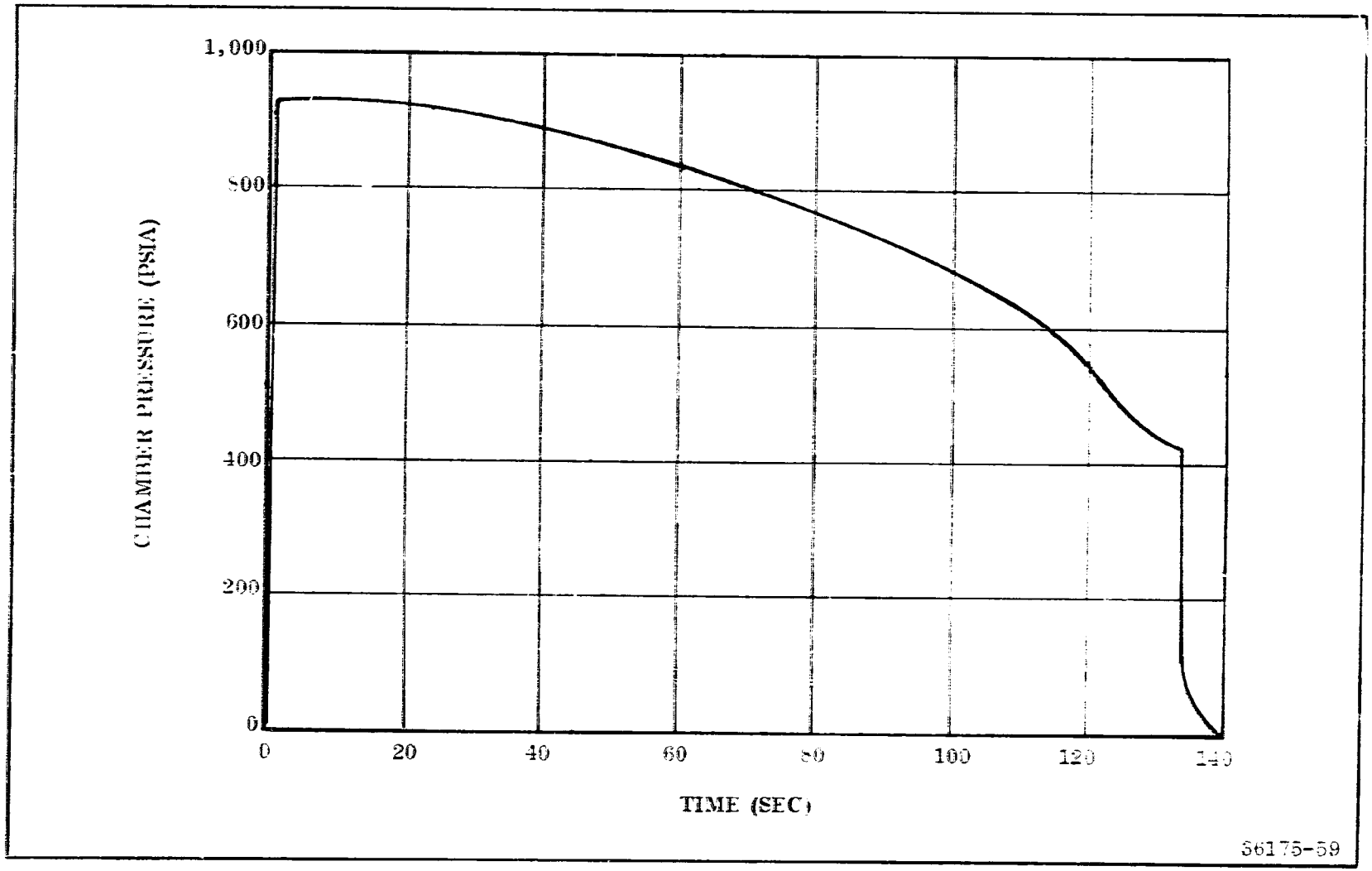

Figure 3-7. Motor Chamber Pressure vs Time Performance, Parallel Configuration

The baseline grain design offers the potential of a wide range of ballistic tailoring without sacrificing simplicity or ease of fabrication. For example, the thrust regressivity can be varied by simply altering the length of the slotted-tube forward segment. A "saddle" thrust trace (in which the thrust is initially highly regressive followed by less regressive performance) can be provided easily by adding one or two additional slots in the headend configuration. Should a more gradual thrust decay during tailoff prove attractive from overall systems considerations, a slight tapering of the port diameter between head end and aft end of each segment can be employed to achieve this. Identical configuration for each cylindrical segment would be retained.

A maximum regressivity value of 0.45 can be produced by substituting a four slot, slotted tube configuration (similar to the forward grain) for the aft grain CP configuration. Further increases in regressivity can be obtained by additional slots in the slotted tube configurations. However, this will produce a "saddle" type thrust-time trace.

A fairly neutral performing grain can be produced by substituting a CP configuration for the slotted tube design used in the headend. This will yield the slightly humped performance characteristic of segmented, end burning CP configurations. This design will be slightly progressive over the first 40 percent of the firing, followed by a slightly regressive performance down to a final thrust that is slightly less than the initial thrust. The ratio of maximum thrust to average thrust is 1.09.

The all CP configuration can be made progressive by inhibiting the propellant surfaces between segments. The maximum progressivity (final thrust/initial thrust ratio) that can be obtained by inhibiting the end surfaces is 2.81.

Considerable performance flexibility exists with the baseline grain configuration. Burntime and thrust level can be varied by adjusting the operating chamber pressure, propellant burning rate, or a combination of both the above.

The discussion which follows is limited to the performance variation which can be achieved within the maximum pressure capability afforded by the baseline case design. Further thrust-time flexibility can be realized by increasing motor operating pressure.

For this particular application, it is probably desirable to effect a burntime increase through a decrease in propellant burning rate while holding the operational chamber pressure constant. This is because an optimum chamber pressure for this system (which has not yet been firmly established) is not likely much less than the pressures used for this motor design.

For the baseline design generated in this study, the option of increasing burntime without decreasing propellant burning rate is not available. This is because the grain design has been optimized to provide maximum propellant loading

density within the limits of port area-to-throat area ratio (erosive burning criteria) constraints. Thus, an increase in throat area (which effects a reduction in chamber pressure and hence a reduction in burning rate) is not possible.

Therefore, to increase the burntime of this motor design, the propellant burning rate must be reduced. The baseline motor design utilizes a burning rate near the mean of the burning rate range demonstrated by this propellant. As a result, considerable latitude is available for the reduction of propellant burning rate.

A 33 sec increase in burntime can be achieved for this motor by reducing the burning rate to the minimum value available while holding the chamber pressure constant. To hold a constant chamber pressure while reducing burning rate, the nozzle throat area must be reduced by the same percentage as the burning rate. Resulting motor thrust would be approximately 2,000,000 lbf.

Further increases in burntime can be achieved by holding throat area constant while reducing the burning rate. This results in a lower chamber pressure which further reduces the motor burning rate. The maximum burntime available using this technique is 192 sec. Corresponding motor chamber pressure and thrust are 528 psia and 1,720,000 lbf, respectively.

These values represent the maximum burntime and minimum thrust available from this motor design without modification of the basic grain configuration.

There is not a great deal of flexibility, within the framework of the baseline design, for the reduction of the burntime. This is because the chamber pressure cannot be increased (due to case design constraints), and increases in propellant burning rate are somewhat limited (without a modest propellant burning rate development program).

Thus, the burntime can be reduced to about 118 sec, without modifying the grain design or undertaking a development program to increase the burning rate. Corresponding motor thrust would be approximately 2,780,000 lbf.

However, only minor modifications to the grain design would be required to effect more substantial burntime reduction. The web thickness could be reduced by increasing the port diameter. This would result in a small reduction of volumetric loading and would require a slight increase in motor length.

A parametric analysis of tailoff thrust imbalance that would be produced by a pair of motors in the parallel Space Shuttle booster system was accomplished. In this analysis, four designs with different tailoff times (different sliver fractions) were evaluated. The thrust differential (between two motors of the same design) produced during tailoff was then determined as a function of the percent difference in their web burntimes.

Figure 3-8 presents the results of this analysis, showing the maximum thrust imbalance produced from a pair of motors for a Space Shuttle mission as a function of percent variation in web burntime (for each of the designs). Theoretically, the baseline design produces a thrust imbalance of greater than one million lb for all web burntime variations in excess of 0.6 percent. This is due to the nature of baseline grain design which has a zero percent sliver fraction.

However, the actual tailoff performance could not realistically be expected to produce the rapid thrust decay indicated by the theoretical calculations. Slight variations in burning rate and effects of erosive burning will produce a slight tapering of the port cavity, resulting in a sliver which prevents the instantaneous propellant burnout predicted in the theoretical baseline performance.

The tailoff performance, produced in the static tests of 156 in. motors which utilized the same grain design required about 5 sec to decay to 10 percent of maximum thrust. The baseline design would be expected to exhibit similar tailoff characteristics.

The other three designs evaluated in this analysis have approximately the same thrust performance over web time as the baseline design. However, slivers have been incorporated in these designs, thus producing more gradual thrust decays than exhibited by the baseline theoretical performance. Figure 3-9 compares the thrust-time performance of all four designs.

As indicated above, the baseline tailoff performance would be expected to be modified somewhat in actual firing. The actual performance, which would be expected to exhibit a tailoff time of about 5 sec. would yield a performance like that of the design with the 5 sec tailoff.

An analysis of the maximum burntime variation that might be expected from motors for the Space Shuttle booster indicates that this variation should be no greater than 0.77 percent. This analysis considered the effects of burning rate variation between motors (predicted to be no greater than 0.3 percent) and the variation in nozzle erosion rate. The dashed line in Figure 3-8 depicts this limiting value.

Figure 3-10 is presented as an aid in selection of tailoff characteristics. It shows the tailoff thrust differential as a function of tailoff time (time from web to action time). The curve shown represents behavior for a web burntime variation of 0.77 percent.

Figure 3-11 presents a "normalized" version of the data shown in Figure 3-8. In Figure 3-11, the maximum thrust differential is shown as a percentage of thrust at web time instead of in pound-force units.

A summary of delivered specific impulse, predicted for the Space Shuttle booster operating conditions, is shown as a function of nozzle expansion ratio at various ambient pressure to stagnation chamber pressure ratios in Figure 3-12.

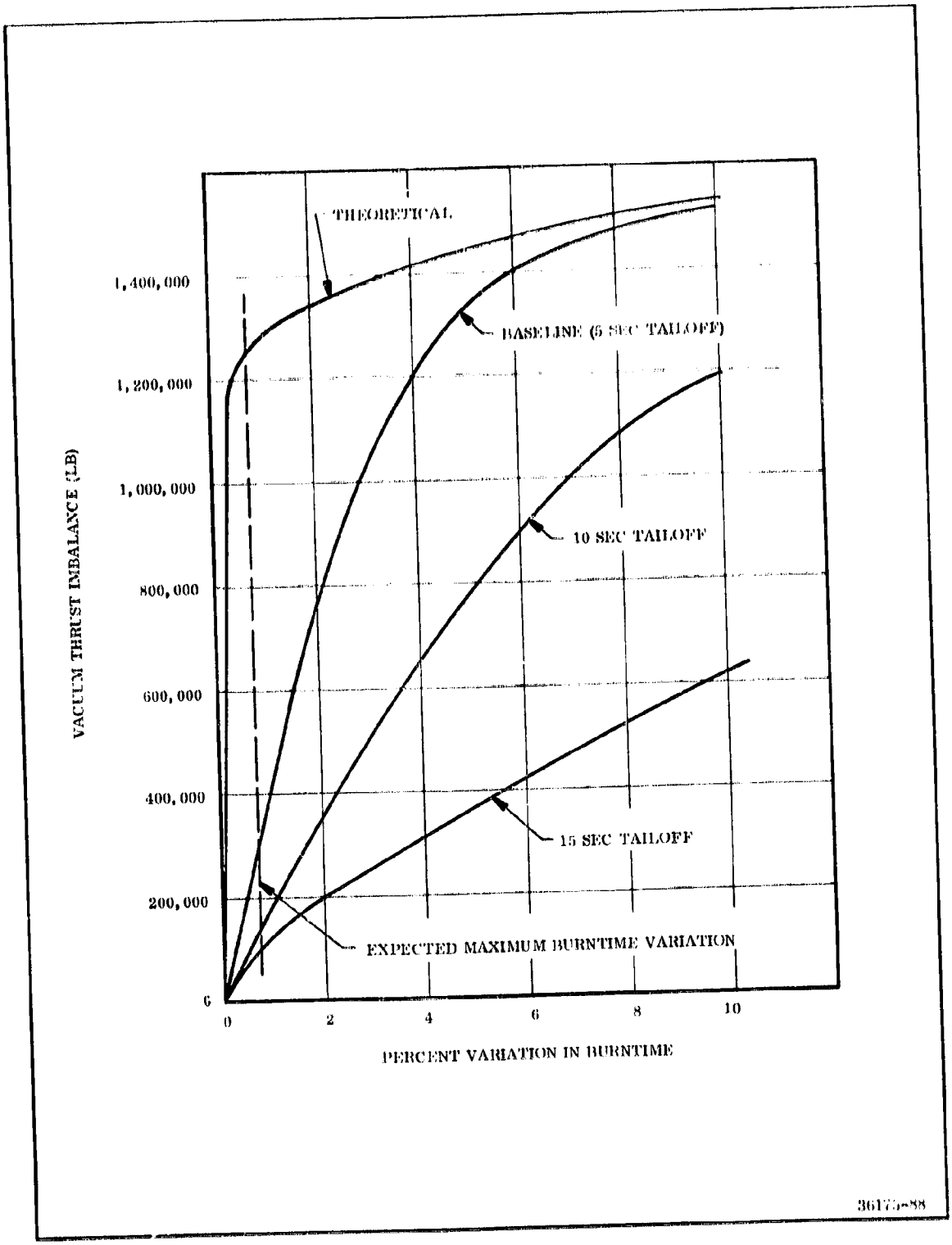

Figure 3-8. Maximum Thrust Imbalance from a Pair of Motors as a Function of Burntime Variation for Motors with Various Tailoff Times

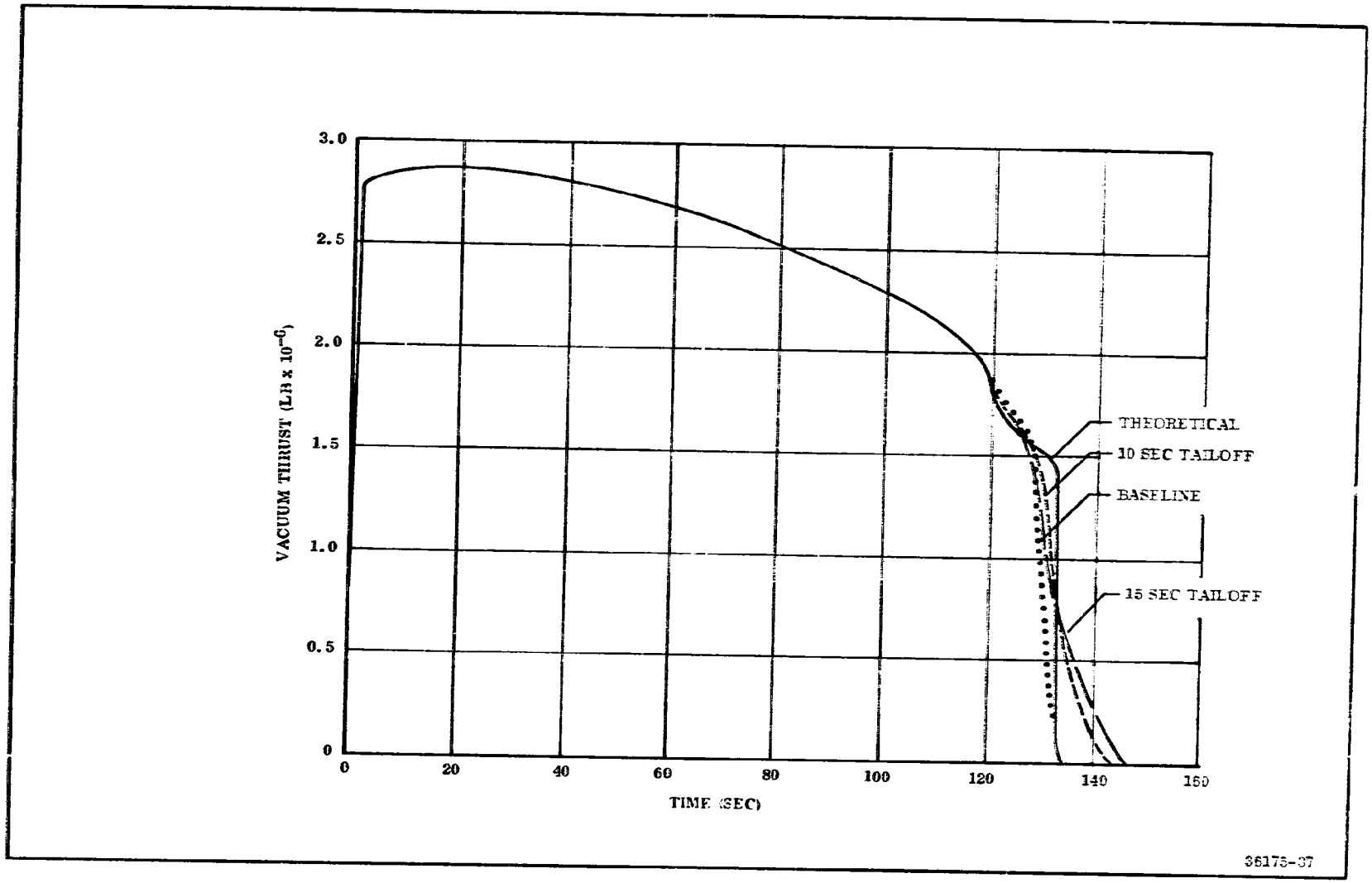

Figure 3-9. Comparison of Thrust Performances

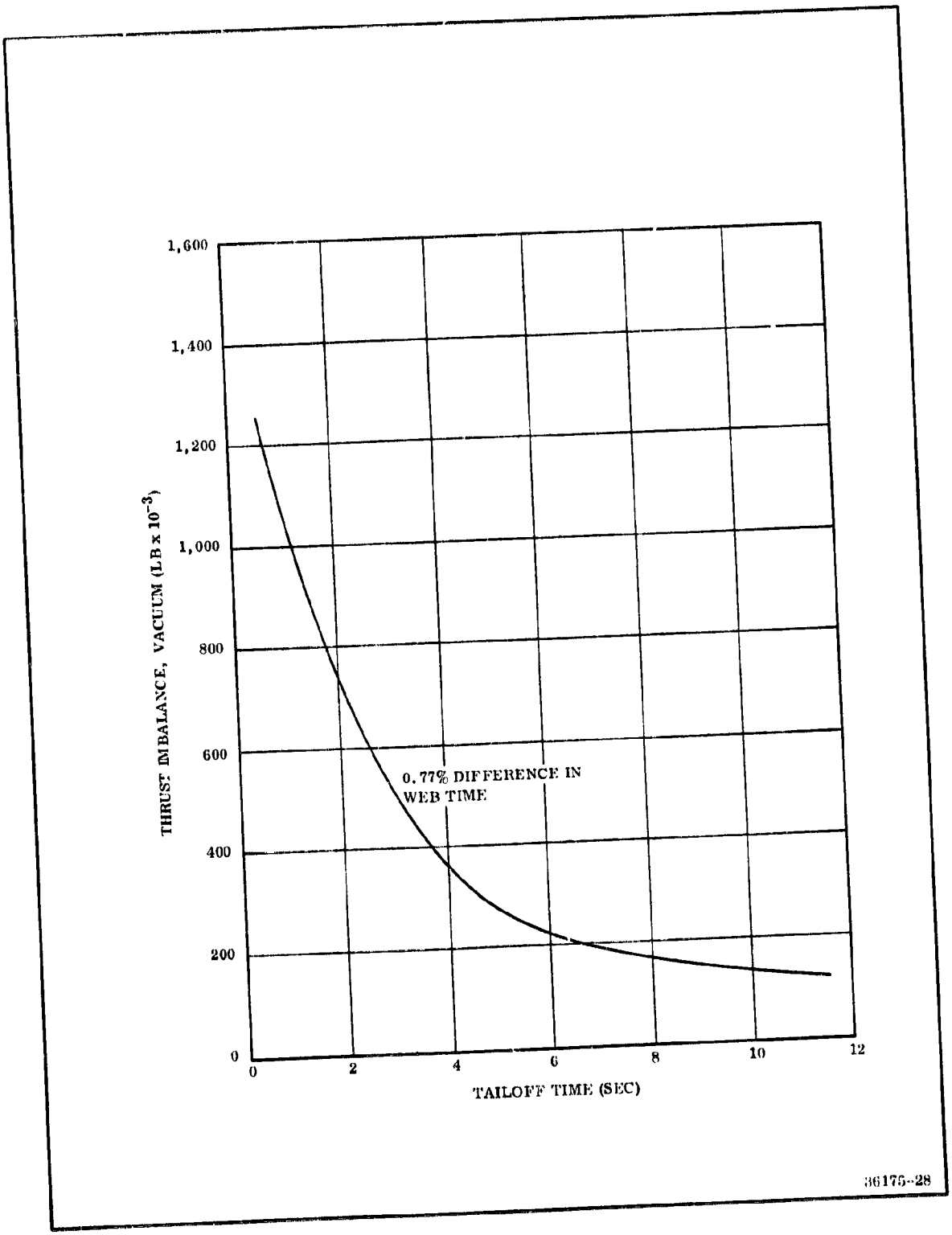

Figure 3-10. Thrust Imbalance from a Pair of Motors as a Function of Time from Web Burnout to End of Action Time

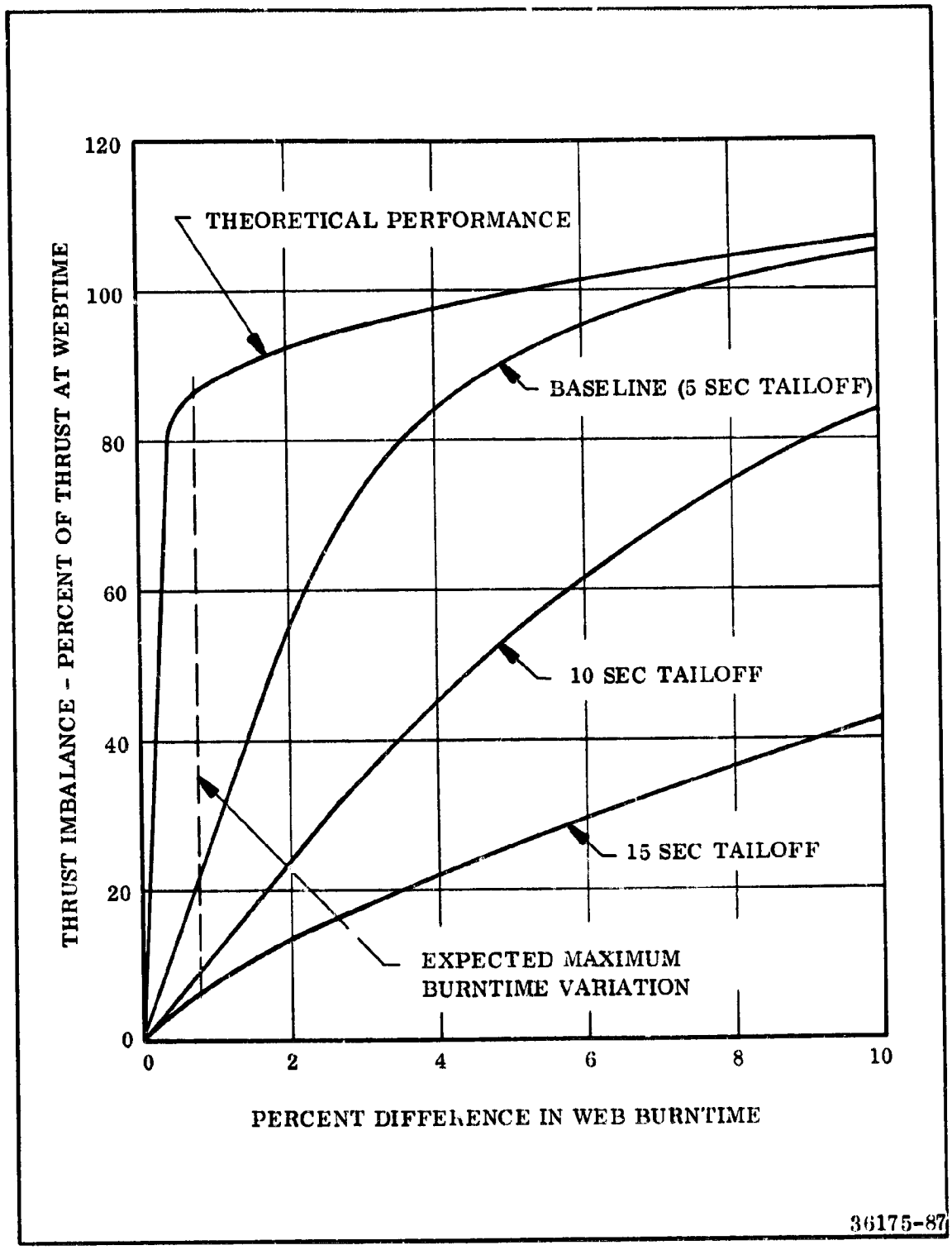

Figure 3-11. Percent Web Time Thrust, Thrust Imbalance Produced by a Pair of Motors of a Booster System Shown as a Function of Percent Difference in Burntime Between Motors

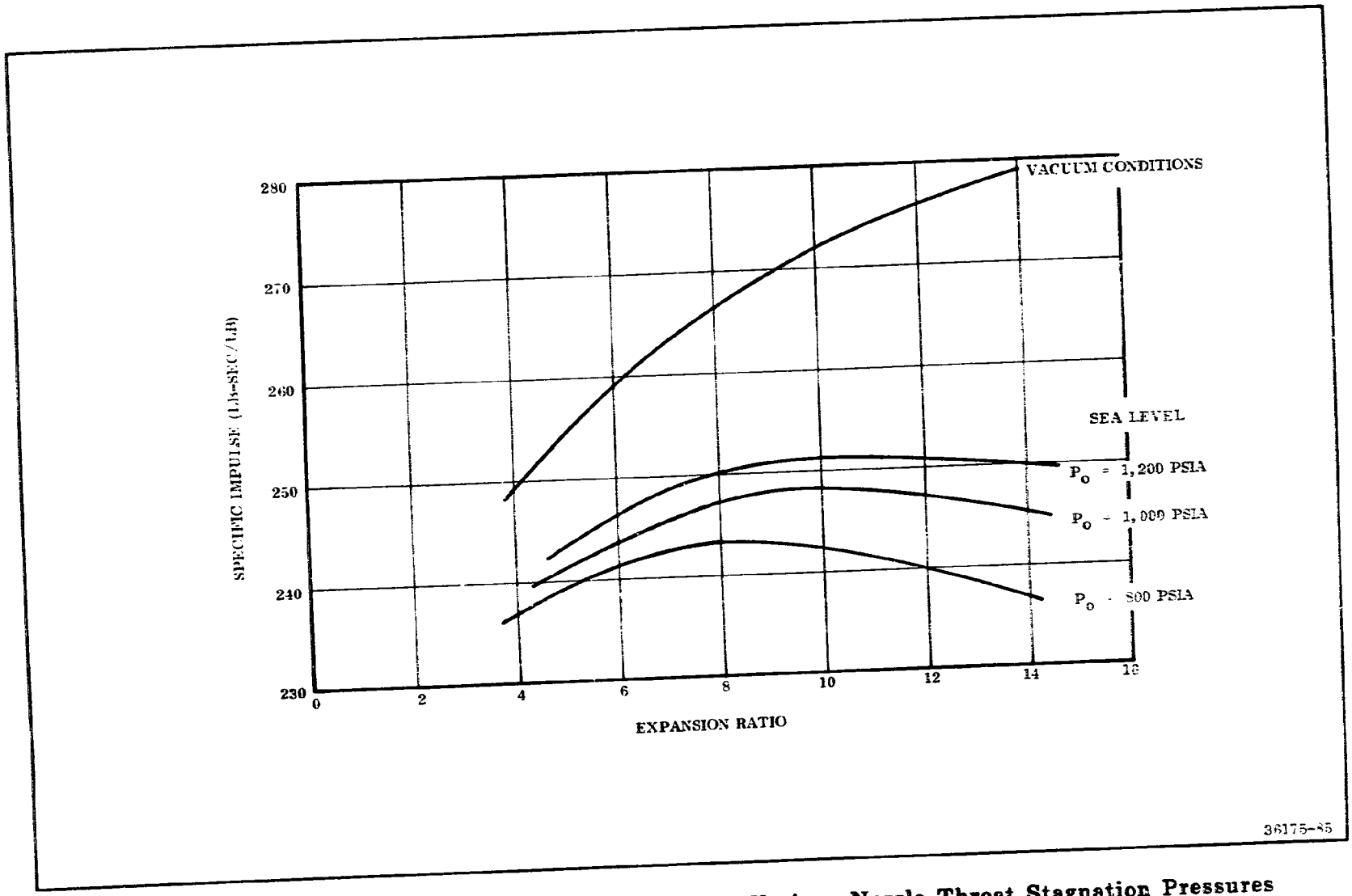

Figure 3-12. Specific Impulse vs Expansion Ratio for Various Nozzle Throat Stagnation Pressures

An analysis was performed to determine the variability in performance parameters that might be expected in the Space Shuttle application. Historical data were used where applicable and analytical methods employed elsewhere. The parameters investigated were the total impulse, vacuum specific impulse, burntime, burning rate, average vacuum thrust, average chamber pressure, and propellant weight. Table 3-9 presents the results of this analysis.

Historical data were reviewed to determine variability in propellant weight, vacuum specific impulse and burning rate since these are generally independent parameters. The Minuteman program, which utilizes the same propellant proposed for the Space Shuttle booster, has demonstrated a variation in vacuum specific impulse of ± 0.6 percent about the nominal value.

Experience on numerous programs has shown that the propellant weight can be held within ± 0.3 percent of nominal.

It is expected that during the Space Shuttle Program, pairs of motors will be produced which exhibit burning rate differences no greater than 0.3 percent (between the pair of motors).

Analytical methods were employed to determine the variability in the remaining parameters, since these parameters are generally dependent on various combinations of the parameters.

The burntime variation is mainly dependent upon nozzle throat erosion variability and propellant burning rate variability. The variability in the nozzle radial throat erosion rate experienced on the Stage I Poseidon motor was assumed, since the selected throat material is the same as used on Poseidon. The resulting analysis indicated a maximum burntime difference of 0.77 percent between motors of a pair.

Experience has shown that the variations in burntime and average chamber pressure are nearly equivalent. Thus the maximum percentage spreads in burntime, shown above, were assumed for average chamber pressure.

The average thrust can be represented by the equation,

$$\text{Average } F = \text{Total impulse/burntime}$$

Thus, the coefficient of variation in thrust can be represented as the sum of the coefficients of variation in total impulse and burntime.

This results in a variation of ± 0.77 percent about the average thrust for pairs of motors.

TABLE 3-9

PERFORMANCE VARIABILITY SUMMARY

Parameter	Maximum Deviation About the Average Value of Two Motors on a Space Shuttle Booster (%)
Specific impulse (sec)	±0.60
Total impulse (lb-sec)	±0.67
Burn rate (ips)	±0.30
Propellant weight (lb)	±0.30
Burn time (sec)	±0.38
Average thrust (lb)	±0.77
Average chamber pressure (psia)	±0.38

The coefficient of variation for total impulse can be considered as the sum of the coefficients of variation of specific impulse and propellant weight. Thus, a variation of ± 0.67 percent about nominal is predicted between pairs of motors.

3.4.2.1.1.1 Grain Structural Analysis

The SRM's proposed for the Space Shuttle Program do not depart from established and well proven state of the art of solid propellant grain design. These motors are larger than any currently in production, however, motors this large (ie, 156 in. diameter) have been designed, fabricated, and successfully static tested at Thiokol/Wasatch and by others. Each assembled motor, consisting of five segments, is about 1,250 in. long. Grain structural considerations are related directly to the motor length-to-diameter ratio (L/D). But, from a grain structural viewpoint, each segment is an entity. Hence, the greatest L/D, 1.79:1, occurs in the center segments. For comparison, the first stages of both the Poseidon and Minuteman ballistic missiles have L/D of 1.72 and 3.4, respectively. All segments feature stress relief flaps at each end of the grain. Each flap is half the length of the grain web fraction or 27 in. The Stage I Poseidon grain also has stress relief flaps at each end. The Stage I Minuteman has only one flap and its stress relief is eliminated during motor cooldown.

Another aspect of grain structural analysis is the grain web fraction and bore contour. These grains have a web fraction of 0.67 and a smooth or cylindrically perforated (CP) bore. In contrast, the Stage I Poseidon with a CP type bore has an 0.80 web fraction. The Stage I Minuteman with a six point star perforation has a web fraction of 0.53. Due to the concentration effects of the starpoints, the Stage I Minuteman is equivalent to a CP with a web fraction of 0.74.

The final structural consideration concerns the external boundary or case-to-propellant bond constraint. The center segment bondline is a straight cylindrical shell as in the Stage I Poseidon grain. However, the dome segments have a cylindrical section of case and some spherical dome bondline. This is similar to the Stage I Minuteman constraint, except the Minuteman has a fully bonded dome. In essence, the dome bonding effectively increases the grain L/D as compared to free ended grain such as in the center segment. However, the forward dome was analyzed to assure that the bonded dome did not cause induced loads exceeding those at the center segment.

Figure 3-13 illustrates, schematically, the important propellant structural features of both the Space Shuttle booster and the comparable Stage I Poseidon and Minuteman features.

A discussion of the only grain loading condition associated with size is in order here. Grain stresses and deformations due to body forces (ie, grain weight and vibrational loadings) are size dependent whereas all other induced stresses and strains are not. Consequently, the Stage I Poseidon and Minuteman analogies used above are not pertinent for body force considerations. However, the 156 in. diameter motors mentioned above provide directly applicable background information on body force loading conditions. In processing one center segment of the 156-1 motor, the segment was suspended vertically without end support for 1 week

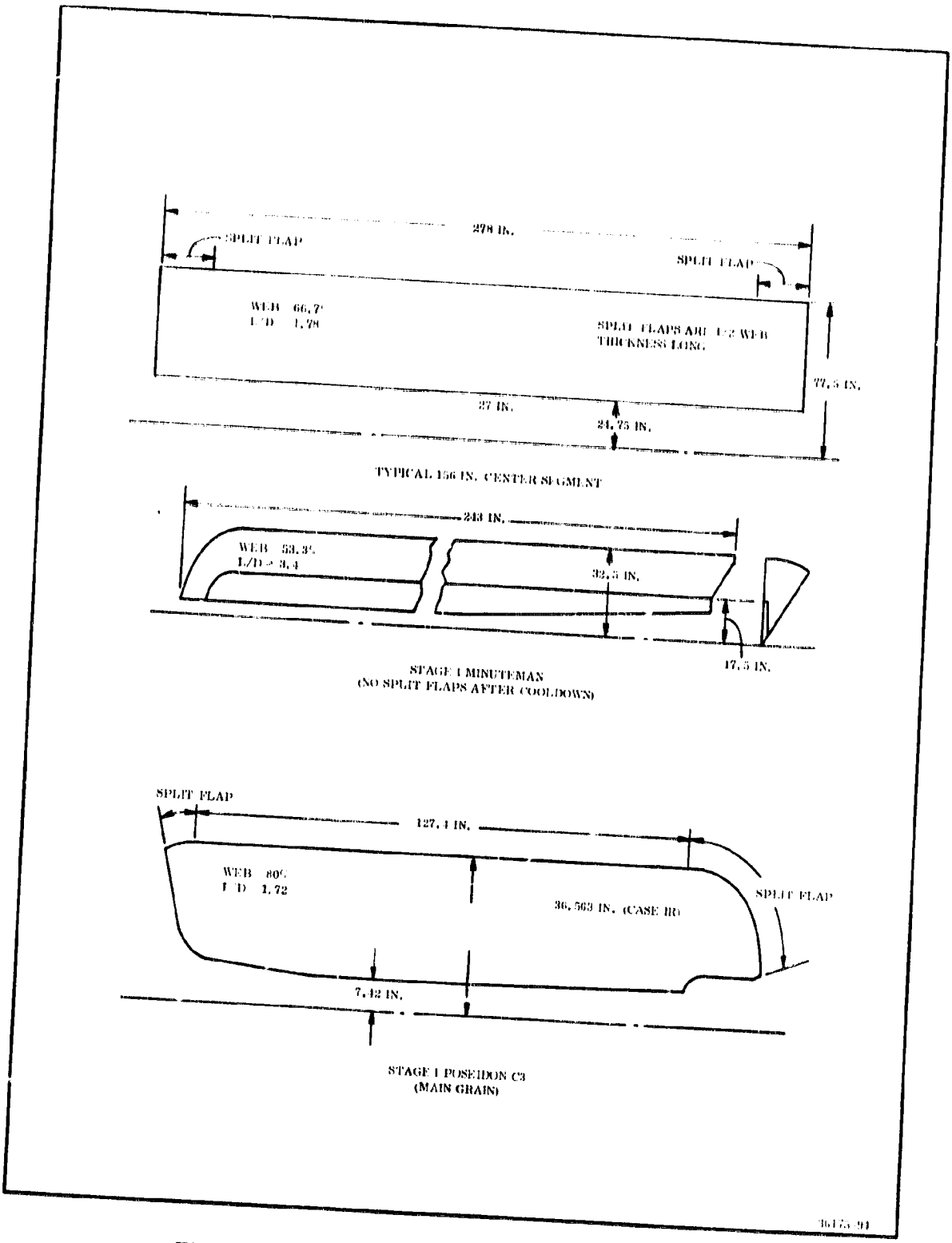

Figure 3-13. Grain Sketches with Typical Grain Structural Parameters and Features

after the core mandrel had been removed. Even though the motor was still warm (propellant is softer when warm), the thermal shrinkage more than compensated for the slump deformation. In other words, at the bore, the down end of the grain was above the level at which it had originally been cast due to thermal shrinkage as shown in Figure 3-14.

As can be observed above, the Space Shuttle solid propellant booster motors will undergo less severe grain structural loading than experienced by the Stage I Poseidon or Minuteman grains. Yet, these latter two motors have been fired reliably after significantly more stringent environmental preloads than the space booster motors will experience. Since the space booster propellant is of the same family as Poseidon and Minuteman, one concludes that it also will be a very reliable grain.

The primary loading conditions inducing stresses and strains in a solid propellant rocket grain are cure and thermal shrinkage and motor pressurization. To a much lesser extent, vibrational loads due to transportation and handling and launch vibrations induce grain loads. Storage slump and launch also induce grain stresses and strains. The larger the motor the lower the launch acceleration will be so that storage and launch are nearly identical at 1 g body force. The vibrational loading is unlikely to be deleterious as shown in a recent Stage I Minuteman program. An aged motor grain was instrumented with grain stress and strain gages, and then subjected to transportation and handling tests. The measured stresses and strains were very low (1.8 psi) with maximum bondline stresses due to (1.16 g at 10 Hz) vibration caused by the transporter being driven over a board coarse. The maximum bore strains were on the order of 0.0005 in./in. Although these loading conditions should not be ignored in a detailed structural analysis, the thermal and pressure environments the grain will be subjected to must be considered as the severest grain design requirements. The only known solid propellant motor failure attributable to a vibration environment was a small tactical motor under unreal and ultrasevere test vibrations. Normal large motor handling and transportation devices or even vibration testing devices capable of inducing such unreal loads into a large motor do not exist.

The capability of the Stage I Minuteman to withstand extended cyclic loading was demonstrated for transportation environments. Results of the test program are shown in Figure 3-15. The load composite for typical 10,000 mi of highway travel was measured. Two motors were subjected to the high load fatigue environment by transporting them across an obstacle course. The motor response was rigid body pitching for both the highway transportation and the obstacle course tests. One motor was subjected to a more severe environment in a vibration facility where it was excited in a flexural mode (both ends in-phase translation). A high degree of confidence was demonstrated when all motors fired satisfactorily after being subjected to these severe environments. Therefore, transportation and handling and launch vibrations must be considered as secondary structural loads.

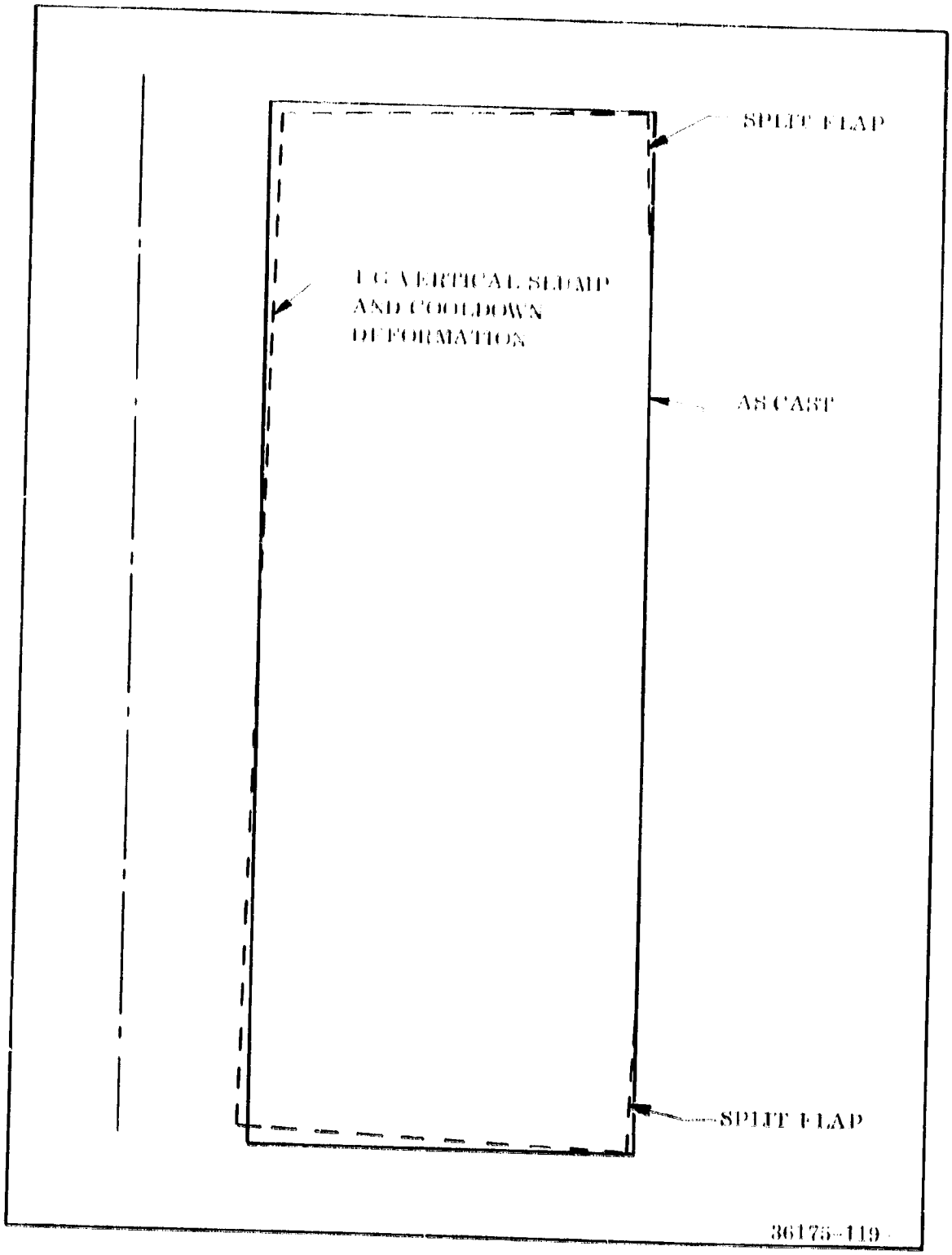

Figure 3-11. Schematic of Actual Vertical Shrink and Cooldown Deformation for 156 In. Center Segment

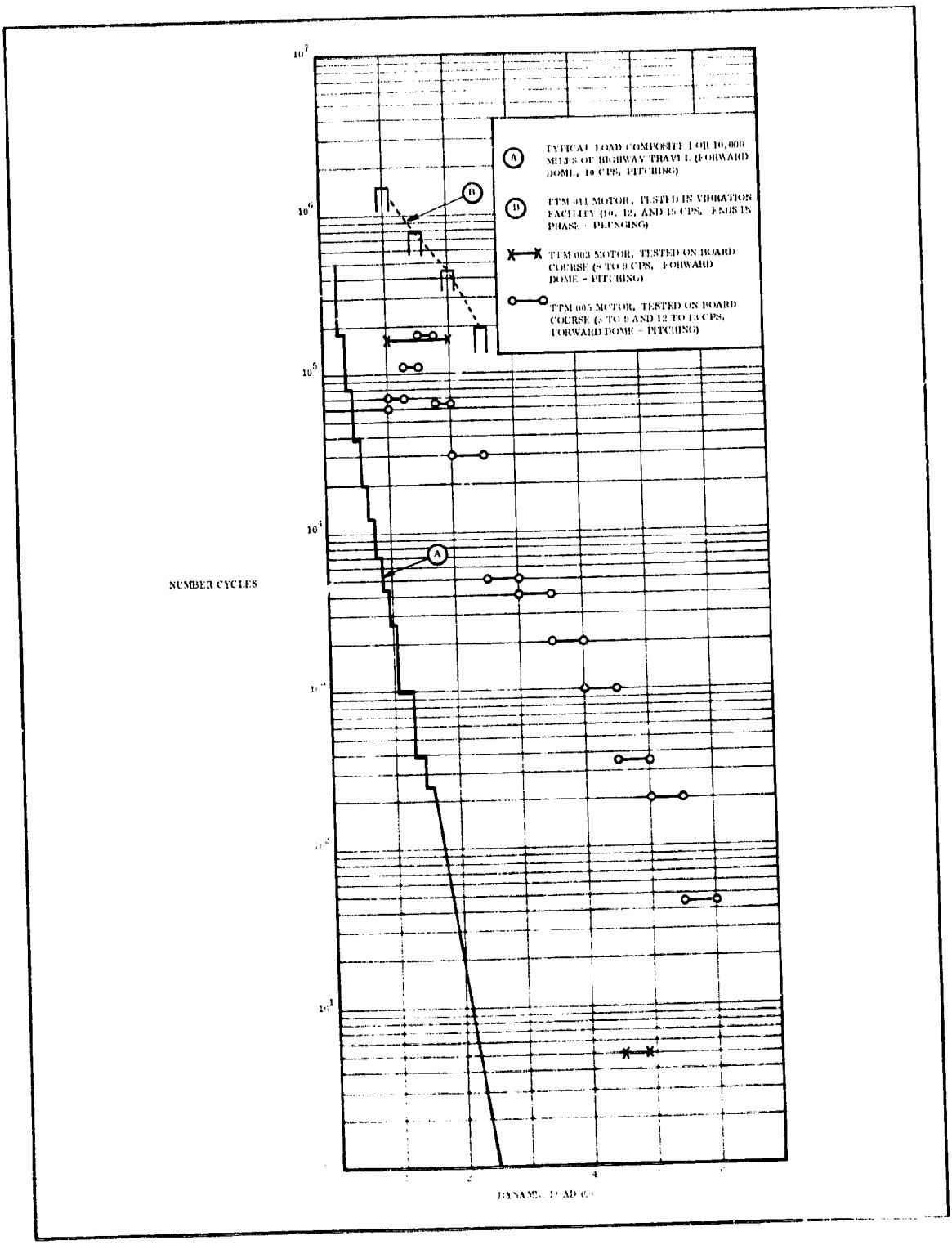

Figure 3-15. Summary Comparison of Load Composite for Typical 10,000 Miles of Highway Travel vs Load Spectrum Experienced by Fatigue Test Motors (Stage I Minuteman)

Normal solid propellant rocket motor processing for the type motor studied requires an elevated propellant cure temperature on the order of 135° F. Since the motor case has a coefficient of thermal expansion 1/10 of that of the propellant, thermal cooldown loads the grain. Some polymerization or cure shrinkage occurs during the 135° F cure time. In large motors, this shrinkage is equivalent to 6° F or less of thermal cooldown. Thus, for a motor to be tested at ambient temperature (70° to 80° F) the effective differential thermal shrinkage is 60° to 70° F. Thermal changes on large motors have the greatest effect on the grain when the entire grain has reached thermal equilibrium at the lower temperature. Fortunately, the equilibrium temperature of these large motors cannot be changed rapidly. As discussed elsewhere, the natural driving temperatures necessary to produce large differential grain temperatures do not occur in continental United States. Hence, a realistic and practical design environment would be about 60° F or an effective thermal differential environment of 81° F.

The motor operational pressure environment for design purposes is usually based on maximum expected operating pressure (MEOP) of the motor after pressure equilibrium has been reached. The predicted pressure trace of the Space Shuttle boosters is near 800 psia. A conservative MEOP, then, would be 1,000 psia where both burning rate and grain temperatures are considered in this MEOP value.

The Space Shuttle SRM grain consists of propellant, liner, and insulation which are all viscoelastic materials. In other words, the material mechanical behavior is time and temperature dependent. To illustrate the mechanical behavior of a viscoelastic material, Figure 3-16 shows a typical propellant stress relaxation modulus vs temperature and time. The high and low end of the modulus curve are denoted as glassy and equilibrium behavior. Liner and insulation have similar characteristics, but different time and temperature sensitivity. Large motors cannot be thermally changed rapidly; thus, propellant under thermal shrinkage loading will exhibit equilibrium modulus behavior. Conversely, the motor pressurization takes place rapidly; and therefore, the effective propellant modulus value will be greater than equilibrium but less than glassy. The grain pressurization time and temperature are not particularly important in a steel case, however. Basically, the propellant, liner, and insulation are incompressible materials when contained in a steel case; thus, the material modulus has little or no effect on the propellant strain due to pressure. Also, thermally induced bore strains are only a function of the thermal coefficient of expansion and Poisson's ratio. Consequently, bore strain predictions for the important loads are modulus independent. Typical stress analysis input parameters for the grain materials are shown in Table 3-10.

Thiokol has demonstrated in Minuteman and Poseidon programs that a maximum principal strain failure criteria is very accurate at the grain bore. Hence, the grain structural behavior parameter of interest is induced bore strain. Figure 3-17 shows a typical strain vs strain rate curve for TP-H1011 Stage I Minuteman propellant. The far right side of the curve represents long term (thermal and slump induced) type

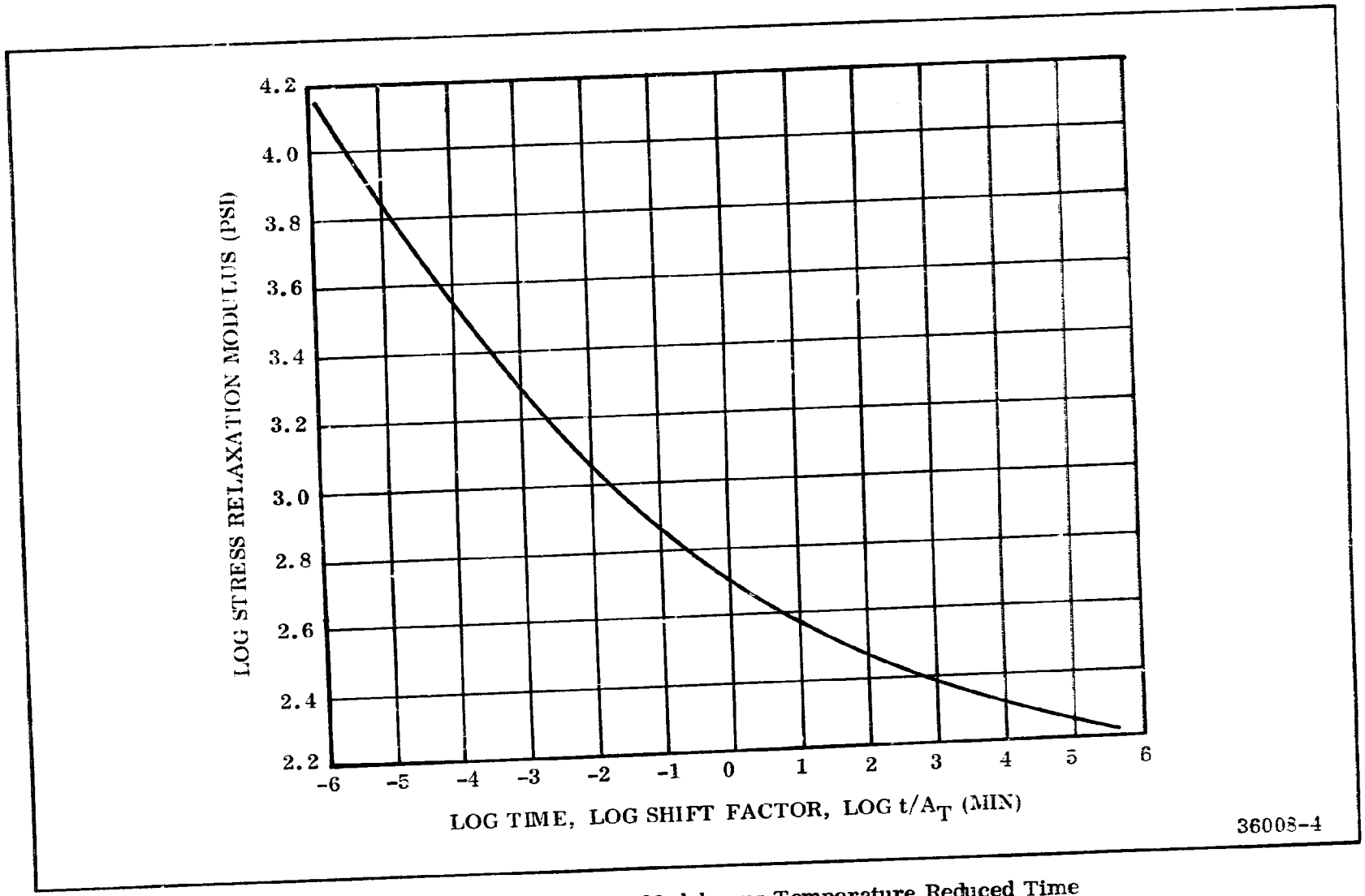

Figure 3-16. Stress Relaxation Modulus vs Temperature Reduced Time

TABLE 3-10

STRESS ANALYSIS INPUT PROPERTIES FOR
SPACE SHUTTLE BOOSTER PROPELLANT GRAINS

Material	Propellant	Liner	Insulation	Case
Shrinkage				
Thermal coefficient of linear expansion (in./in./°F)	5.24×10^{-5}	45×10^{-6}	40×10^{-6}	6×10^{-6}
Poisson's ratio*	0.499	0.499	0.499	0.27
Modulus (psi)	150	130	1,600	30×10^{6}
Pressure				
Modulus (psi)	1,000	130	1,600	30×10^{6}
Poisson's ratio*	0.499	0.499	0.499	0.27

*Poisson's ratio is near or at 0.5 but a value of 0.499 decreases computer running time significantly without serious effect on the results.

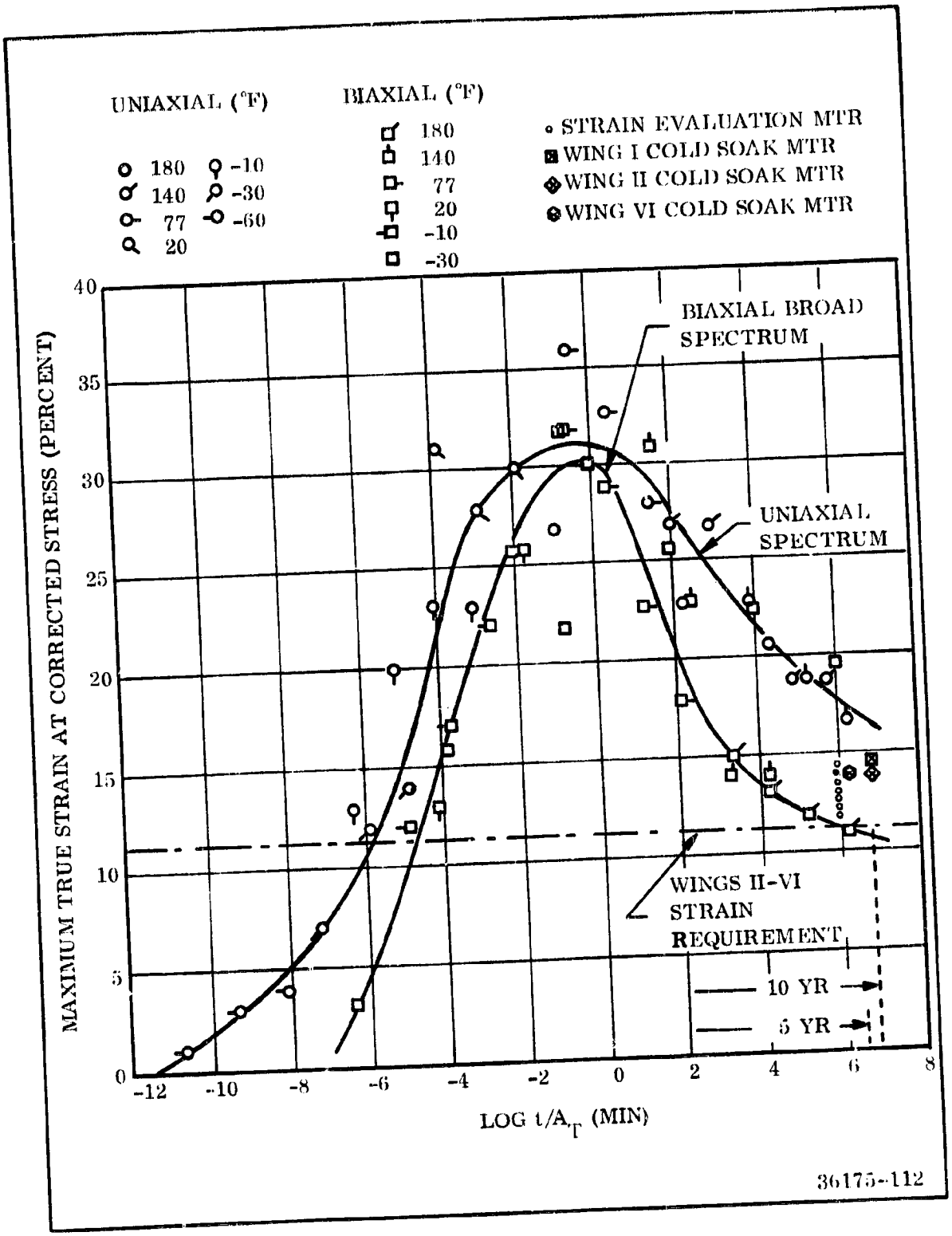

Figure 3-17. Propellant Capability Data

strain capability. Pressure strain capability is near the apex of the curve. The primary loading condition can be assessed accurately by current analytical techniques discussed in the next section. Similarly, slump induced strains are also predictable as the viscoelastic materials are behaving elastically with the equilibrium modulus.

Current grain design structural analysis techniques have been applied to the Space Shuttle grain for the two primary grain loads and vertical slump. Briefly, these techniques involve a finite element stress analysis computer code for axisymmetric bodies. The segment geometry is described to the computer by a grind as shown in Figure 3-18. The input mechanical properties were presented in Table 3-10. The program is not based on viscoelastic theory but rather on elastic theory. Thus, limit values of relaxation modulus are used for input. Superficially, this approach may appear questionable, but the prediction accuracy has been verified several times for shrinkage and slump induced strain calculations and the instrumented Stage I Minuteman results verified both bondline stress and bore strain predictions. The pressure induced stresses are not as well verified at present; however, in a steel case grain the bondline is under compression and hence is not very critical. In other words, the grain's incompressible materials compressed against a much stiffer constraining case are not susceptible to failure. The bore strain prediction accuracy was studied in the Poseidon program, and these results indicated conservatism. In other words, using the effective or limit modulus predicts greater strains than measured in experimental motors. Results of the stress analysis conducted for the baseline grain design are shown in Table 3-11. The comparable propellant capability for TP-H1011 propellant, shown along with attendant margins of safety (including safety factor at 1.5), also are shown in Table 3-11. As can be seen, the Space Shuttle grains will be very reliable, the lowest margin of safety is 2.29.

Structurally, the Space Shuttle 156-in. grain will be very reliable. The techniques required to fabricate such grains have been established and demonstrated. The propellant, liner, and insulation used in these grains have been characterized more extensively than any propellant ever used in SRM's. No other propellant has ever been made in the quantities and for as long a time as this propellant. The grain configurations designed for this grain are very amenable to structural analysis. Furthermore, adequacy of the stress analysis techniques required have been demonstrated repeatedly. The use of a proven propellant in conjunction with proven analysis techniques results in the utmost confidence in the predicted reliability of these grains.

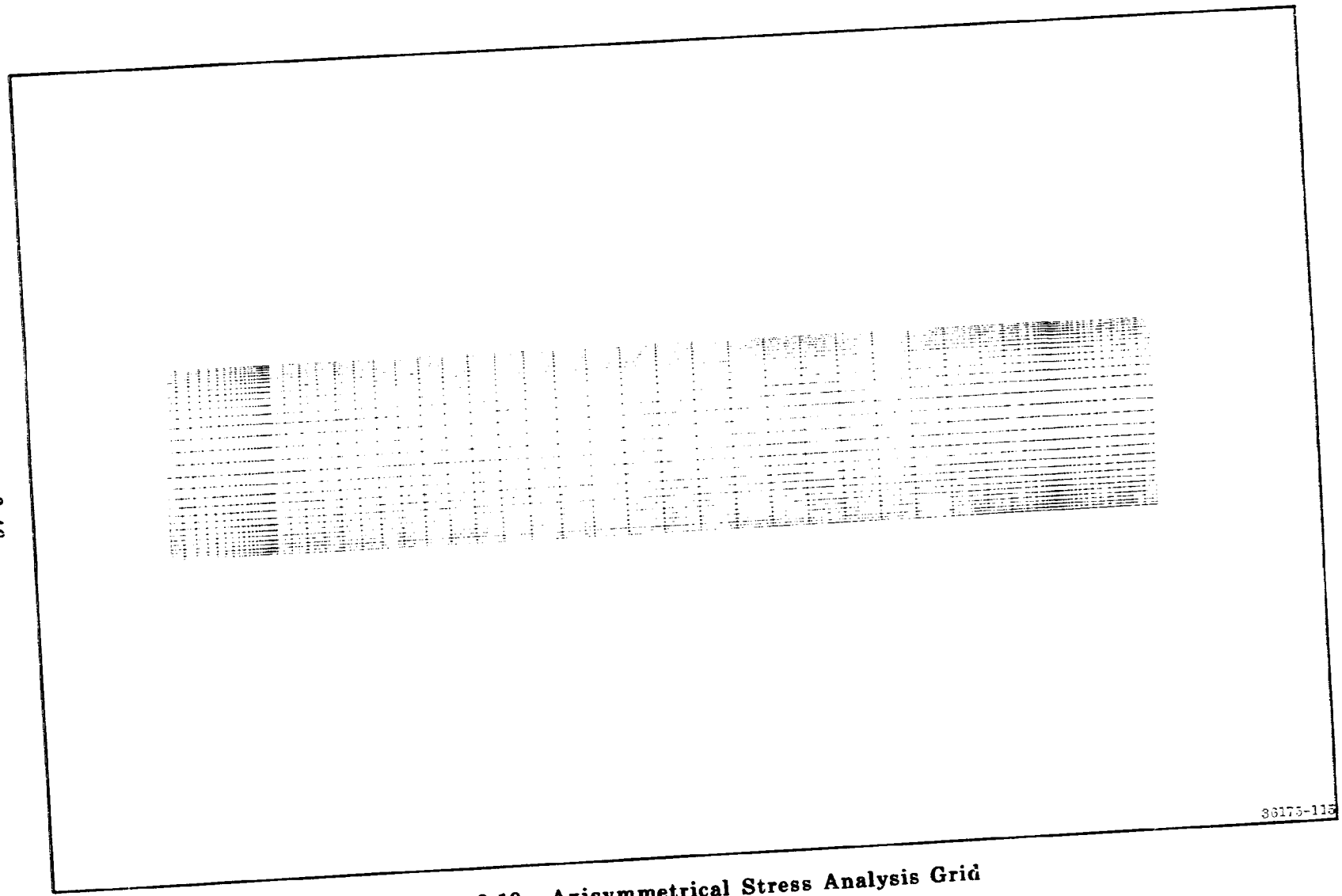

Figure 3-18. Axisymmetrical Stress Analysis Grid

TABLE 3-11

STRESS ANALYSIS RESULTS FOR SPACE SHUTTLE BOOSTER GRAINS WITH COMPARISON TO STAGE I MINUTEMAN AND POSEIDON GRAINS

Load Condition	Space Booster Center Segment	Stage I Minuteman	Stage I Poseidon
Shrinkage to 60°F			
Bore strain (in./in.)	0.033	0.105	0.056
Propellant strain capability (in./in.)*	0.17	0.17	0.17
Least margin of safety**	2.43	0.08	1.02
Shrinkage plus 1 g vertical slump			
Bore strain (in./in.)	0.033	0.113	0.057
Least margin of safety**	2.43	0.0	0.99
Pressure			
Bore strain (in./in.)	0.044	0.100	0.149
Propellant strain capability (in./in.)*	0.38	0.38	0.38
Least margin of safety**	7.6	2.8	1.6
Combined pressure and shrinkage to 60° F			
Bore strain (in./in.)	0.077	0.213	0.213
Propellant strain capability (in./in.)*	0.38	0.38	0.38
Least margin of safety**	2.29	0.19	0.19

*Propellant capability = aged, lower three sigma strain capability

**Margin of safety = $\frac{\text{capability}}{\text{reduced} \times 1.5} - 1$

3.4.2.1.1.2 Plume Characteristics

The Space Shuttle booster motors produce a large exhaust plume. An analysis was performed to determine the size of the booster motor exhaust plume and also provide a description of some of its properties (velocity, temperature). The booster motor operates between sea level conditions up to about 100,000 ft altitude. Analyses were conducted for plume conditions at sea level and 100,000 ft. Also of interest was the exhaust plume from the TT ports at 100,000 ft altitude.

The sea level booster plume was analyzed using an exhaust plume model which includes plume mixing and afterburning in air developed by the Naval Weapons Center (NWC)*. The NWC exhaust plume model along with models developed by Lockheed Propulsion Company and AeroChem Research Laboratories have been evaluated by Thiokol** to determine which model shows the best comparison with test data. The model evaluation work indicated that the NWC model was more accurate than the others. The analysis also indicated means of improving the prediction capability of the NWC model. These improvements have been incorporated into the NWC model at Thiokol. This model is now used to predict the characteristics of low altitude, low speed, and nearly optimum expanded plumes with negligible missile base effects. The Space Shuttle booster motors at sea level fit these conditions.

The results of the sea level Space Shuttle booster motor plume analysis are shown in Figure 3-19. The lines of constant temperature and velocity give a good description of the plume size and physical makeup. The reaction of the exhaust gases with air (afterburning) causes an increase in temperature within the exhaust plume. The afterburning of the exhaust gases and air also causes the plume to be much larger than a nonreacting exhaust plume.

The booster motor plume at 100,000 ft was analyzed using a method of characteristics solution for supersonic flow of an ideal, frozen or equilibrium reacting gas mixture (MOC)***. This type program has been used extensively and has been accepted as the standard means for calculating exhaust plumes at high altitudes where afterburning does not occur. The Space Shuttle booster plume was predicted with the MOC program using an ideal gas solution with equilibrium chemistry. The results of these predictions are shown in Figure 3-20. The plume

*Victor, A. C. and Buecher, R. W., "An Analytical Approach to the Turbulent Mixing of Coaxial Jets," NOTS-TP-4070, Naval Ordnance Test Station, China Lake, California, October 1966.

**Webb, J. K. and Smoot, L. D., "Comparison of Rocket Exhaust Plume Microwave Attenuation Prediction Models," Thiokol Chemical Corporation, to be published.

***"Computer Program for Nozzle and Plume Analysis," Thiokol Chemical Corporation, Program No. S3179, February 1968.

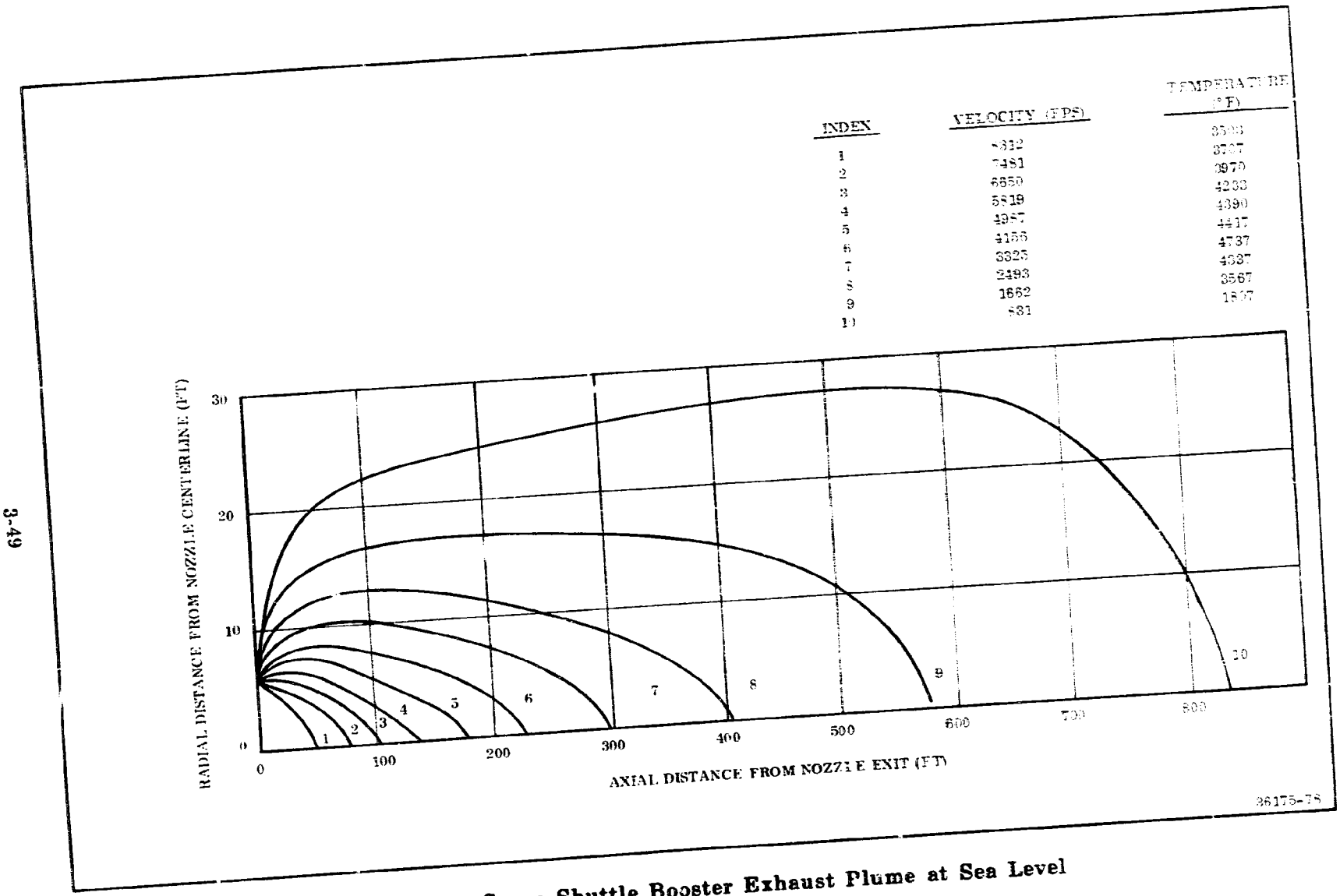

Figure 3-19. Space Shuttle Booster Exhaust Plume at Sea Level

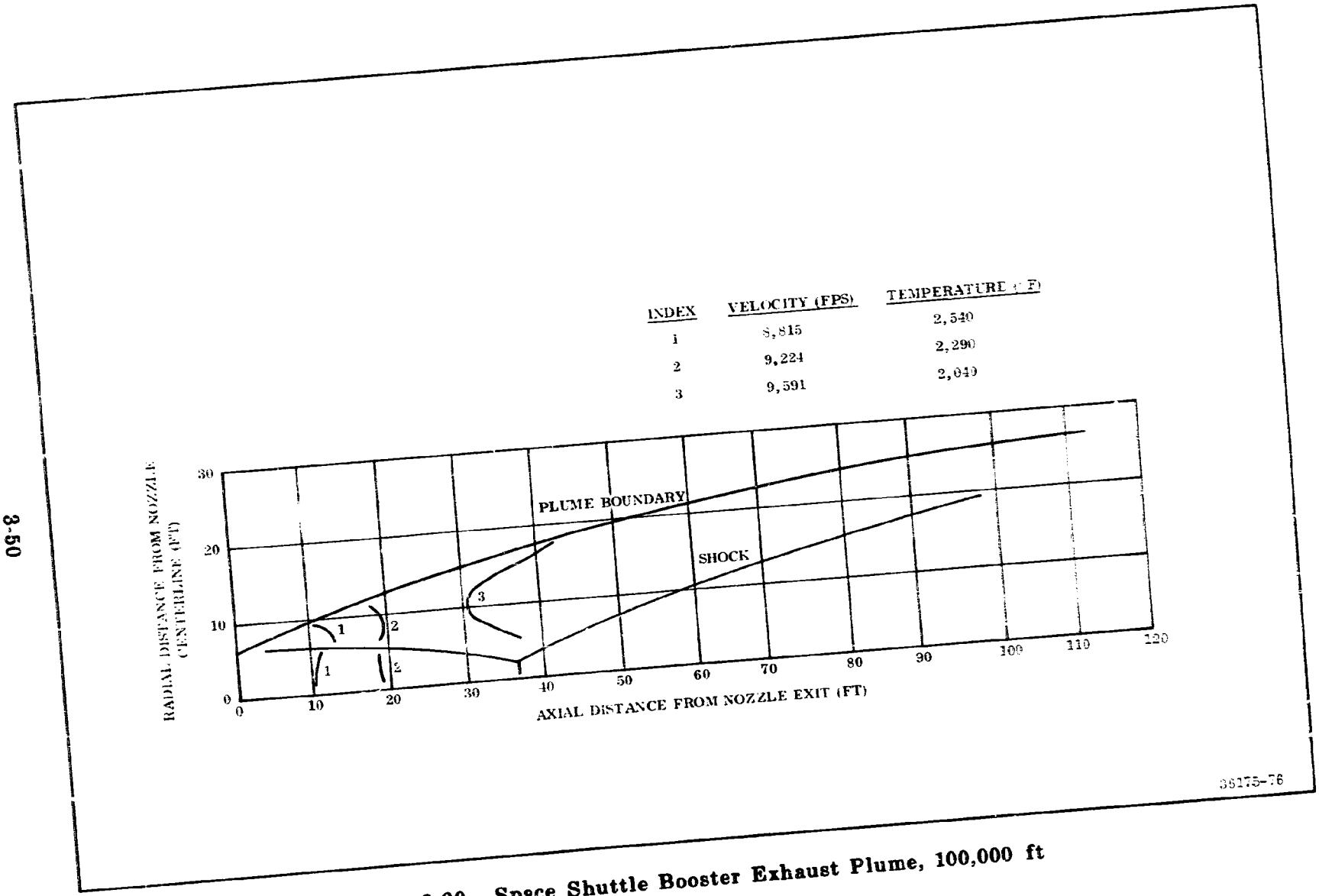

Figure 3-20. Space Shuttle Booster Exhaust Plume, 100,000 ft

boundary, shock structure, and lines of constant temperature also are shown in Figure 3-20.

In comparing the exhaust plumes at sea level and the 100,000 ft condition, the sea level plume is larger. The sea level plume experiences afterburning and a near zero velocity; these conditions tend to produce a large exhaust plume. The 100,000 ft exhaust plume experiences a lower free ambient pressure than the sea level plume, but because of the lack of the afterburning and compression effect resulting from a vehicle Mach number of about 5, the exhaust plume is smaller.

The exhaust plume predictions for the 156 in. parallel motor discussed above can be used to determine the plume properties of the other designs. The methods used to calculate the exhaust plume structure and composition are directly proportional to throat radius. Therefore, to obtain a description of exhaust plumes, the data presented above must be scaled by the ratio of throat radii.

3.4.2.1.2 Propellant

The propellant selected is the Minuteman polybutadiene acrylonitrile (PBAN) propellant. Thiokol/Wasatch has processed 125 million lb of this propellant.

In making this selection, it was considered necessary that the propellant meet the following criteria.

1. Have demonstrated ballistic performance and mechanical properties.
2. Be readily processible in volume quantities.
3. Have adequate sources of raw material supply available at reasonable cost.
4. Exhibit a high degree of reproducibility of both physical and ballistic properties.
5. Have a Class 2 explosive classification.

Experience in the use of propellant based on PBAN polymer has been gained during a period of more than 10 years. This experience has evolved from the production of the Stage I Minuteman, Stage I Poseidon, and 156 and 260-in. development motors. In these applications, it has been demonstrated that propellant reproducibility is excellent and that motor performance can be reliably and accurately predicted utilizing laboratory and subscale motor data.

The past successful history in the use of this basic propellant provides confidence that the SRM booster for the Space Shuttle system can be designed and

and successfully produced without requiring major development. A minor propellant tailoring program, very limited in scope, may be necessary for the purpose of effecting minor adjustments of propellant burning rate. This would primarily consist of determining the optimum particle size distribution of the ammonium perchlorate and/or the required iron oxide percentage.

Because of the success of the Stage I Minuteman and Stage I Poseidon programs, the demonstrated reliability of propellants based on PBAN polymer is extremely high. There have been over 1,000 test firings of motors using PBAN polymer propellant formulations without a propellant failure. While a few of these tests exhibited failures of components other than the propellant system, there has never been any indication of a propellant system failure.

PBAN propellants have excellent demonstrated aging characteristics. These results are based upon both long term carton aging programs and on long term motor aging programs. The most pertinent data have been obtained from the propellants taken from motors as old as 6 years. These data have shown that the propellant mechanical properties do not change after the initial 3 months. In addition, Stage I Minuteman motors have been fired successfully after being stored for over 10 years.

The composition, theoretical thermochemical, and physical properties of this propellant (Thiokol designation TP-H1011) are summarized in Table 3-12.

PBAN propellants have the lowest cost of any presently being used in large motors. The present cost of the PBAN propellant is approximately $0.51/lb.

The processing procedure will consist of casting (under vacuum conditions) propellant directly into the insulated and lined case segments. Upon completion of casting, the vacuum is released and the segments cured for about 96 hr at cure temperature. After cure, the mandrel is removed and the grain is cooled down. The individual segments are then ready for nondestructive testing and final assembly. A more detailed discussion of the manufacturing method is presented in the manufacturing plan.

During casting, propellant sampling will be done at appropriate intervals. Ballistic test samples (5 in. CP motors) and JANNAF standard physical specimens will be prepared from these propellant samples. Testing of these specimens then will characterize the ballistic and physical properties of propellant (and segment).

Alternate Propellant System

Hydroxol Terminated Polybutadiene Polymer (HTPB) is a relatively new but extremely promising material for use in solid propellants. Thiokol has over 2 years of experience in the development, evaluation, and scaleup of these propellants. Mixes as large as 1,500 lb have been made and no problems have been encountered.

TABLE 3-12

PROPELLANT PARAMETERS

Type	PBAN
Thiokol designation	TP-H1011
Composition	
Aluminum (%)	16.0
Ammonium perchlorate (%)	70.0
Binder (%)	14.0
Theoretical thermochemical data (reference conditions)	
Characteristic velocity (fps)	5,186
$C^* - P_c$ exponent	0.0057
Burning rate coefficient exponent	0.35
Expansion ratio	10
Chamber specific heat ratio	1.143
Exit pressure (lb/sq in.)	15.1
Chamber pressure (lb/sq in.)	1,000
P_c temperature sensitivity (π_K/deg)	0.0015
Temperature exponent	0.0248
Density (lb/cu in.)	0.064
Theoretical vacuum specific impulse (sec)	286.2
Chamber temperature (°K)	3,462
Molecular weight of exhaust gas	28.59
Physical properties	
Stress (psi)	95
Strain at maximum stress (%)	31
Modulus (psi)	431
Strain at rupture (%)	39

However, further development is required to qualify HTPB propellants for Space Shuttle application.

Since experience is limited using this propellant system, less confidence exists in its reliability. However, industry experience indicates that high reliability could be expected.

The HTPB polymer does not contain carboxyl cardons; therefore, no hydrogen bonds exist as they do in PBAN to raise propellant viscosity. Therefore, at the same molecular weight, HTPB has a lower viscosity and at the same solids loading, these propellants are easier to process. Thiokol has demonstrated solids loadings as high as 90 percent and these propellants have been scaled up successfully to 150 gal vertical mixers to the 1,500 lb baten size.

Burning rates of 0.3 to 0.8 ips at 1,000 psi have been obtained with 90 percent solids propellants. Higher and lower burning rates could be obtained readily at lower solids loadings. Again, because of the low viscosity of the HTPB polymer burning rate, tailoring is easily performed.

While the aging characteristics of these propellants have not been studied extensively, the results after 1 year indicate excellent aging stability. Additional effort is underway to extend this period of time. An additional advantage of HTPB propellant is that a lower temperature cure can be obtained. This allows a reduction in the thermal shrinkage of the propellant and thereby reduces the thermally induced stress and strain in the propellant grain.

As previously mentioned, Thiokol has over 10 years experience with PBAN propellants and while they have as much experience as anyone in the industry with HTPB this amounts to only over 2 years development experience. No production motor experience is available for HTPB propellants.

Propellants based on PBAN must be considered more reliable than those based on HTPB because of the vast amount of experience and data available. HTPB on the other hand, may prove to be just as reliable when more experience is gained.

It is possible to obtain about 2 percent higher solids loading with HTPB propellants than with the PBAN propellants. It is further significant that the HTPB would have as good or better mechanical properties and equivalent processing characterisities at the higher solids level.

HTPB is more versatile than PBAN because of easier processing which allows a wider range of particle size distributions and because of the inherently lower burning rate of the HTPB propellants system.

PBAN propellants have demonstrated excellent long term aging characteristics. HTPB may prove to age equally as well but comparative data are not available.

HTPB is superior to PBAN in all pertinent characteristics at any given solids loading and has the same mechanical properties at approximately 2 percent higher solids loading.

HTPB, because of its lower viscosity, is easier to process than PBAN. Both propellant systems have been successfully processed at 88 percent total solids and, while they both are slightly pseudoplastic, both can be successfully cast using very large motor techniques.

The current price of PBAN polymer is $1.40/lb while that of R-45M is $0.54/lb. However, the R-45M does not include antioxidant or Aerospace Quality Control standards. Arco Chemical, the producer of R-45M, estimates that at a production rate at 1.8 million lb/year they can supply R-45M containing an antioxidant and with Aerospace Quality Control standards at $0.60/lb at bulk quantities and $0.64/lb at truckload drum quantities. In large production quantities, it is estimated that the comparable price of PBAN could be as low as $0.80/lb.

Although HTPB propellants show promise for future, long range utilization they were not seriously considered by Thiokol for Space Shuttle applications. Considerably more production program experience is required before these propellants can be considered qualified for Space Shuttle use.

3.4.2.1.3 Case

The basic design of the 156 in. diameter Space Shuttle motor case would be essentially unaffected by the type of material ultimately selected for use in the case, however, the fabrication techniques would, of course, be grossly different.

The baseline case consists of a cylindrical tube, closed at the ends with two hemispherical end domes. The entire assembly is subdivided into five sections (segments) for purposes of convenience in transportation and handling. The three center segments are 281.5 in. long and are cylindrical in cross section. The aft and forward segments contain 224 and 154 in. of cylindrical length, respectively, and also include hemispherical end domes with reinforced polar cutouts of the size required to accommodate the nozzle and igniter assemblies, respectively. At the intersection of the domes and cylindrical sections, both fore and aft, thickened tapered sections provide for the attachment of an additional short cylindrical member. The thickened tapered sections are referred to as the Y-rings and the short cylinders as skirts.

The function of the Y-rings is essentially twofold: (1) to provide a convenient means of attaching the skirt without having to weld directly on the pressure dome, and (2) to provide a gradual transition of thickness which tends to minimize discontinuity stress in the area. A somewhat synergistic effect realized from the Y-joint structure is that it also tends to help spread out concentrated loadings induced onto the skirts by such items as point supports and thrust reactions.

This general type of Y-joint design has been utilized in numerous successful rocket motor case programs including the Stage I Minuteman case and previous 156 in. demonstration rograms.

When cutouts are made at the apex of each dome to accommodate the nozzle and igniter, additional material must be placed in the bore of the cutout in order to partially replace the stiffness of the membrane, which is lost, and to provide a mass to which the nozzle or igniter assembly can be attached (in this case bolted). Ideally, the combined stiffness of the reinforcement ring and the added component exactly replaces the stiffness and displacement characteristics of the lost membrane, however, in actual design practice, this condition is never quite obtained and therefore additional bending and shear stresses (discontinuity forces) are induced into the dome. A gradual tapered transition is provided to help attenuate these additional stresses before basic dome thickness is reached.

When TT ports exist, the same discussion applies. In fact, one significant advantage of a hemispherical dome design is the true circular locus of the intersection of a hemispherical dome and a cylinder whose centerline is normal to the dome surface.

The cylindrical skirts have proven to be an efficient way of reacting the thrust and support loads normally encountered in conventional solid propellant rocket motor applications. Each of the individual segments are connected by the use of a clevis type segment joints. This general type of joint has enjoyed extensive usage in past large motor programs. Thiokol has successfully built and tested both 120 and 156 in. diameter cases using the clevis joint concept. Also in preparation for these programs a good deal of bench testing was accomplished in order to demonstrate the basic load carrying ability of the concept. In addition to Thiokol experience, the Titan IIIC strap on motors also have utilized the clevis joint concept on a successful basis.

Two variations of the clevis joint are: the tapered pin and the straight pin. The tapered pin was originally conceived to insure interchangeability between segments, and as an aid in segment-to-segment assembly. The concept was successfully employed in both 120 and 156 in. sizes. In both cases, complete interchangeability between segments at any circumferential orientation was demonstrated. Additional industry experience in the Titan program has served to demonstrate that, through the proper use of good tooling techniques, interchangeability also can be achieved with the straight pin joint along with the cost, weight, and pin retention advantages inherent with the straight pin concept. For these reasons, the straight pin concept was selected for the 156 inch space shuttle case design. A circumferential band type retainer was selected for pin retention.

The functionality of all subcomponent designs employed in the selected case design has been amply demonstrated in previous large case programs.

The following requirements were established for the design of the 156 in. diameter case.

1. All associated components: case wall, clevis joint, dome wall, dome reinforcement area, etc, are to have a minimum safety factor of 1.4. The safety factor is defined as the predicted stress limit (maximum expected) loading, divided into the minimum ultimate strength capability of the component involved.

2. The assembly shall be capable of undergoing a preliminary hydrotest of MEOP (1,000 psig) plus 20 percent or 1,200 psig without gross yielding or excessive permanent deformation in any component.

3. The assembly shall be capable of repeated reuse (recycle) for 10 firings and associated 120 percent hydrotests without any behavior in violation of item 2 above.

4. The assembly must be capable of withstanding the rigors of ocean recovery with its associated high velocity impact,

penetration and support loading. At this time, exact recovery environments and requirements are to be determined, however typical requirements would be:

- 100 fps impact
- 66 ft total submergence (nose tip)
- 20 psi max saddle pressure on secondary entry

5. The assembly must be capable of accepting a salt water environment for a reasonable period of immersion, without any deleterious effects on the functionality of the case.

In addition to the above listed requirements certain additional requirements also are imposed for convenience and cost considerations.

1. The assembly must be capable of being statically fired in a horizontal attitude while supported only at the skirt ends.

2. The individual segments must be capable of 50 psi Pneuma-Grip pressure over a 10 ft length while being held circular at the ends by a spider arrangement.

The fabrication technique to be employed for the case is highly dependent upon the material from which the case is being fabricated. The basic D6AC material will be vacuum arc remelted and made into ring rolled forgings for spinning of the center segments and into hot or cold forgings for the dome segments.

Present spinning and heat treatment facilities require that the maximum segment length be limited to 160 in. This, of course, means that center segment must be further divided with an additional joint. The assumption is made, that if it should prove to be economically advantageous, both spinning and heat treating facilities and capabilities will be developed to handle a full segment of 281.5 in.

The spun D6AC segment would be heat treated and then the clevis joint configuration machined into the end of each segment. This machine-after-heat-treat procedure is required to obtain the close tolerances required for the clevis joint. Prior to final machining, the entire assembly must be subjected to rigorous nondestructive inspection in order to preclude the existence of critical flaws.

The end segments will be rough machined to contour and then heat treated. Final cleanup machining including the clevis joint and dome reinforcement will be done at this time. TT ports will be contour machined with most of the cutting required in the heat treated condition.

About the only alternative to this procedure would be the inclusion of one circumferential weld at the midpoint of each center segment prior to heat treat. This would preclude the requirement to spin longer cylinders than presently available (160 in.) but would require a welding operation with its associated X-ray inspection requirements.

The basic component thickness for the D6AC motor has been sized consistent with the appropriate pressures and design requirements. At this point, no detailed structural analysis will be presented and would in fact be superfluous since exact design conditions such as prelaunch, launch and flight conditions are yet to be identified. The predicted MEOP may also change as final design perturbations are made.

At the appropriate time in the program, detailed studies will be conducted to make meaningful predictions concerning the state of stress of each area of the case. Of particular interest will be:

1. The action of the clevis joint in various tolerance conditions.

2. The discontinuities that surround the various dome reinforcements such as the polar bosses and the TT ports.

3. The effect of various loading conditions on the clevis joint.

4. The effect of rather concentrated loading on the forward and aft thrust skirts.

Thiokol has a full complement of structural analysis techniques programed on the electronic computer for optimum usage. These programs include both 2D axisymmetric and fully 3D finite element programs, as well as many standard ring and frame and axisymmetric discontinuity analyses. Both elastic and plastic behavior can be analyzed in many programs.

The accuracy and efficiency of these techniques have been fully demonstrated in previous successful case programs.

Solid rocket motor case materials are, generally, evaluated and selected to prescribe cost/performance criteria. Technical requirements peculiar to the mission must be satisfied in total.

This section of the report summarizes the considerations and results leading to selection of D6AC steel for the baseline case. The dependent parameters considered are listed in order of their importance.

1. Cost Credibility -- Large case production experience and substantiated vendor quotes will provide maximum credibility.

2. Reliability and Manrating -- By the development of appropriate failure criteria, safety factors, proof testing, verification testing, and quality control criteria, adequate reliability can be predicted for all materials considered. Some materials, though, will be inherently more satisfying for this application.

3. Satisfaction of Design Requirements -- Since many SRM design requirements will be flexible prior to a more final or detailed definition of the system, the choice of case materials must not constrain the flexibility of SRM stage design.

4. Low Cost -- The relative evaluation of the impact of material selection on case cost will include the impact of the differential case weights and fabrication constraints on the motor and/or stage cost.

The following materials are considered candidates for large segmented solid rocket motor cases.

1. 18 Percent Ni Maraging - 250 Grade (vacuum melted) -- This alloy has been used extensively in aerospace applications which include in the air-melt variation, pressure vessels for previous 156 in. motors. Its advantages include high toughness for the particular strength level, a relatively simple heat treat, and highly predictable dimensional changes in heat treatment so that most, if not all, machining can be done in the soft condition. Its disadvantages include susceptibility to stress corrosion in salt water environment and susceptibility to pitting corrosion in humid environment.

2. 18 Percent Ni Maraging - 200 Grade (vacuum melted) -- This alloy was used for the successful 260 in. motors. Of higher toughness than the 250 Grade materials, its advantages and disadvantages are as described for the 250 Grade.

3. D6AC (vacuum melted) -- This alloy has had extensive use in aerospace vessels, including the Stage I Minuteman

and the 120 in. Titan IIIC motors. It is a quench and temper material with toughness sensitive to quench rates. The material also may be expected to exhibit stress corrosion sensitivity in salt water.

4. 18 Percent Ni Maraging - 190 Grade (vacuum melted) This slightly lower molybdenum variation of the other 18 percent Ni maraging steels affords somewhat improved toughness using essentially the same technology.

5. HY-180 Candidates (two varieties) - Development of these alloys have been funded by the Naval Ships Systems Command as part of a series of alloys designed to provide high resistance to crack propagation, initially for submarine applications, both varieties are readily fabricated using shipyard practice.

   a. 12 Percent Ni Maraging (double vacuum melted) - This material has been used in 0.75 in. thick test vessels having leak-before-burst capability. Interest in it for submersibles has waned because in those applications it affords insufficient resistance to stress corrosion in salt water. Along with the 18 percent Ni alloys, it would require, in the present application, a highly effective coating system. Its advantages include exceedingly high toughness in the parent metal and weld zones, 100 percent weld efficiency, leak-before-burst capability in the anticipated thickness and a simple postweld heat treat. Its disadvantages include relatively little use to date.

   b. 9 Percent Ni Maraging (vacuum melted) -- This material, a replacement for the 12 percent Ni alloy, is being used for the Navy's Deep Submersible Search Vehicle Prototype. Its advantages include exceedingly high toughness in the parent metal and weld zones (using TIG in small-bead, multipass configuration), 100 percent weld efficiency, leak-before-burst capability in the anticipated thickness, and no postweld heat treat. Its disadvantages include little use to date.

6. HY-140-5NiCrMoV (air melt) -- Another of the Navy's HY series steels, this material has had extensive

use in naval applications and some pressure vessel use as well. Its advantages include exceedingly high toughness in the parent metal and weld metal, affording leak-before-burst capability in the present application, 100 percent weld efficiency, high stress corrosion resistance, low cost, and easy availability to fabrication using shipyard practices.

Only D6AC material satisfied the cost credibility criteria. The Stage I Minuteman and Titan IIIC SRM cases are produced from this material. The only substantiated vendor price quotes (Rohr and Ladish) were for the D6AC material. The D6AC case is considered technically acceptable, particularly with no welds and adequate quality control or inspection. In the final analysis, the required reliability will be established through the development of safety factor or safety margin criteria from extensive materials and component verification testing.

The 200 Grade 18 Ni and the HY materials are attractive based on fracture mechanics and fabrication considerations. Of these, the HY-140 is most attractive technically and should be evaluated in depth prior to final SRM case material selection. The cost credibility of the support study will stand since an HY-140 case will be less costly even when the increase in motor size required to balance the increase in case weight is considered.

Therefore, considering design flexibility through weldability and ease of fabrication; reparability through weldability and leak-before-burst; inherent safety through leak-before-burst, environmental insensitivity, and material use history--HY-140 is the most attractive candidate technically. The 18 Ni (200) and D6AC (200) are acceptable technically also. Of the acceptable materials, only D6AC satisfies the cost credibility criteria and has, therefore, been selected as the baseline case material.

3.4.2.1.4 Internal Case Insulation

The insulation design for the motor is state of the art both in material selection and application. The design approach used includes all the standard design considerations such as thermal protection, reliability, weight constraints, and cost. This motor is part of a manrated system. Therefore, the design approach must possess proven reliability with an extra margin of safety.

The insulation is an integral part of the propellant grain retention system and must have within its design the ability to relieve stresses incurred in the grain during cure and thermal shrinkage. This capability is provided in the form of stress relief flaps in the forward and aft domes and each end of the cylindrical segments.

The thickness of the insulator is dependent upon the material characteristics (char/erosion rate, thermal conductivity, exposure time and thermal flow environment). In regions of low exposure time, such as the midpoint in each segment, a minimum thickness is required. However, near the segment joints and in the domes, the insulator is relatively thick due to the increased exposure time.

The designation of a manrated system requires the use of an insulator system of proven reliability, which necessitates that the thermal properties and variability of these properties shall be fully characterized.

The mechanics of designing the basic insulator system utilizing these data follow.

1. The maximum predicted thickness of material affected by the thermal/flow environment is calculated by multiplying the maximum predicted erosion/char rate by the exposure time. This is then multiplied by 2 to provide a safety factor.

2. The additional insulator material thickness required to provide thermal protection to the chamber is calculated using a two moving boundary, thermal analysis computer program. Program input includes: the internal chamber environment, insulator material thermal properties, the predicted material affected (erosion/char) rate, the allowable insulator-to-case wall interface temperature, etc. The maximum allowable insulator-to-case wall interface temperature is usually based on case structural integrity and usually is fixed at 250° to 300°F for nonmanrated systems; for this manrated system it was assumed to be 75°F.

The material loss rates used to design this motor are empirical in nature and are based on data from numerous applications of this material in motors of a similar size and with a similar internal environment. All of the data used to design the motor are substantiated by both production and demonstration motor firings.

The detail insulator design is depicted on Figure 3-3 and the critical areas are depicted on Figure 3-21.

The effect of the submerged nozzle on the insulator design is reflected in the low material affected rate experienced at section E-E in Figure 3-21. This is due to a lower gas flow velocity across the insulator than would be experienced with an external nozzle.

The grain stress relief flap thickness was designed to provide thermal protection to restrain the backside temperature rise to well below the autoignition temperature of the propellant.

Asbestos, silica filled NBR is an insulation material which is used as state of the art throughout the industry. This material has been demonstrated in several production programs such as Minuteman, Poseidon, and Titan IIIC SRM.

Material selection was based on consideration of the following factors: (1) compatibility with case and propellant/liner, particularly with respect to processing, (2) chemical and physical stability with respect to motor aging, (3) industry experience and familiarity with fabrication techniques, (4) cost impact of raw materials and fabrications, (5) demonstrated reliability. The material properties of this asbestos, silica filled NBR material are listed in Table 3-13.

The steel case internal surface will be grit blasted and solvent cleaned with MEK prior to installing the insulation. Chemlok 205 primer and 220 adhesive will be applied to the cleaned case and allowed to dry before installing the first ply (sheet) of uncured rubber. Care will be exercised to insure that no air is trapped between the case and the rubber before applying the filler plies which form the insulation configuration. All joints in each ply will be skived, rolled, and stitched to insure maximum contact between pieces and joints in subsequent plies will be offset. Each ply of rubber is thoroughly rolled to insure intimate contact and that all entrapped air is removed before installing the succeeding ply. The last ply of rubber covers the entire insulator including the 6.08 in. thick piece in the center portion of the case segment. This final ply provides a smooth base for propellant bonding. See Figure 3-22 for a typical ply layup of a segment joint.

The 0.18 in. thick propellant stress relief flaps are formed by placing a release material between the last two plies of the insulator to prevent bonding. The lengths of these flaps are shown on the motor layout (Figure 3-5).

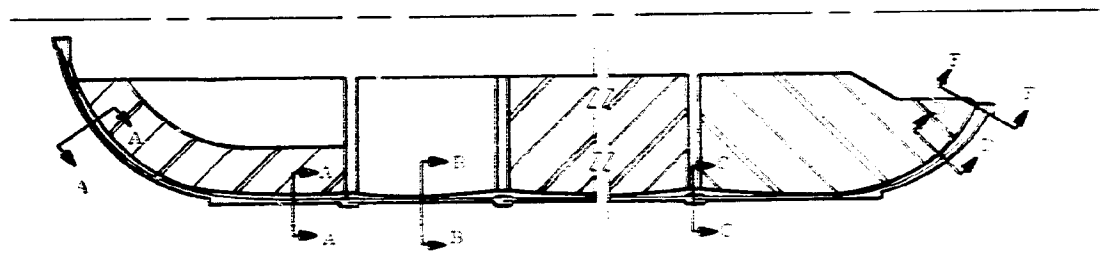

SECTION	EXPOSURE TIME (SEC)	PREDICTED MATERIAL LOSS RATE (MILS/SEC)	PREDICTED MATERIAL LOSS THICKNESS (IN.)	ADD FOR SAFETY FACTOR (IN.)	ADD FOR THERMAL PROTECTION (IN.)	TOTAL THICKNESS (IN.)	[illegible] (IN.)	INSULATION MATERIAL
A-A	.05	8.0	0.017	0.015	[illegible]	[illegible]	[illegible]	[illegible]
B-B	0	0	0	0.125	[illegible]	[illegible]	[illegible]	[illegible]
C-C	193	3.0	0.465	0.139	[illegible]	[illegible]	[illegible]	[illegible]
D-D	90	12.0	0.540	0.162	[illegible]	[illegible]	[illegible]	[illegible]
E-E	156	12.0	0.468	0.140	[illegible]	[illegible]	[illegible]	[illegible]

Figure 3-21. 156 Inch Diameter Motor Insulation

TABLE 3-13

ASBESTOS SILICA FILLED [illegible]
MATERIAL PROPERTIES

Material	Asbestos [illegible] Silica Filled [illegible]
Density (lb/cu ft)	50
Tensile Strength (psi)	1,700
Hardness (Shore A)	80
Thermal Conductivity (Btu/hr-ft-°F)	0.127
Specific Heat (Btu/lb °F)	0.42
Diffusivity (sq ft)	0.0036

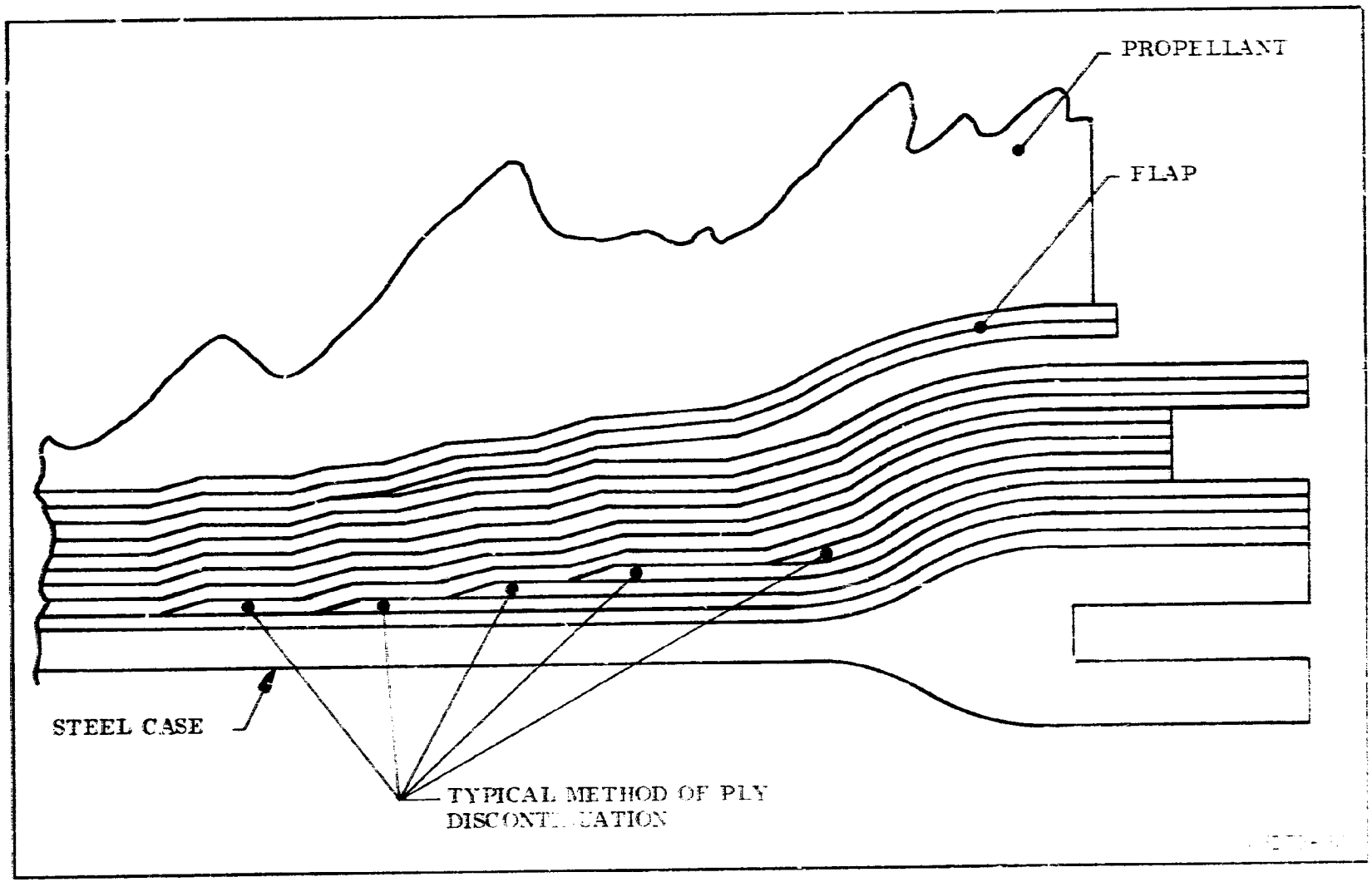

Figure 3-22. Schematic of Typical Insulation Layup

The detail configuration of the insulation which forms the segment joints and polar boss interface is formed during rubber layup by an adjustable tooling fixture. The insulation is vacuum-bagged and the case segment is subjected to an elevated temperature cure in an autoclave. The cure will be at a minimum temperature of 270°F and a pressure of 80 to 100 psia for approximately 4 hr.

The large size of this motor restricts the fabrication of the rubber insulator to either in-case integral fabrication or externally formed insulator segments.

A segmented insulator could be fabricated by a high pressure, closed dye mold process, but this would produce an insulator which is inherently less reliable than a one piece insulator. The fabrication and installation of segmented components involves all the problems inherent to a one piece component plus the additional problems of segment orientation and joint filling. Therefore, this technique was not selected.

Another area of consideration for evaluation is the use of mastic insulation materials which are either castable, trowelable, or sprayable. One such material is TI-II-704B, an asbestos/carbon black/ammonium-phosphate-filled HC polymer (liquid polybutadiene carboxyl terminated) material which was demonstrated in the 260 in. diameter space booster development program. Another candidate material is UF-1140, an asbestos filled epoxy polysulfide, which has been used successfully in heavyweight test motors.

Mastic insulators have been demonstrated in limited application in many types and sizes of SRM's. The initial cost of the raw materials is much lower but the mastic materials have the characteristic of being difficult to process.

The high viscosity characteristic designed into mastics to allow their application without slump creates a problem of air entrapment and porosity. In the past, this problem has created the need for numerous repairs on motors using this type of material. An extensive program would be required to demonstrate the feasibility of this material in a manrated system. This would be relatively expensive and precludes the use of this approach.

3.4.2.1.5 Liner

UF-2121 liner has been demonstrated in the production Stage I Minuteman and Genie motors and in numerous development motors. The extensive use of this liner system for grain retention has enabled the thorough characterization of (1) the processing methods and procedures to be used for its formulation and application and (2) its compatability and bondability with numerous insulation materials and particularly with the asbestos, silica filled NBR material and propellant selected for the baseline motor. All materials used in this formulation are commercially available in the large quantities required.

The UF-2121 liner system has demonstrated excellent physical and thermal properties in both laboratory and full scale motor testing. Laboratory testing of this bond system has shown that the failure is 100 percent cohesive in the propellant. Table 3-14 shows details of material properties data.

The UF-2121 liner has demonstrated excellent aging characteristics in the surveillance program for Stage I Minuteman motors. No storage motor fired to date has shown any performance anomaly attributable to aging. (See Figure 3-23 for Stage I Minuteman firing history.)

The liner is applied to the insulation/propellant interface to a nominal thickness of 0.065 in. by means of sling lining equipment. The insulation, including the stress relief flap, is buffed and solvent cleaned with MEK before installation of the liner.

The design parameters used in selecting the liner system are: (1) state-of-the-art materials and processing approach, (2) material compatability, (3) reliability adequate for a manrated system, and (4) chemical and physical stability sufficient to assure aging capability of the motor.

3.4.2.1.6 Nozzle

The nozzle for the baseline parallel burn SRM is a fixed, submerged, convergent-divergent, state-of-the-art design. Its size, configuration, and materials are typical of those of the 156-7 nozzle successfully demonstrated by static test in 1966 by Thiokol. It is also similar in many respects to numerous other nozzles both large and small which have been successfully designed, fabricated, and tested.

The nozzle is tailored to the performance requirements of the SRM motor while at the same time incorporating all possible features to assure a low cost, highly reliable assembly. Because of its proposed use in a manrated system, higher margins of safety have been applied in design and sizing the ablative materials and structures than are generally used in SRM nozzle design.

TABLE 3-14

MATERIAL PROPERTIES, DC-2424

Pot life, ambient (hr)	3
Stress (psi)	248
Strain (in./in.)	1.46
Density (gm/cm)	0.908
Thermal conductivity $\frac{\text{Btu-ft}}{\text{sq ft-hr-}^\circ\text{F}}$	0.100
Tensile adhesion to TP-H1011 propellant (psi)	106

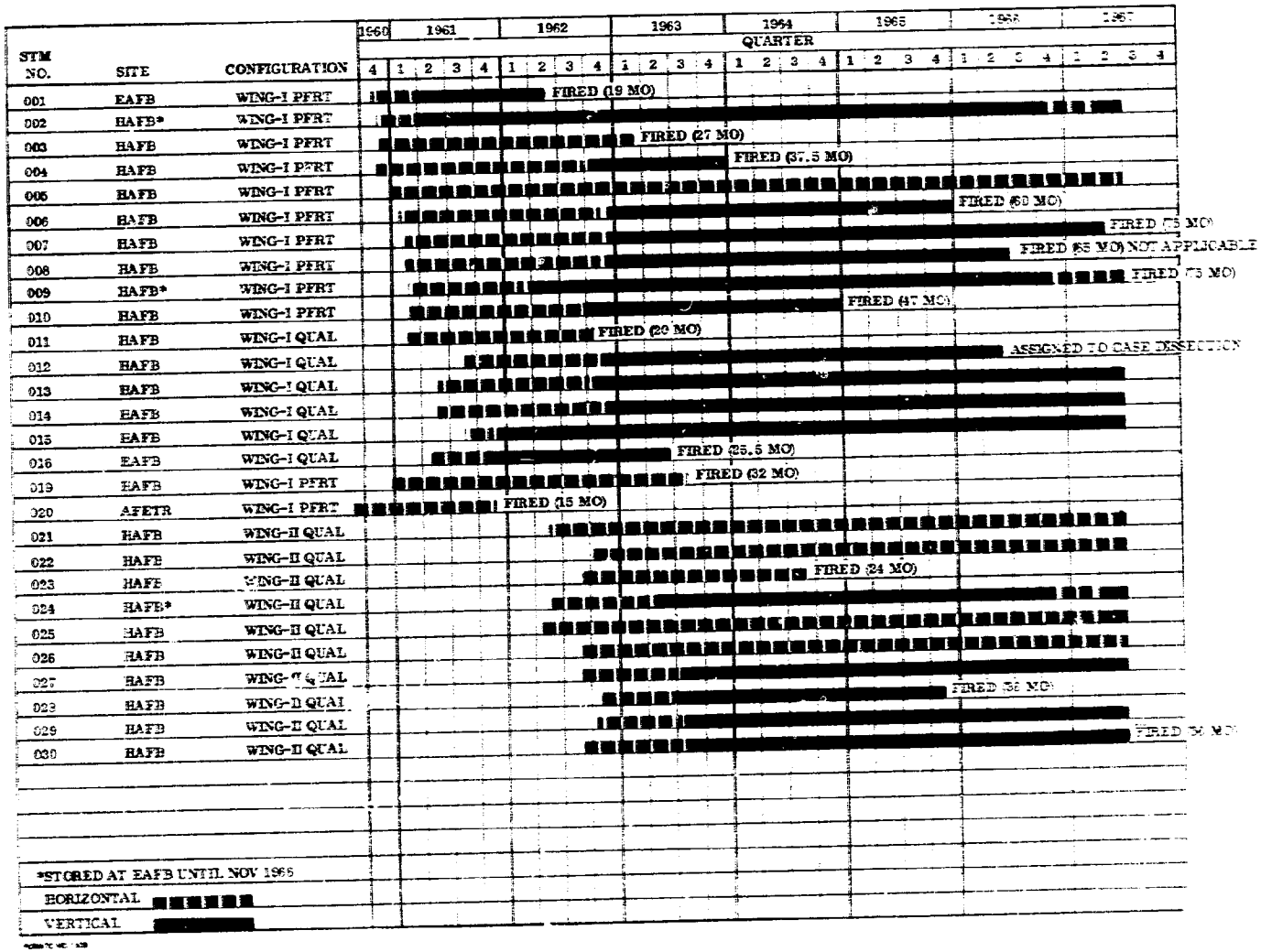

Figure 3-23. Motor Storage History

Flow contours around the nose and into the throat are designed to achieve uniform gas acceleration through the inlet section, thus assuring smooth, uniform erosion. To minimize erosion and tendency to spall and delaminate, the ablative components material plies are edge-oriented to the gas flow rather than ply oriented. This has been proven effective in numerous tests.

The divergent cone has a 17.5 deg half angle and is 165 in. long from throat to exit plane. The required structural and ablative material thicknesses at the exit result in an outer diameter of 150 in., well within the motor diameter.

The exit cone half angle (17.5 deg) is the same as that of the 156-1 and 156-9 nozzles and was selected because of the availability of previous design and fabrication experience and test and performance data from these nozzles.

The exit cone is fabricated as two components. The forward cone is bonded to and contained within the steel structure. The aft cone is assembled and bonded into the flange structure, then pinned and both structure and cone are overlaid with glass cloth gore panels for added joint strength and cone retention. The adhesive and gore strips are redundant safety features since the shear pins are designed to provide full retention.

All components are bonded to each other and to the structure. In addition, components are seated on ramps or entrapped by other components wherever possible to insure positive retention if loss of bond should occur.

Every effort has been made to minimize the number of components and create simplicity of their configurations and of the assembly in order to facilitate ease and economy of fabrication.

The design is shown in Figure 3-24. Criteria employed in the design of the nozzle are listed in Table 3-15.

The ablative and insulative materials selected are materials which have been used consistently in nozzles of all sizes for many years and which have been extensively tested and proven in both R & D and operational SRM systems. Of particular significance is their use and successful performance in the large nozzles of previous 120, 156, and 260 in. motor programs conducted by Thiokol, Lockheed, Aerojet, and UTC. The materials and their physical and thermal properties are well defined as are their ablative and insulative performance characteristics; also, processing and fabrication methods have been developed and standardized to the point that consistency and reproducibility of properties and performance from part to part is assured.

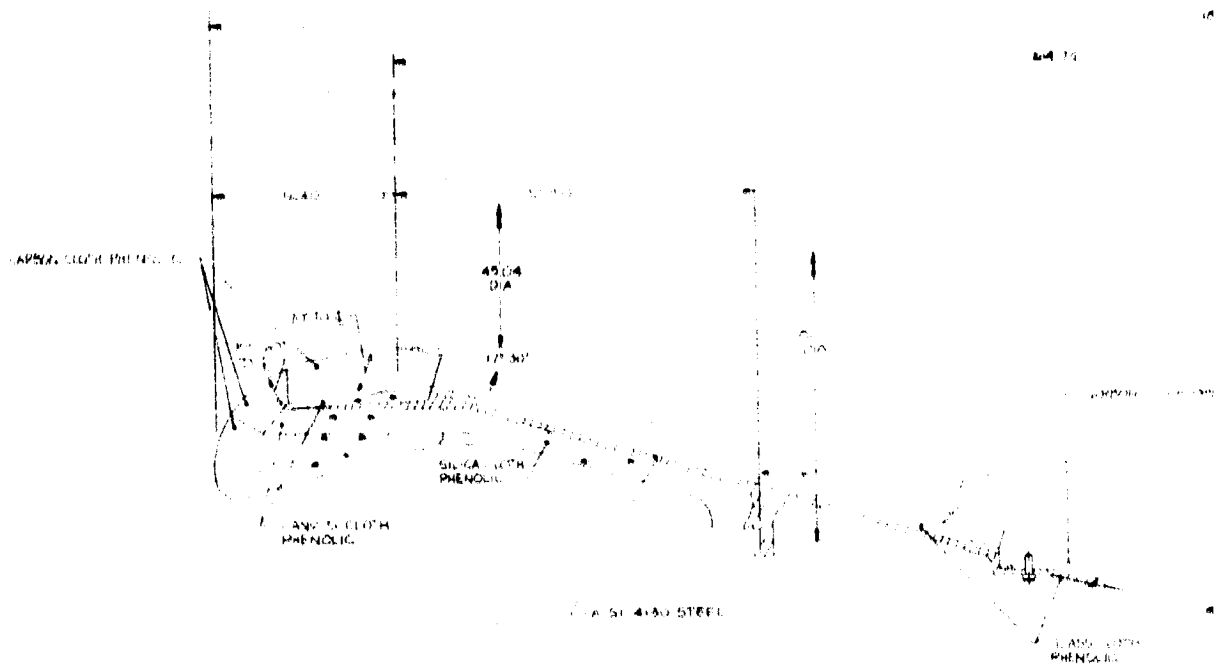
49.04
DIA
SILICA CLOTH
PHENOLIC
CARBON CLOTH
PHENOLIC
A SI 4130 STEEL

Figure 3-21

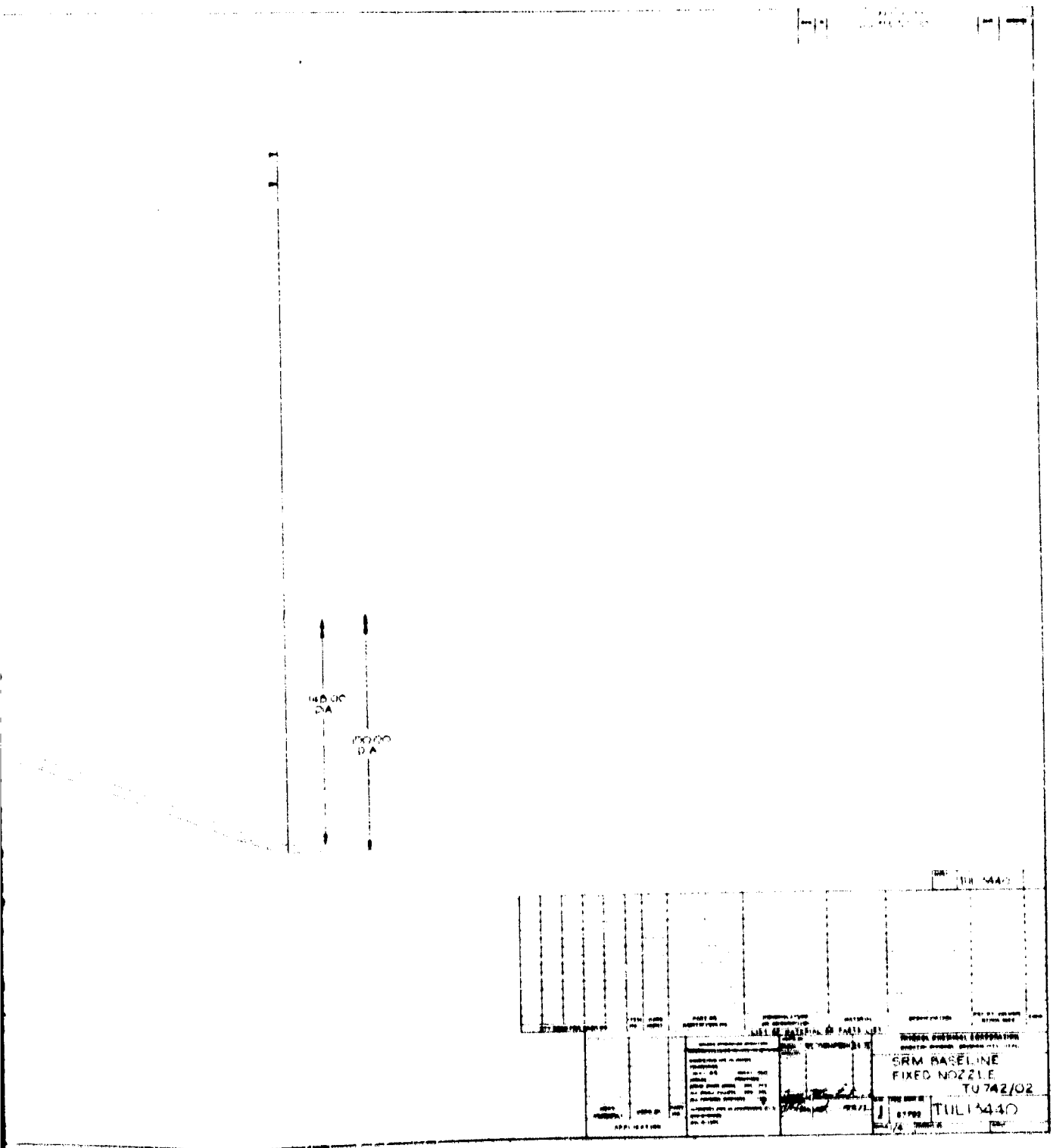

Figure 3-24. SRM Baseline Fixed Nozzle

TABLE 3-15

NOZZLE CHARACTERISTICS DESIGN CRITERIA

Throat diameter, initial (in.)	45.04
Throat area, initial (sq in.)	1,593.26
Exit diameter, initial (in.)	148.6
Exit area, initial (sq in.)	17,295.10
Expansion ratio, initial	10.851
Exit cone half angle (deg)	17.5
Submergence (%)*	19.6
Pressure, average (psia)	830
MEOP (psia)	1,000
Safety factors	
Ablatives	2.0
Structure	1.4
Nozzle weight (lb)	10,149

*Submergence, $\% = \frac{\text{Length, Throat-to-Flange}}{\text{Length, Throat-to-Exit}} \times 100$

Silica cloth phenolic is utilized both as the ablative and insulative liner on the submerged fixed portion of the nozzle and in the aft exit cone section where the thermal environment is relatively mild. Canvas cloth phenolic, a lower cost material, was considered for these areas, but because of its lower resistance to erosion and much higher char rate than silica, considerably more material is required. Finished component costs are then essentially the same for each material while the canvas cloth phenolic component is considerably heavier since densities of the two cured materials are essentially the same.

In the nose, throat and upper exit cone areas, where the thermal environment is severe, carbon cloth phenolic is the selected liner material. This material provides excellent, predictable erosion resistance and has a long history of successful performance in these areas in both large and small nozzles.

Beneath the nose and throat section liners, canvas cloth phenolic is employed as both insulator and filler in order to take advantage of its low cost.

The upper cone insulator and the aft cone overlay are of glass cloth phenolic which provides both thermal protection and structural support to the cone liners. Selection of this material is based on its high strength, low cost, and previous usage.

The structural element of the nozzle is heat treated AISI 4130 steel. This material is relatively inexpensive, readily available and easy to work with from the fabrication standpoint, while providing the necessary strength and stiffness required for the nozzle structure.

The ablative and insulative plastic components will be fabricated by tape wrapping the raw materials on mandrels, the tape being oriented to produce the desired ply angle for each part and then cured at the specified temperature, pressure, and time which will produce the desired properties in the finished part. For the throat section and upper and lower exit cones which are composites of two materials, the inner liner is tape-wrapped and debulked; the outer surface machined, then overwrapped with the second material and the composite cured as a unit. Curing may be done by either hydroclave or autoclave method, both being standard processing techniques and producing essentially the same end result in the finished part. Following curing, the parts are machined to final configuration for assembly into the nozzle structure.

The foregoing fabrication methods are standard in the industry and have been well developed and proven for nozzle plastic components of all sizes. Adequate equipment and facilities exist and the processing techniques are already established for fabrication of plastic components for large booster nozzles.

The nozzle structures will be machined from rolled and welded plate or from a forging. No unique processes or equipment are required or need to be developed.

Final assembly of the nozzle involves bonding of the various plastic components into position, installing the exit cone retention pins and overwrapping and curing the glass structure at the exit cone joint.

To arrive at a credible nozzle design, preliminary layouts were prepared and a series of analyses made to establish the final configuration. Nozzle nozzle configuration and inlet contour were obtained from an aerodynamic design computer program developed specifically for nozzles. A flow analysis was performed to verify the flow pattern of the exhaust gases into the throat and to define heat transfer coefficients along the entire flow surface. The heat transfer data were utilized in making a thermal analysis, the results of which defined the required ablative and insulative liner thicknesses and the resultant erosion and char profiles. Actual motor operating parameters and exhaust gas properties were used in the analyses to insure accuracy of the results.

Structural members were sized and designed to withstand pressure loadings under conditions of 1.4 times MEOP. Both stress and deflection were considered in the analysis.

In all cases, the appropriate safety factors, as listed in Table 3-15, have been incorporated to insure design and performance integrity. Excessive margins of safety, however, have been avoided in order to minimize weight and cost.

Erosion and char profiles resulting from the analyses are shown in Figure 3-25. Mass properties of the design are listed in Table 3-16.

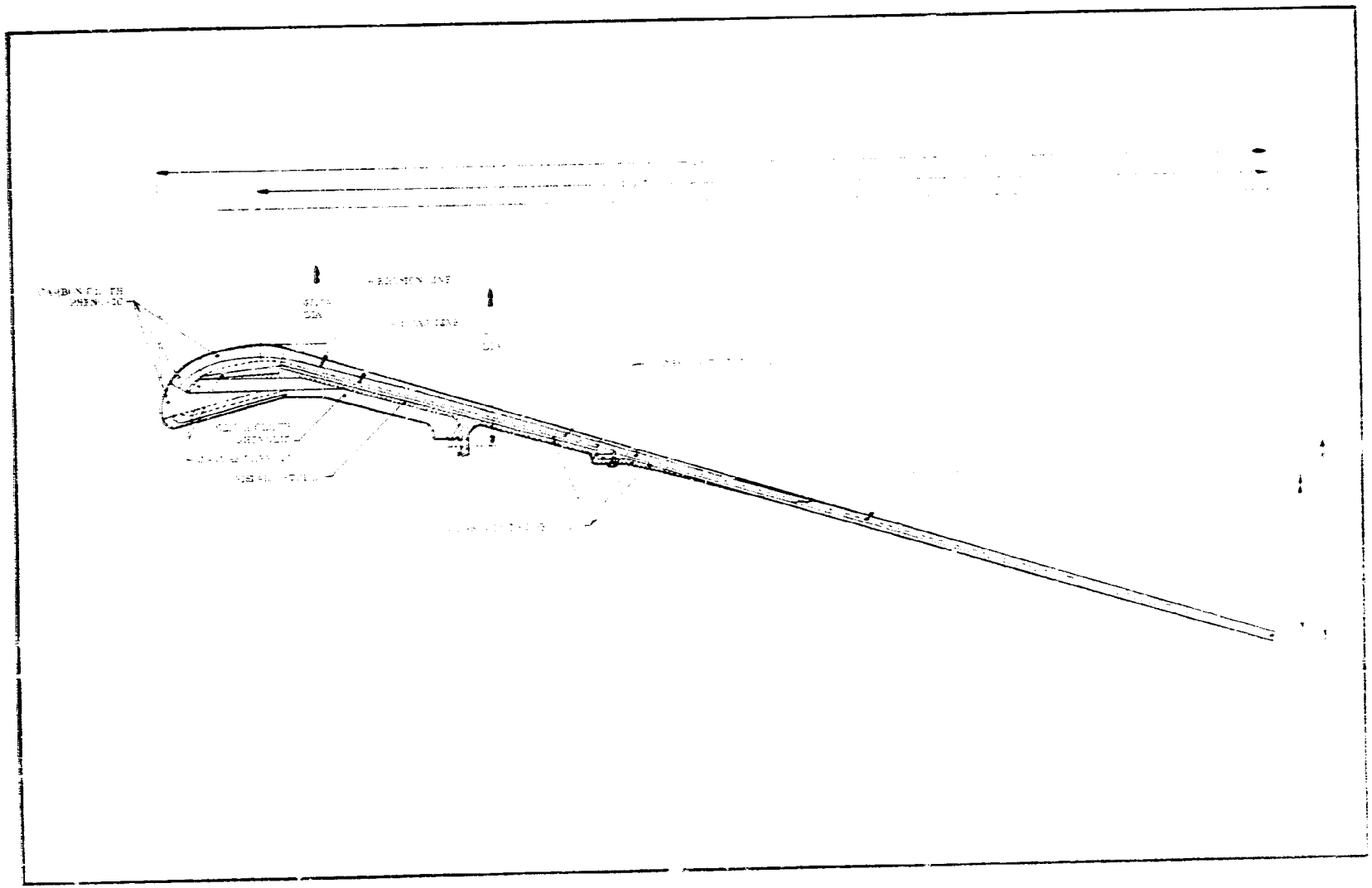

Figure 3-25. Nozzle Erosion and Char Profile, TU-[illegible]

TABLE 3-19

SRM BASELINE FIXED NOZZLE MASS PROPERTIES DATA

	[illegible]	[illegible]	[illegible]	[illegible]	[illegible]	[illegible]	[illegible]
TOTAL NOZZLE--FIXED	10148.593	127.677	[illegible]	[illegible]	1761.745	[illegible]	[illegible]
NOSE CARBON CLOTH	[illegible]	71.15[illegible]	[illegible]	[illegible]	[illegible]	[illegible]	[illegible]
FWD INSERT CARBON CLOTH	[illegible]	[illegible]	[illegible]	[illegible]	[illegible]	[illegible]	[illegible]
THROAT CARBON CLOTH	[illegible]	[illegible]	[illegible]	[illegible]	[illegible]	[illegible]	[illegible]
THROAT LINER--CANVAS CLOTH	[illegible]	[illegible]	[illegible]	[illegible]	[illegible]	[illegible]	[illegible]
BACK LINER-- CANVAS CLOTH	247.[illegible]	95.796	[illegible]	[illegible]	[illegible]	[illegible]	[illegible]
BACK INS.--SILICA CLOTH	[illegible]	[illegible]	[illegible]	[illegible]	[illegible]	[illegible]	[illegible]
STRUCTURE--STEEL	3214.905	[illegible]	[illegible]	[illegible]	[illegible]	[illegible]	[illegible]
EXIT CONE LINER--GLASS	374.430	[illegible]	[illegible]	[illegible]	[illegible]	[illegible]	[illegible]
EXIT CONE CARBON CLOTH--FWD	[illegible]	[illegible]	[illegible]	[illegible]	[illegible]	[illegible]	[illegible]
EXIT CONE CARBON CLOTH--AFT	754.307	148.447	[illegible]	[illegible]	192.402	[illegible]	[illegible]
EXIT CONE GLASS--AFT	[illegible]	[illegible]	[illegible]	[illegible]	541.87[illegible]	[illegible]	[illegible]
EXIT CONE SILICA CLOTH	[illegible]	197.7[illegible]	[illegible]	[illegible]	[illegible]	[illegible]	[illegible]

3.4.2.1.7 Ignition System

The ignition system for the booster rocket motor will be a head-end mounted Pyrogen system (Figures 3-26 and 3-27). The ignition system is similar to those used on other large motors.

The ignition assembly is composed of five main subassemblies: (1) safety and arming device, (2) pyrotechnic booster assembly, (3) initiating Pyrogen igniter, (4) booster Pyrogen igniter, and (5) the igniter cap (adapter).

1. Safety and Arming Device--The igniter safety and arming device will be a modified Minuteman device. The modifications will be primarily the replacement of ES0003 squibs with 1 amp, 1 w squibs and the incorporation of additional circuits in the control connector to allow fire pulse monitor in the SAFE position. This modification will provide a device with the same functional characteristics as the device used on the Titan IIIC and the improved control features of the standardized Minuteman device. These features include switch contacts which are less subject to damage and contamination and a control switch design which does not permit midcycle hangup during marginal control power operation.

   The proposed squib is the S22510 qualified and produced by Hercules Incorporated and is the same design as used in the Titan IIIC device.

2. Pyrotechnic Booster--The pyrotechnic booster provides the ignition train between the safety and arming device and the initiating Pyrogen igniter and will contain 30 grams of 2A boron-potassium nitrate pellets.

3. Initiating Pyrogen Igniter--The initiating Pyrogen igniter has a high strength steel multiport chamber loaded with TP-H1016 propellant in a 30 point star configuration. The initiator system will operate at 1,800 psi (Figure 3-28) and will provide a mass discharge rate of 5.5 lb/sec for 0.14 sec.

4. Booster Pyrogen Igniter--The booster Pyrogen igniter assembly has a high strength steel case, NBR external and internal insulation, UF-2121 liner and TP-H1016 propellant. The grain is cast in a 30 point star configuration. The igniter will operate at 1,500 psia (Figure 3-29)

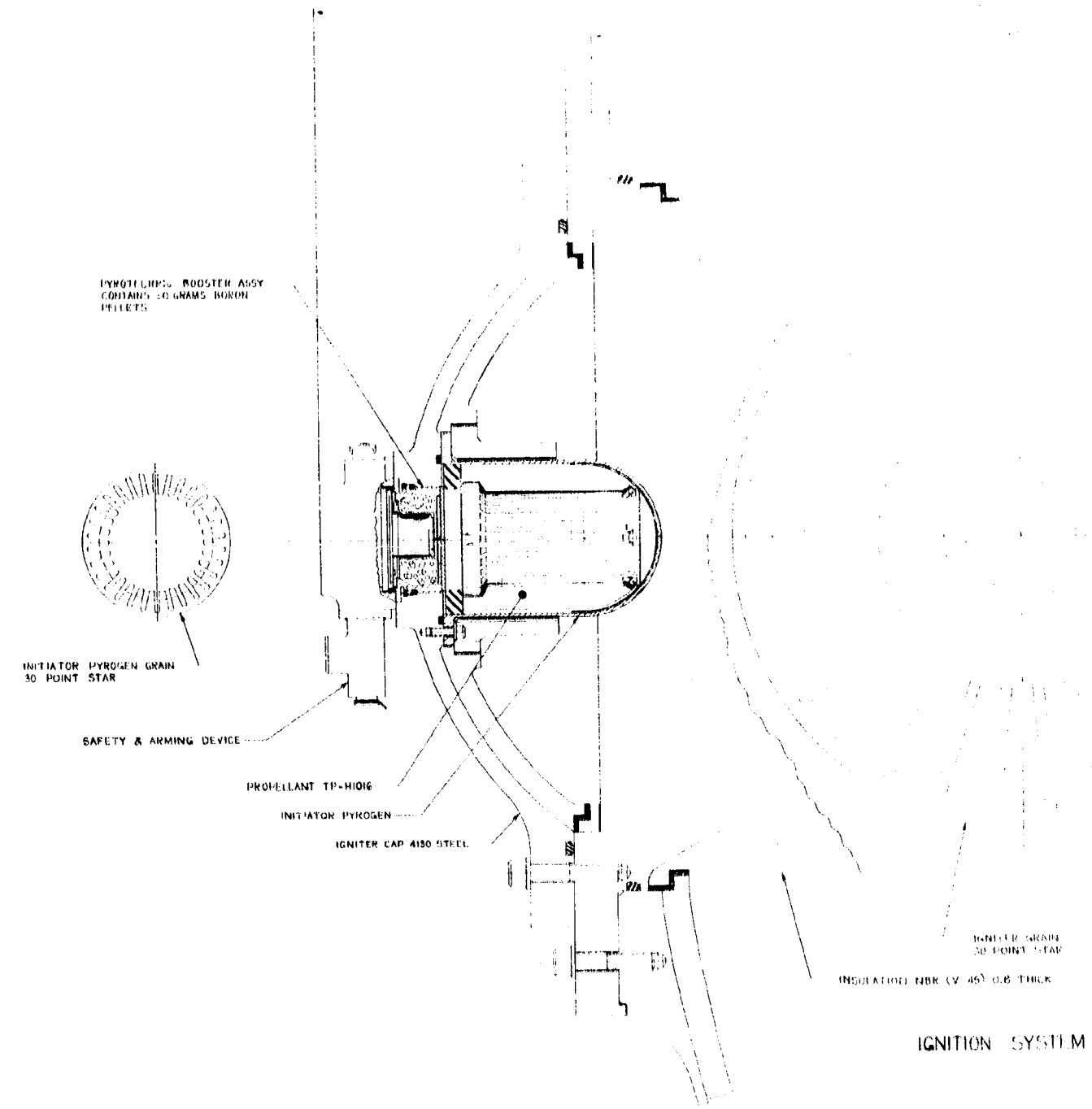

IGNITION SYSTEM

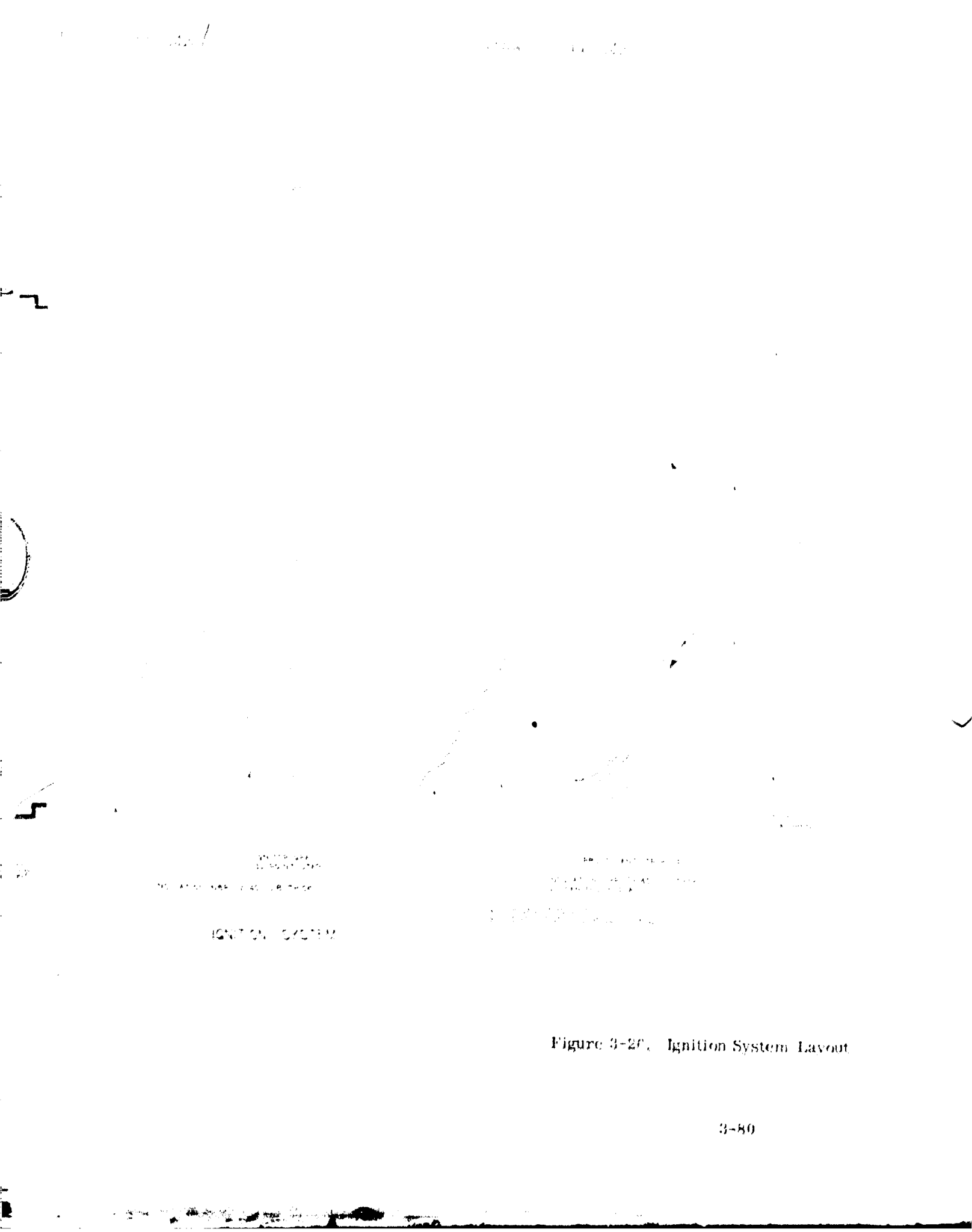

Figure 3-26. Ignition System Layout

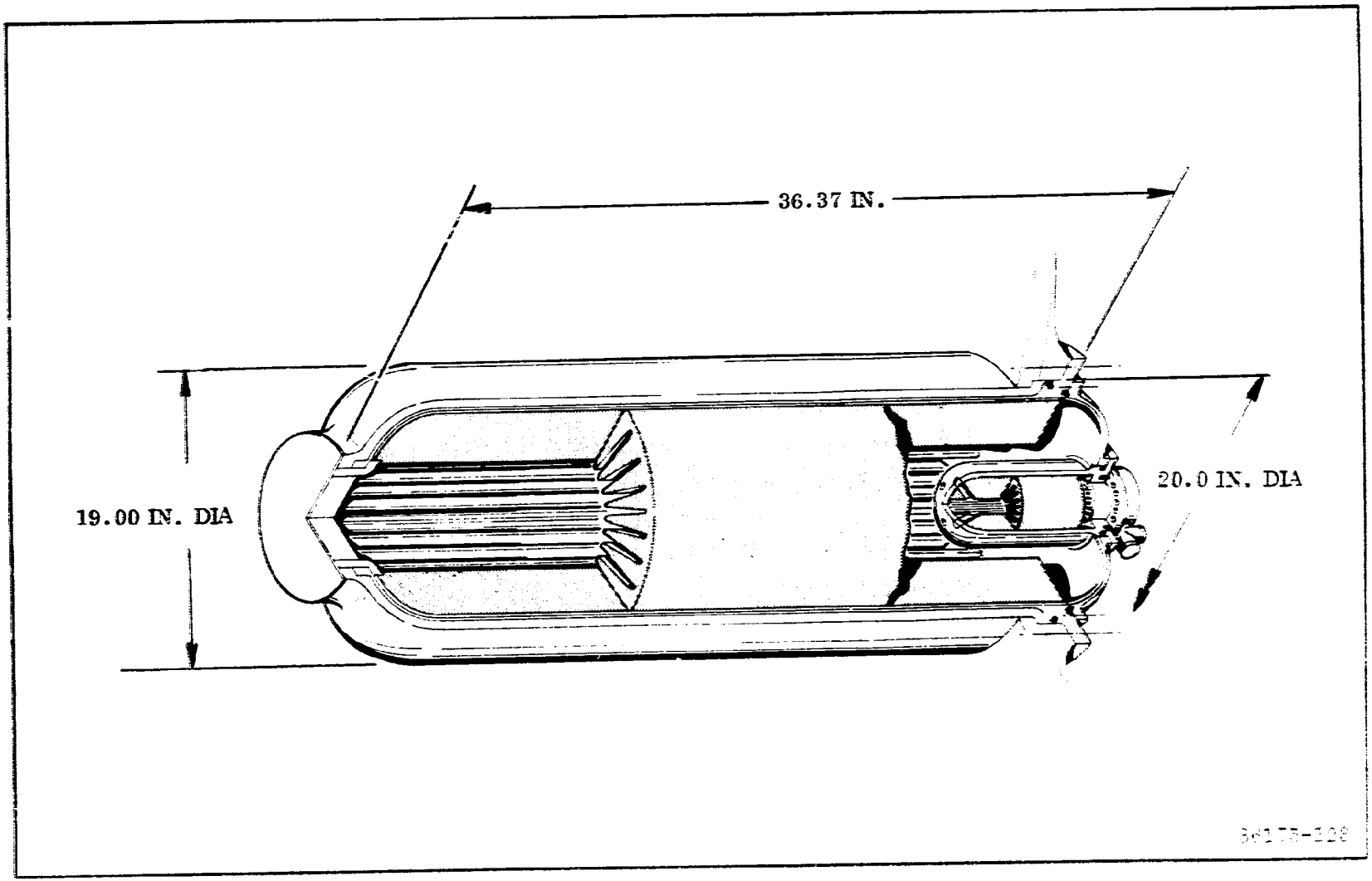

Figure 3-27. Ignition System

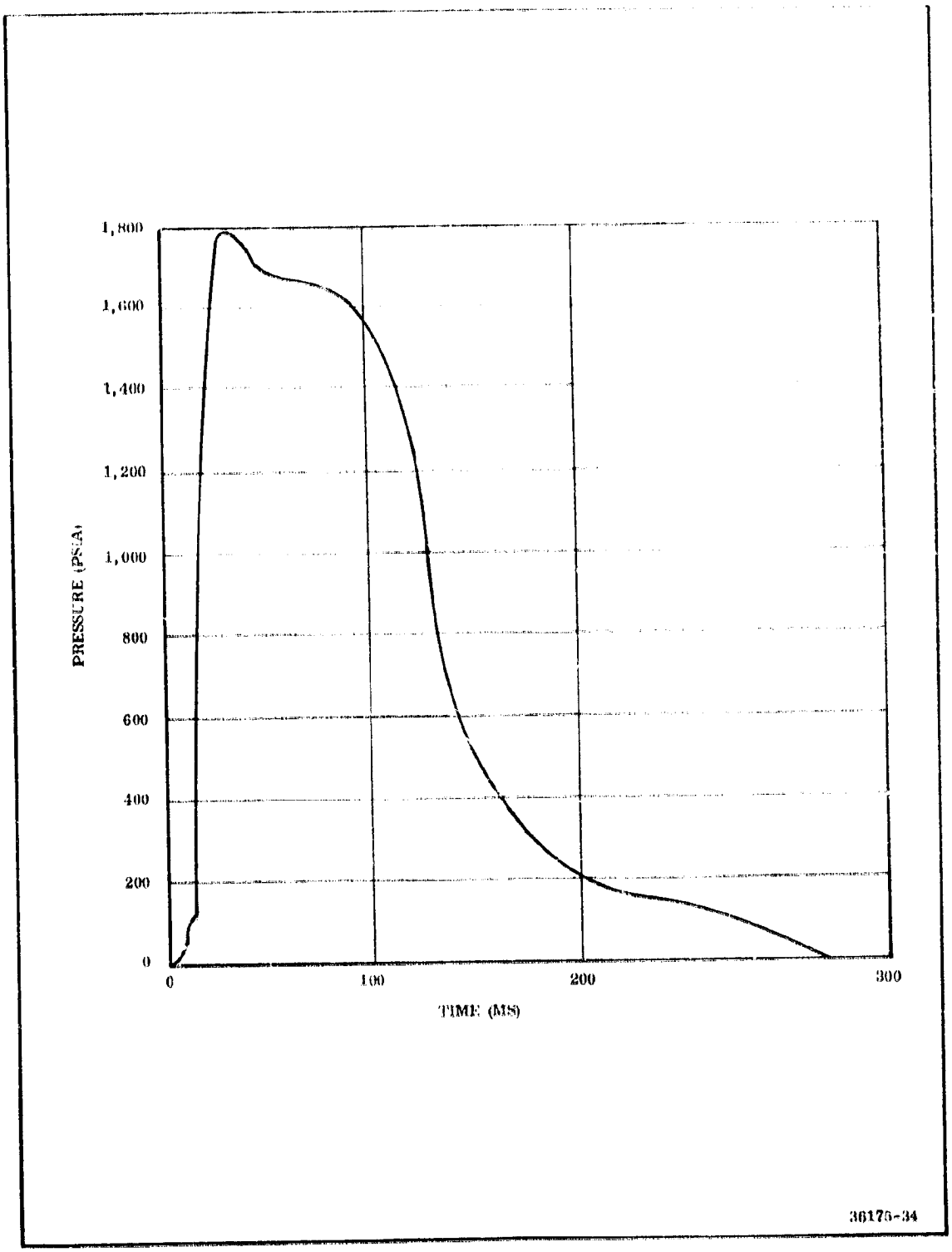

Figure 3-28. Pyrogen Initiator Pressure-Time Trace

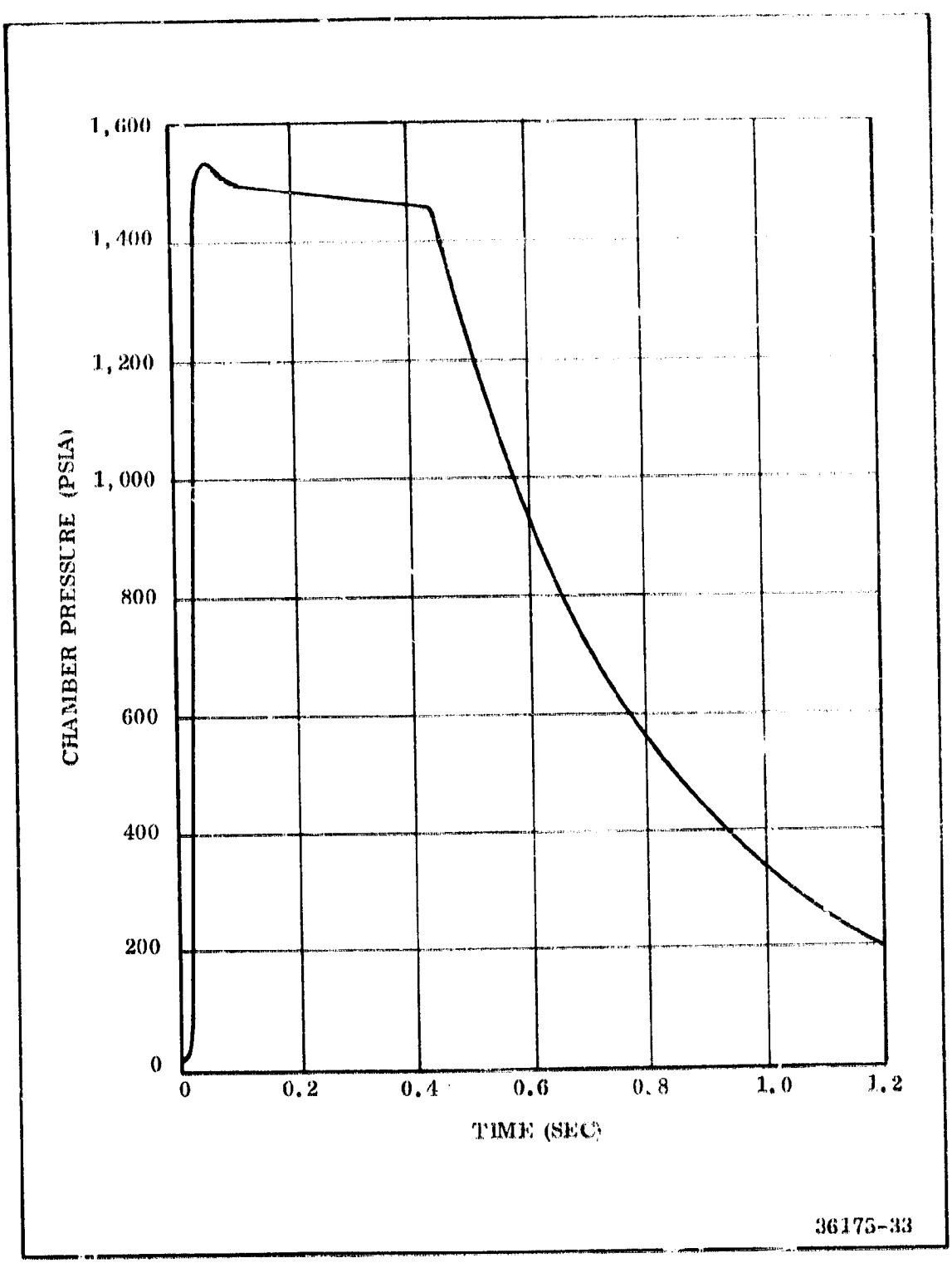

Figure 3-29. Pyrogen Igniter Performance

and will provide a mass discharge rate of 286 lb/sec for approximately 0.6 sec.

5. Igniter Cap (Adapter)--The igniter cap provides for attachment of the initiating Pyrogen igniter, booster Pyrogen igniter, booster assembly and the S & A device into one integral unit. The igniter cap is made of high strength steel.

The desired igniter propellant characteristics are high burning rate at reasonably low pressure, a relatively high flame temperature, good cured physical properties, and a relatively low casting viscosity. To meet these requirements the Stage I Minuteman igniter propellant (TP-H1016) was selected for use in the Pyrogen initiator and the Pyrogen igniter.

Initiator and igniter design performance summary is shown in Table 3-17.

The sequence for motor ignition is: (1) the S & A device is electrically armed and the two squibs are electrically initiated, (2) the flame and pressure created by the squibs ruptures two windows (diaphragms) and ignites the booster assembly, (3) the flame from the booster charge ignites the initiating Pyrogen igniter, and (4) the initiating Pyrogen igniter exhaust gases ignite the booster Pyrogen igniter. The ignition transient of a motor is made up of four relatively distinct time periods which are identified as follows.

1. Igniter response time.

2. Time to achieve motor pressure-igniter output equilibrium prior to motor propellant ignition.

3. Lag time or time between equilibrium pressure achievement and first ignition of motor propellant.

4. Flame spreading time or time from end of lag time until all surfaces of the motor grain have been ignited.

The ignition transient for the large booster baseline motor was predicted. The prediction includes an equilibrium calculation which begins at the end of lag time and ends with achievement of motor equilibrium pressure. The prediction is based on ballistic and physical characteristics of the large booster motor grain, the ignition parameters of the proposed ignition system, estimated time of first ignition, and flame spreading rates over all surfaces of the motor. Motor pressure, thrust, mass flow rate and surface area ignited plus igniter pressure and mass flow rate are computed as functions of time.

TABLE 3-17

IGNITER DESIGN AND PERFORMANCE

Characteristic	Value
Grain diameter (in.)	16.5
Grain design	30 point star
Grain cylindrical volumetric loading	0.653
Cylindrical length (in.)	23.50
Total grain length (in.)	27.07
Propellant weight (lb)	224
Throat area (in.)	29.95
Maximum pressure (psia)	1,490
Weight flow rate at max P_c (lb/sec)	286.3
Burn (0-web burnout) time (sec)	0.448
Time to 95% P_{max} (sec)	0.035
Chamber free volume (cu in.)	2,592
Initiator flow rate (lb/sec)	5.5

The predicted chamber pressure transient for the large booster motor is illustrated in Figure 3-30 . The design parameters and characteristics shown in Table 3-18 were used to size the booster igniter to achieve required motor ignition characteristics.

The electrical initiation redundancy from the power supply to the S & A device is shown in Figure 3-31 . The S & A device also contains its own redundant initiators and firing circuits.

A tradeoff study (cost, function, and reliability) was conducted to evaluate modification of the Minuteman S & A device vs using the qualified Titan IIIC device. The study revealed that modification and requalification of the Minuteman S & A device outweighed the cost disadvantages of the Titan IIIC device.

The modifications of the Minuteman S & A device are primarily the replacement of the ES003 squib with a 1 amp, 1 w squib and the incorporation of additional circuits in the control connector to allow fire pulse monitor in the SAFE position. This device will provide the same functional characteristics as the Titan IIIC device and the improved control features of the standardized device. These features include switch contacts which are less subject to damage and contamination and a control switch design which does not permit mideycle hangup during marginal control power operation.

The proposed squib is the qualified S225D0 as produced by Hercules Incorporated and which is used currently in the Titan IIIC device.

The propellant selection for use in both the initiating and main Pyrogen igniters is TP-H1016. This is the Stage I Minuteman igniter propellant and has been selected because it meets all ballistic requirements, and it is a fully characterized propellant with excellent physical properties, high density, and a high flame temperature.

TP-H1016 propellant has a liquid terpolymer, butadiene-acrylic acid, acrylonitrile (HB) mixed with a liquid epoxy resin for the binder system, iron oxide burning rate catalyst, 2 percent spherical aluminum and ammonium perchlorate oxidizer. The burning rate of TP-H1016 is 0.84 ips at 1,000 psi. The igniter grain design is shown in Figure 3-17 .

The igniter chambers for the initiating and main Pyrogen igniters will be made from 4130 or 4340 high strength steel, spin forged and/or machined and heat treated to 160 ksi minimum tensile strength. This selection is based on a minimum cost and weight analysis.

The main Pyrogen igniter will operate at a chamber pressure of 1,500 psi. A safety factor of 2.0 will be used in design of this chamber. The additional weight incurred by this higher safety factor will be insignificant and is desirable in igniters where it is necessary to obtain a high mass flow rate in a short time interval.

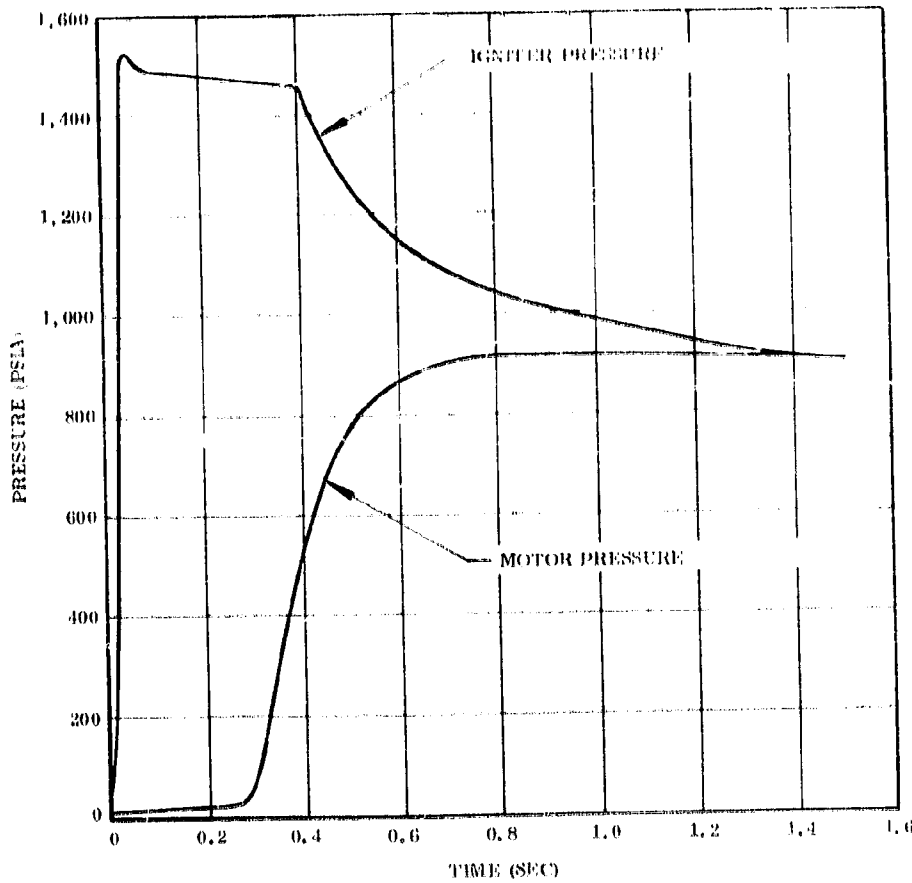

Figure 3-30. Motor Ignition Transient

TABLE 3-18

IGNITER DESIGN PARAMETERS AND CHARACTERISTICS

Characteristic	Value
Igniter coefficient	0.18
Igniter burntime (sec)	0.4–0.5
Port to throat ratio	1.8
Pressure produced by the igniter in the motor (psi)	30
Igniter flame temperature, exit (°K)	2,363
Igniter aluminum content (%)	2
Igniter length to diameter ratio	2.2
Number of nozzles	1
Igniter electric initiator, no-fire power load	1 amp, 1 w

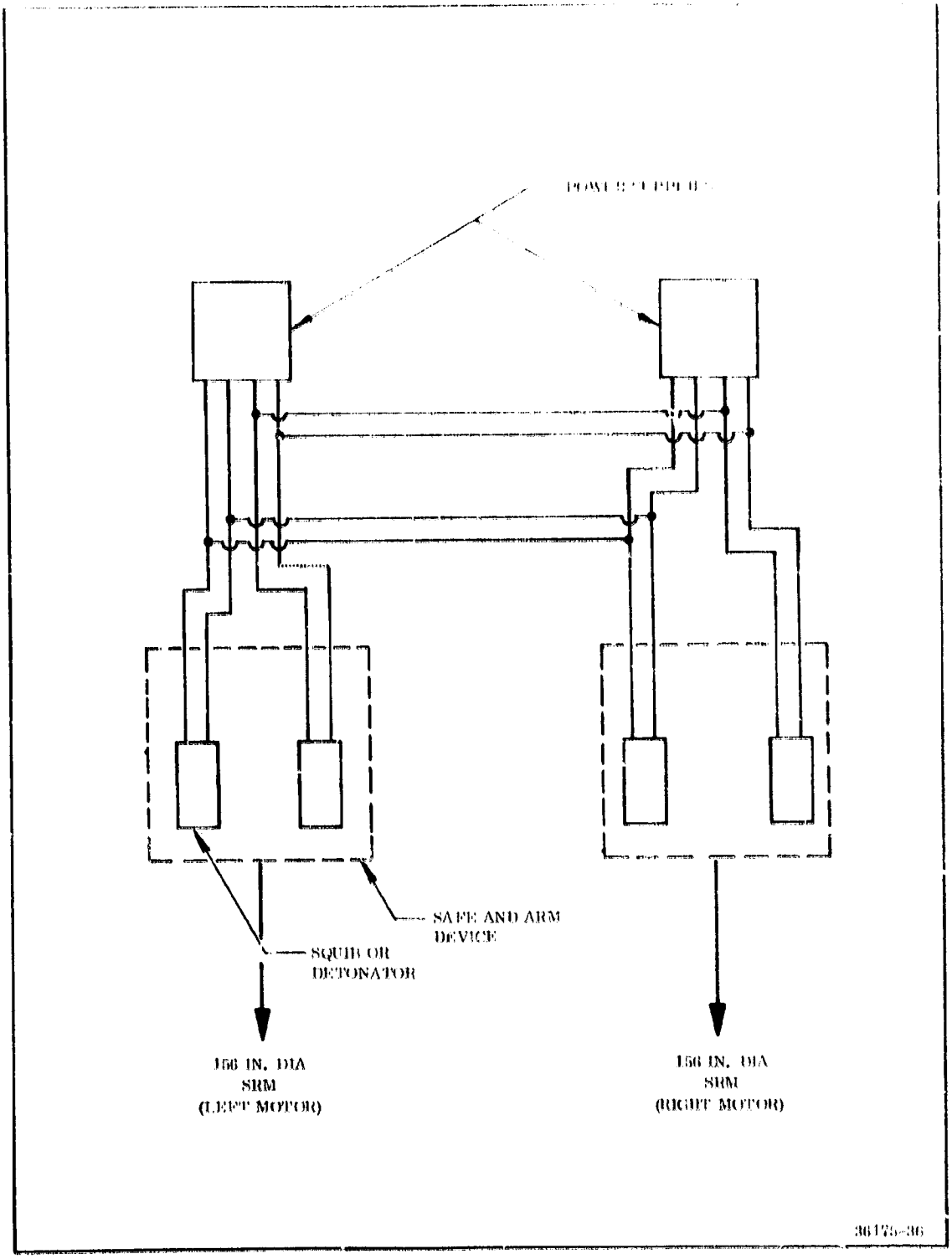

Figure 3-31. Initiation System Ordnance Redundancy for Ignition, Thrust Termination, and Destruct

The steel chamber will be insulated both internally and externally. The external insulation consists of 0.8 in. of asbestos filled NBR laid up and solvent cut in place. Tapering of the insulation will allow controlled burnback consumption of the steel Pyrogen case. The insulation is based on a char rate of 1.1 mils/sec with a 1.5 safety factor.

The internal insulation protects the igniter case from over heating (which could cause external insulation bondline failure if permitted) during both the igniter and motor action times.

The internal and external insulators can be vulcanized in place, thereby eliminating the tolerance problems normally associated with molded rubber parts. The insulation will be a filled NBR rubber.

The procured S & A device will be electrically checked, and a weighed quantity of pyrotechnic pellets will be packed in the container in the device. A foam plastic cushion and perforated cover plate will seal the pellet container.

The steel chamber will be a procured item. The chamber will be brush lined and cured. Plugs in the nozzle orifices will seal the nozzles and act as guides for the casting mandrel. The propellant will be bayonet-cast into the chamber to a preset level and then the mandrel pressed into the uncured propellant. After cure, tooling disassembly, and propellant cutback,the igniter will be ready for use.

The main Pyrogen chamber will be a procured item. It will be hydrotested at the supplier. After receipt, it will be cleaned and insulation applied, vacuum bagged, and cured in a pressurized heated autoclave.

The Pyrogen grain starpoints are wide enough to permit pressure casting of the propellant through the igniter nozzle with the mandrel in place. After the propellant has filled the chamber to a predetermined level, the mandrel is seated into the casting base. After cure, tooling disassembly, core removal, and cutback, the igniter will be ready for use.

A high density foam plastic plug will be bonded into the nozzle of the Pyrogen igniter to provide a moisture seal.

The motor forward closure with initiating Pyrogen igniter and main Pyrogen igniter assembled to it will be assembled to the motor forward segment as a unit. The S & A device will be assembled to the initiation assembly prior to shipment. An igniter S & A device in the SAFE position presents no additional hazard to the system.

Aft-end-mounted Pyrogen ignition systems of the launcher retained variety were considered for this application. They have been demonstrated by Thiokol, Aerojet, and UTC. The largest rocket motors tested to date (156 and 260 in.

diameter motors) have been ignited by launcher retained Pyrogen igniters. Other 120 and 120 in. motors have been ignited by headend Pyrogen igniters. The design parameters for aft end ignition are well known and accepted in the industry. The design parameters for the headend igniters are also well known and well demonstrated for very large motors. The advantages of aft end mounted launcher retained Pyrogen igniters are

1. The inert components of the igniter are not carried with the motor and present a weight savings.

2. The ignition system does not have to be made lightweight heavy materials can be used because the weight is not carried with the motors.

3. A headend igniter port is not required in the motor.

4. A full headend propellant web may be utilized.

The reduced inert component weight and increased propellant weight both result in improved motor performance. When the motor ignites and accelerates away rapidly after ignition, a very simple support for the igniter is all that is required.

In systems such as the Space Shuttle, the launch vehicle will be tied down to the launch structure and will not be released until full thrust is achieved. The igniter cannot be left in the nozzle for this length of time. It would be necessary to provide some sort of retraction mechanism for the ignition system which would withdraw it when a desired motor chamber pressure has been achieved. The cost of ignition system retraction mechanisms would far offset the savings achieved in the use of heavyweight components.

Static tests of large aft end ignited motors are complicated. A support structure, release mechanism and a sled and track are all required to hold the igniter until the motor is ignited and then to remove it from the nozzle after the motor has ignited. Therefore, based on design simplicity of the launch pad and the improved ignition characteristics for the rocket motors, a headend Pyrogen ignition system was selected for the Space Shuttle motors.

A fiberglass igniter chamber has many attractive features and was considered. Internal and external insulators for the igniter would not be required. The igniter chamber could be allowed to burn back throughout the duration of motor burntime. Fiberglass chars in such a way as to protect the internal igniter components from excessive heating. The igniter propellant grain designs require long starpoints and a very thin case propellant web. This requirement dictates that the igniter chamber have at least one end open to the full diameter of the chamber to pass the casting mandrel. Small fiberglass igniter chambers have been designed for small Pyrogen igniters with a full opening on one end achieved by tapering or coning the fiberglass

outward at the open end and sandwiching it between an inner and outer steel ring. This technique cannot be scaled up to the diameter required for the Space Shuttle without making the steel rings excessively heavy and, therefore, precludes the use of fiberglass cases.

3.1.2.1.8 Electrical

The electrical and electronic systems are comprised of two separate categories of equipment and associated cable.

1. Electrical subsystem.
2. Instrumentation subsystem.

The design of the various subsystems will be based on the functional description and the system requirements of each category. In all cases, qualification to manrated flight operation will be a design requirement.

The Space Shuttle SRM electrical system processes and distributes SRM airborne electrical signals, ground power, and blockhouse controls for operating the SRM ignition and instrumentation systems.

Design requirements will be satisfied by using qualified components. The following electrical components make up the electrical subsystem.

1. Instrumentation battery.
2. Power transfer switch.
3. Cable assembly.
4. Instrumentation enclosure.

Wire gages, types, configuration, and capacities will be equal or exceed the required specification. The use of twisted shielded wire and overall cable assembly shielding is consistent with that used on manrated flight qualified systems. Overall design characteristics of the complete assembly will be as good or better than the design specification. The components meet the requirements of the environment as shown as Table 3-18A.

Guidance common circuit isolation and the vehicle single point ground characteristics will be consistent with design criteria. Separate conductors are provided in the cable assemblies for these circuit returns.

The SRM electrical system is required to supply airborne power and provide for distribution of power from both airborne and ground sources to the vehicle monitoring, ordnance, and instrumentation systems. The system also must distribute orbiter command signals and must distribute power supplied by the orbiter for SRM igniter squib ignition.

Monitoring capability for countdown and hold, ground checkout tests, and combined systems tests are required. Additional vehicle electrical system requirements include:

TABLE 3-18A

ENVIRONMENTAL DESIGN REQUIREMENTS

	Transportation and Handling	Vibration	Acceleration	EMI	Temp Altitude	Shock
Instrument battery	X	X			X	X
Power transfer switch		X		X		
Cable assembly		X		X	X	X
Instrument enclosure	X	X	X	X	X	X

1. Distribution of airborne instrumentation signals conditioned to the proper margin levels to the SRM Space Shuttle electrical interface.

2. Distribution and isolation of the redundant ignition current and the provision of current limiting for all ordnance circuits.

3. Provision of switching capability for power transfer from ground to airborne power.

4. Isolation of the guidance common circuit.

5. Compatibility with a vehicle single point ground.

6. Provision and distribution of regulated instrumentation excitation power.

7. Provision for stray voltage detection for the ignition ordnance.

All electrical connections between the SRM and the Space Shuttle are through the forward staging connections. Electrical components are interconnected using independent cable assemblies with one or more connectors on each end.

The SRM instrumentation signals for flight and handline data are conditioned in the instrumentation enclosure. Power for the instrumentation system is provided by the airborne instrumentation battery and conditioned to the proper levels inside the instrumentation enclosure.

Adequate provisions are made in each cable assembly for distributing vehicle monitor power for countdown and hold, ground checkout, and combined systems test monitoring requirements.

The electrical configuration will be investigated to locate the individual worst case circuit (cable run, resistance, gaging) and analyze that circuit to determine the effect of changes in configuration, wire length, and the type of wire.

The layout of the instrumentation system is shown in Figure 3-32.

The SRM instrumentation system supplies vehicle events and conditioned information for performing SRM analyses and evaluation. The systems are divided into two categories: prelaunch system and postlaunch (flight) system. This division distinguishes between parameters monitored prior to launch that no longer require monitoring following launch and the inflight measurement parameters. The prelaunch instrumentation subsystem senses events and conditions within the SRM and supplies an electrical measure of the function through the umbilical to the ground facility for recording. The inflight

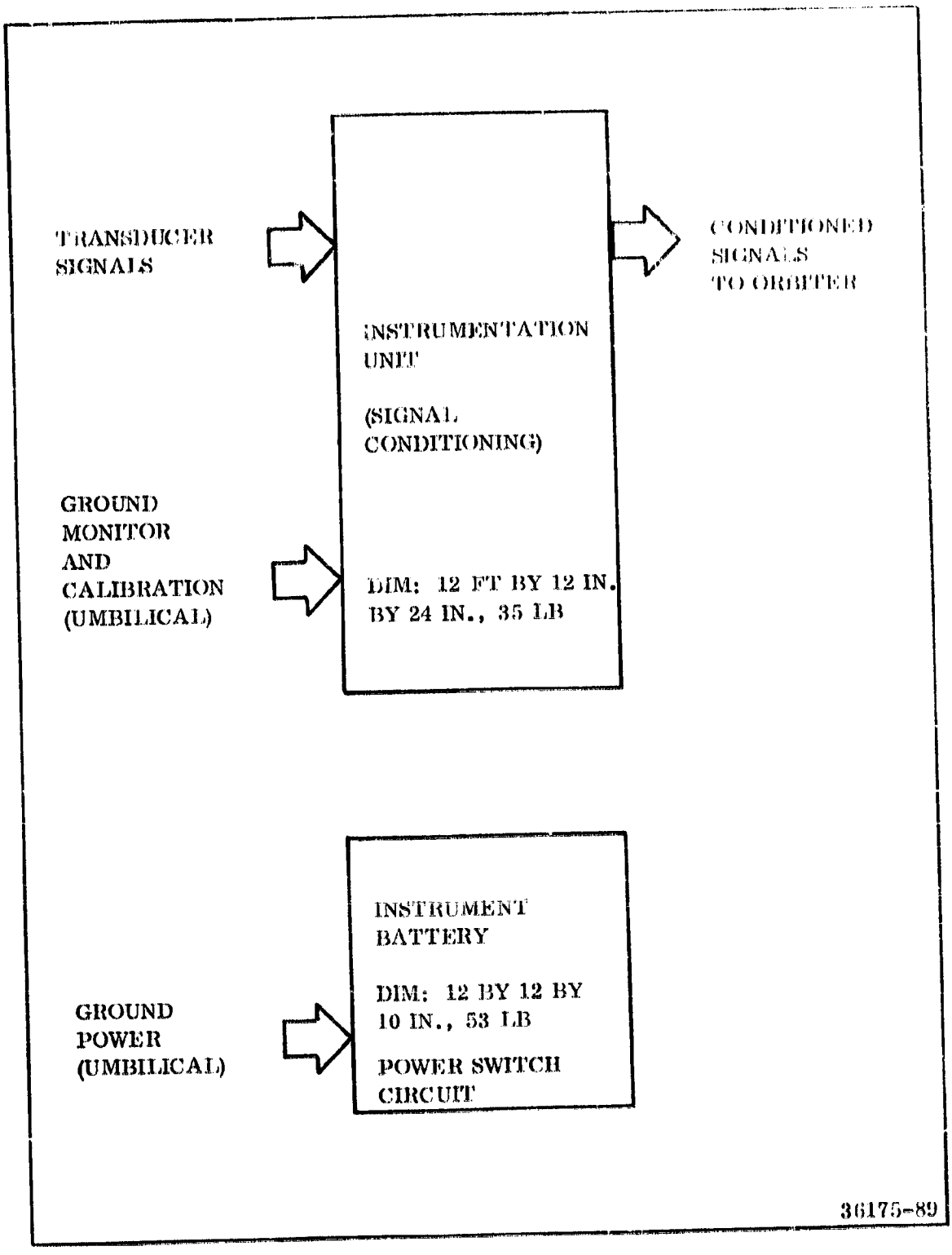

Figure 3-32. Instrumentation System Layout

instrumentation system senses events and conditions within the SRM, conditions these signals and sends them to the orbiter for telemetry to ground facilities.

The SRM instrumentation system provides electrical analog signals of vehicle conditions and events for verifying and evaluating vehicle performance before and during flight. Provisions will be made on each SRM for 108 channels of data.

The recommended flight instrumentation as shown on Table 3-19 is for the one unmanned and the five manned flights.

Proposed configuration and detailed mission requirements dictate the need for customer approval of the proposed measurement list prior to implementation. The inclusion of any item of instrumentation must be designed with a sufficient margin of safety to preclude failure of the flight vehicle due to instrumentation failure. Techniques of high burst pressure ratings, electrical safety resistors, minimization of structural complexity, proper electrical impedance matching and minimization of electromagnetic interference in design will be employed.

The required accuracy of 0.5 percent (three-sigma) relates to the customer needs for accurately defining the vehicle performance. Consequently, this accuracy will be representative of the total stimulus to forward staging disconnect, with traceability to the National Bureau of Standards. A high confidence level of system performance will be obtained to assure compliance with these requirements.

Output impedance at the forward staging disconnects of the instrumentation signals will not exceed 500 ohms or 500 ohms maximum shunted by 0.1 μf capacitance to insure proper coding by the Space Shuttle (PCM) encoder or multiplexer.

The instrumentation will be powered by ground power or an airborne power supply with final switching to the airborne supply approximately 11 sec before launch.

All instrumentation components will survive environments of flight, handling, and transportation, and be compatible with the reactants involved on the total vehicle. Maintenance will be provided for the vehicle single point grounding system with isolation of the guidance common circuitry. System design allows compliance with the hold and turnaround requirements.

The prelaunch instrumentation includes the calibration of instrumentation channels, as well as the monitoring of battery voltage, stray voltage on ignition line and safety and arming indication. Also the operation check of the ground to airborne power switch is a prelaunch function.

The postlaunch instrumentation includes some prelaunch tests on the operation of the nozzle actuation system. This monitoring continues into flight.

TABLE 3-19

RECOMMENDED FLIGHT INSTRUMENTATION LIST

2	Pressure measurements	
2	Radiometer measurements	
2	Calorimeter measurements	
15	Temperature measurements	
15	Acceleration measurements	
1	Thrust termination measurement	(optional)
1	ISDS measurements	(optional)
1	Destruct command measurements	(optional)
1	Staging command measurements	(optional)
2	Nitrogen squib valve monitors	
2	Nitrogen regulation pressures	
2	Monofuel pressures	
2	Decomposition chamber pressures	
2	HPU - starter grain No. 1	
2	HPU - starter grain No. 2	
2	Turbine speed magnetic pickups	
2	28 vdc power bus A	
2	28 vdc power bus B	
4	EDV (pump) monitors	
2	Lube oil temperatures	
2	Hydraulic system pressures	
2	Hydraulic system return	
4	Differential pressures	
8	TVC commands	
8	TVC feedbacks	
4	Failure indicator switches	
8	Arm-disarm signals	
4	Battery initiator monitors	
4	Control box monitors	

therefore,it is classed as postlaunch. Also included in the postlaunch instrumentation are the SRM performance monitor channels, pressure, temperatures, and acceleration.

The instrumentation unit individually conditions each channel of data to be sent to the multiplexer on the orbiter. This conditioning includes bridge balance units, temperature reference ovens, accelerometer amplifiers, and event conditioners.

The battery required for the instrumentation system was selected on the basis of being qualified for manrated flight systems and with the requirement of meeting the onboard flight specifications. The instrumentation battery provides the regulated excitation power and the signal conditioning power for all channels of data throughout the SRM mission.

The subsystem assembly has switching capability from ground power to battery power. Switching circuits to switch from ground power for preliminary and functional checkout to battery power for final checkout, calibration, and flight performance are designed into the subsystem using flight qualified electronic and electromechanical components for reliability of performance.

The design of the cables for the distribution of the power uses wires of a sufficient size to carry the intended current without an appreciable line loss of power in the cables. All cables terminate in flight qualified electrical connectors. The cables are shielded against any electromagnetic interference (EMI). The control leads and the instrumentation leads are fabricated in separate cables to minimize inductive pickup between leads.

The packaging and mounting of the subsystems take into consideration the environmental conditions to which the systems will be subjected. The cases have a watertight seal with hermetically sealed electrical connectors. The battery and electronic circuits are shock mounted to impede the inherent shock and vibration of the SRM assembly through liftoff, flight, separation, and ocean splashdown.

The subsystems with the associated cables are capable of continuous operation for checkout and calibration throughout the complete flight mission from either ground power or from the onboard batteries.

3.4.2.2 Additional Design Features

The design features discussed below are presented separately from the baseline design in accordance with the NASA direction to provide visibility as to the effect (primarily on cost) of a TVC and abort system. The TVC system consists of a movable nozzle with a flexible bearing, an actuation system, a hydraulic power unit (HPU), and the associated electronics.

The abort system is comprised of thrust termination ports at the head end of the motor, a malfunction detection system, and an optional motor destruct system. The necessary electronic equipment relative to the stage is also discussed.

Figure 3-33 shows the parallel burn SRM Stage incorporating these additional design features.

3.4.2.2.1 TVC System

The TVC system selected is based upon the use of a flexible bearing to achieve nozzle thrust deflection capability. This system has been successfully tested on 156 in. motors and is currently employed on both stages of the Poseidon weapon system. The flexible bearing is the logical selection, based upon experience and demonstrated capability. Further rationale leading to its selection is presented below.

Numerous studies have been performed over the past few years by Thiokol, Aerojet, Lockheed, and NASA investigating the various types of TVC nozzles that could be readily adapted for use on a large solid propellant booster. These studies considered the following nozzle types:

1. Forward pivoted flexible bearing nozzle
2. Aft pivoted flexible bearing nozzle
3. Hot gas secondary injection TVC (HGTVC) nozzle
4. Liquid injection TVC (LITVC) nozzle
5. Gimbaled nozzle
6. Mechanical interference TVC systems such as:
   a. Jet tabs
   b. Jetavators
   c. Jet vanes

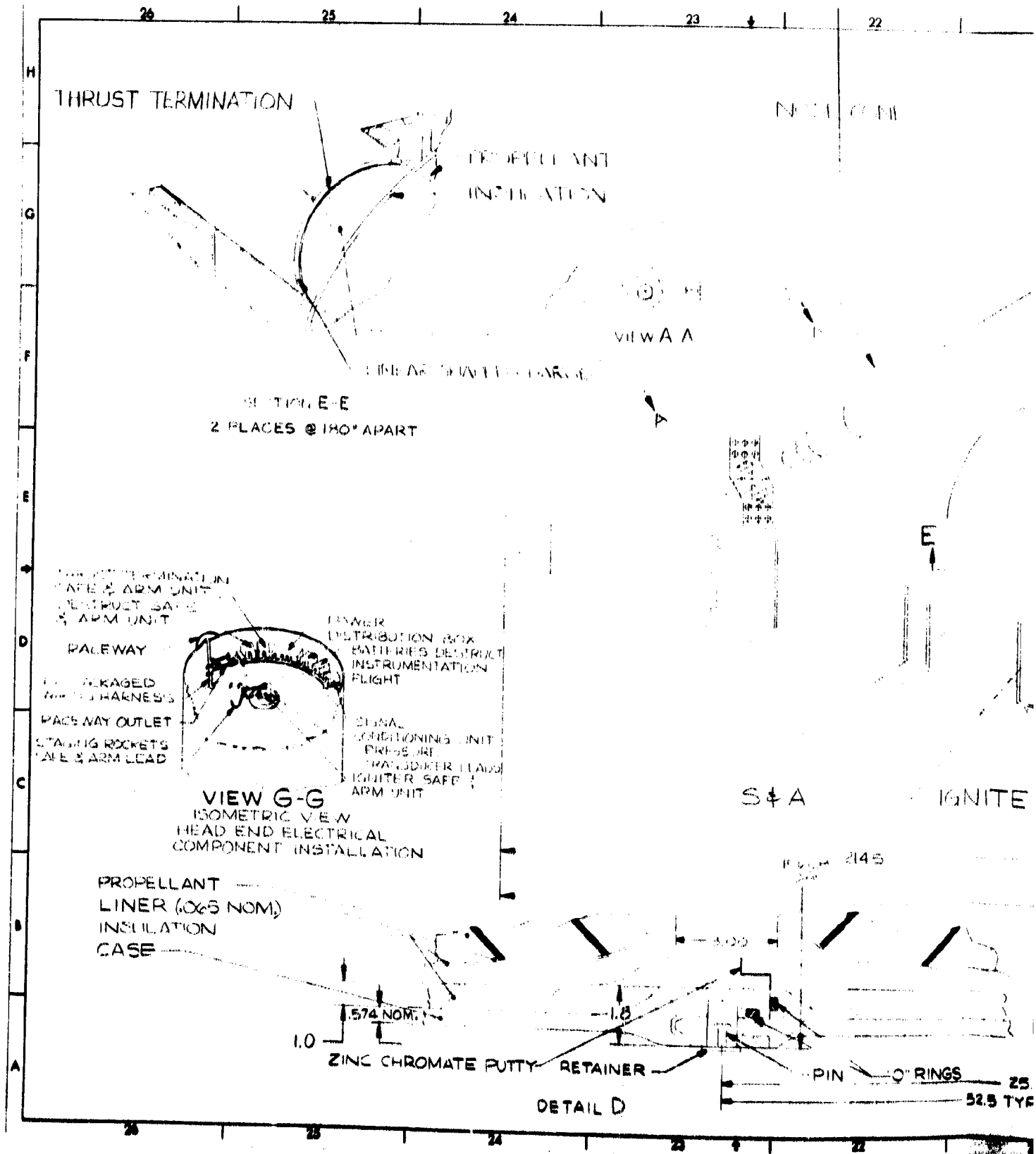
THRUST TERMINATION
PROPELLANT
INSULATION
VIEW A A
SECTION E-E
2 PLACES @ 180° APART
RACEWAY
PACS WAY OUTLET
STAGING ROCKETS
SAFE & ARM LEAD
POWER
DISTRIBUTION BOX
BATTERIES DESTRUCT
INSTRUMENTATION
FLIGHT
SIGNAL
CONDITIONING UNIT
PRESSURE
TRANSDUCER LEADS
IGNITER SAFE
ARM UNIT
VIEW G-G
ISOMETRIC VIEW
HEAD END ELECTRICAL
COMPONENT INSTALLATION
S & A
IGNITE
PROPELLANT
LINER (.065 NOM.)
INSULATION
CASE
.574 NOM.
1.0
ZINC CHROMATE PUTTY
RETAINER
PIN
O" RINGS
52.5 TYP
DETAIL D

FOLDOUT FRAME

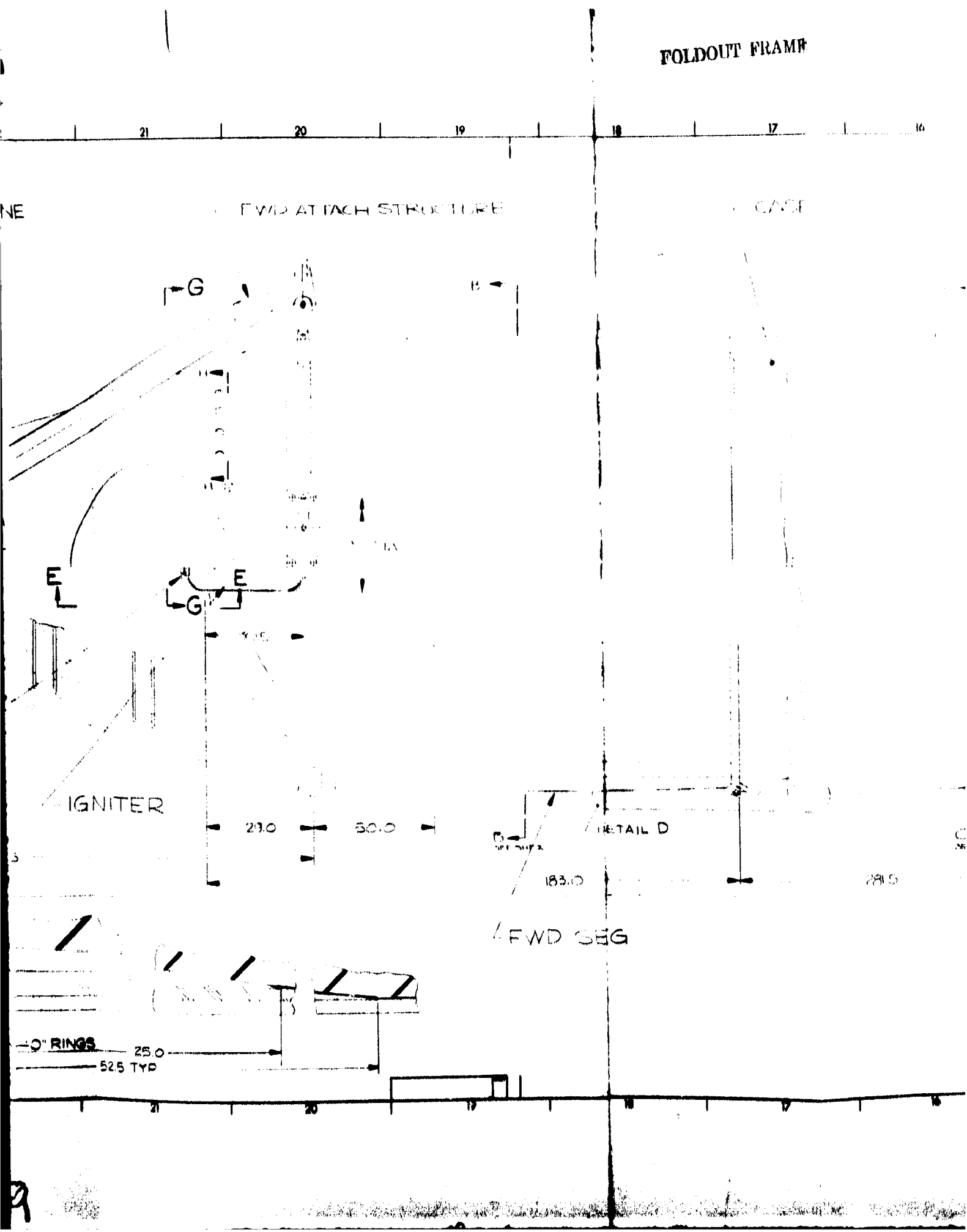

/

FOLDOUT FRAME 3

15 14 13 12 11 10

281.5

281.5

CYL SEG (3 REQD)

15 14 13 12 11 10

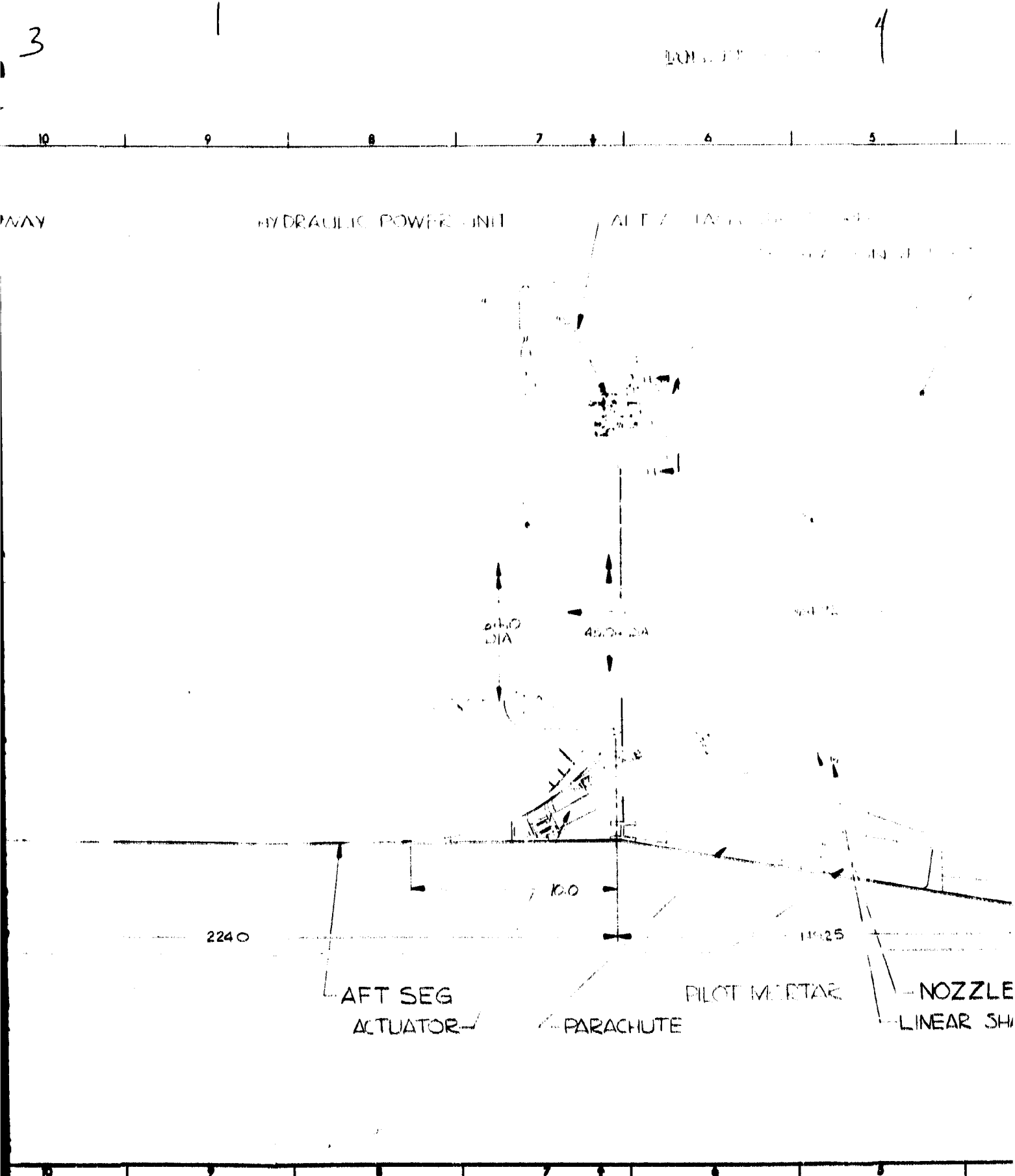
HYDRAULIC POWER UNIT
AFT SEG
ACTUATOR
PARACHUTE
NOZZLE
2240

Figure 3-33. 1

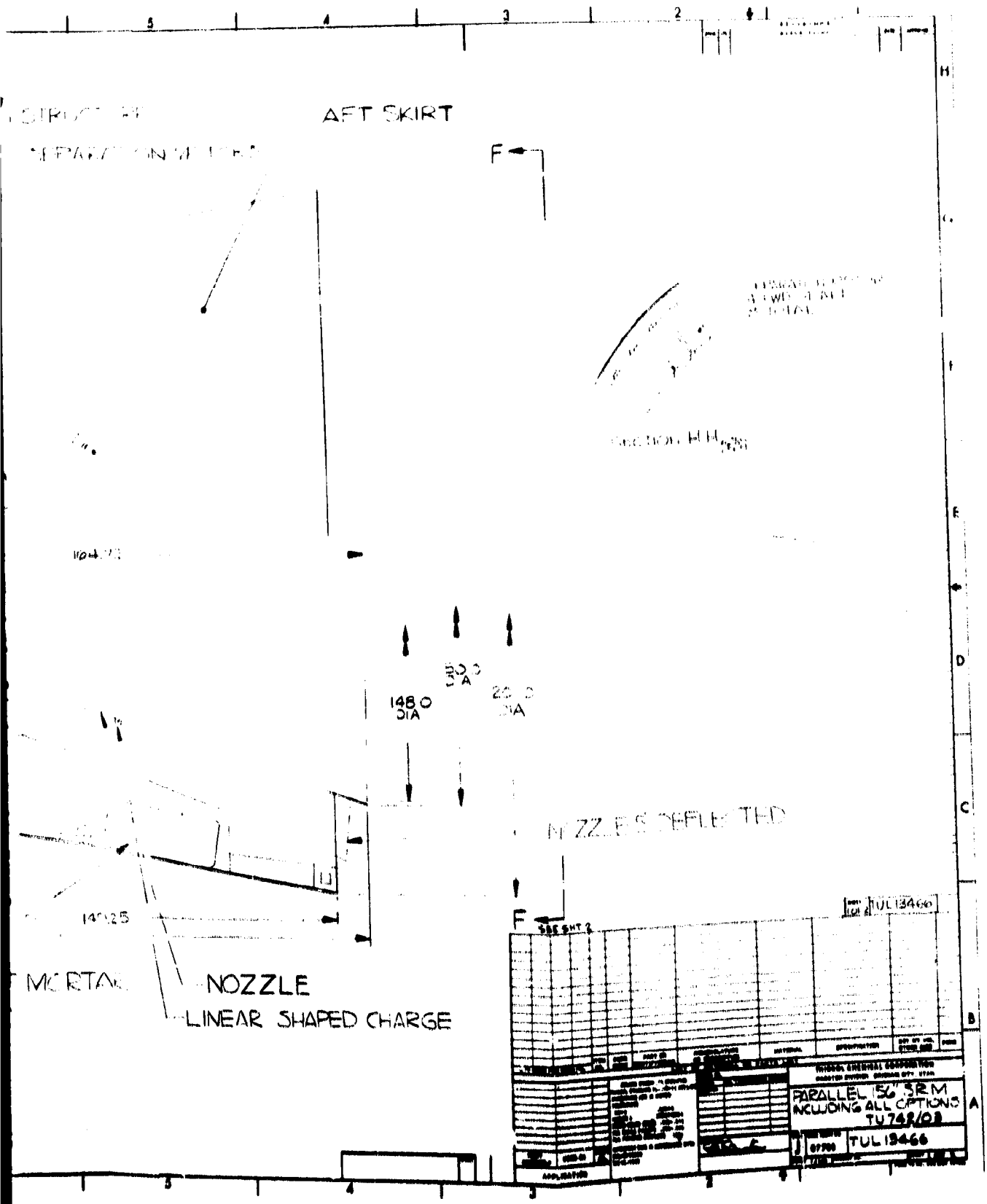

Figure 3-33. 156 Inch Baseline SRM Stage, Parallel Configuration with all Options (Sheet 1 of 2)

FOLDOUT FRAME

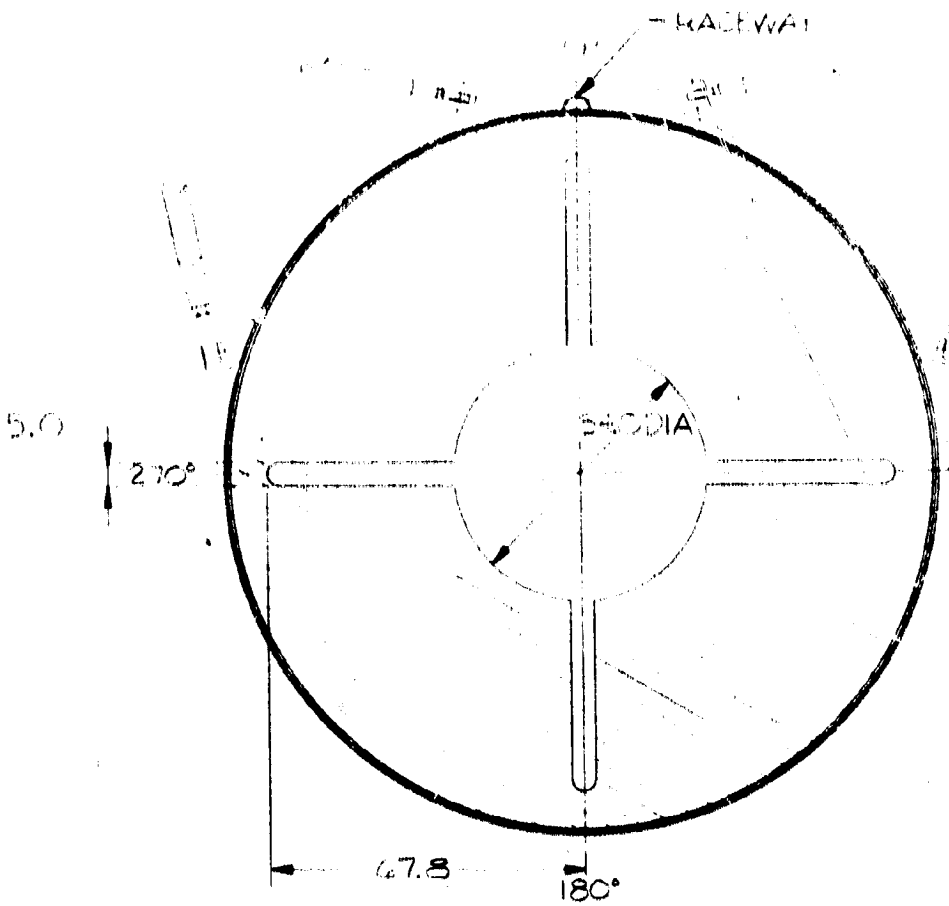

SECTION B-B

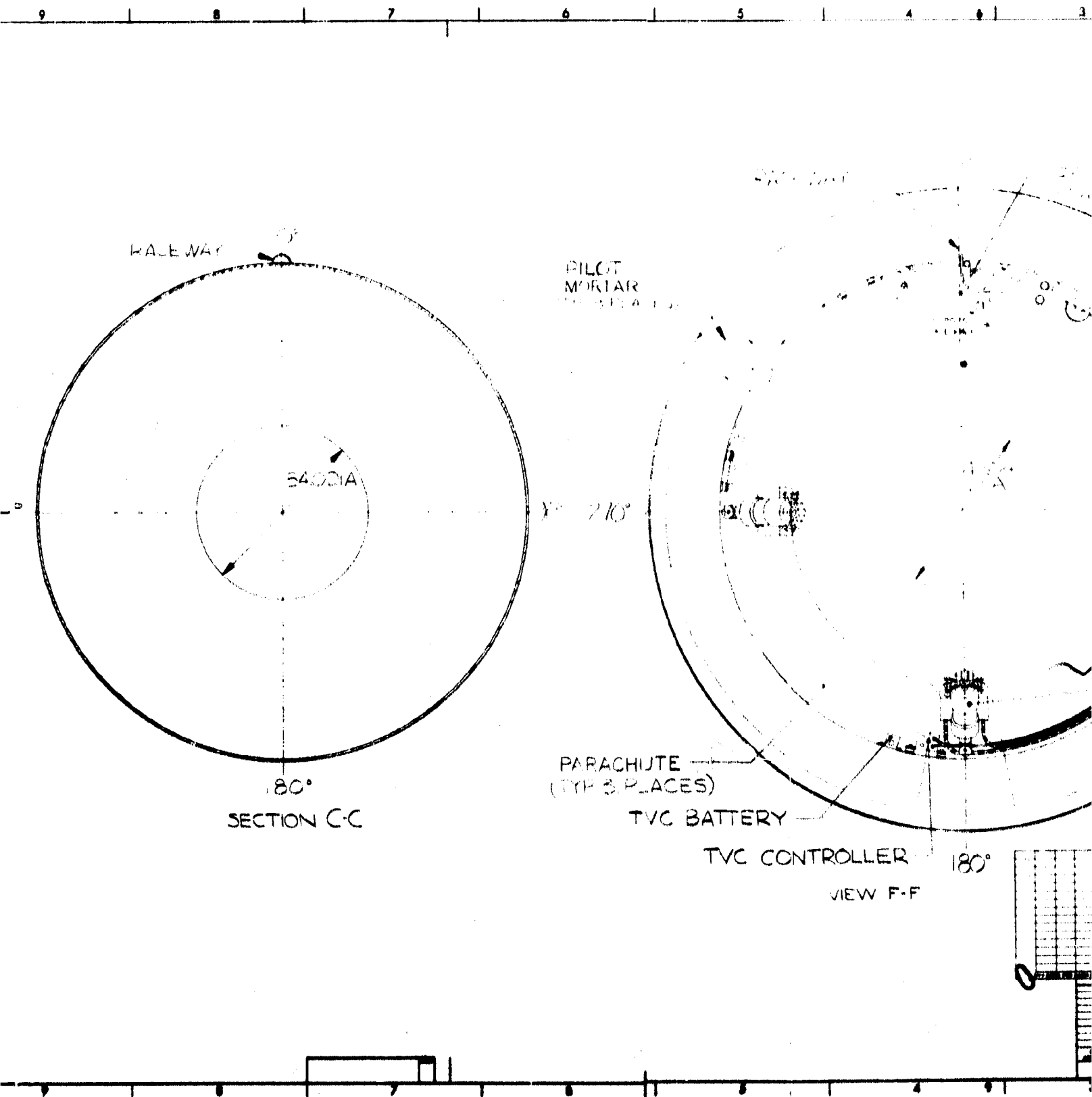

Figure 3-33. 156 Inch Baseline SRM St

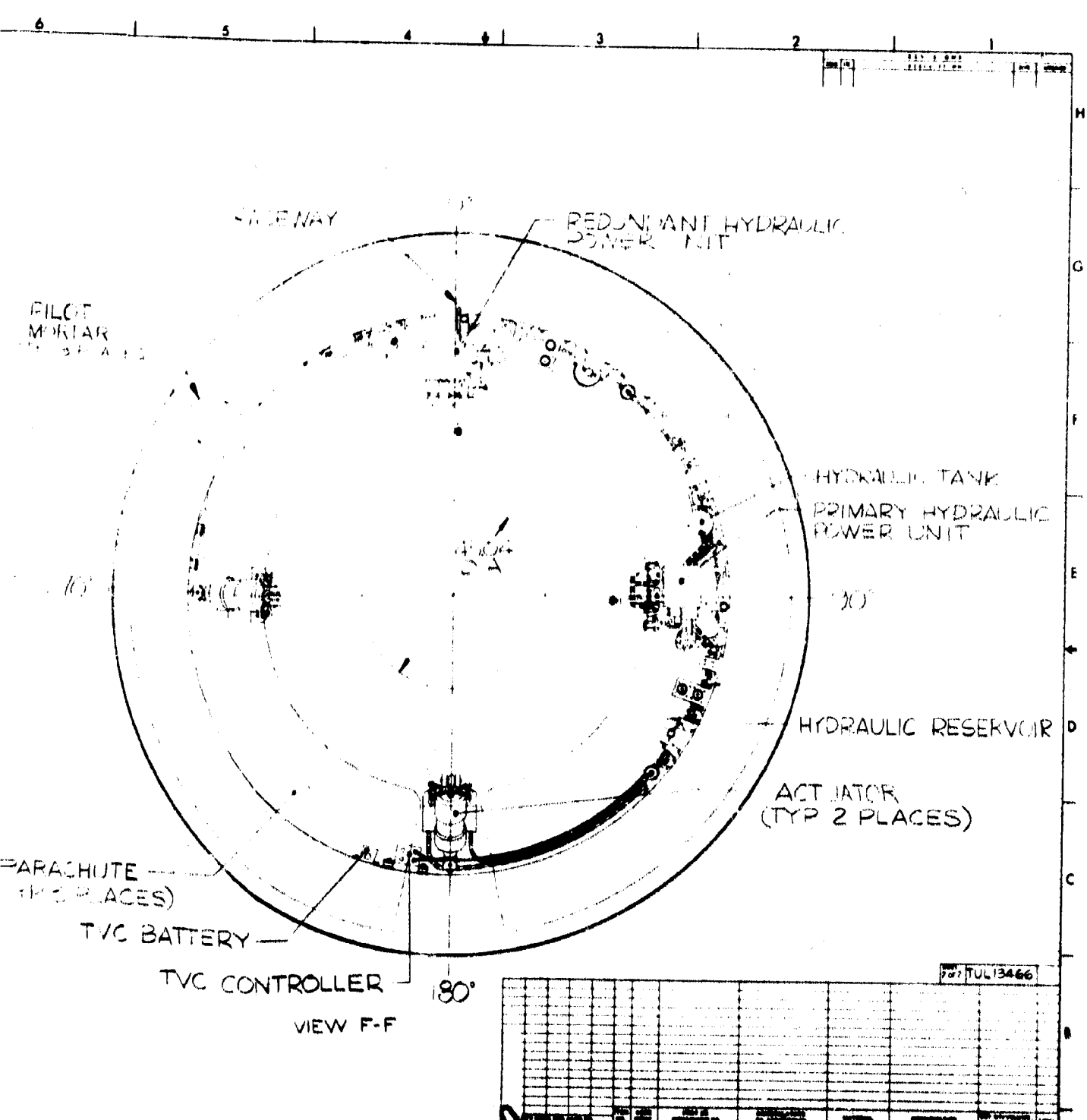

Figure 3-33. 156 Inch Baseline SRM Stage, Parallel Configuration with all Options (Sheet 2 of 2)

d. Supersonic splitline

e. Mechanical probes

7. Dual flexible bearing nozzle

8. Techroll movable nozzle

The studies indicated that none of the mechanical interference systems warranted further investigation as it was concluded that development risks (and cost) were greater than other TVC techniques, primarily because of the severe materials problems. Additionally, high nozzle and actuation system weight penalties and performance losses were encountered.

Of the many TVC systems investigated, the dual flex concept is by far the most attractive with regard to total system weight (the sum of nozzle and actuation system weight), required actuation system output horsepower, and cost. However, although the dual flex has been successfully demonstrated in an actual subscale static test, it is not as fully developed as are the single flexible bearings which have been fabricated and successfully flight tested on the Poseidon and Minuteman systems and successfully bench and static tested on 156 in. motors. Considerable development effort and cost would be required to advance the dual flex concept to the same relative state.

Studies performed by NASA* and others on TVC systems for the 260-in. diameter motors showed LITVC to be considerably inferior to the movable flexible bearing nozzle from both weight and cost standpoints, even for small thrust vector angle requirements. The LITVC system weight was found to be about three times that of the flexible bearing system and the cost nearly 81 percent higher. A comparison of typical systems for a 156-in. motor indicated approximately the same results.

If large vector angles are desired, as in the proposed system, the flexible bearing system has demonstrated a thrust vectoring capability up to $\pm$ 17.5 deg in smaller tactical missile system nozzles. Studies and analyses have shown such vector capability can be readily achieved in larger size flexible bearings. The LITVC system is limited to a maximum achievable effective angle of 4 to 5 deg.

The hot gas thrust vector control technique has the same disadvantages as the LITVC method with the additional drawback of not being state-of-the-art. This technique would also necessitate an extensive development program prior to its acceptance as a reliable means of thrust vectoring.

*Ref NASA Technical Memorandum NASA-TMX-67912.

The gimbaled nozzle has the advantage of being state-of-the-art and has the capability of attaining large vector angles, but weight and fabrication cost are prohibitive regardless of the required vector angle.

The Techroll Movable Nozzle concept being developed by UTC appears quite promising from the standpoint of having lower system torque and, therefore, reduced actuation system power requirements and weight. The concept has been demonstrated on some small nozzles but is far from being state-of-the-art, particularly for the large size nozzles being considered. Extensive development would be required. Cursory investigation of a typical Techroll system for the 156-in. size nozzle indicates that the end rings would be quite massive and much heavier than those for a flexible bearing system. In addition, the radial clearances required between the inner and outer rings would permit excessive radial movement and offset the thrust centerline unless an additional restrictive system was developed and incorporated.

The aft pivot flexible bearing system is nearly equivalent to the forward pivoted system. It would require a greater actuation system power capability, however, since the available moment arm length is considerably less than that of the forward pivoted system.

In summary, investigation of the forward pivoted flexible bearing nozzle indicated it to be the most suitable system for the 156-in. SRM booster motors. It is a highly reliable, relatively lightweight system as well as being considerably lower in cost than the other systems evaluated.

3.4.2.2.1.1 TVC Nozzle

The TVC nozzle is a partially submerged, movable, omniaxial, state-of-the-art design providing $\pm$ 5 deg thrust vector control capability. Its size, configuration, gimbaling mechanism, and materials are typical of those of the 156-9 nozzle successfully demonstrated by static test in 1967.

The gimbaling mechanism is a forward pivoted flexible bearing consisting of alternate laminae of metallic and elastomeric shims integrally bonded to and between forward and aft end rings which in turn interface with the nozzle movable and fixed sections to form the complete assembly.

With exception of the gimbaling mechanism, the nozzle is essentially identical to the baseline SRM nozzle and contains the same basic design features, redundancies, and margins of safety.

The nozzle design is shown in Figure 3-34. Criteria employed in developing the design and dimensional characteristics of the nozzle are listed in Table 3-26. Figure 3-35 shows a cross section of the flexible bearing assembly.

FOLDOUT FRAME

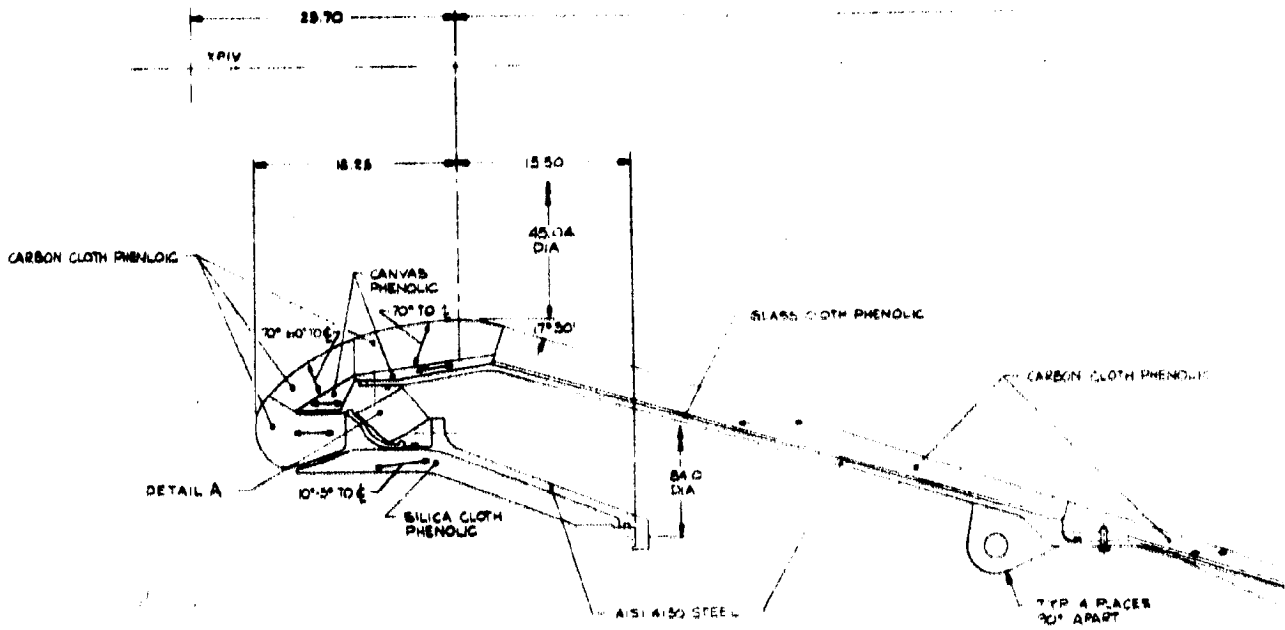

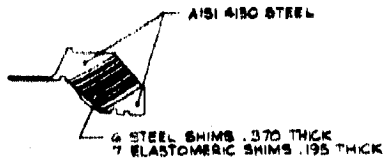

DETAIL A

FOLDOUT FRAME 2

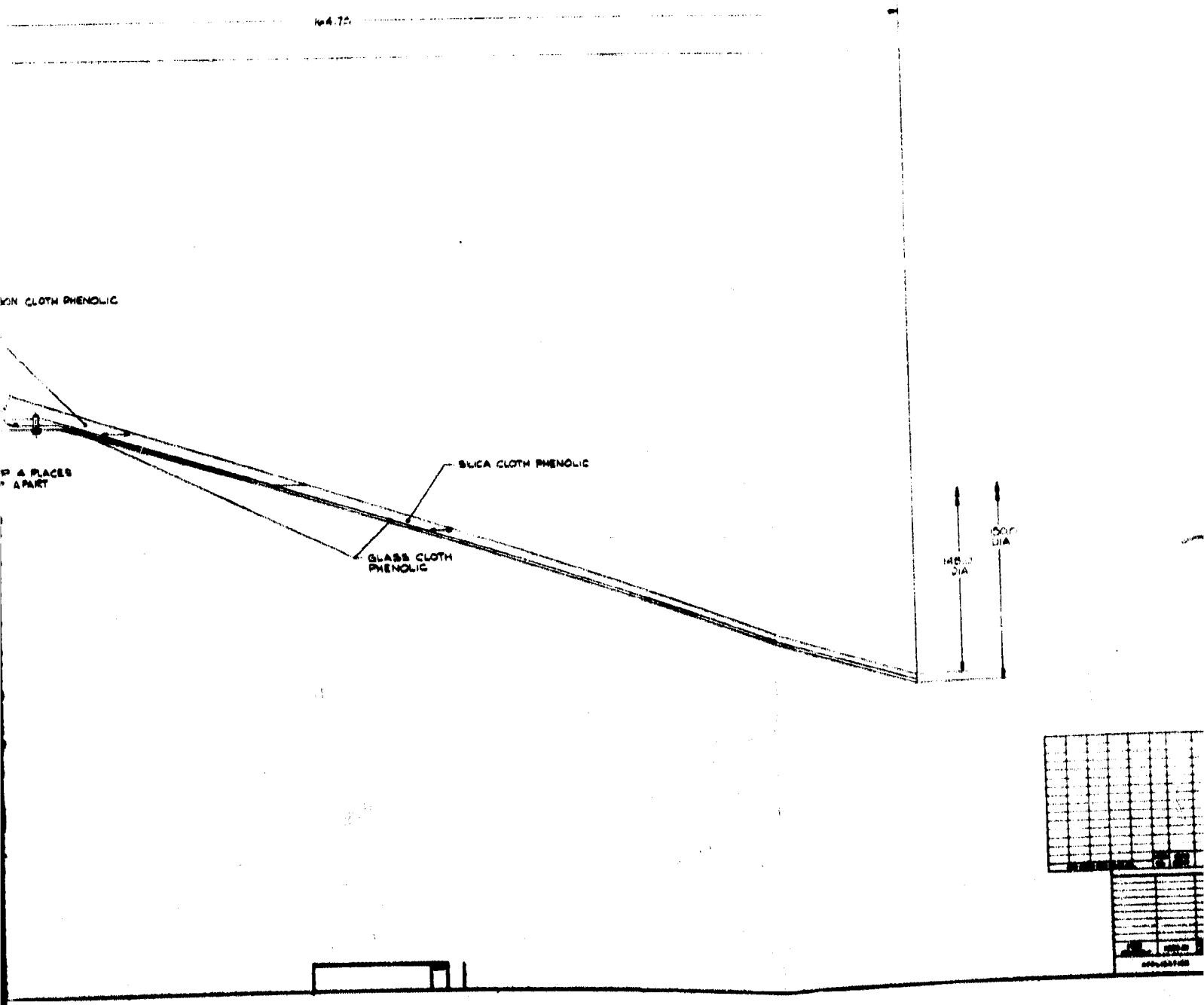

Figure 3-34. SRM Baseline Mov

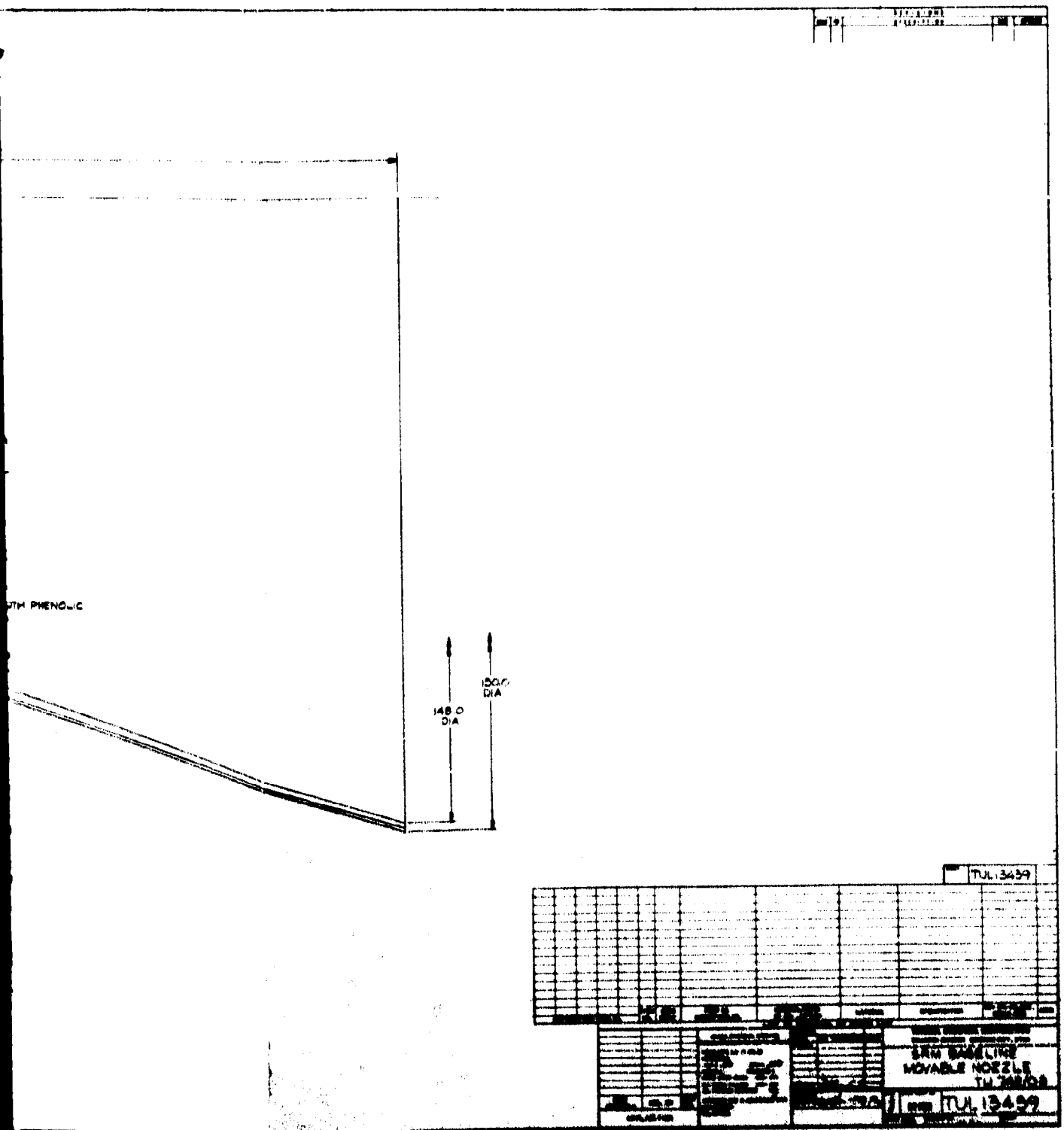

Figure 3-34. SRM Baseline Movable Nozzle, Parallel Configuration

TABLE 3-20

NOZZLE CHARACTERISTICS DESIGN CRITERIA

Throat Diameter, Initial (in.)	45.04
Throat Area, Initial (sq in.)	1,593.26
Exit Diameter, Initial (in.)	148.0
Exit Area, Initial (sq in.)	17,203.4
Expansion Ratio, Initial	10.8:1
Exit Cone Half Angle (deg)	17.5
Submergence (%)*	9.4
TVC Capability (deg)	±5
TVC Slew Rate (deg/sec)	5
Pressure, Average (psia)	830
MEOP (psia)	1,000
Safety Factors	
Ablatives	2.0
Structure	1.4
Proof Pressure Test, Flex Seal	1.2 x MEOP
Nozzle Weight (lb)	11,890.38

*Submergence (%) = $\frac{\text{Length, Throat to Flange}}{\text{Length, Throat to Exit}}$ x 100

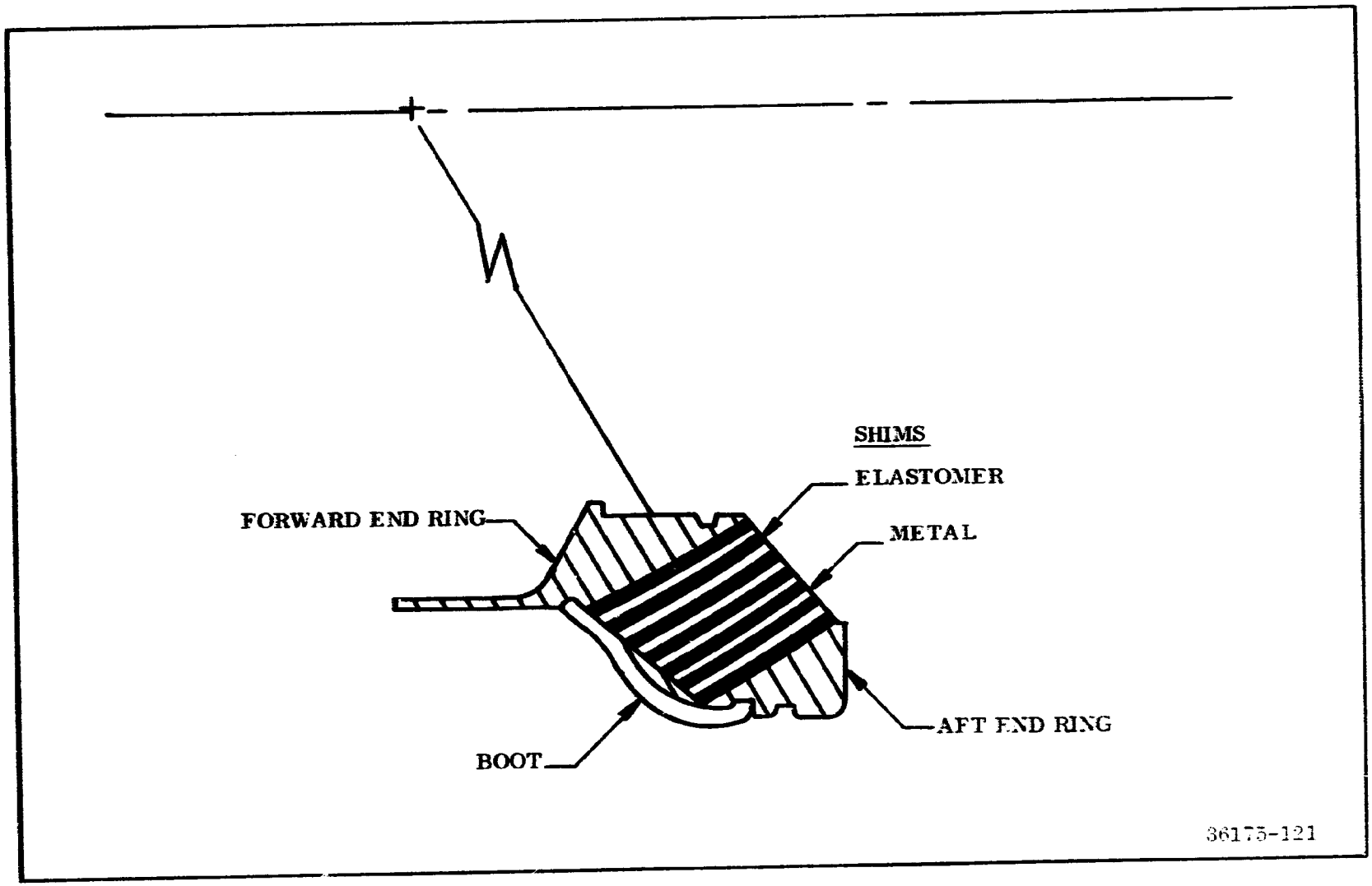

Figure 3-35. Flexible Bearing Cross Section

The ablative and insulative materials are identical to those of the baseline fixed nozzle, are used in the same manner throughout this design, and were selected for the reasons cited previously.

The structural elements of both the movable and fixed sections of the nozzle are heat treated AISI 4130 steel, as are the end rings and metallic shims of the flexible bearing. This material is relatively inexpensive, readily available, and easy to work with from the fabrication standpoint, while providing the necessary strength and stiffness required for the nozzle and bearing structural elements.

For the flexible bearing elastomer, both natural rubber and synthetic polyisoprene have been used extensively, and there is little or no difference in performance. Polyisoprene has a somewhat higher shear strength than the natural rubber, however, and therefore, has been selected for this design. The flexible bearing insulative boot is of V-44, an asbestos/silica filled elastomeric material which also has been tested previously and proven in this and other applications.

Fabrication of the nozzle structural elements and ablative/insulative liners is accomplished in the same manner previously described for the baseline fixed nozzle.

In fabricating the flexible bearing assembly, the end rings are machined from ring forgings, and the metal shims are either spin or explosive formed from sheet stock. After trimming, surface preparation and cleaning of the metal shims is completed, appropriate thicknesses of the uncured elastomer are laid up on each shim, and the shims then stacked between the end rings in a mold fixture which holds the shims in their proper position. Correct spacing of the shims is also provided for by the fixture to insure proper thicknesses of elastomer are obtained. Heat and pressure are then applied to the assembly to cure and vulcanize the elastomer and metallic laminae into an integral unit.

The bearing insulative boot is fabricated in a similar manner, the raw material being laid up in a mold cavity, the die closed, and heat and pressure applied to effect cure of the part. The die molded boot is then bonded to the end rings to complete the flexible bearing assembly. This is the same procedure developed and proven in fabricating three 156-9 nozzle bearings, and also is used currently for flexible bearing fabrication for the first and second stage nozzles in the Poseidon production program. Following fabrication, the bearing assembly is thoroughly tested to verify functional capability and structural and sealing integrity.

Final assembly of the nozzle involves bonding of the various plastic components into position, joining the fixed and movable structures to the flexible bearing assembly, installing the cone retention pins, and overlaying and curing the glass cloth structure at the exit cone joint.

To arrive at a credible nozzle design, preliminary layouts were prepared and a series of analyses made to establish the final configuration. The same but

somewhat more extensive series and sequence of analyses were performed for this design as for the baseline fixed nozzle. Although both nozzles are essentially the same, separate analyses were required since point loads from the actuation system had to be considered in designing the structure of the movable nozzle, and an extension of the analyses was necessary to cover the flexible bearing assembly. In addition, past test data and experience has shown that movable nozzles experience slightly greater erosion than fixed nozzles, and therefore it was necessary to modify some parameters in the ablative analysis.

In all cases, the appropriate safety factors, as listed in Table 3-20, have been incorporated to insure design and performance integrity. Excessive margins of safety, however, have been avoided in order to minimize weight and cost.

Erosion and char profiles resulting from the analyses are shown in Figure 3-36. Mass properties of the design are listed in Table 3-21. Analysis of the flexible bearing produced the torque values given in Table 3-22.

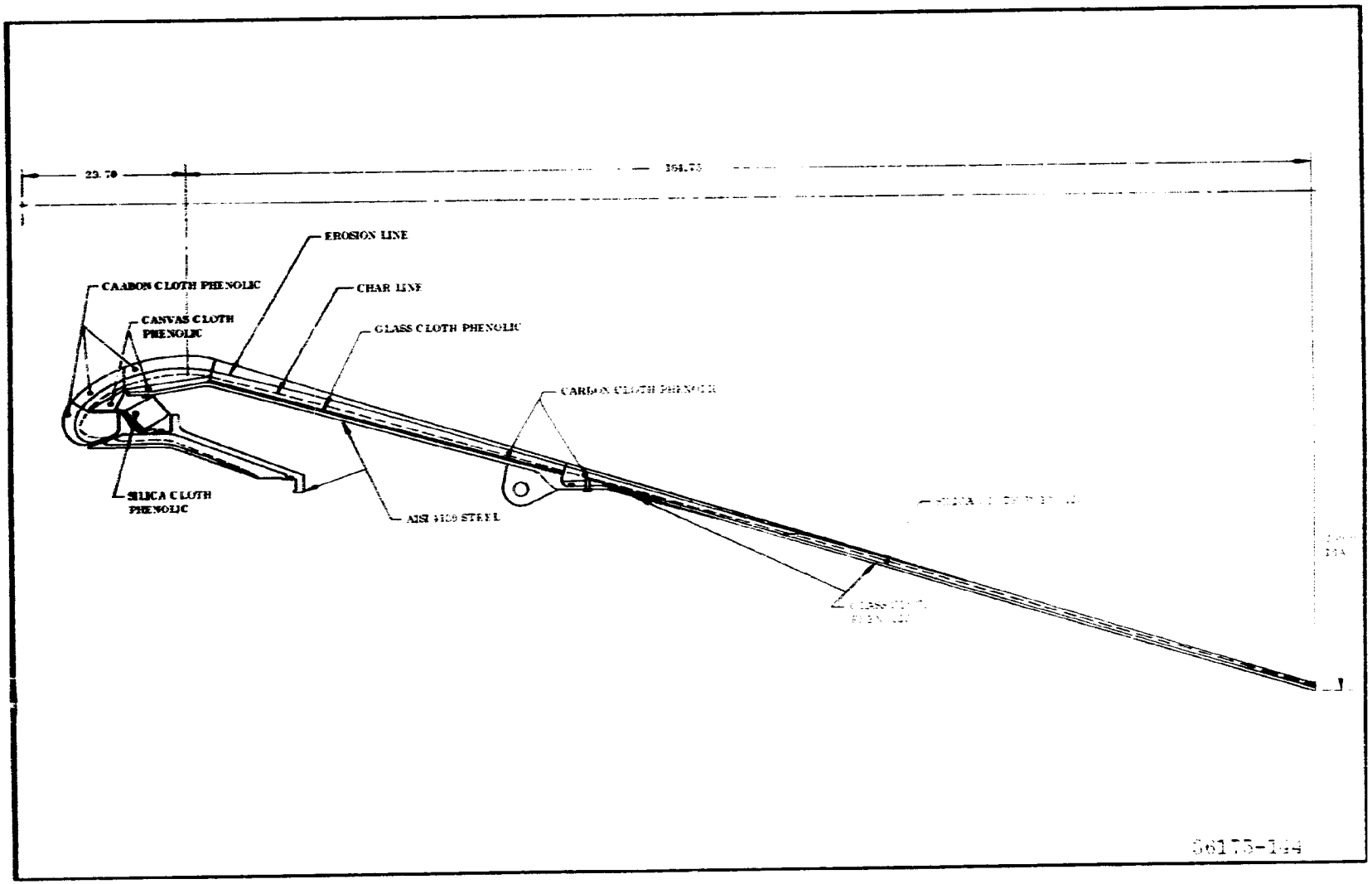

Figure 3-36. Nozzle Erosion and Char Profile, TU-742 [illegible] Motor

TABLE 3-21

SRM MOVABLE NOZZLE MASS PROPERTIES DATA, OPTIONAL

	WEIGHT (LBS)	CENTER OF GRAVITY LONG.	LAT.	VERT.	MOMENT OF INERTIA PITCH	ROLL	YAW
NOZZLE ASSEMBLY	11862.340	1558.735	200.000	200.000	7.963	4.365	7.963
FIXED PART	2627.926	1525.529	200.000	200.000	0.420	0.770	0.420
STRUCTURE	1788.675	1527.092	200.000	200.000	0.282	0.521	0.282
FLEXSEAL ADAPTER	305.466	1517.799	200.000	200.000	0.035	0.071	0.035
NOZZLE ATTACH FLANGE	1483.209	1529.005	200.000	200.000	0.239	0.451	0.239
INSULATION	836.918	1522.180	200.000	200.000	0.135	0.247	0.135
EXPENDED PAT	5.557	1518.812	200.000	200.000	0.001	0.002	0.001
EXPENDED TDAT	244.553	1518.812	200.000	200.000	0.038	0.071	0.038
UNEXPENDED EAT	586.807	1523.615	200.000	200.000	0.095	0.174	0.095
O RINGS	2.333	1528.941	200.000	200.000	0.000	0.001	0.000
MOVABLE PART	9097.414	1568.677	200.000	200.000	6.666	3.551	6.666
STRUCTURE	3616.036	1567.349	200.000	200.000	2.238	1.360	2.238
FLEXSEAL ADAPTER	457.032	1512.732	200.000	200.000	0.043	0.085	0.043
BASIC SHELL	2217.305	1552.950	200.000	200.000	0.511	0.609	0.511
ACTUATOR ATTACH RING	0.0	0.0	200.000	200.000	0.0	0.0	0.0
EXIT CONE GLASS	941.699	1627.760	200.000	200.000	0.549	0.666	0.549
NOSE INSULATION	193.825	1506.052	200.000	200.000	0.028	0.056	0.028
EXPENDED PAT	3.076	1503.780	200.000	200.000	0.000	0.001	0.000
EXPENDED TDAT	135.364	1503.780	200.000	200.000	0.016	0.031	0.016
UNEXPENDED EAT	55.385	1511.731	200.000	200.000	0.011	0.023	0.011
BACK INSULATION	370.821	1508.514	200.000	200.000	0.030	0.060	0.030
EXPENDED EAT	3.711	1508.368	200.000	200.000	0.000	0.001	0.000
EXPENDED TDAT	163.299	1508.368	200.000	200.000	0.013	0.026	0.013
UNEXPENDED EAT	203.811	1508.649	200.000	200.000	0.017	0.033	0.017
THROAT INSULATION	365.127	1518.319	200.000	200.000	0.025	0.048	0.025
EXPENDED PAT	4.631	1518.841	200.000	200.000	0.000	0.001	0.000
EXPENDED TDAT	203.784	1518.841	200.000	200.000	0.013	0.024	0.013
UNEXPENDED EAT	156.712	1517.625	200.000	200.000	0.012	0.024	0.012
NOSE LINER	63.246	1509.905	200.000	200.000	0.006	0.012	0.006
THROAT LINER	88.724	1518.372	200.000	200.000	0.007	0.014	0.007
EXIT CONE INSUL. FWD	1294.696	1549.576	200.000	200.000	0.205	0.291	0.205
EXPENDED PAT	17.315	1549.592	200.000	200.000	0.003	0.004	0.003
EXPENDED TDAT	761.922	1549.592	200.000	200.000	0.117	0.165	0.117
UNEXPENDED EAT	515.460	1549.551	200.000	200.000	0.085	0.123	0.085
EXIT CONE INSUL. CENTER	723.506	1592.299	200.000	200.000	0.174	0.316	0.174
EXPENDED PAT	8.305	1592.750	200.000	200.000	0.002	0.004	0.002
EXPENDED TDAT	365.436	1592.760	200.000	200.000	0.085	0.155	0.085
UNEXPENDED EAT	349.765	1591.806	200.000	200.000	0.087	0.158	0.087
EXIT CONE INSUL. AFT	1515.459	1642.242	200.000	200.000	0.728	1.204	0.728
EXPENDED PAT	14.693	1643.533	200.000	200.000	0.007	0.012	0.007
EXPENDED TDAT	646.574	1643.533	200.000	200.000	0.317	0.513	0.317
UNEXPENDED EAT	854.191	1641.242	200.000	200.000	0.403	0.680	0.403
EXIT CONE LINER	214.536	1552.138	200.000	200.000	0.037	0.055	0.037
O RINGS	2.727	1555.076	200.000	200.000	0.001	0.001	0.001
FLEXSEAL	622.594	1515.658	200.000	200.000	0.065	0.128	0.065
RUBBER SEAL	26.118	1513.772	200.000	200.000	0.003	0.006	0.003
NOZZLE ATTACH PROVISIONS	137.000	1535.586	200.000	200.000	0.022	0.044	0.022
BOLTS	111.000	1536.250	200.000	200.000	0.018	0.036	0.018
SEALANT	26.000	1532.750	200.000	200.000	0.004	0.008	0.004

MOMENT OF INERTIA IS IN SLUG FEET SQUARED DIVIDED BY 1000 ABOUT AXES
THRU THE CENTER OF GRAVITY

TABLE 3-22

FLEXIBLE BEARING NOZZLE ACTUATION
TORQUE, TU-742/03 MOTOR
(Million In.-Lb)

Component	
Internal Aerodynamic	1.143
Offset	0.353
Seal Spring (5 deg vector)	0.904
Seal Boot Spring (5 deg vector)	0.045
Gravity (considered only for horizontal static test)	0.543
Total	2.988

3.4.2.2.1.2 TVC Actuators

The reliability and redundancy requirements of the Space Shuttle system necessitate the use of multiple, failure-correcting servoactuators for the SRM thrust vector control (TVC) system. The TVC actuation subsystem consists of two hydraulically operated, tandem servoactuators per motor. Each actuator consists of servovalves which control the flow of hydraulic fluid, the main ram which provides power to position the SRM movable nozzle, and position transducers for feedback. Also included in the servoactuator are the failure detection functions of the actuator subsystem. Since the principal reliability problem area is the servovalve, reliability is improved by the use of redundant channels, automatic detection of failures, and the bypass of a failed channel.

The selected TVC servoactuator is shown schematically in Figure 3-37. The TVC actuation requirements are listed on Table 3-22A. This actuator is an electrohydraulic two channel, tandem piston configuration. This operate/fail/operate actuator is an implementation of redundant hydraulic control, employing an intra-system monitoring capability. The actuator consists of two independent, hydraulically isolated, channels with each channel capable of controlling the tandem piston. Only one channel controls the actuator at any one time. With a malfunction in the controlling channel, an automatic switch is made to the standby channel; thus, there is neither a loss in output force nor a performance degradation.

When hydraulic pressure is applied to the servoactuator, the solenoid valves are pulsed to engage the system. Once pulsed, the solenoid valves are held on the seat with hydraulic pressure. This in turn energizes the system engage valve and activates channel No. 1. The active servovalve in channel No. 1 then acquires control of the actuator.

An auxiliary flapper nozzle develops pressure proportional to the position of the second stage servovalve spool. The auxiliary pressures from the active and monitor servovalves are fed to opposite ends of the comparator spool. If no malfunction occurs, the two monitor pressures will remain equal in magnitude and the comparator spool will remain centered. If a malfunction occurs, the output pressures of the active and monitor servovalves will differ. This will cause a pressure difference on the comparator spool creating motion of that spool. When the pressure difference exceeds a predetermined threshold, motion of the comparator spool will dump the supply pressure, holding the engage valve in the engage position. The engage valve of channel No. 1 will be forced by a spring into the bypass position where it blocks the output of the active servovalve of channel No. 1. The engage valve responds by moving one step, and channel No. 2 becomes the active channel and operates in exactly the same manner as channel No. 1 had acted previously.

Failure threshold of the comparator can be easily varied by spring rate and overlap of the comparator spool. Once the optimum threshold is determined, it will remain fixed in the design.

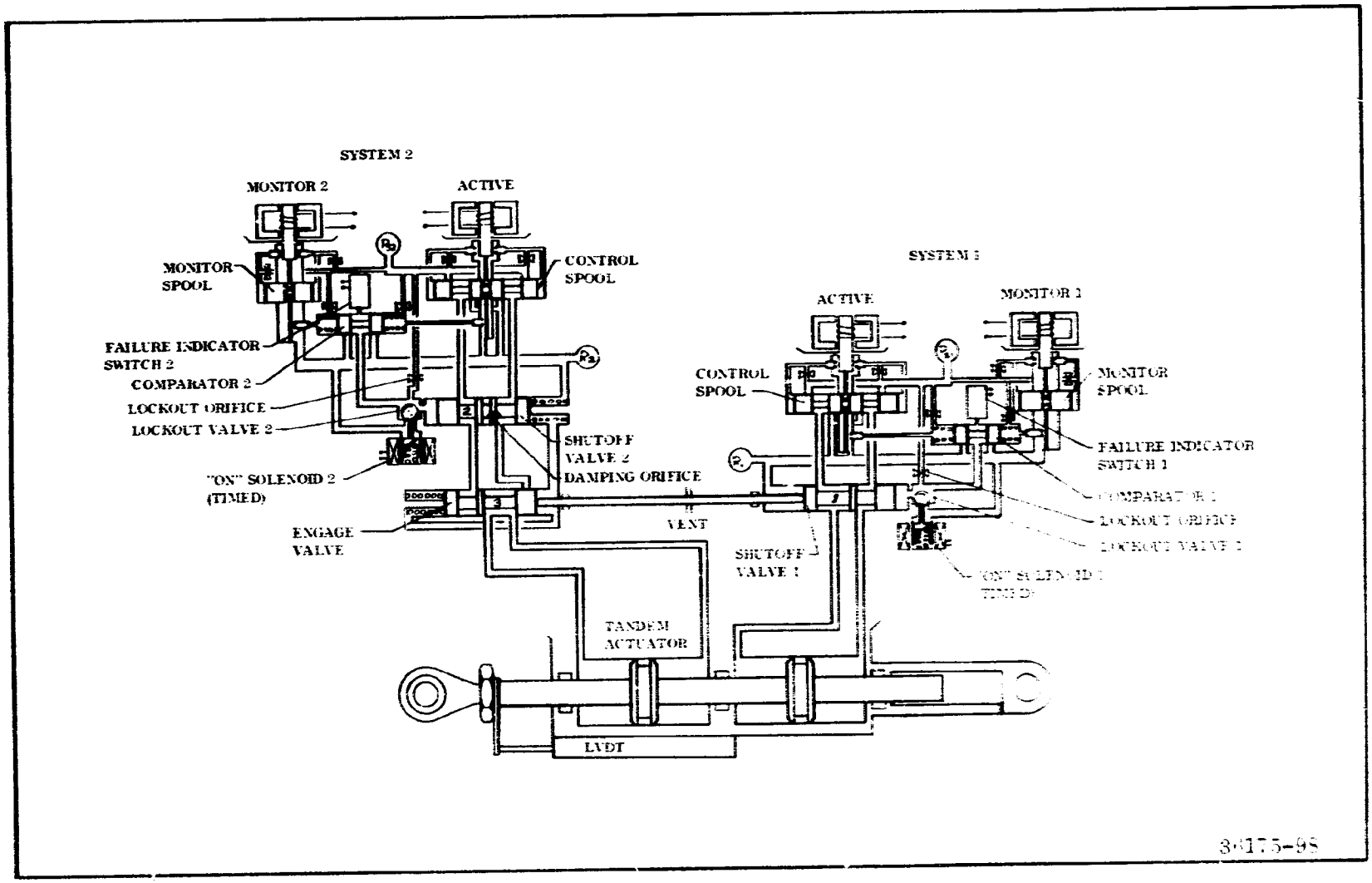

Figure 3-37. TVC Servoactuator System Schematic

TABLE 3-22A

TVC ACTUATOR REQUIREMENTS

TVC angle (deg)	5
TVC slew rate (deg/sec)	5
Load (lb)	41,000
Area (sq in.)	13.8
Stroke (in.)	16.1
Supply pressure (psi)	4,000
Flow rate (gpm)	18.5
Max pump horsepower	60.5
Redundancy	Active/standby

A failure in channel No. 2 will cause the actuator to fail in a bypass mode or nulled condition. Channel failure is monitored by a pressure switch on the comparator valve, and a signal is transmitted to the shuttle vehicle.

A decrease in hydraulic system pressure which exceeds a predetermined threshold in a channel will cause the solenoid valve to unseat, thus, switching to the unfailed channel.

After a malfunction, a channel will not come back on line until the solenoid valve is again pulsed by the flight crew. If the malfunction has been corrected, pressure will hold the solenoid valve on its seat. Input to the comparator spool from the active and monitor servovalves will be identical, the engage valve will be pressurized, and the pressure switch will cycle, thus returning the channel to normal operation. If a malfunction is still present, the channel will immediately switch off line as before.

Attached to the actuator piston are four position feedback linear variable differential transformers (LVDT). One LVDT is utilized for each of the four channels for servostabilization as shown in Figure 3-38. Since hydraulic monitoring is utilized downstream of the servovalve, failures in the LVDT, servoamplifier, servovalve, and guidance signals are detected and automatically corrected without appreciable actuator movement.

The two basic types of actuator feedback considered were mechanical and electrical. Mechanical feedback actuators are currently being utilized for engine positioning on several space boosters, including the Saturn launch vehicle. The reason for this selection is the contribution of the mechanical feedback system to the TVC system reliability. The basic contribution to reliability is achieved through elimination of the LVDT position transducers together with their associated cabling and power supply. Even more significant is the reduction of hardover failures. The mechanical feedback actuator "fails neutral" with a loss of electrical control. In the nonredundant electrical feedback actuator, if the feedback transducer opens, an actuator cable is severed, or the servoamplifier malfunctions, a hardover actuator results.

The major disadvantages associated with mechanical feedback actuators occur during the development phase. However, extensive use of analog computers for initial sizing of the actuator feedback parameters greatly reduces the trial and error selection of loop gains, pressure feedback sensitivity, and other characteristics which are mechanically rather than electrically actuated. Once the feedback actuator has been built, it is necessary to disassemble and rebuild it if a loop gain change is required. The servovalve is not easily removed or replaced and is usually attempted only at the manufacturer's facility.

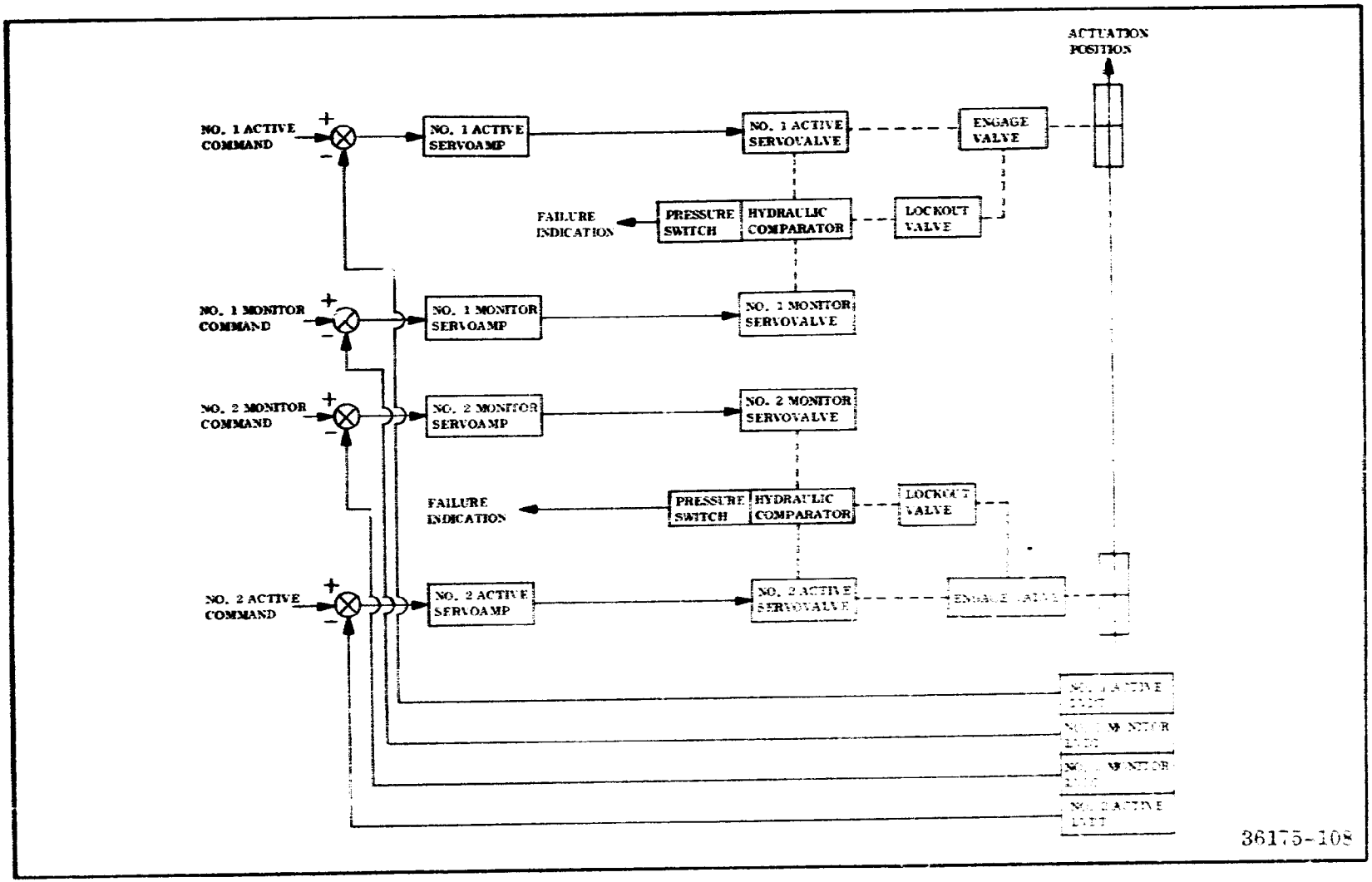

Figure 3-38. Active/Standby Actuation Schematic. Block Diagram

Table 3-23 summarizes the key actuator feedback considerations. Mechanical feedback actuators improve the system reliability by eliminating the electrical feedback transducer, cables, and power supply. Also provided are inherent "fail neutral" tendencies. This reliability improvement is achieved at the expense of some loss in static positioning accuracy and some inconvenience in the ability to change servoloop parameters. However, the Space Shuttle redundancy requirements necessitate the use of redundant TVC actuators. Redundancy was achieved in the manrated Saturn launch vehicle through the use of four engines each gimbaled with a mechanical feedback actuator in each axis. Loss of one of the four TVC systems would not result in a mission failure. However, in the solid propellant Space Shuttle booster, the number of nozzles available for TVC control (excluding the shuttle) is reduced to two. It becomes apparent that redundant actuators are required, since loss of one TVC system would jeopardize the mission success.

Techniques have been demonstrated to develop redundant actuators utilizing electrical feedback. These actuators are capable of sensing and eliminating single actuation and guidance system failures. There are no known actuators in use or in development utilizing redundant mechanical feedback. Typically, redundancy with mechanical feedback actuators is achieved through multiple actuators. Based on this fact and coupled with the costly development required for mechanical feedback actuators, the selected TVC actuator feedback concept is one of electrical utilization of automatic failure detection and correcting techniques.

There are two basic types of redundant control systems, monitorless and monitor. A monitorless redundant control system minimizes the effect of any one component failure by the use of multiple operational units. The operational units are connected so that failures tend to be canceled out by the remaining "nonfailed" components or channels.

A monitor redundant control system is based on the principle of continuous performance comparison of multiple operational channels and the removal of the effects of the fail channel by switching techniques.

For the purpose of this study, only active/standby system monitoring is considered. For this monitoring technique, the control channels can be selectively coupled to the actuator. Only one control channel is coupled at any one time to the actuator. No performance degradation occurs as in force sharing monitoring since each control channel is made similar to the others.

The basic requirement of the TVC actuator is that it must withstand any first internal failure or external input or power supply failure with no performance degradation. While performance degradation may be acceptable, it certainly is not an advantage. The second requirement is that upon any second failure, transfer of the actuator to a bypass condition must occur. A hardover condition as a result of a second failure is unacceptable. The monitoring technique assumes that independent electrical and hydraulic power supplies are available to achieve control

TABLE 3-23

TVC SERVOACTUATOR FEEDBACK CONSIDERATIONS

Item	Electrical Feedback	Mechanical Feedback
Initial engineering development costs	Nominal	Much higher due to special nature of the design
Development flexibility	Easily modified gains and compensation	Require disassembly of actuator for gain change, etc. Computers are used to minimize changes
Troubleshooting	Many components to check; ie, amplifier servovalve, feedback	Simple replacement of actuator
Replacement of servovalve	Easy	Only at manufacturer's facility, usually replace total actuator
Accuracy	Dependent on feedback linearity and servoloop gain	Dependent on stability of current driving amplifier
Servoamplifier requirements	High gain operational amplifier for signal summing and compensation	Low gain, high stability, low drift
Torque motor availability	Many sizes available	Various sizes not readily available. Development of torque motor required
Typical failure mode	Hardover	Fail-safe - typically the actuator goes to neutral - large reduction in hardover failure modes
Overall reliability	Nominal	Improved

channel isolation. Four TVC actuator concepts are evaluated on the basis of weight, reliability, ease of development, ease of manufacture, simplicity, ease of maintenance and cost.

System No. 1--Active/Standby - External Monitoring

System No. 1 is shown in Figure 3-39. The actuator consists of a tandem power ram and incorporates two servochannels. Two independent hydraulic supplies provide completely redundant channels. The normal operation of the actuator is such that the engage valve allows operation of the power actuator by servovalve No. 1 while channel No. 2 is in a standby mode. Normal operation occurs until an external signal from either the flight crew or the guidance system activates the engage valve, thus bypassing channel No. 1 and activating channel No. 2. A second failure to the actuation system, as sensed by the guidance system, places the actuator in a neutral condition bypassing both channels. Reliability of the actuation system is improved due to the redundancy of the electrical and electrohydraulic components. A disadvantage of this system stems from the external nature of the channel switching command. Since monitoring of actuator failures is downstream of the power ram, large actuator transients may occur since external effects such as attitude rate are monitored to detect TVC failures.

System No. 2--Triple Channel - Majority Voting

System No. 2 shown in Figure 3-40 is an active standby configuration of redundancy. This system is designed so that the operational characteristics of the standby channel are similar to the active channel. Both channels are fed through a three position engage valve. Upon commands from the internal hydraulic monitoring and logic section, the engage valve transfers the system through its redundancy operating modes.

Monitoring is carried out at spools of the servovalves, using a hydraulic position transducer. A third servovalve is used as a reference monitor channel. For any first failure, the system either transfers to the standby channel, or in the situation where the first failure is the standby channel, activates itself so that the standby channel cannot be engaged upon occurrence of a second failure. Since monitoring is carried out at the servovalve spool prior to the actuator ram, hardover failures of the servovalve, command input, servoamplifier, and position transducer are detected without requiring a deviation of the actuator from the commanded position. Additional advantages of this redundant concept are:

1. The actuator transfer time is easily made very short since solenoid valves are not utilized.

2. Single component failures causing total control system failures are limited to components historically having an extremely low failure rate.

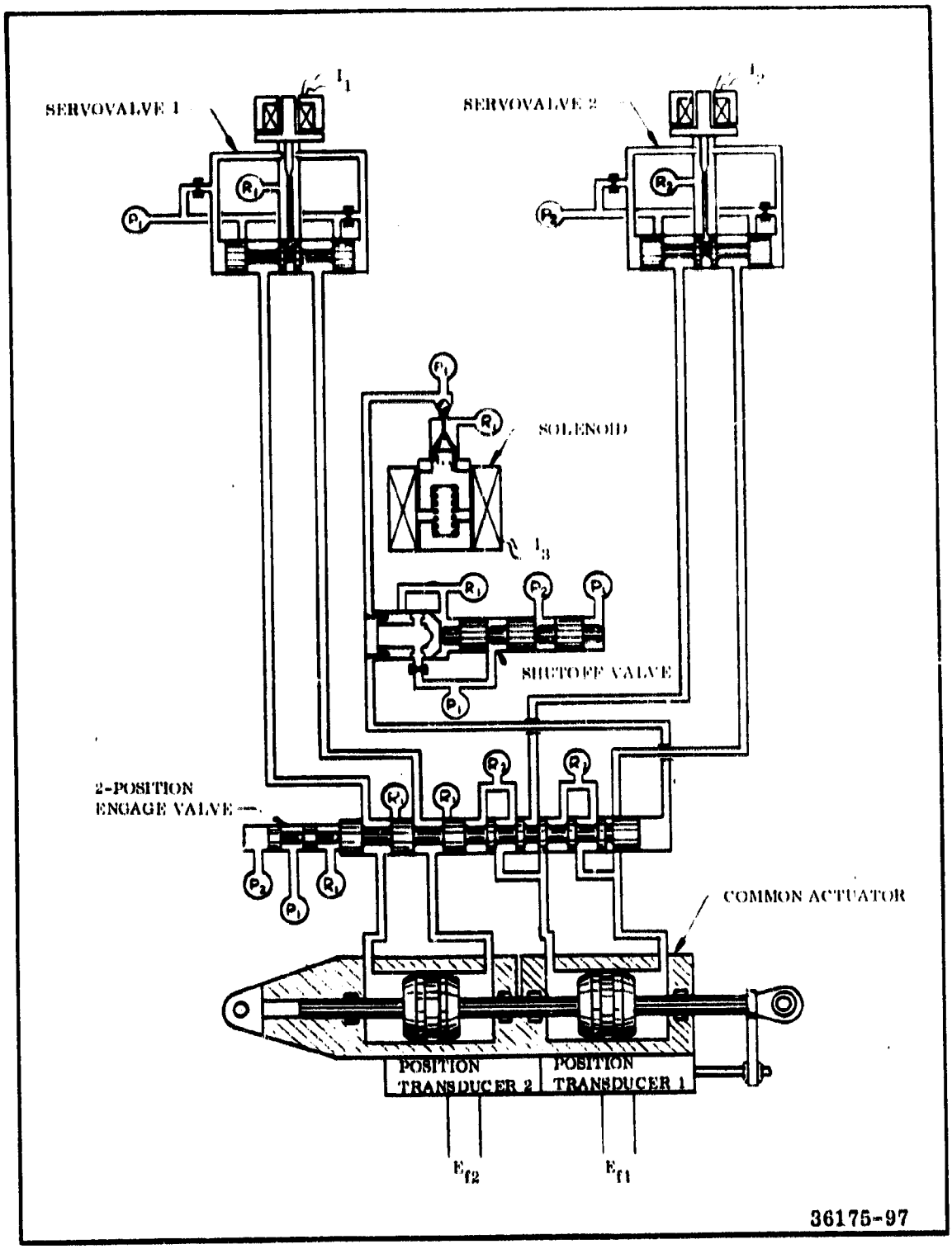

Figure 3-39. System 1, Active/Standby, External Switching Actuator

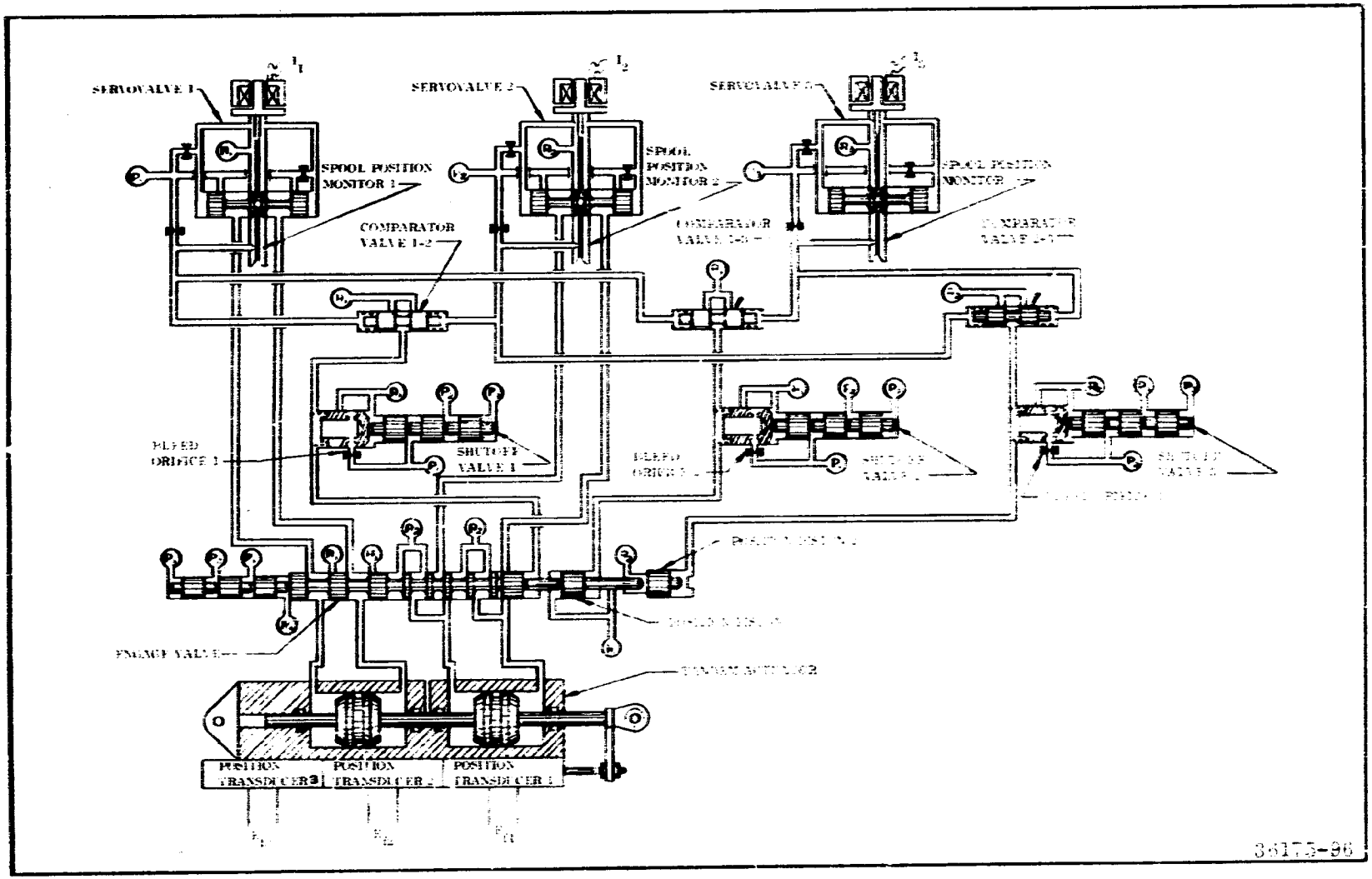

Figure 3-40. System 2, Triple Channel, Majority Voting Actuator

3. Monitoring and logic kept in the hydraulic energy media is relatively insensitive to environmental conditions.

4. The monitoring system is insensitive to load variations in the output ram.

System No. 2 has the following general unfavorable characteristics

1. A third servovalve is required as a monitor.

2. Three hydraulic comparators and shutoff valves are required.

3. A third independent hydraulic power supply is required.

4. A third position transducer and servoamplifier are required.

System No. 3--Active/Standby - Dual Channel - Internal Switching

System No. 3 shown in Figure 3-41 consists of two independent systems with complete hydraulic isolation controlling a tandem actuator. Only one system controls the actuator at a time. With a malfunction in the controlling system, an automatic internal switch to a fully operational standby system is made, thus eliminating any loss in output force or performance degradation. System No. 3 has the general favorable characteristics of System No. 2 while requiring only two independent hydraulic systems. System No. 3 has the following general unfavorable characteristics.

1. A fourth servovalve is required.

2. Two comparators and two shutoff valves are required.

3. A fourth position transducer and servoamplifier are required.

System No. 4--Active/Standby - Triple Channel - Internal Switching

System No. 4 shown in Figure 3-42 consists of three independent systems with complete hydraulic isolation controlling a triple tandem actuator. Only one channel controls the actuator at a time. With a malfunction in the controlling system, an automatic internal switch is made to the fully operational standby system. The obvious advantage of System No. 4 over System No. 3 is that the actuator can withstand three failures before the actuator is rendered useless.

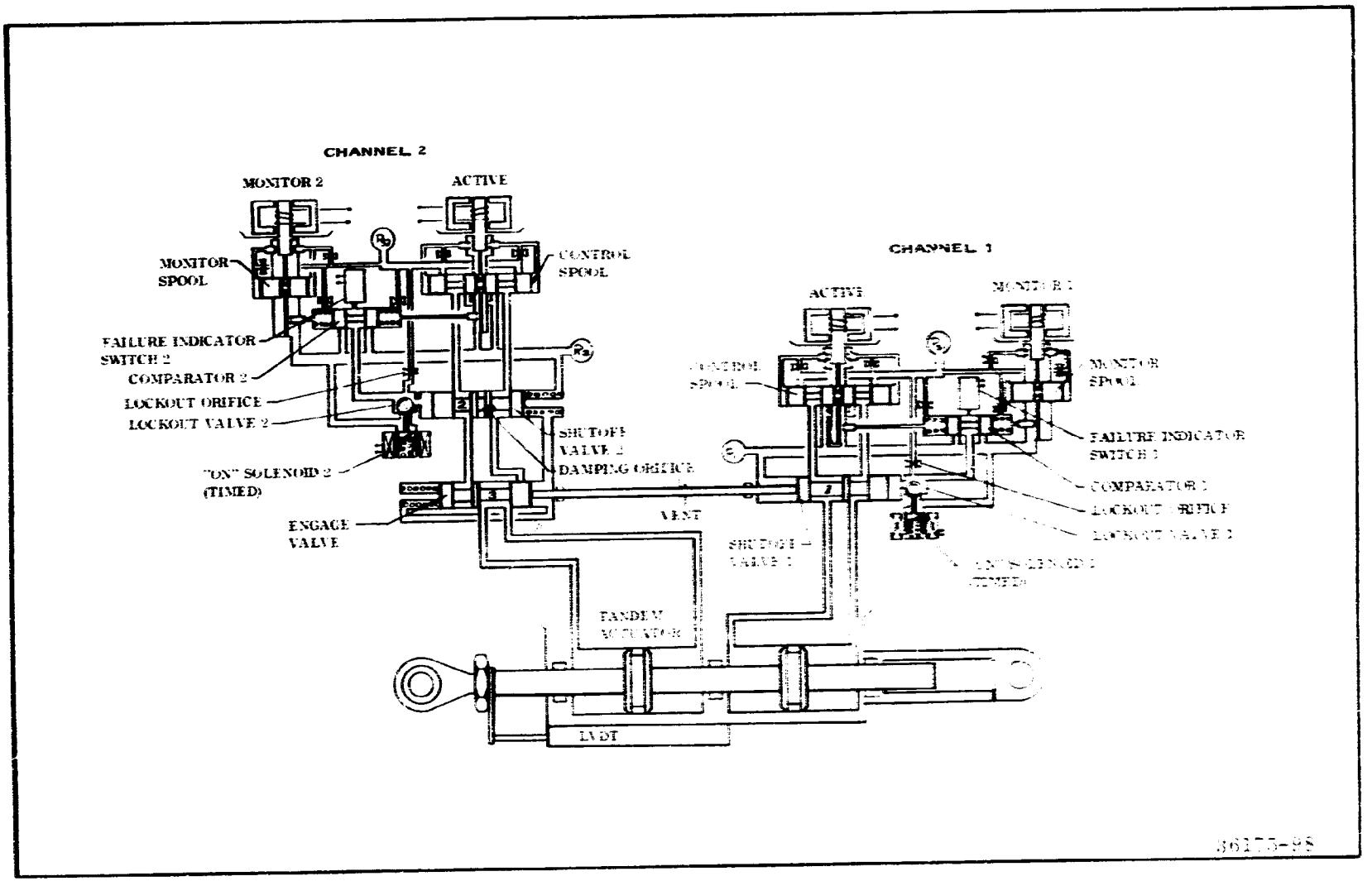

Figure 3-41. System 3, Active/Standby, Dual Channel, Internal Switching Actuator

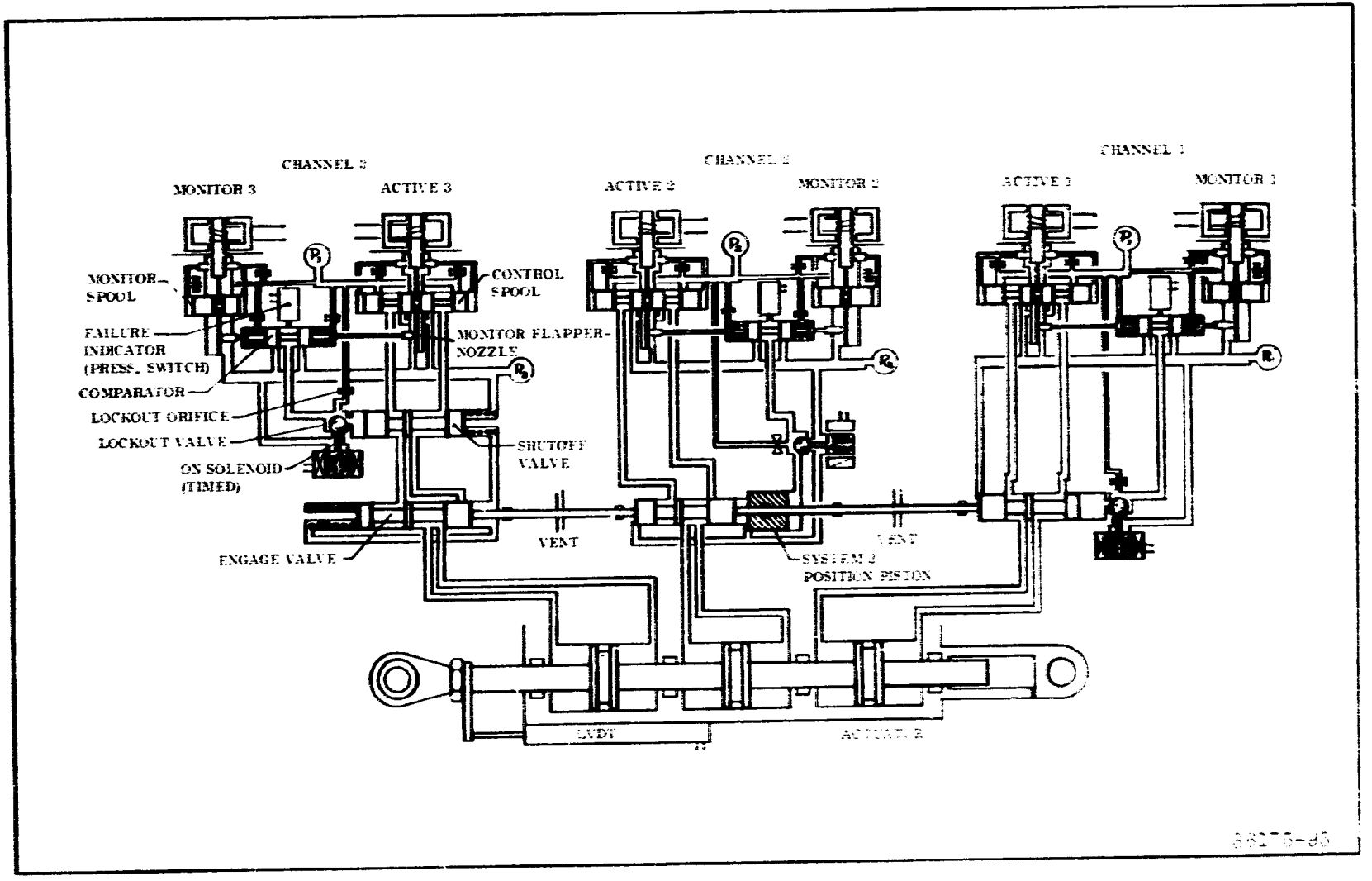

Figure 3-42. System 4, Active/Standby, Triple Channel, Internal Switching Actuator

System No. 4 has the following general unfavorable characteristics:

1. Six servovalves are required.

2. Six feedbacks are required.

3. Six servoamplifiers are required.

4. An additional comparator and shutoff valve are required.

In the following discussion, each of the four redundant systems are evaluated on the basis of weight, reliability, ease of development, ease of manufacturing, simplicity, ease of maintenance, and cost. The effects of actuator redundancy requirements upon additional HPU requirements are also discussed.

Weight

As shown in Table 3-24, the TVC actuator weight for the four redundant systems is relatively constant due to the large weight of the power ram. However, there is a significant weight penalty when considering Systems 2 and 4, since these systems require a third HPU based on the actuator redundancy mechanization. For System No. 2, the additional HPU could be a low power unit since its only function is to provide hydraulic power to the monitoring system.

Reliability

A reliability summary is presented in Table 3-25. With the minimum reliability requirement given as 0.9999, all four systems exceed the minimum reliability requirements. The mean time between failures (MTBF) for all redundant systems exceeds 5,000 hr.

Ease of Development

All of the actuators considered in this tradeoff study have been fabricated and tested. There appears to be no hidden development risks. Only a modest scale-up due to hydraulic flow rate is required. The systems with their corresponding backgrounds are as follows:

1. Active/Standby - External Switching (developed by LTV Electro System for the X20 Dyna-Soar Space Glider).

2. Triple Channel - Majority Voting (developed by Hydraulic Research and proposed for C5A and SST).

3. Active/Standby - Dual Channel - Internal Switching (actuator developed by Hydraulic Research).

TABLE 3-24

TVC SYSTEM EVALUATION

TVC Actuator Evaluation Category	Weighting Factor	System Number 1 Rating	1 Weighted Rating	2 Rating	2 Weighted Rating	3 Rating	3 Weighted Rating	4 Rating	4 Weighted Rating
Weight	5	1.00	5.00	0.96	4.80	0.94	4.70	0.73	3.65
Reliability	25	0.90	22.40	0.98	24.50	0.96	24.00	1.00	25.00
Ease of development	10	1.00	10.00	0.90	9.00	0.95	9.50	0.85	8.00
Ease of manufacture	5	1.00	5.00	0.95	4.75	0.95	4.75	0.90	4.50
Simplicity	20	1.00	20.00	0.67	13.40	0.51	10.20	0.35	7.00
Ease of maintenance	10	1.00	10.00	0.95	9.50	0.95	9.50	0.90	9.00
Cost	25	1.00	25.00	0.88	220	0.81	20.20	0.70	17.50
Total TVC actuator			88.40		87.95		82.85		75.12
Relative TVC actuator rating			1		2		3		4
HPU evaluation category									
Weight	5	0	0	-100	-500	0	0	-300	-1,500
Simplicity	20	0	0	-50	-1,000	0	0	-300	-6,000
Cost	25	0	0	-42	-1,050	0	0	-94	-2,350
Total HPU			0		-2,550		0		-9,850
Relative HPU rating			1		3		1		4
Total TVC system			88.40		-2,462.05		82.85		-9,774.88
Total TVC system rating			1		3		2		

TABLE 3-25

TVC SYSTEM RELIABILITY SUMMARY*

System	Reliability - First Failure	Mean Time to First Failure (hr)	Reliability - Second Failure	Mean Time Between Failure (hr)	Relative Reliability
0	0.998544	343	0	343	0.06
1	0.998538	340	0.9999121	5,688	1
2	0.996589	116	0.9999975	200,000	35
3	0.998296	587	0.9999960	125,000	22
4	0.998296	587	0.9999980	250,000	44

*Reliability analysis based on 30 min operation.
System "0" is nonredundant electrical feedback.

4. Active/Standby - Triple Channel - Internal Switching (actuator developed by Hydraulic Research and Evaluated by NASA for the Space Shuttle).

Ease of Manufacture

All of the systems considered are complex devices requiring many manufacturing steps. The total number or major components and assemblies provide the basis for this evaluation. An increase in redundancy requirements reduces the ease of manufacture.

Simplicity

As the degree of redundancy increases, the relative simplicity decreases due to the increased number of components. There is a significant simplicity penalty when considering Systems No. 2 and 4 due to the requirement of a third HPU to provide the required actuator redundancy.

Ease of Maintenance

The maintenance evaluation assumes that the primary activities will involve system checkout of control functions. All actuators are considered line replaceable items. Due to the increased redundancy requirements, System No. 1 has the highest rating.

Cost

The redundancy requirements increase the cost of the TVC actuator. The basic assumptions are that the servovalve production cost is $1,200 and the HPU production cost is $50,000. Again, there is a significant cost penalty for Systems No. 2 and 4 due to the requirement of a third HPU to provide the required actuator redundancy.

Table 3-24 summarizes the ratings previously discussed and applies the weighting factors to establish total weighted ratings for each system. Following is a listing of the relative standings of the various systems, together with the total weighted rating. Ratings are based on a maximum possible total score of 100. Negative numbers reflect penalties due to the requirement of having a third HPU to provide the required actuator redundancy.

System No. 1	Active/Standby - External Switching	88.40
System No. 3	Active/Standby - Dual Channel - Internal Switching	82.85

System No. 2	Triple Channel - Majority Voting	-2,462.05
System No. 4	Active/Standby - Triple Channel - Internal Switching	-9,524.88

Based on the foregoing evaluation, both System No. 1 or System No. 3 are suitable for the Space Shuttle booster TVC system. However, System No. 3 is recommended because of its internal failure detection and correction techniques. This internal detection and correction technique reduces large vehicle transients that would be caused by external sensing of attitude rate. Error detection for System No. 3 is ahead of the power ram rather than wholly within the vehicle guidance system or flight crew systems.

3.4.2.2.1.3 Hydraulic Power Unit

The selection of a flexible bearing necessitates the requirements for a suitable actuation and control scheme. Preliminary design studies and applicable tradeoffs by the aerospace industry indicate that several attractive methods can satisfy the 156 in. Space Shuttle booster performance requirements. Evaluation of these studies for the baseline hydraulic power supply reveals that redundant monofuel powered turbine driven hydraulic systems best satisfy the manrated Space Shuttle boosters needs. The rationale and credibility criteria are summarized in Table 3-26. Schematic representation of the entire baseline nozzle actuation and control system is shown in Figure 3-43. A general arrangement layout of the major equipment locations is shown in Figure 3-44.

Several types of hydraulic power units (HPU) were considered which could be used to drive the hydraulic servoactuators on movable nozzle systems. The primary candidates are:

1. Solid propellant warm gas generator-turbine-pump.
2. Solid propellant warm gas generator blowdown.
3. Cold gas passive blowdown.
4. Monopropellant warm gas generator-turbine-pump.
5. Warm gas motor pump.

In addition to these systems, several other HPU types were investigated but were not selected as primary candidates. Included in this category are the free piston pump, pneumatic (warm gas) actuators, and the turboactuator.

The free piston pump is essentially a hydraulic pump consisting of a single piston driven by pneumatic pressure (a warm gas generator in this case). The piston is made to oscillate by alternately pressurizing each end of the piston rod. The resulting hydraulic flow is a function of the cyclic rate and the piston area. This system is especially attractive from a weight and simplicity standpoint up to about 40 horsepower.* From the referenced study, the weight of a free piston pump system would be approximately 225 lb for the program under consideration; however, lack of development and consequent confidence was the primary reason for discontinuing study of this type of HPU.

*P. H. Stahlhuth, "Study Determines Uses of Free Piston Pump." Hydraulics and Pneumatics (May 1971), pp 93-96.

TABLE 3-26

HYDRAULIC POWER UNIT (HPU) EVALUATION

Evaluation Category of HPU	Weighting Factor	Systems: Liquid Fuel Turbine Pump (Variable)		Liquid Fuel Turbine Pump (Fixed)		Solid Propellant Turbine Pump (Fixed)		Solid Propellant Turbine Pump (Variable)		Solid Propellant Warm Gas Blowdown		Cold Gas Blowdown		Solid Propellant Warm Gas Motor Pump (Fixed)	
		Rating Factor	Wt of Rating	Rating Factor	Wt of Rating	Rating Factor	Wt of Rating	Rating Factor	Wt of Rating	Rating Factor	Wt of Rating	Rating Factor	Wt of Rating	Rating Factor	Wt of Rating
Weight	5	0.95	4.8	0.9	4.5	0.9	4.5	1.0	5.0	0.8	4.0	0.7	3.5	0.8	4.0
Reliability	25	0.95	23.8	0.97	24.4	0.97	24.4	0.95	23.8	0.97	24.4	0.97	24.4	0.95	23.8
Development Status	10	1.0	10.0	0.95	9.5	1.0	10.0	9.5	9.5	0.9	9.0	0.9	9.0	0.80	8.0
Ease of Manufacturing	5	1.0	5.0	0.95	4.8	1.0	5.0	0.95	4.8	0.95	4.8	0.95	4.8	0.90	4.5
Simplicity	20	0.95	19.0	0.95	19.0	0.96	19.2	0.95	19.0	0.97	19.4	1.0	20.0	0.95	19.0
Ease of Maintenance (Checkout)	10	1.0	10.0	1.0	10.0	0.90	9.0	0.95	9.5	0.5	5.0	0.95	9.5	0.95	9.5
Cost	25	0.95	23.8	0.95	23.8	0.95	23.8	0.92	23.0	0.96	24.0	1.0	25.0	0.95	23.0
			96.4		96.0		95.9		94.6		93.6		96.2		91.8

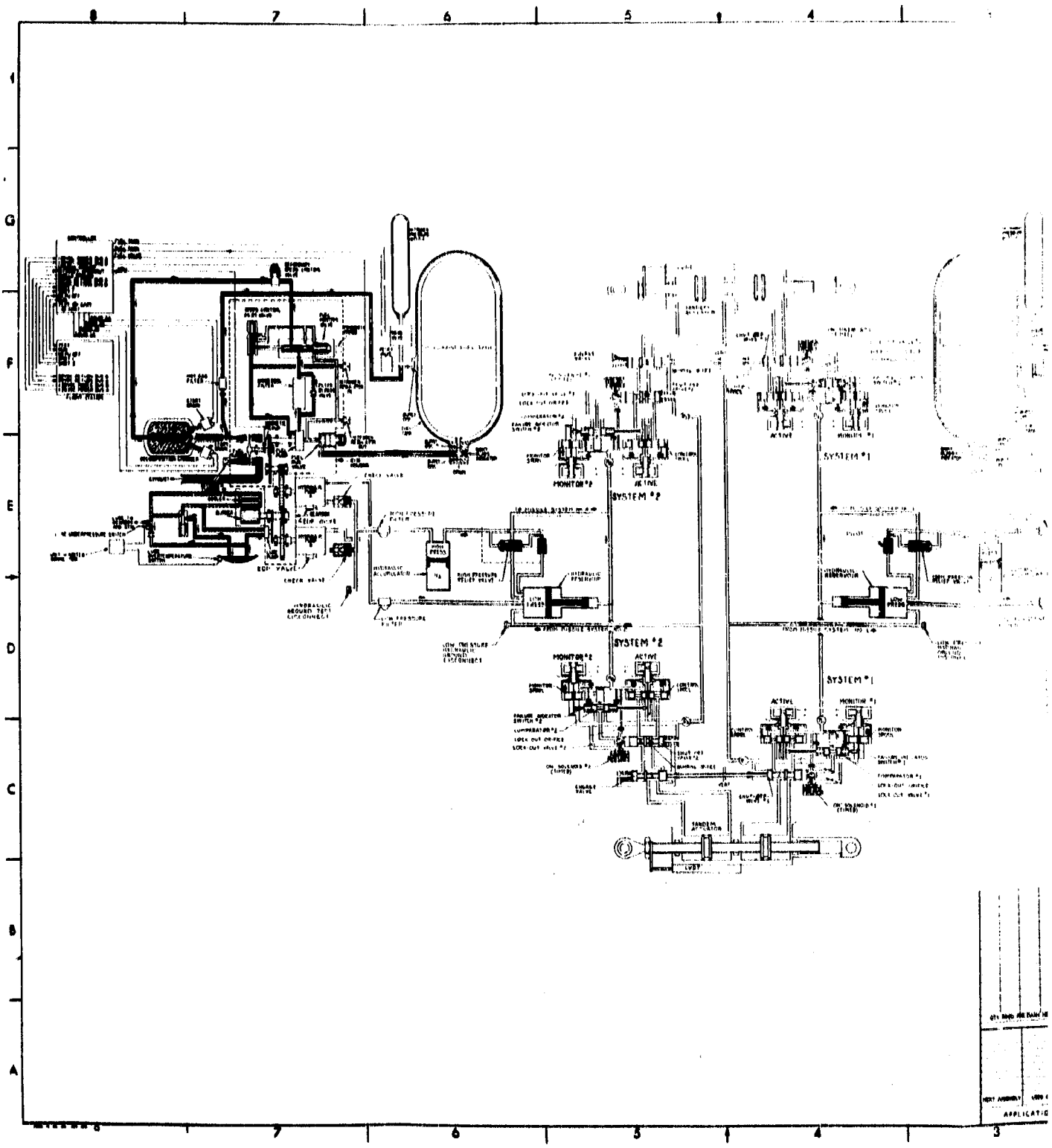

Figure 3-43. Schemat

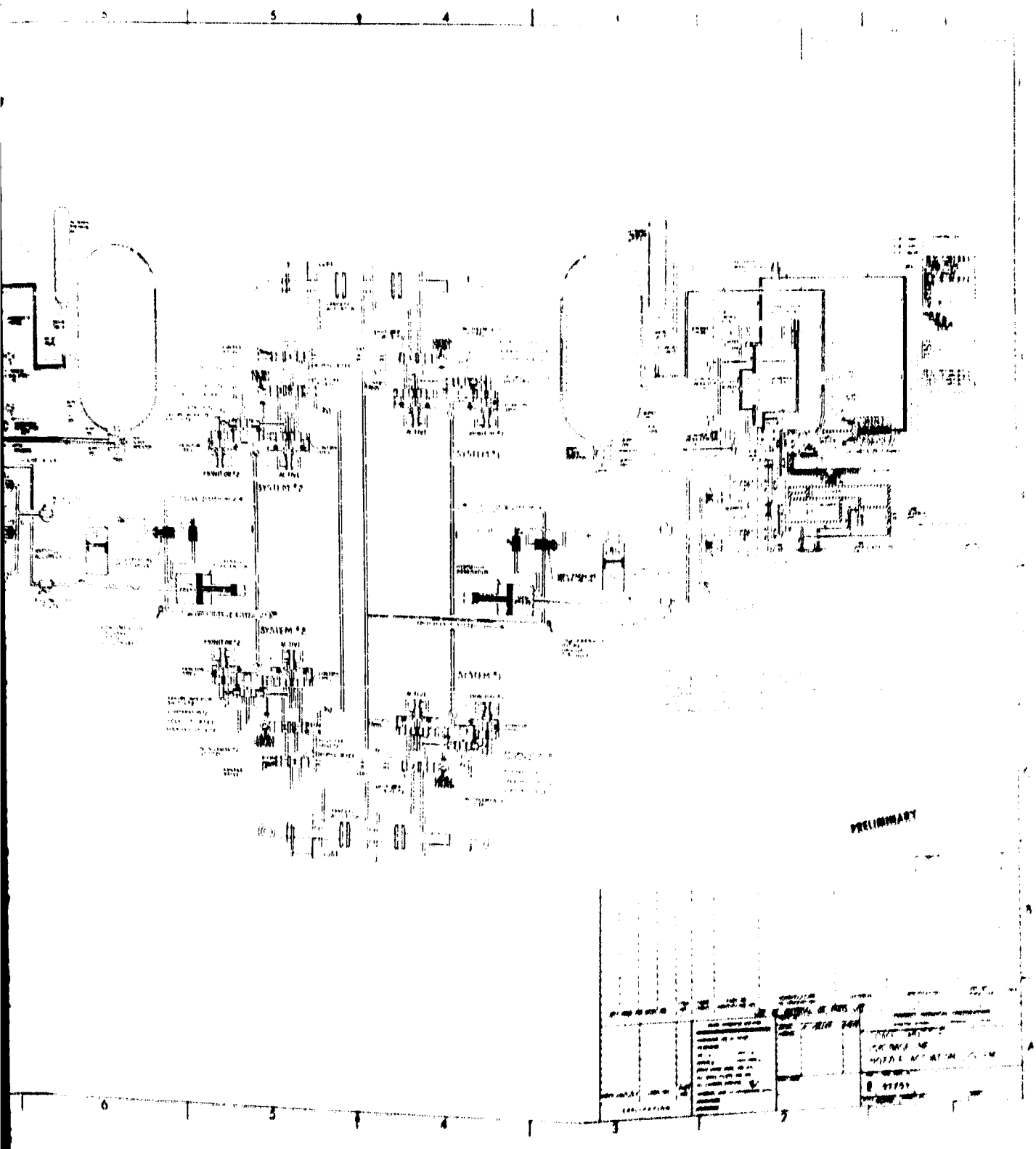

Figure 3-13. Schematic of Complete HPU and Actuation System

FOLDOUT FRAME 1

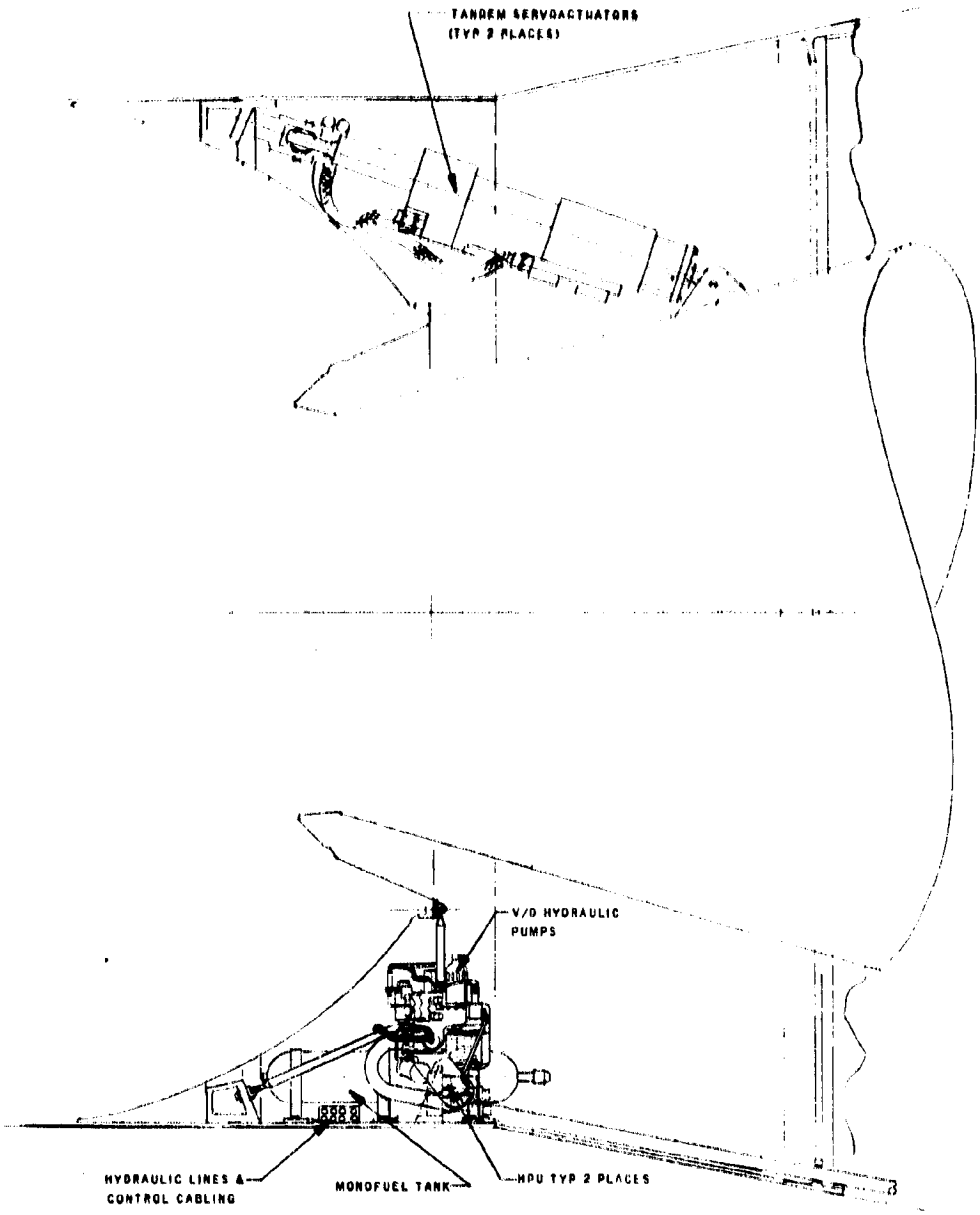

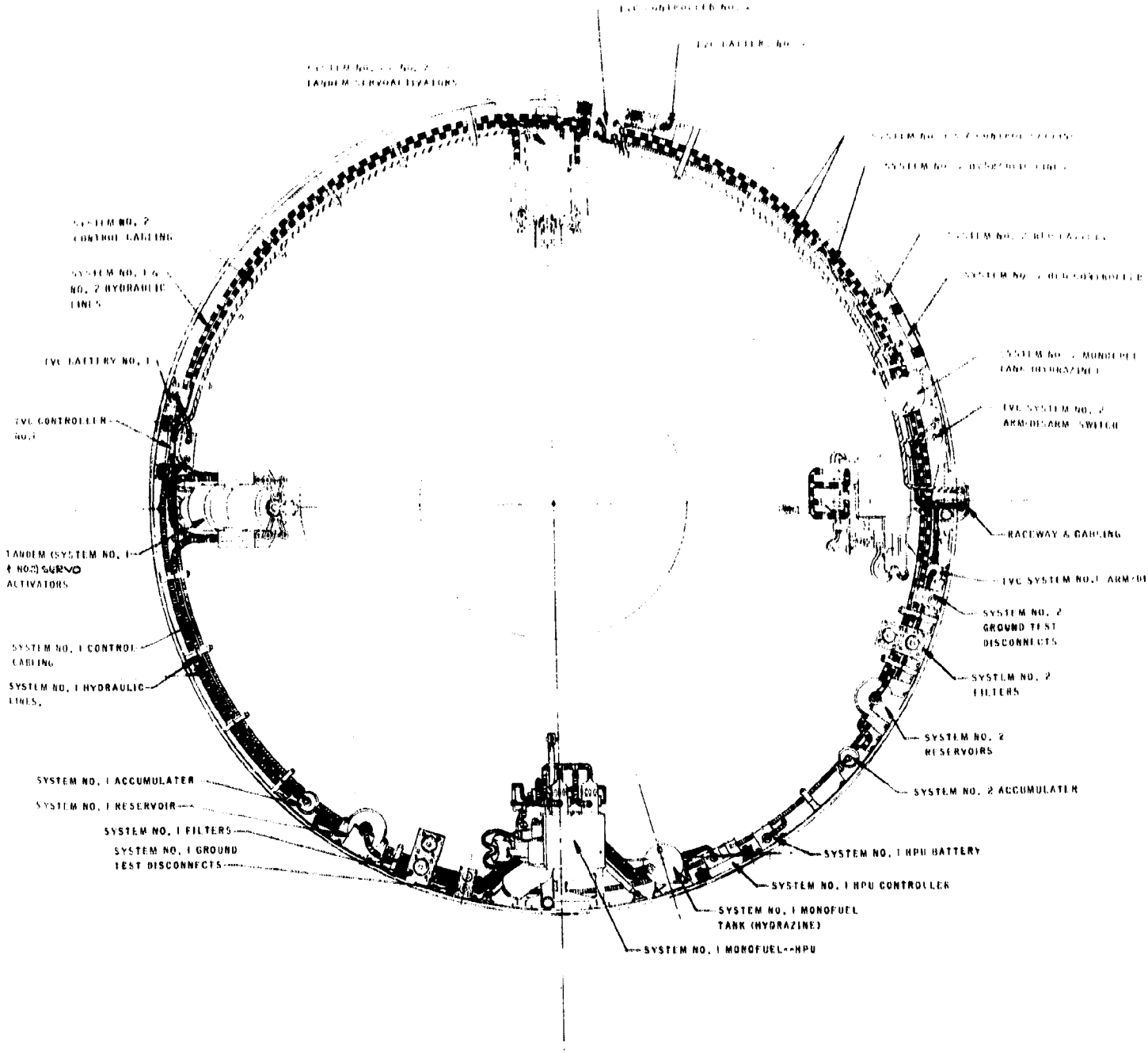

Figure 3-44. TVC System Arrangement

The turbo- and pneumatic actuators were excluded primarily for the same reason. Although there is little doubt that such systems could be developed, it is felt that the development time and risk are not compatible with program requirements. The turboactuator suffers another deficiency in that it is more difficult to obtain redundancy than with other systems.

Solid Propellant Warm Gas Generator - Turbine - Pump

The design and operation of the solid propellant warm gas turbine pump system (WGTP) is similar to that of the selected hydrazine fueled system except that a solid propellant is used as the means of supplying warm gas.

Two variations of the WGTP system were studied. One method used a variable displacement pump (VDP) while the second used a fixed displacement pump (FDP). The VDP has a definite weight advantage over the FDP; however, it is more complex. The VDP discharges hydraulic fluid on demand; consequently during periods of no demand (or very low demand), the pump requires little input power. The turbine, sized to run at maximum load, will tend to overspeed during these low demand periods unless a turbine speed control is incorporated in the design. This speed control, not required with a fixed displacement pump, results in increased complexity.

The fixed displacement pump produces flow at a constant rate throughout its operational period. If there is no demand for flow by the actuators, then the flow is bypassed to the reservoir. The hydraulic power produced by the pump is converted into heat and consequently the oil will increase in temperature throughout the operational time of the pump. For this reason, a large reservoir must be provided so that the oil can absorb the heat produced. Although the VDP and FDP weights are similar, the addition of the large reservoir and hydraulic oil to the FDP system results in a significantly heavier system.

Simplified schematics of the VDP and the FDP system are shown in Figures 3-45 and 3-46, respectively.

Table 3-27 gives a weight comparison of the systems studied. Note that the weights of the actuators, controls, tubing, etc, are not included since it is assumed these components will be common to both systems and have the same weight as long as system pressure remains at 4,000 psi.

The design parameters used to evaluate systems are shown in Table 3-28.

Turbine shaft horsepower is computed by:

$$SHP = \frac{HP}{E_1}$$

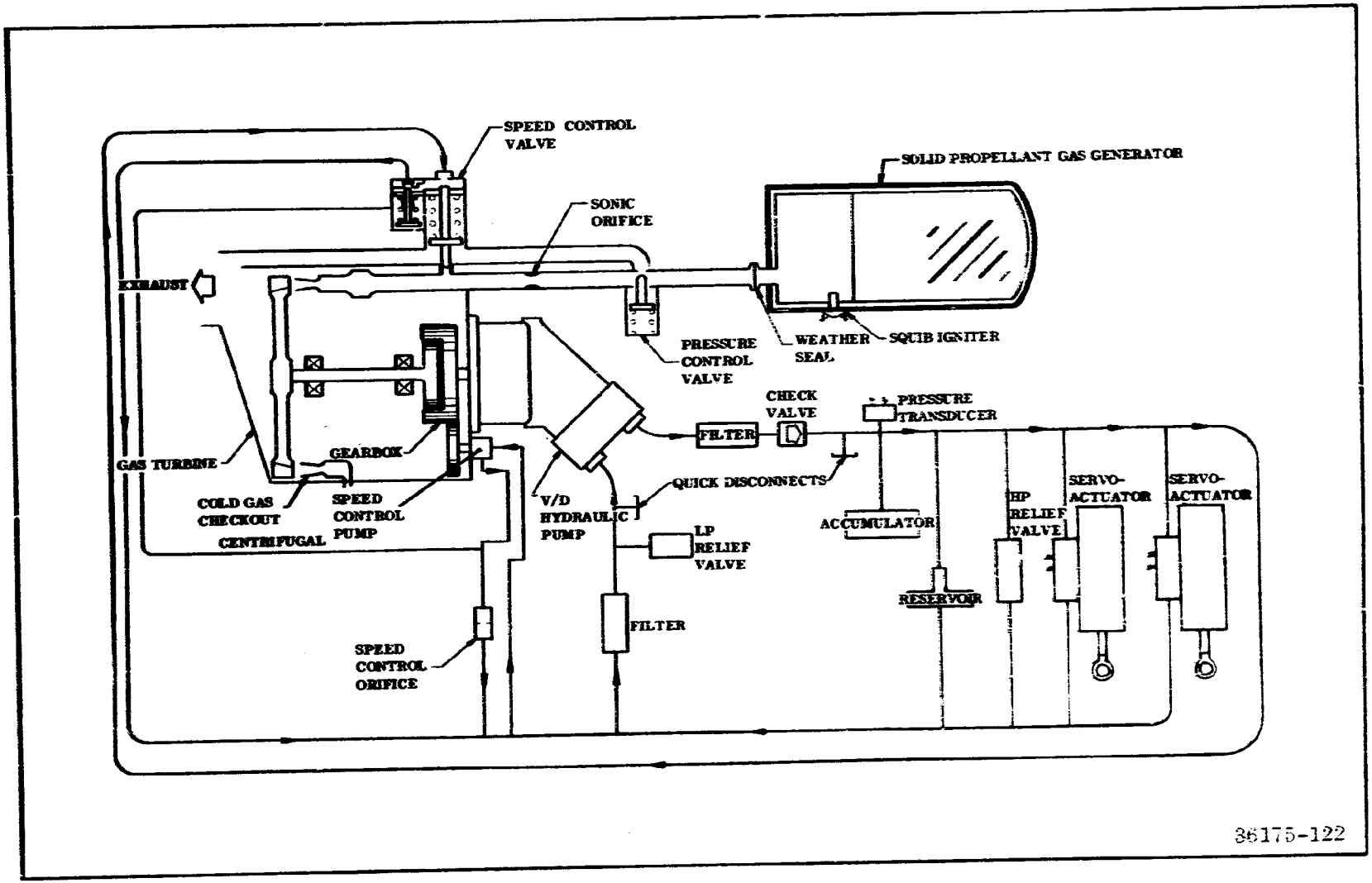

Figure 3-45. Schematic of Variable Displacement Pump Approach

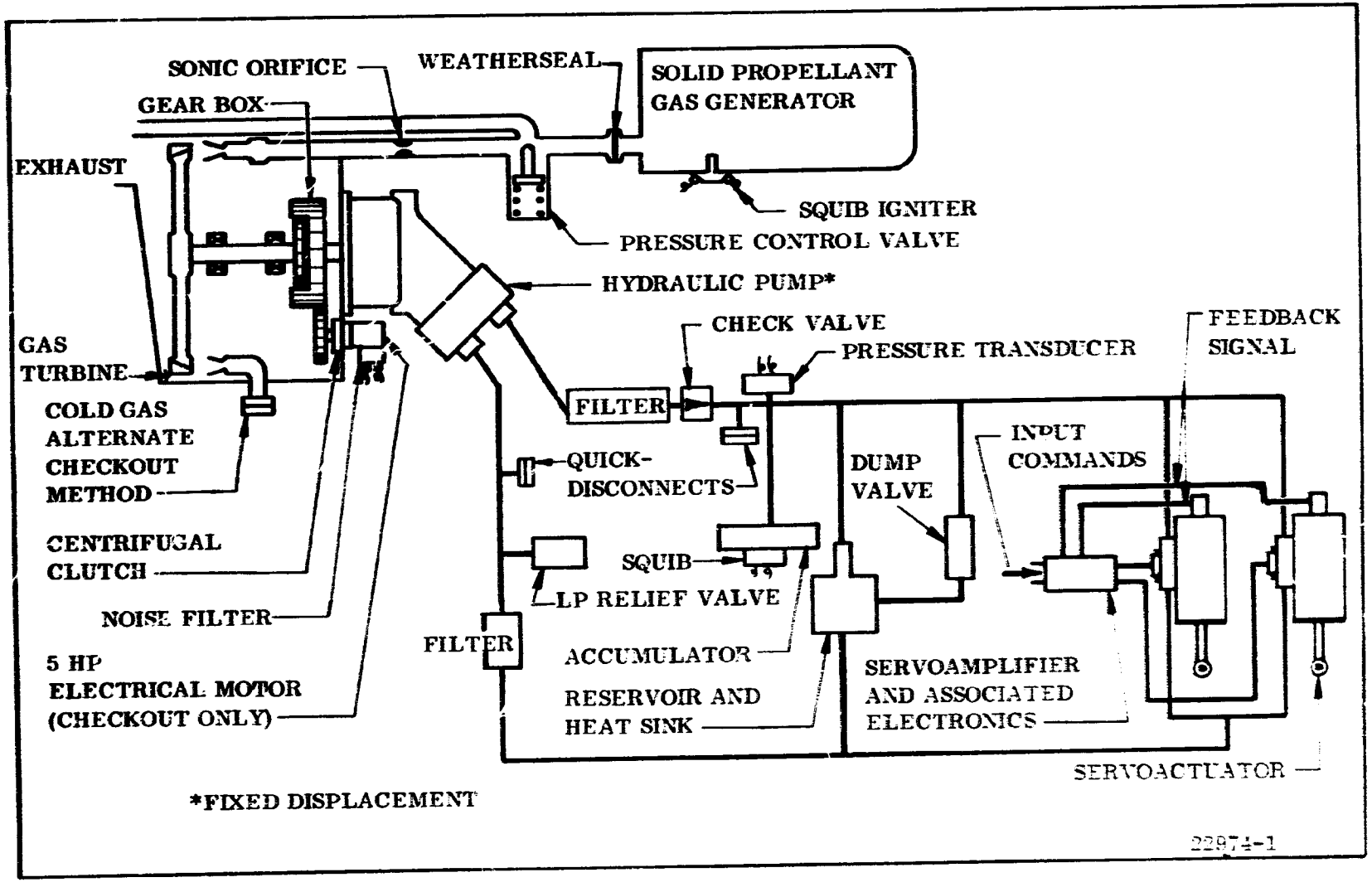

Figure 3-46. Schematic of Warm Gas Turbine Fixed Displacement

TABLE 3-27

WEIGHT COMPARISON OF CANDIDATE HYDRAULIC POWER UNITS

Component	System (lb)						
	Liquid Fuel Turbine Pump		Solid Propellant Turbine Pump		Solid Propellant Warm Gas Blowdown	Cold Gas Blowdown	Solid Propellant Warm Gas Motor Pump
	Variable	Fixed	Fixed	Variable			
Gas generator			50	50	60		109
Pump	13.2	13.2	11.5	11.5			
Turbine-gear box			37	37			
Accumulator	17.5	17.5	17.5	17.5	150		
Reservoir	10.0	30.0	30.0	10.0			
Oil	7.5	50.0	50.0	7.5	76	75.6	
Relief valve			1.0	1.0	1		
Controls	4.4	3.0	3.0				
Fuel	23.7	23.7					
Tank	40.0	40.0				285	
GN_2						92	
Accessories	72.0	68.0				20	
Motor pump							185
Total	188.3	242.4	200	137.5	287	472.6	294

TABLE 3-28

DESIGN PARAMETERS

Parameter	Parallel	Series
Torque (in. -lb)	2.45×10^6	3.08×10^6
Hydraulic horsepower	60.5	77
Actuator area (sq in.)	13.8	17.3
Actuator flow (gpm)	18.5	23.2
Stroke (in.)	± 6.4	± 6.4
Action time (sec)	140	140
Max vector angle (deg)	± 5	± 5
Max slew rate (deg/sec)	5	5
Design horsepower	87	87
"G" loading	3	3

Where - HP is the hydraulic horsepower and E_1 is the pump and gearbox efficiency.

Gas horsepower (GHP) is in turn obtained by dividing SHP by the efficiency of the turbine. Warm gas flow rate ($\dot{W}$) was computed from the equation:

$$\dot{W} = \frac{GHP\ (550)}{Ha_d}$$

Where - Ha_d is the adiabatic head in feet.

The grain weight is then:

$$Wg = \dot{W}\ (t_g + 10)$$

Where - t_g is the action time.

It was assumed that the system would be started approximately 10 sec before launch in order for the system to be up to pressure at the initiation of motor operation. A mass fraction (σ) of 0.75 was used to compute the total weight of the gas generator. This value was used for all cases where the gas pressure was 1,000 psi.

The weight of remaining components was taken from curves used in the Thiokol TVC computer program. This program, "Advanced Thrust Vector Control Preliminary Design Computer Program," produced in 1968 under Contract AF 04(611)-11647, computes the weight of the TVC systems as part of the preliminary design. From Table 3-27 it may be noted that the FDP system is approximately 62 lb heavier than the corresponding VDP system.

Solid Propellant Warm Gas Generator Blowdown

The warm gas blowdown (WGB) system is shown in a simplified schematic on Figure 3-47. The primary components are a solid propellant warm gas generator, relief valve, and a blowdown reservoir.

Knowing the maximum hydraulic flow rate required (Q) from the system, the gas flow from the gas generator is computed from:

$$W = \rho Q$$

Where ρ is the density of the gas.

The weight of the gas generator is computed by the same method as for the turbine systems.

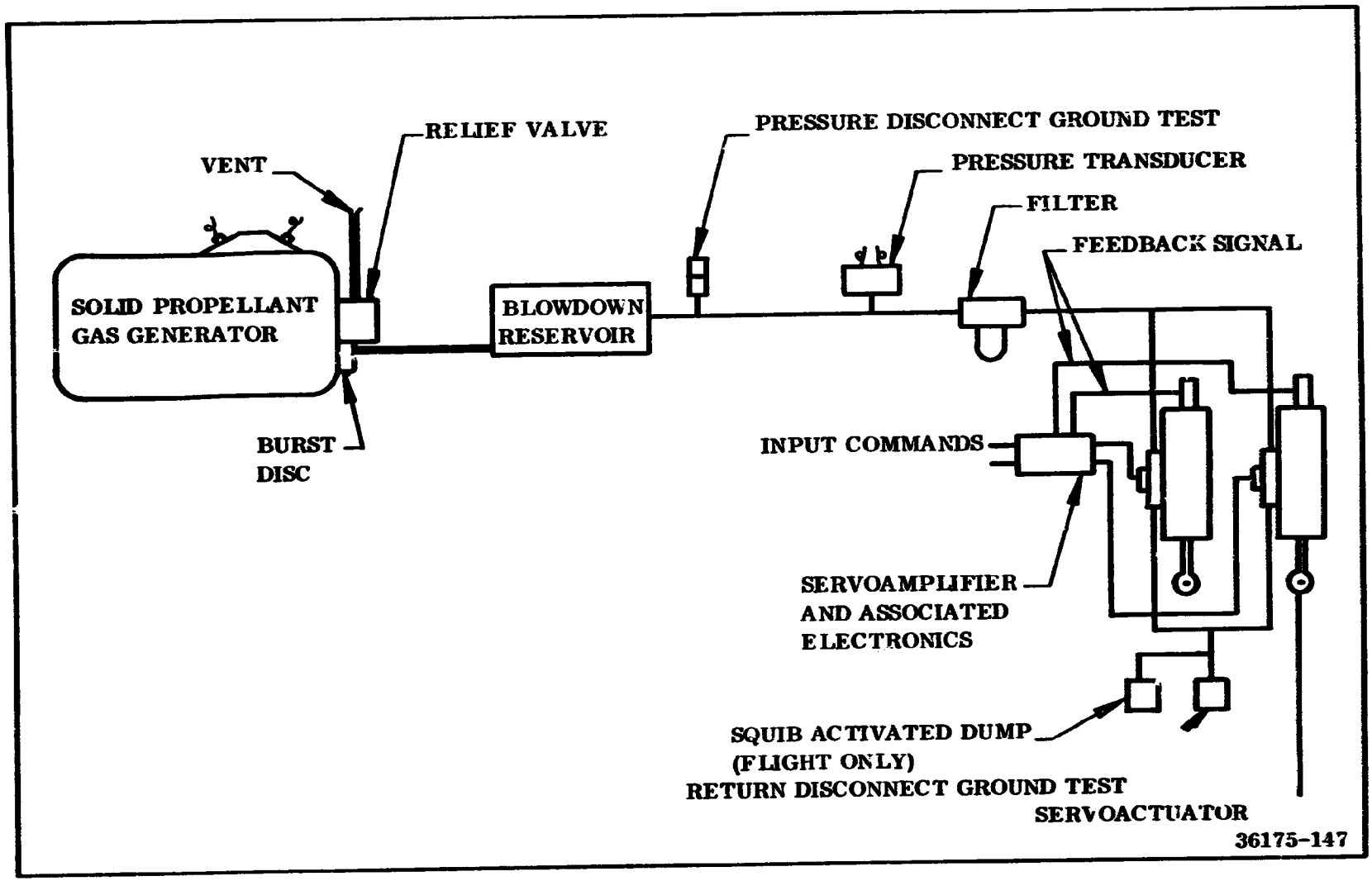

Figure 3-47. Schematic of Warm Gas Blowdown System

The gas generator pressure was assumed to be 3,000 psi and consequently the hydraulic supply pressure would have the same value. This would require slightly larger servoactuators. Although not expected to be great, this factor must be included in the complete tradeoff.

In sizing any blowdown system, a thorough knowledge of the duty cycle must be available. For this study, use was made of the duty cycle used in the design of a TVC system for a 260 in. solid propellant motor under NASA Contract NAS3-12040 in 1969. The duty cycle presented by NASA-Lewis included a 0.2 cps limit cycle oscillation with an amplitude of 0.1 deg.

The volume of fluid displaced is computed by the equation:

$$V = \frac{Ap\ l}{57.3} \int_{t=-10}^{t=+140} (|\dot{S}y| + |\dot{S}p|)\ dt + Q_L t$$

Where:

Ap = actuator piston area, sq in.

l = lever arm, in.

$\dot{S}p, y$ = pitch and yaw rate, deg/sec

Q_L = servovalve leakage flow, cu in./sec

t = time, sec

The integral in the above equation was multiplied by a factor of two to account for the larger vector angle requirement in the present program. It was assumed that servovalve leakage flow is 1 gpm per valve. The total volume of hydraulic oil used is 2,395 cu in. An expulsion efficiency of 95 percent was used to bring the total volume of oil to 2,520 cu in.

The total weight of the WGB system as noted on Table 3-27 is 287 lb. To this must be added a small amount to differentiate between the weight of the actuation for a 4,000 psi system versus a 3,000 psi system. It should also be remembered that any change in duty cycle requirements may considerably change the size and weight of the system. It is relatively simple in that it has few components and moving parts. It has the disadvantage of not being readily adapted to prelaunch checkout; however, provisions can be made for checkout at the additional cost of weight and complexity.

Cold Gas Passive Blowdown

A simplified schematic of the cold gas passive blowdown system (CGB) is shown in Figure 3-48. Pressurized gaseous nitrogen is used as a power source to provide hydraulic flow to the servoactuators. The pressurized gas is stored in the same container as the hydraulic fluid. A hydraulic pressure regulator is located at the outlet of the tank to maintain a constant 3,000 psi pressure to the servosystem. Initial tank pressure is 5,000 psi. During operation the gas expands as fluid is discharged, and at the end of firing the final gas pressure is 3,200 psi. The amount of oil expelled is 2,395 cu in. as was used for the warm gas blowdown system. The total tank volume required is 8,970 cu in.

The weight of the cold gas system is shown on Table 3-27 as 473 lb. This is considerably more than the other systems; however, it has a great advantage because of the simplicity and low cost. It was because of this simplicity and resulting reliability that NASA-Lewis chose a passive CGB system over a turbine system in the study referred to previously.

As with the warm gas blowdown system, the disadvantages are the checkout procedure and the duty cycle limitations. A checkout technique can be designed into the system using a quick disconnect as shown on the schematic. Ground hydraulic power can be attached at that point and used to position the movable nozzle. The duty cycle must be defined with sufficient safety factor to insure an adequate supply of hydraulic fluid.

Liquid Fuel Turbine Pump

This system uses the same components as previous designs except for the gas generator and accessories necessary for the liquid propellant (monofuel) gas generator. For the warm gas liquid fueled generator scheme, hydrazine is used as a fuel and pumped to a catalyst bed by a centrifugal fuel pump. A simplified schematic of the liquid fueled system is shown in Figure 3-49. Fluid is pumped through a fuel valve which controls flow to the catalyst bed and hence to the turbine. The fuel pump can be mounted on a common shaft with the turbine so that it will always turn at turbine speed. The output pressure of the fuel pump is essentially independent of flow but a direct function of pump speed and consequently turbine speed. The fuel valve senses pump output pressure and varies flow to the turbine as a function of this pressure. Thus, turbine speed is controlled and can be maintained at almost constant speed over the entire hydraulic flow range. Low pressure warm gas is bled off at the turbine and fed back to the fuel tank to create a slight backpressure on the fluid. The system is started by firing a cartridge propellant which drives the turbine to its operating speed. This cartridge also raises the temperature of the catalyst bed to assist decomposition of the fuel during startup.

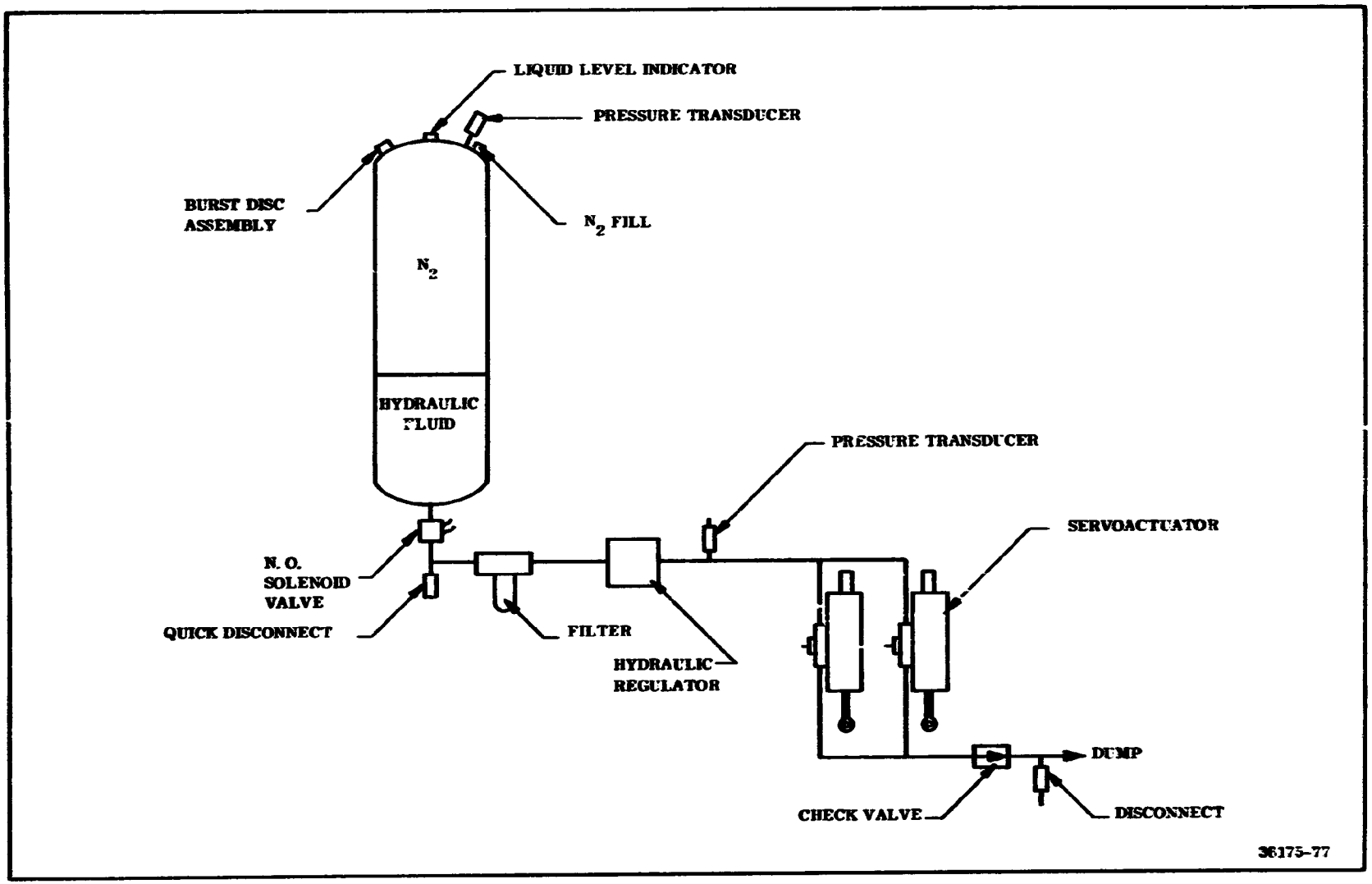

Figure 3-48. Schematic of Passive Cold Gas Blowdown System

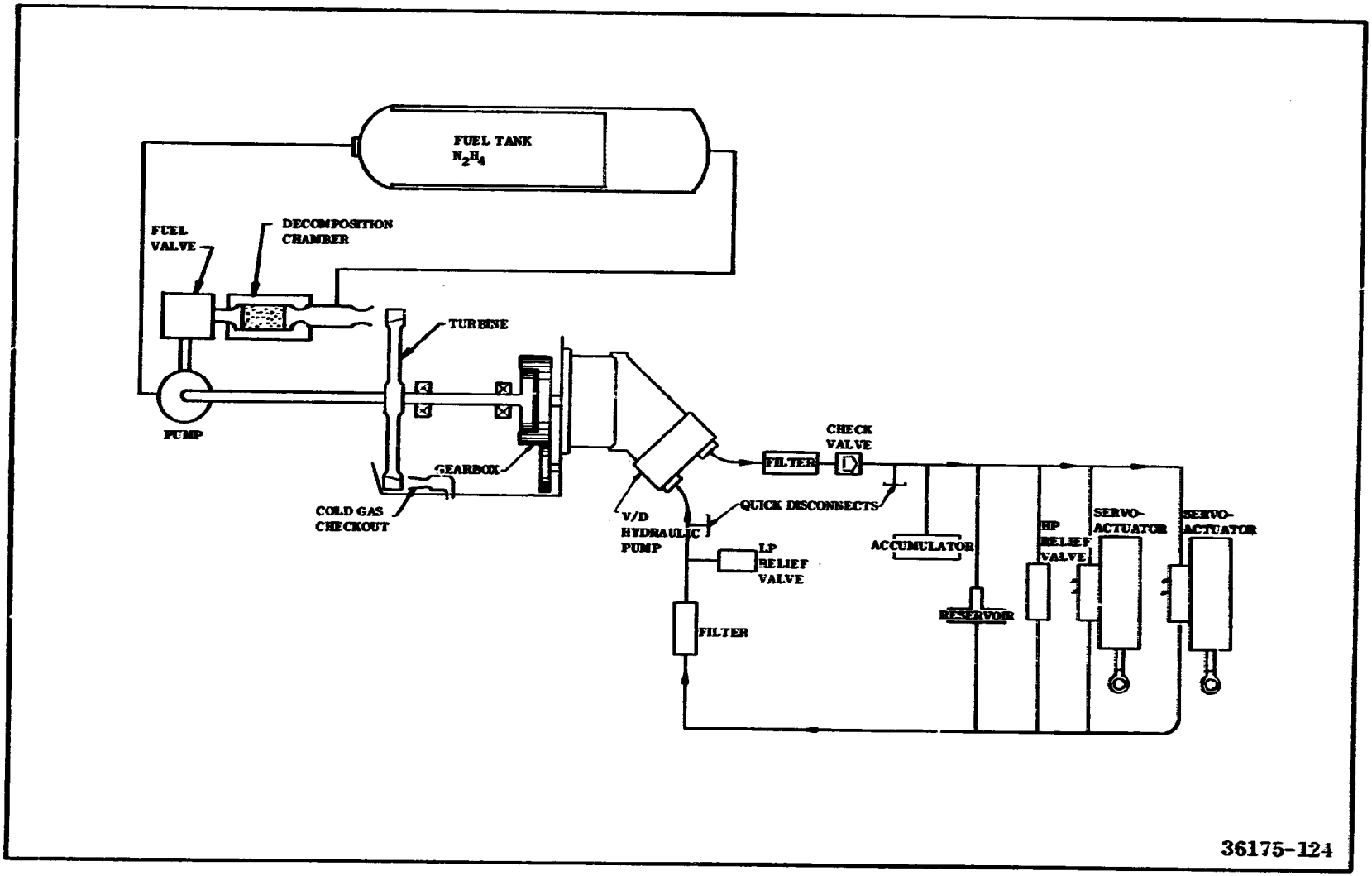

Figure 3-49 Liquid Fuel System (Hydrazine)

The system was sized using both a variable displacement and a fixed displacement pump. Weights are given in Table 3-27. A more detailed description of this system is presented later. System weights were obtained by scaling down the present Concorde system which has a 480 sec operating time to a 150 sec time. The fixed displacement pump version is essentially the same except a larger reservoir is used to absorb the heat generated by the fixed displacement, constant flow hydraulic pump.

Warm Gas Motor Pump System

The warm gas motor pump system consists of an integrated warm gas motor-hydraulic pump. The warm gas motor is powered by a solid propellant warm gas generator. A simplified schematic of the system is shown in Figure 3-50. The integrated system concept lends itself to a favorable packaging arrangement.

A 100 hp unit has been developed by Vickers for application with a Gatling gun drive. The unit has been produced and undergone considerable testing. Warm gas motors, as such, have been designed and tested since 1958 with many improvements since that date. High reliability is obtained since the design is simple and the rotating components operate at relatively low speed.

The weight of the warm gas motor pump system is noted on Table 3-27. The weight of the motor pump includes the warm gas motor, pump, hydraulic reservoir, fluid, valves, etc, as an integrated package. The system was sized using 87 hp and 150 sec duration as with the other HPU's.

Hydraulic Power Unit

The baseline hydraulic power unit (HPU) is composed of four basic modules: the gas turbine module, the gearbox, the turbine controller, hydrazine monofuel tank and supporting hydraulic components (see Figure 3-43). The entire unit is located in the 156 in. solid rocket motor stub skirt, allowing ready accessibility to all components from the aft end of the vehicle. Access doors may be required in the stub skirt for either maintenance or ground checkout of the HPU. The total baseline system weight breakdown for the entire actuation system is shown on Table 3-29.

In reviewing major sources for HPU's applicable to the SRM system needs, it was found that several are available. The first, shown in Figure 3-51, was developed by Sundstrand Aviation for the Concorde SST Aircraft as an emergency hydraulic power unit and has a shaft horsepower rating of 95 hp. The other source is the system that AiResearch Manufacturing Company developed for the Spartan missile application as shown in Figure 3-52. It has a rating of 90 hydraulic hp. Either of these units could be easily adapted to the 156 in. Space Shuttle needs. Thiokol has selected the Sundstrand (monofuel) unit over the AiResearch (solid gas generator) unit because of its current production status, qualification status and its reuse and restart capabilities.

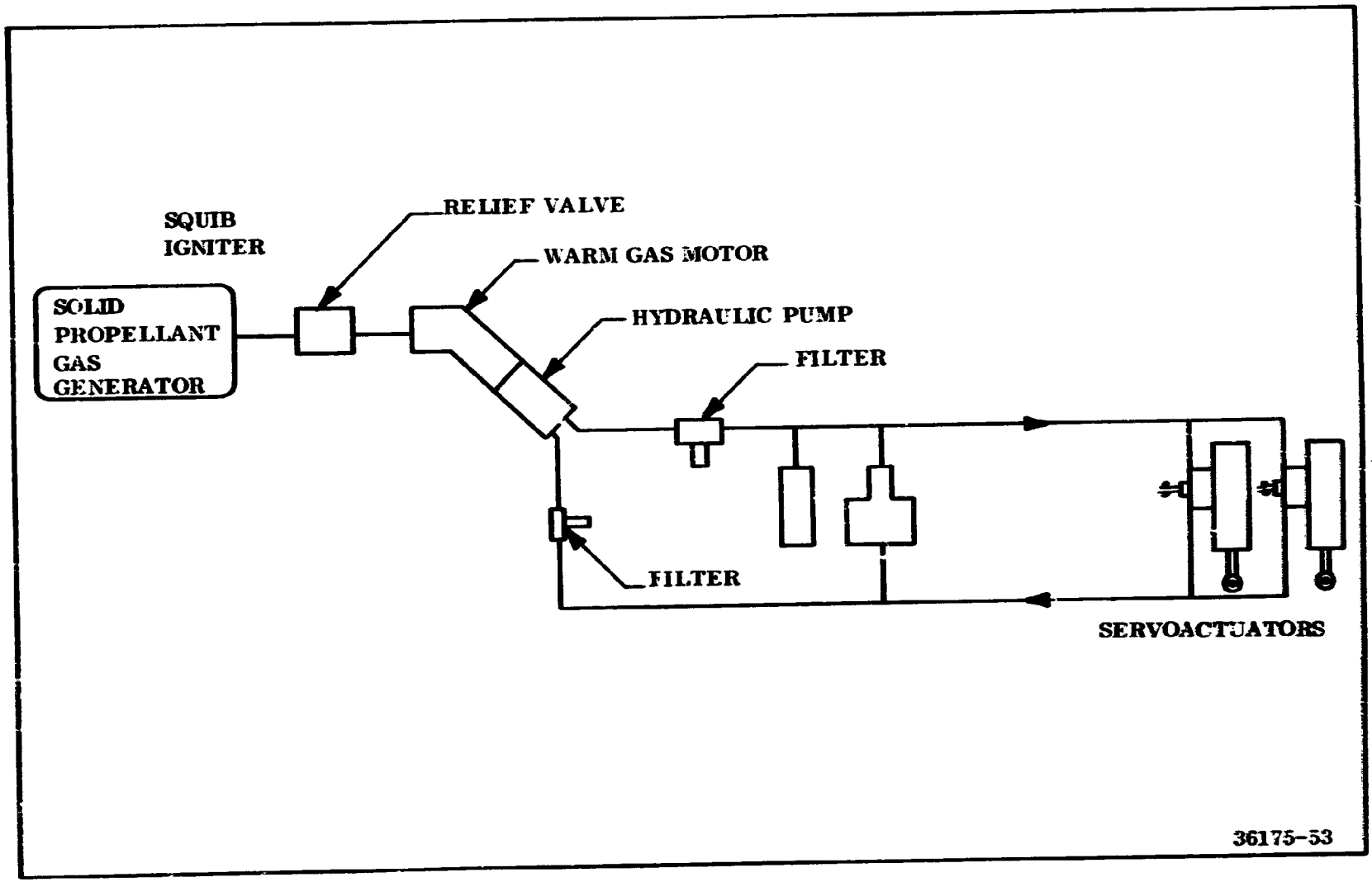

Figure 3-50. Schematic of Warm Gas Motor Pump

TABLE 3-29

TVC ACTUATION SYSTEM WEIGHT ESTIMATE

	System 1	System 2
HPU (Concorde unit)	72 lb	72 lb
Tank (wet) - monofuel 8 min	125	125
HPU controller	5	5
HPU battery	6	6
Hydraulic reservoir (400 cu in.)	15	15
Hydraulic accumulator (200 cu in.)	18	18
High pressure filter (40 gpm)	6	6
Low pressure filter (40 gpm)	6	6
High pressure, quick disconnect (1 in.)	2	2
Low pressure, quick disconnect (1-1/4 in.)	2	2
TVC controller	20	20
TVC battery	6	6
Arm/disarm (2)	4	4
Tandem actuators (2)	312	*
Support for HPU (1 set)	25	25
Support for reservoir (1 set)	8	8
Support for accumulator (1 set)	5	5
Hydraulic tubing (w/fluid)	137	*
Hydraulic fluid	20	*
Miscellaneous supports	150	*
Electrical cabling (1 set)	660	*
Hydraulic pump (2)	30	30
Total	1,634 lb	355 lb
Total Weight	1,989 lb	

*Common to both systems.

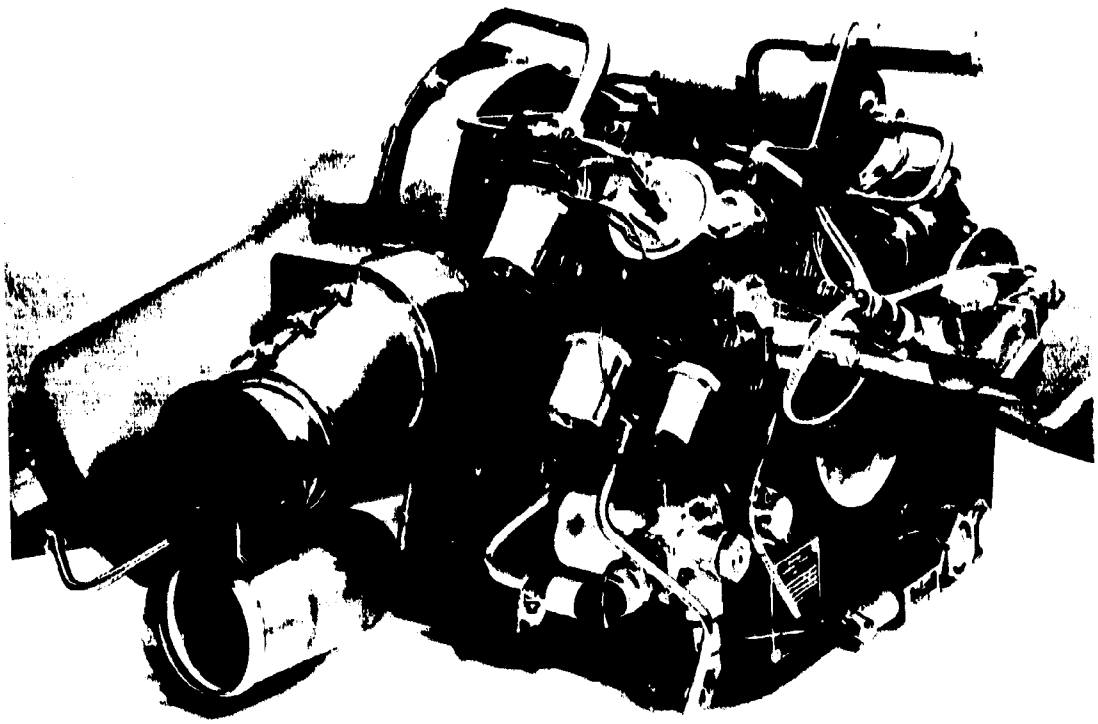

Figure 3-51. Concorde Monofuel Powered HPU

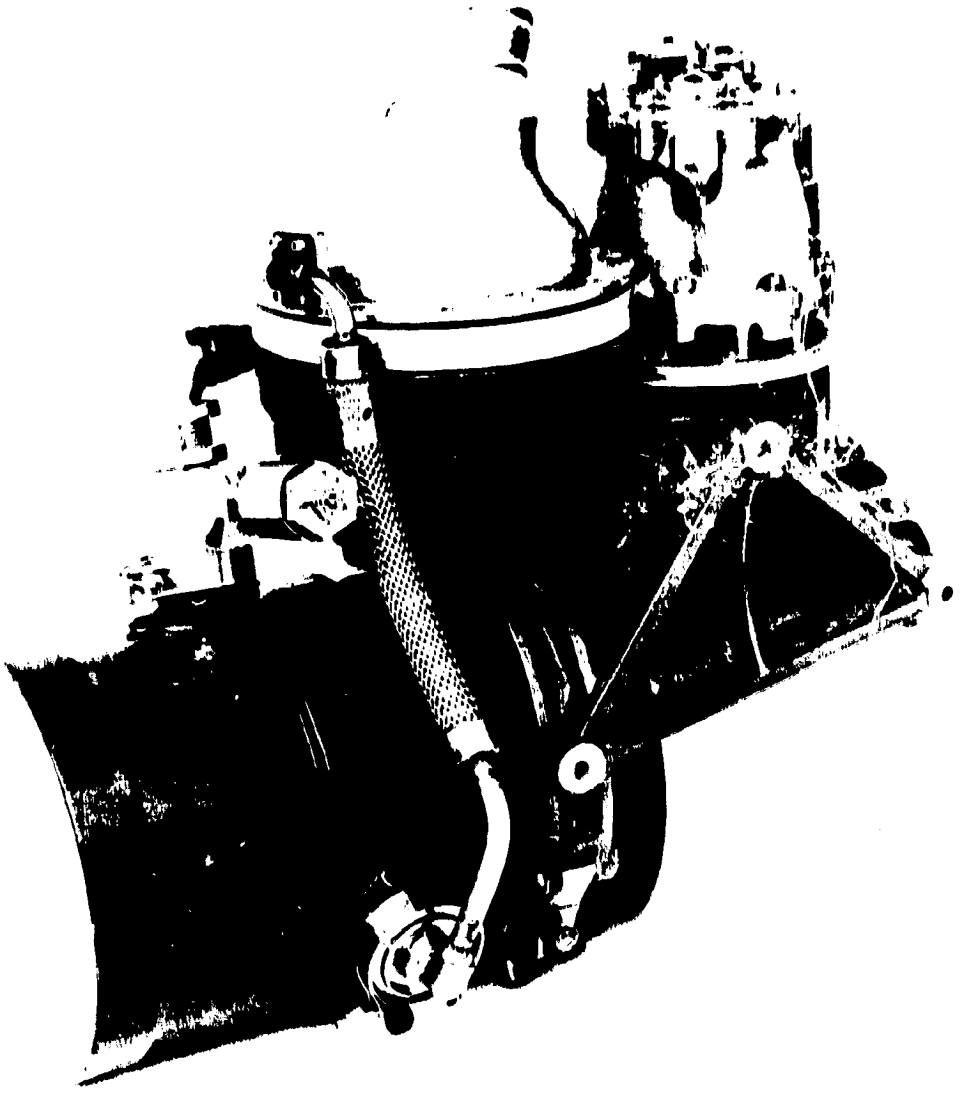

Figure 3-52. Spartan Solid Propellant Powered HPU

Sizing of the prime mover during system design showed that a minimum hydraulic power output capability of 60.5 hp was required. The 95 shaft hp Sundstrand unit selected for this system, when converted through known efficiency factors for hydraulic systems, gives a hydraulic power output of 87 hp, thus providing a comfortable margin over system requirements. This also allows for system versatility and potential growth if needed.

Two alternate HPU systems which offer simplicity over the baseline HPU at the expense of development, cost, and weight have been investigated and are briefly presented here for consideration.

Alternate 1 is a modification of the monofuel (Concorde) HPU. By removing most of the turbine speed control equipment and by operating the turbine against a constant load (fixed displacement pump), major complexity can be eliminated. However, the HPU will become heavier and be limited in operational duration. This approach will require additional hydraulic oil volume in the system to absorb the heat generated during the low vectoring periods. The initial sizing for the differential weight indicated that it will increase by 80 lb per HPU. Figure 3-53 reflects this general configuration.

The major disadvantages to this approach are additional weight, HPU temperature limitation, shorter checkout duration, larger fluid components, and a modest development requirement. The significant advantages are lower complexity and reduced costs.

Alternate 2 consists of identical equipment as Alternate 1 except the prime mover fuel is a solid propellant. Being a constant load turbine driven system the weight will increase by 80 lb for the necessary heat absorption during low vectoring periods.

This approach is the simplest turbine driven HPU available. Currently, the Nike-Zeus, Poseidon, and Spartan missiles use this type of prime mover. The major disadvantages are additional weight, single start capability, limited checkout, larger fluid components and a modest development effort. The significant advantages are maximum simplicity, lower costs and good historical data. This system is shown in Figure 3-54.

The baseline HPU serves as the source of hydraulic power for operation of the 156 in. solid rocket motor thrust vector control nozzle. The power derived from hot gas driving a turbine wheel is transmitted through an integral gearbox to the hydraulic pump. Actuation of the gas turbine motor may be automatically induced by launch control sequence circuitry or it may be actuated by a manual signal from the launch console. The present unit will provide 8 minutes of full power output. The dual squib arrangement provides a second start capability. To prevent firing of the gas turbine motor while the vehicle is still on the launch pad, an arm/disarm switch has been provided for arming the system from the launch control sequence.

FOLDOUT FRAME

FOLD

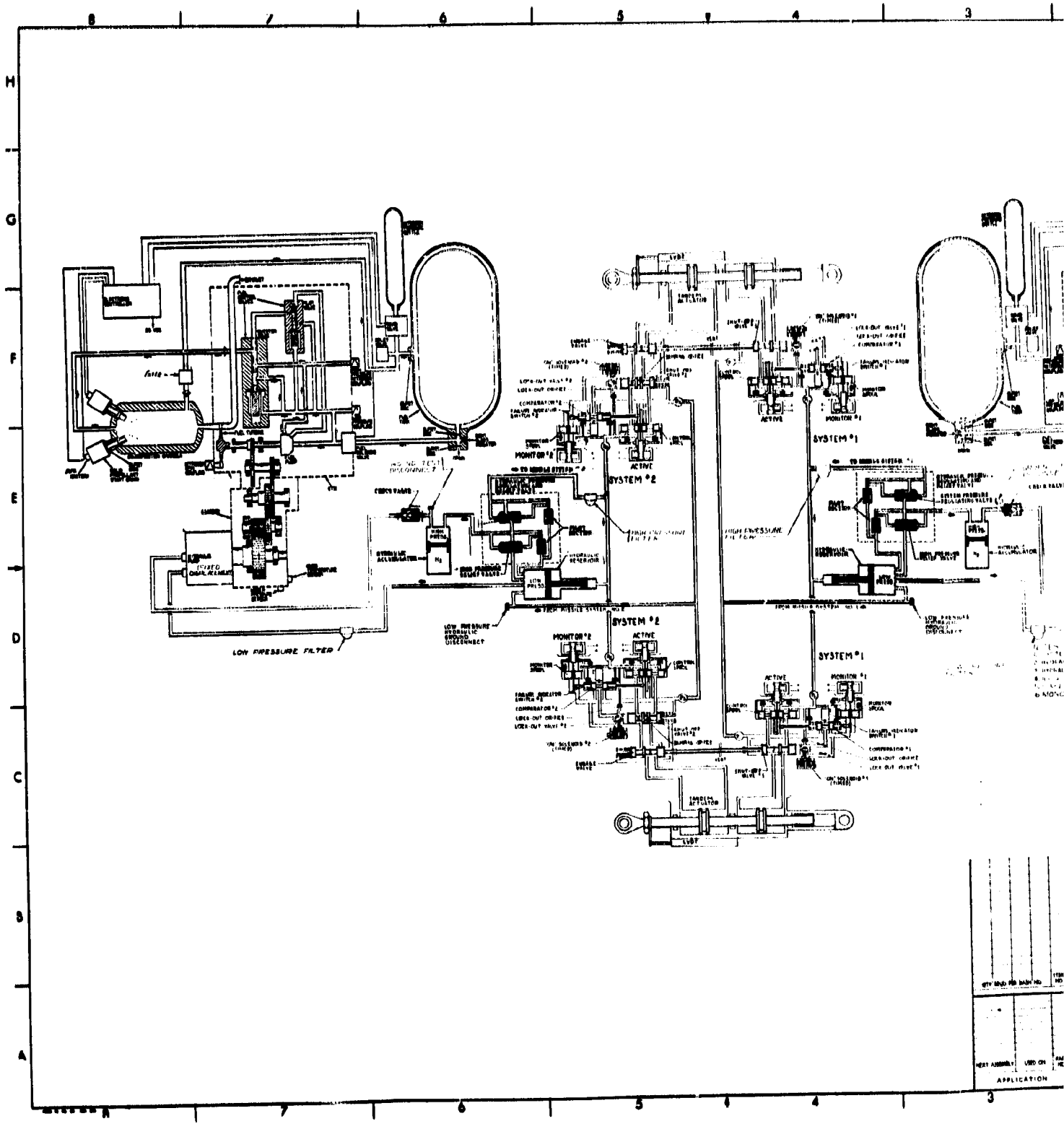

Figure 3-53. Schematic of Alterna

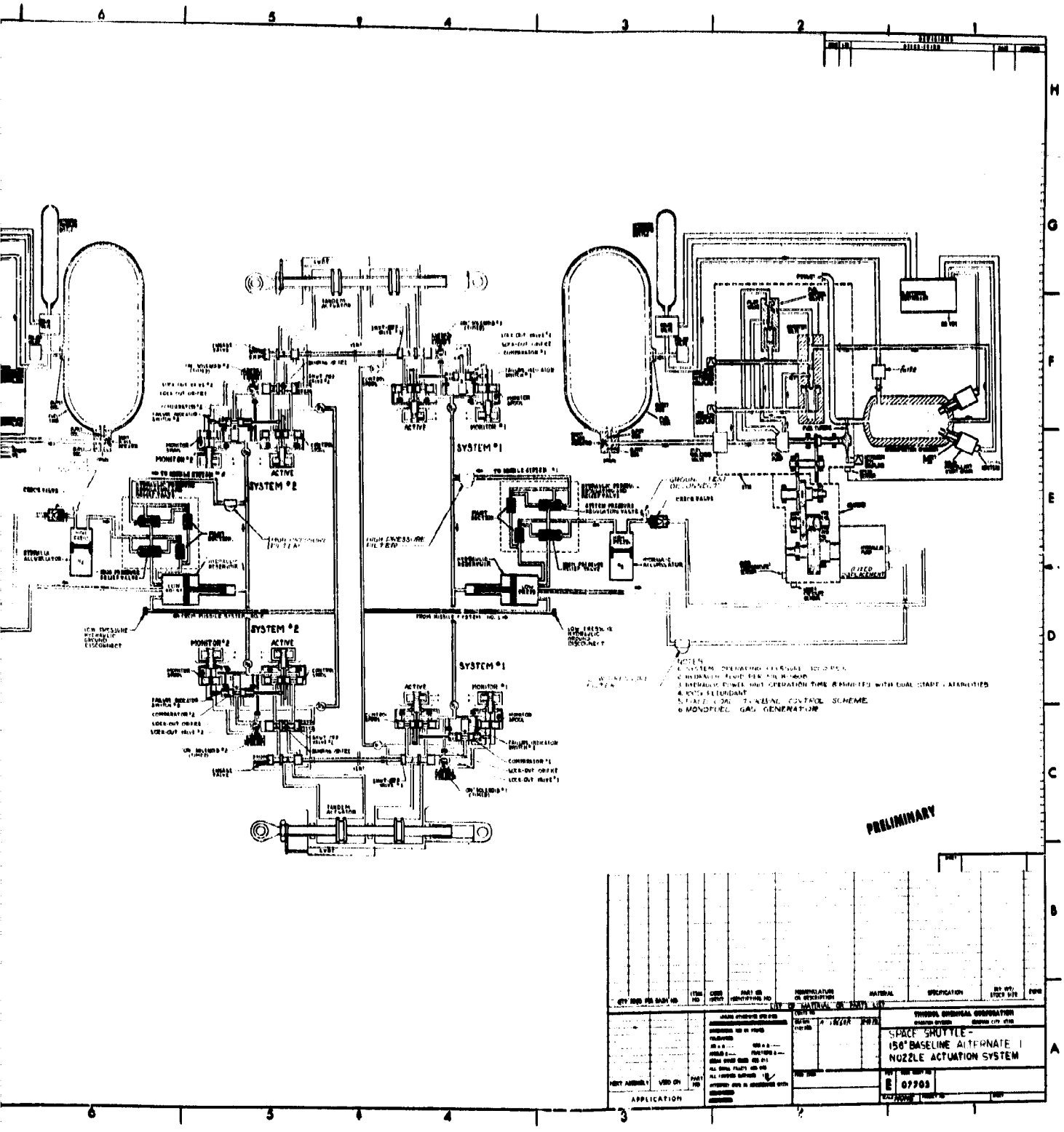

Figure 3-53. Schematic of Alternate No. 1, Nozzle Actuation System

FOLDOUT FRAME

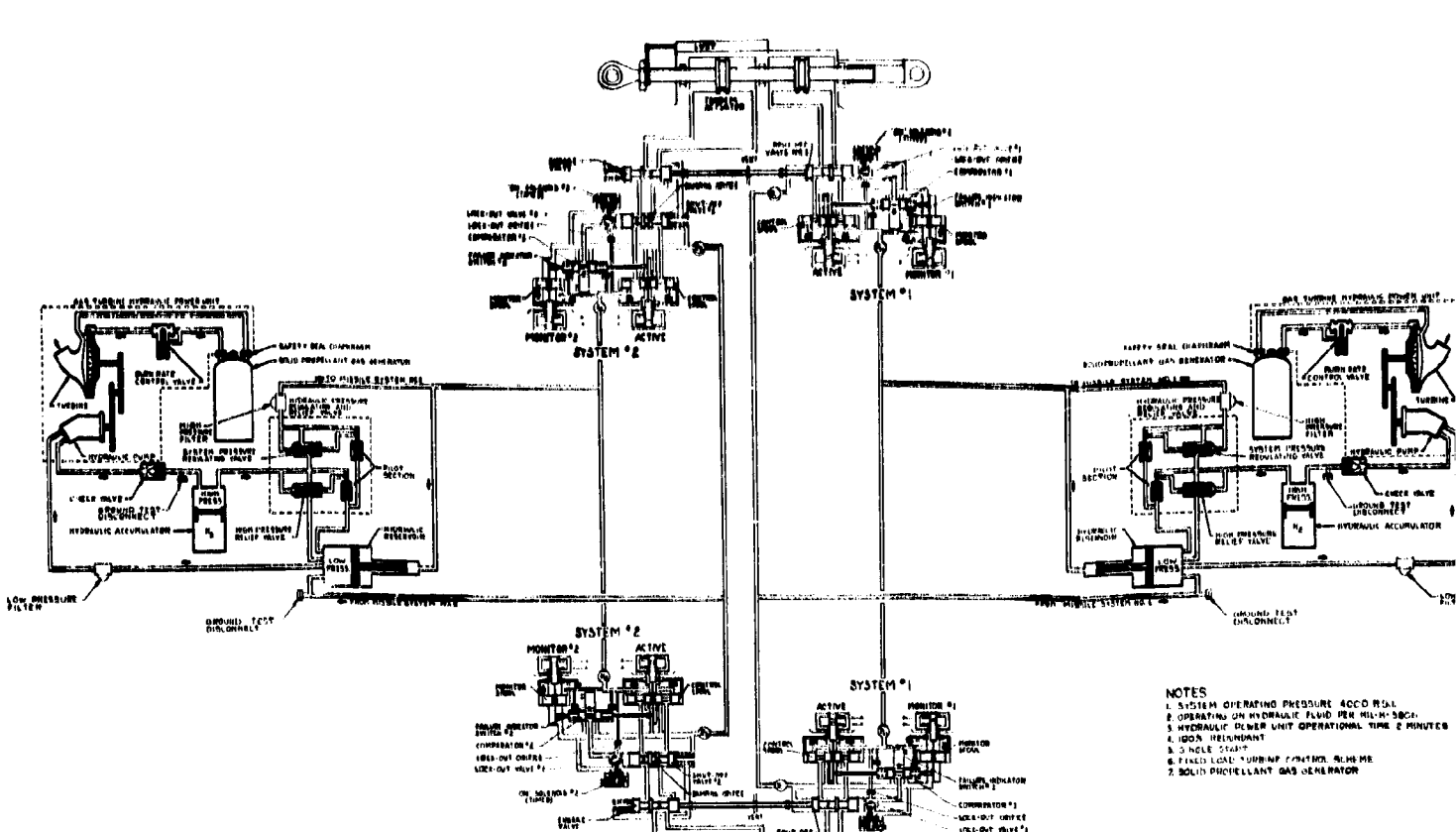

Figure 3-54. Schematic of Alternate No. 2, Nozzle

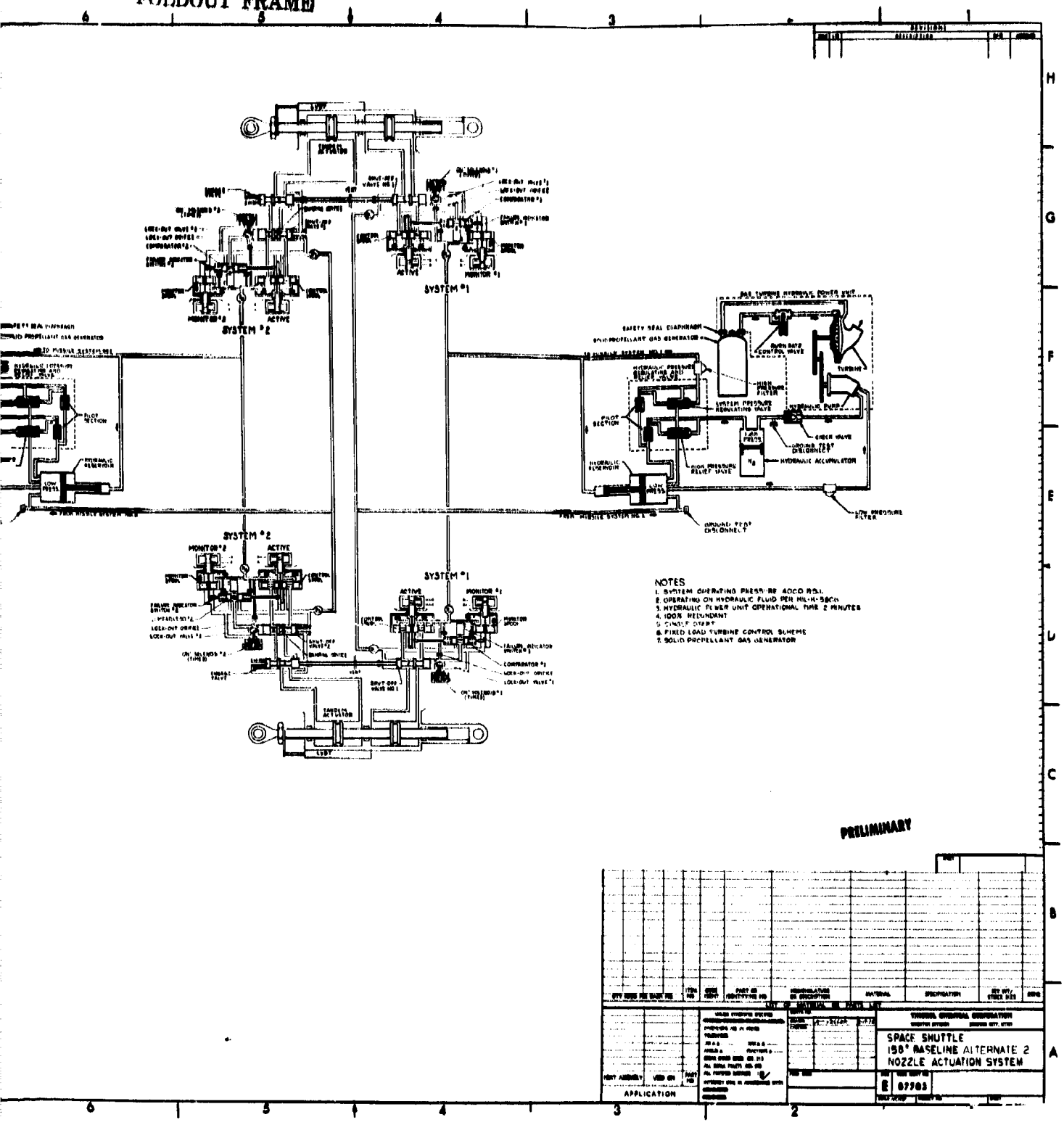

Figure 3-54. Schematic of Alternate No. 2, Nozzle Actuation System

The vehicle attitude control systems operation is initiated by closing the circuits to the arm/disarm switches, thus isolating the eight squibs in each system. After the switches are in the arm mode and the short removed from all squib leads, the system can operate. This is accomplished by an electrical signal that opens the solenoid valve (hydrazine) and ignites one of the solid propellant start initiator grains. At the same time the start initiator grain is ignited, the controller also effects the release of gas from the nitrogen cylinder by a squib valve. Action of the squib valve bursts the disc on the pressurant inlet port, initiating fuel expulsion to the fuel pump. Gas from the solid propellant starter grain passes through the turbine nozzle and causes rotation of the turbine and its gear train. The fuel pump, driven by the turbine shaft, develops fuel pressure and fuel begins flowing to the decomposition chamber as start grain pressure decays.

Simultaneously, solid propellant gas pressurizes and transfers heat to the decomposition chamber. As the grain approaches burn completion, the pressure in the decomposition chamber begins to drop. When the chamber pressure drops and turbine speed thereby decays, fuel is sprayed into the preheated chamber. Fuel decomposition begins when heat absorbed by the chamber is transferred to the atomized fuel.

Predetermined cartridge energy and burn rate enables the fuel pump to prime the fuel system and generate a pressure head sufficient to initiate fuel flow into the decomposition chamber. As the fuel reaches the decomposition chamber, the hot decomposition gas is directed through converging-diverging supersonic nozzles to the turbine blades. Turbine acceleration brings the unit to full speed within 1.0 sec from the receipt of the start command.

The electronic controller, operating in conjunction with the speed sensing magnetic pickup and fuel solenoid valves, provides overspeed control for the unit.

Fuel decomposition by the heat transfer characteristics of the multipath thermal regenerative bed sustains HPU operation. Gas generation will continue until terminated by closure of the solenoid operated fuel valve or by fuel exhaustion.

Shutdown can be accomplished at any time by closure of the fuel solenoid valve. Upon shutdown of the HPU, the residual hydrazine fuel in the filter, diverter valve, and associated lines is automatically purged through the decomposition chamber. The hot decomposition chamber decomposes the low pressure fuel into gas which exits through the exhaust duct.

Units that are considered "line replaceable" are the gas turbine module, controller, hydrazine fuel tank and start initiators.

3.4.2.2.1.4 Electronics

To support the redundant TVC actuator concept, redundant control electronics, hydraulic power and electrical power are required. Four identical TVC electronic control boxes are provided (two per solid rocket motor), each housing four servoamplifier channels. The pitch-yaw No. 1 channels are located in control unit 1 while the pitch-yaw No. 2 channels are located in control unit 2. Figure 3-55 shows a block diagram of control unit 1.

Four identical silver cadmium batteries (two per solid rocket motor) provide the necessary electrical power required by the HPU and TVC control units. Silver cadmium batteries were selected due to their ability to provide many recharge cycles and their relative high specific energy of 36 watt hours per pound.

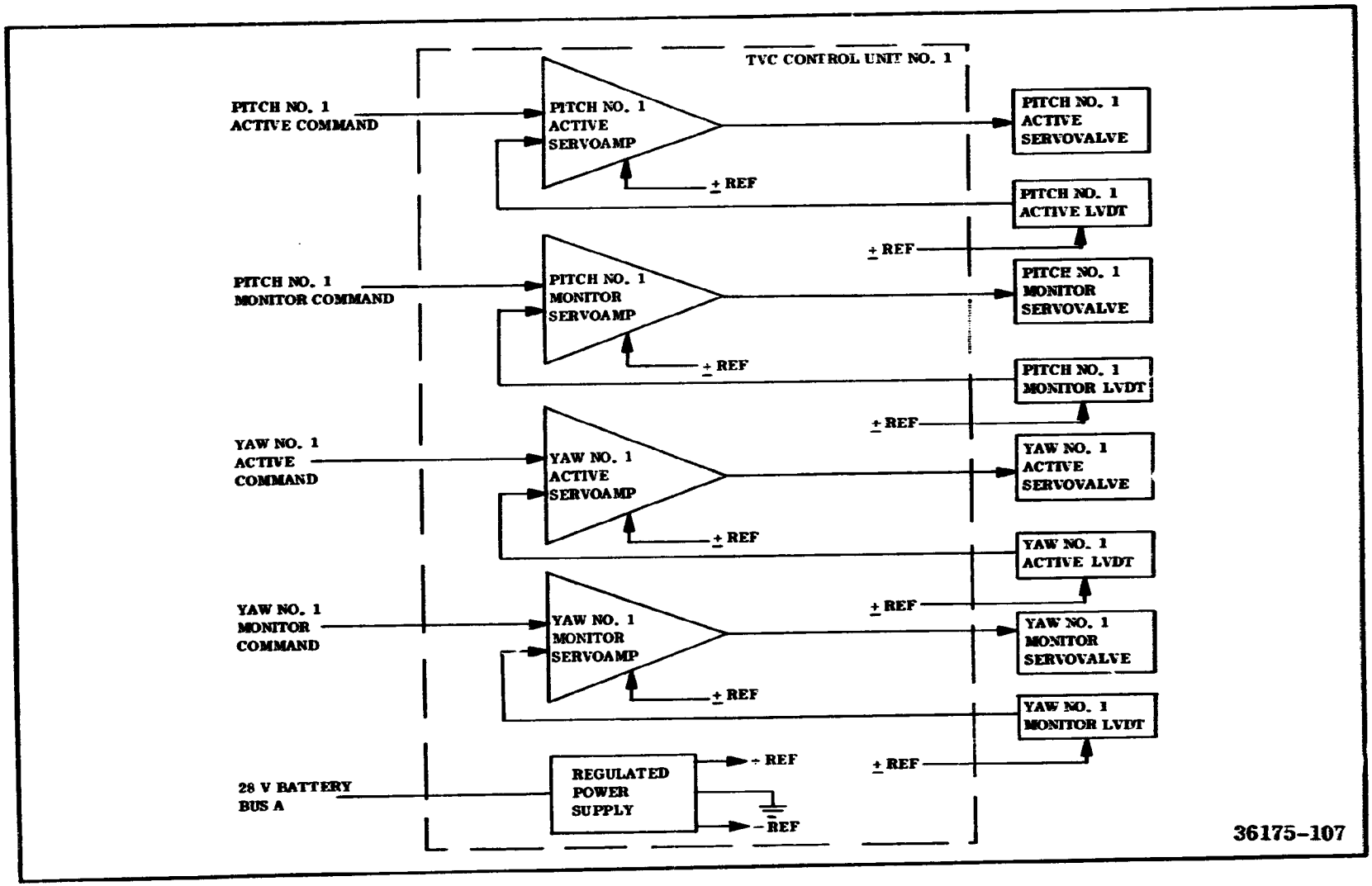

Figure 3-55. TVC Control Unit No. 1, Block Diagram

3.4.2.2.2 Abort System

Throughout the entire design and manufacture of the complete shuttle vehicle, large amounts of time and effort will be spent in design, manufacturing process control, inspection, and nondestructive testing to assure that a mission abort will not occur. However, the contingency exists and must be planned for. During the boost phase operation, malfunctions requiring mission abort could occur in either the orbiter avionics, the orbiter propulsion or in the SRM stage. Thiokol has made no attempt to define the possible malfunction modes in the orbiter. A detailed study of the SRM stage reliability and possible failure modes was conducted and the results are contained in Section 7.0 of this report. The study shows that the SRM stage is extremely reliable and that the probability of occurrence for failure modes which do exist can be significantly reduced by identifying the failure mode and proper design.

A plan which provides an abort sequence from time zero to SRM staging is shown on Table 2-2 . The abort plan requires only two special capabilities on the SRM stage:

1. The ability to hold down on pad for full SRM burntime without thrust termination (TT) of SRM should malfunction occur prior to liftoff.

2. The ability to thrust terminate the SRM at any time during flight.

A malfunction detection system (MDS) to provide data on abnormalties in SRM operation is included in the stage avionics.

The stage aft structure is designed to withstand full SRM and orbiter thrust as discussed in 3.4.2.3. This provides a preliftoff checkout capability and allows abort capability in the unlikely event that an SRM should not ignite, if a TVC system does not operate, if an orbiter problem occurs prior to liftoff.

The MDS and TT systems are discussed below.

3.4.2.2.2.1 SRM Malfunction Detection System

The MDS system on the SRM stage will have two capabilities, the ability to monitor and compare chamber pressure between the two motors on the stage and the ability to monitor the hydraulic pressure and position at the nozzle actuators.

The detection and display of differences in chamber pressure between the two SRM's will be accomplished by solid state electronic circuits. The pressure difference between the chambers of the two SRM's will be continuously displaced in the orbiter. If the difference becomes excessive, an indicator will identify the SRM at fault.

The design to accomplish this will use redundant pressure measurements from each SRM. Three pressure transducers on the headend of each SRM will measure the chamber pressure. Signals from these transducers are fed to a solid state electronic comparator circuit, where the signals from e two transducers on each SRM that are nearest the same level are selected to provide a chamber pressure signal to the orbiter. The chamber pressure signals from the two SRM's are fed to a differential comparator circuit, which will detect and indicate to the pilot the deviation of chamber pressures between SRM's.

The response time of the MDS will be limited by the frequency response of the indicator. The order of magnitude willbe in the millisecond range response time. The MDS will also monitor and display the hydraulic pressure at the nozzle actuators and indicate the nozzle position.

The MDS system is an advisory system only. It will not initiate abort procedures, only indicate SRM status. This approach is taken because of the good possibility of continuing a mission with an abnormal motor pressure differential or even with a TVC failure on one motor. Also, with this approach, a failure in the MDS system could not create a false abort.

Design and qualification specifications will require the MDS to perform its normal function after being subjected to transportation and handling, vibration, shock, and temperature environments. Also the MDS must operate within the specified accuracy during the flight environment, acceleration, vibration, and temperature altitude.

The ordnance distribution box will contain provisions to elecrically "enable" or "disable" the MDS circuitry by command signal received from the orbiter.

3.4.2.2.2.2 Thrust Termination System

Thrust termination on the SRM stages can be accomplished at any time during motor burn by opening two ports in the headend of the motor. Opening the headend ports accomplishes two purposes: (1) it reduces the motor chamber pressure to a low level, thus reducing the thrust from the nozzle, and (2) it provides "nozzles" on the headend with a reverse thrust.

The TT port design selected for use in the 156 in. SRM Space Shuttle booster is the ductile bubble design. This is shown in Figures 3-56 and 3-57. The design incorporates a secondary, low radius of curvature dome which is bolted to the reinforcement ring of the port hole in the primary motor dome. The thickness of the secondary dome will be approximately 0.10 in. and it will be fabricated from a material which is capable of large plastic strains without frangible failure. This will allow the dome to open in a ductile manner when a cross pattern is cut by a shaped charge. The baseline pattern for the charge is a cross which will divide the dome into four equal sections but it would be a simple matter to redesign for a more dense cutting pattern should requirements dictate a need.

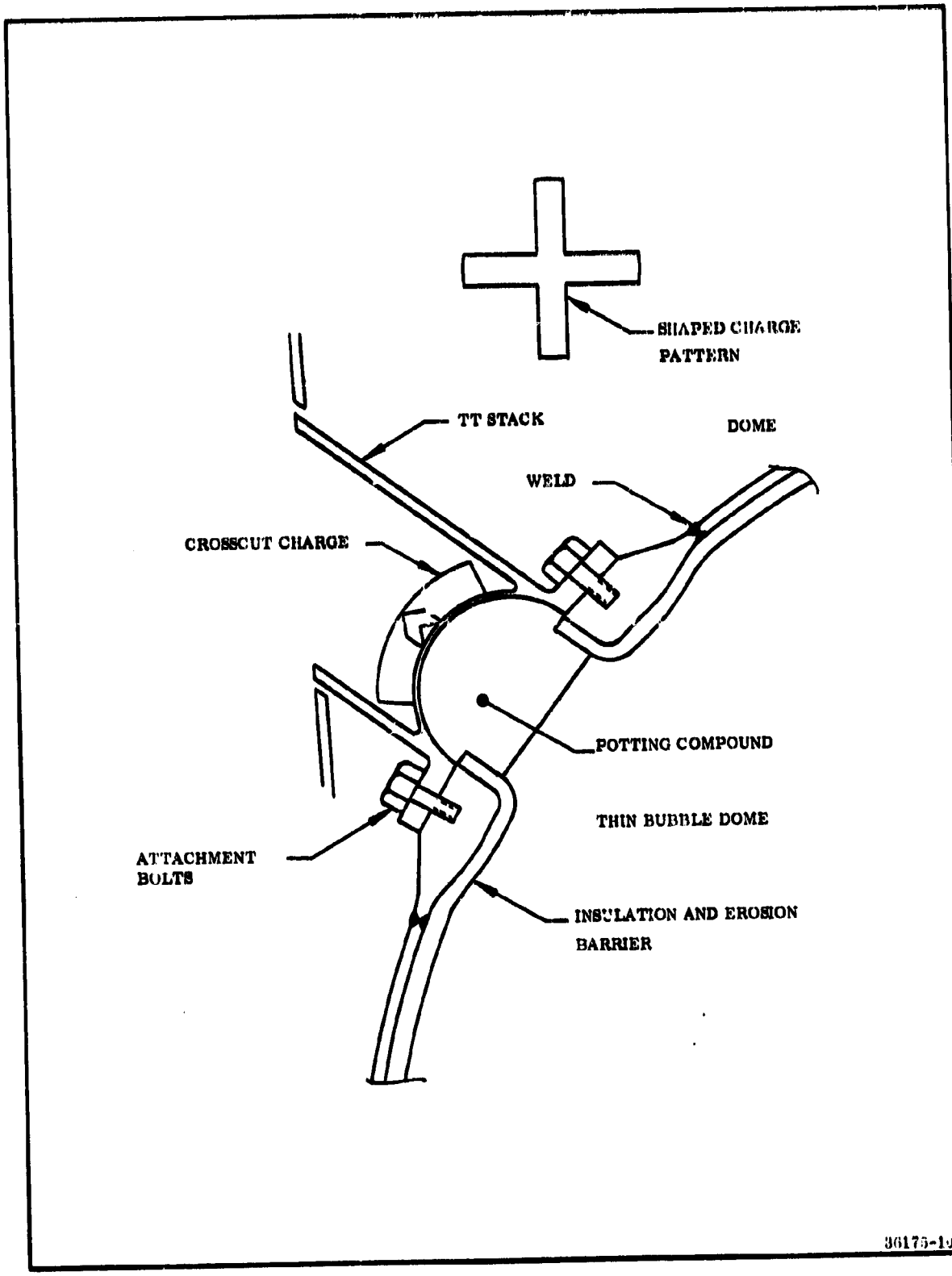

Figure 3-56. Ductile Bubble Concept

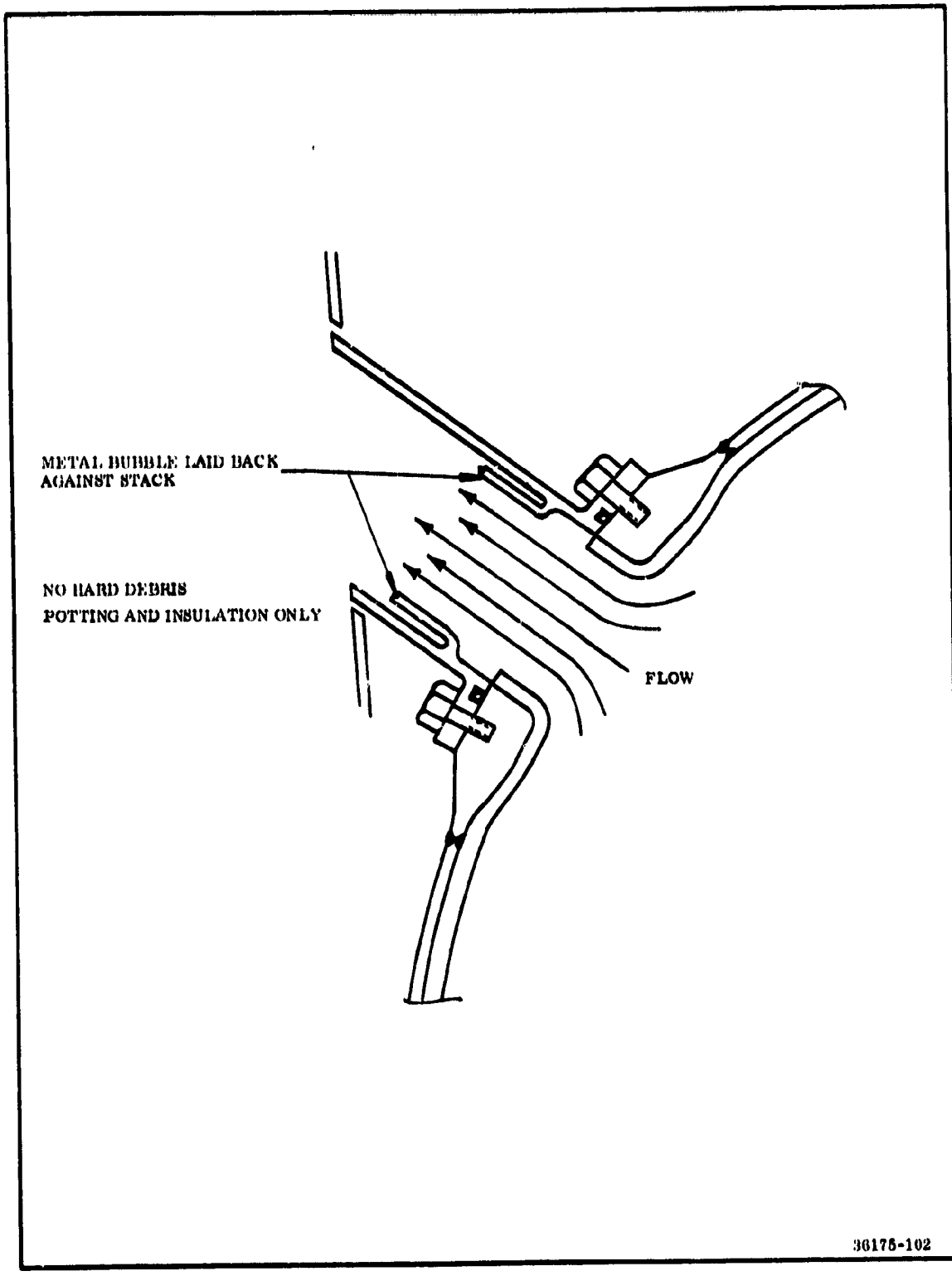

Figure 3-57. Ductile Bubble Concept Flow Schematic

In the approach shown, a pressure seal will be accomplished by a standard O-ring assembly with the groove cut into the flange of the port cover.

An erosive-resistant insulation collar will be placed in the orifice of the port to protect the reinforcement flange from the gas flow during TT port operation. This will accomplish several desirable objectives. The forward segment of the motor can probably be reused even after a ported firing, the reliability of the port operation over relatively long firing is increased and the insulation collar provides a more efficient flow orifice.

An S&A device will be provided. This device will be armed before launch and will be ready to fire when required.

The TT ports are opened by shaped charges (Figure 3-58). The TT system ordnance function time from the receiving of the electrical initiating pulse at the S&A device until the shaped charge cuts the ports will be from 0.30 to 1.0 ms.

Negation of the rocket motor thrust takes place as soon as the ports are cut.

The time requirement at the most severe condition will be 0.5 sec.

Thrust termination functioning time specification for the Stage III Minuteman motor is from 0.219 to 0.705 ms. The Stage III Minuteman has six ports cut within this time, verifying that the 0.30 to 1.0 ms requirement for the shuttle motor can be easily achieved even though the detonation transfer leads are comparatively longer. Each shaped charge will be initiated in three places to provide redundancy for reliability (Figure 3-58).

Thrust Termination Tradeoff Studies - There are several major TT port design concepts presently considered for use in solid propellant rocket motors. The variations of these major designs are many,and once a general system is selected,a design effort must be expended to optimize the final design.

For the purpose of this discussion, three general systems are considered.

1. The cut dome plate concept (Figures 3-59 and 3-60).
2. The ductile bubble dome concept (Figures 3-56 and 3-57).
3. The frangible burst disc concept (Figures 3-61 and 3-62).

In all three design concepts studied there are similar baseline design constraints.

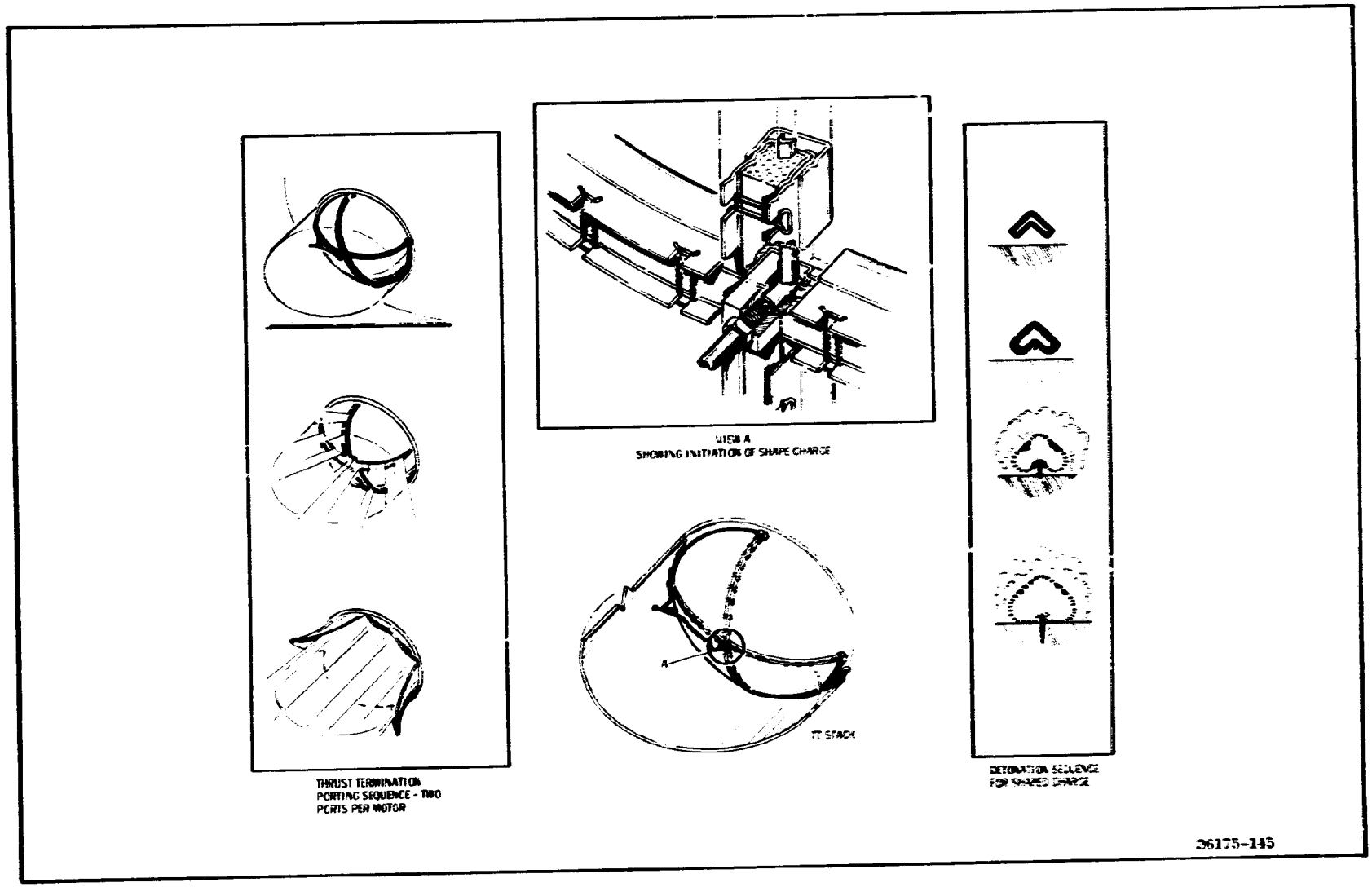

Figure 3-58. Thrust Termination System

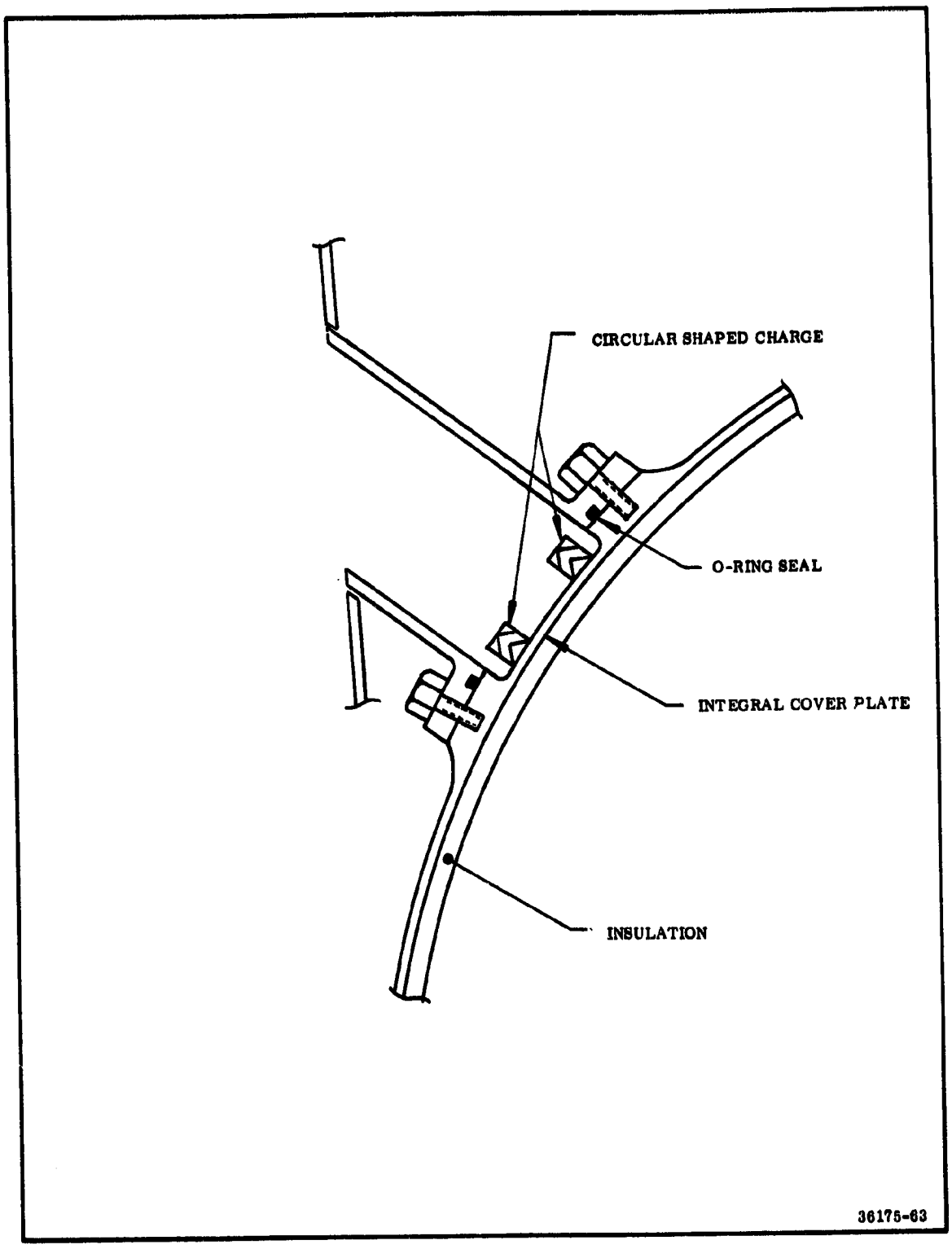

Figure 3-59. Cut Dome Plate Concept

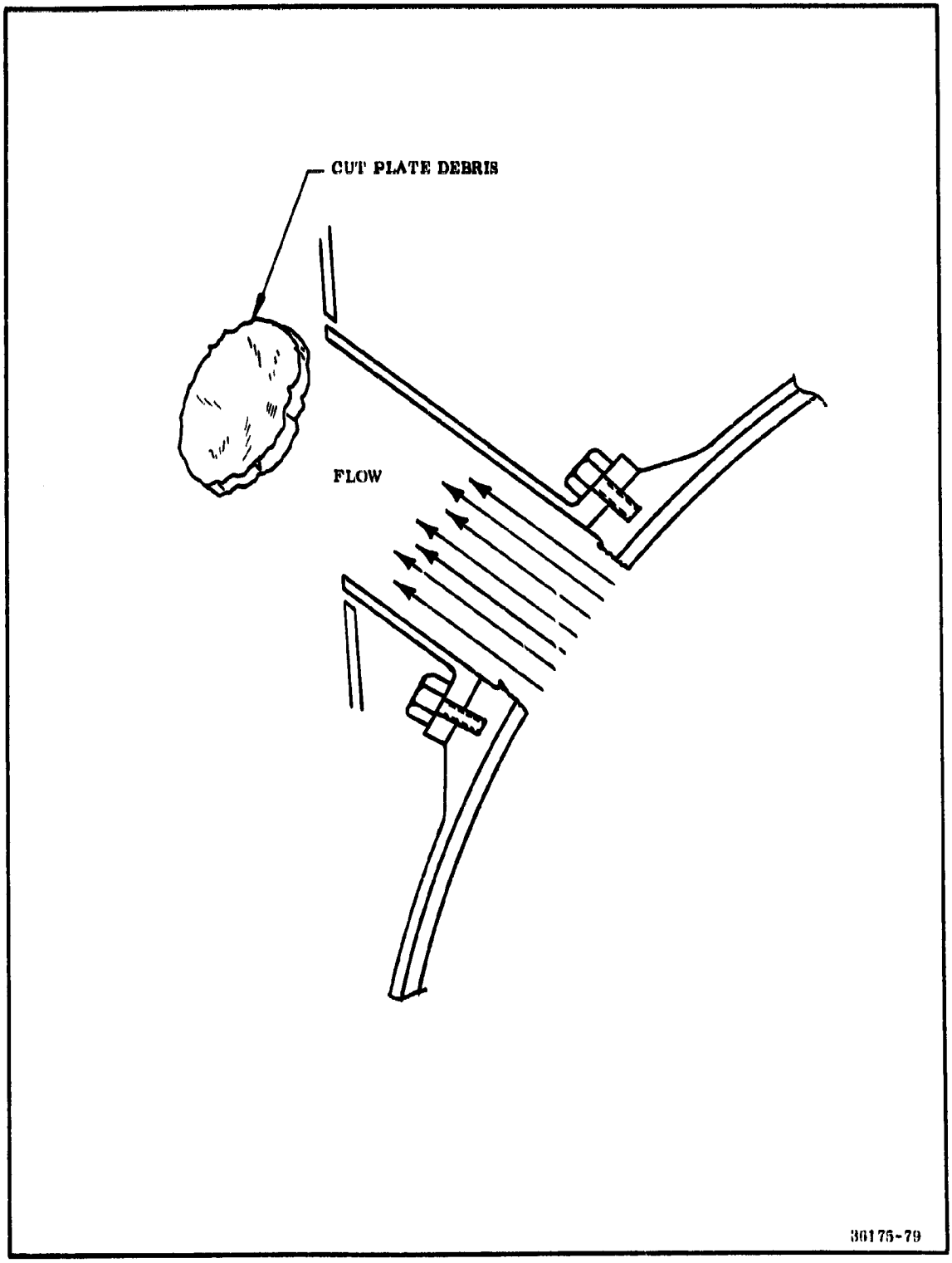

Figure 3-60. Flow Schematic of Actuated Cut Dome Plate Concept

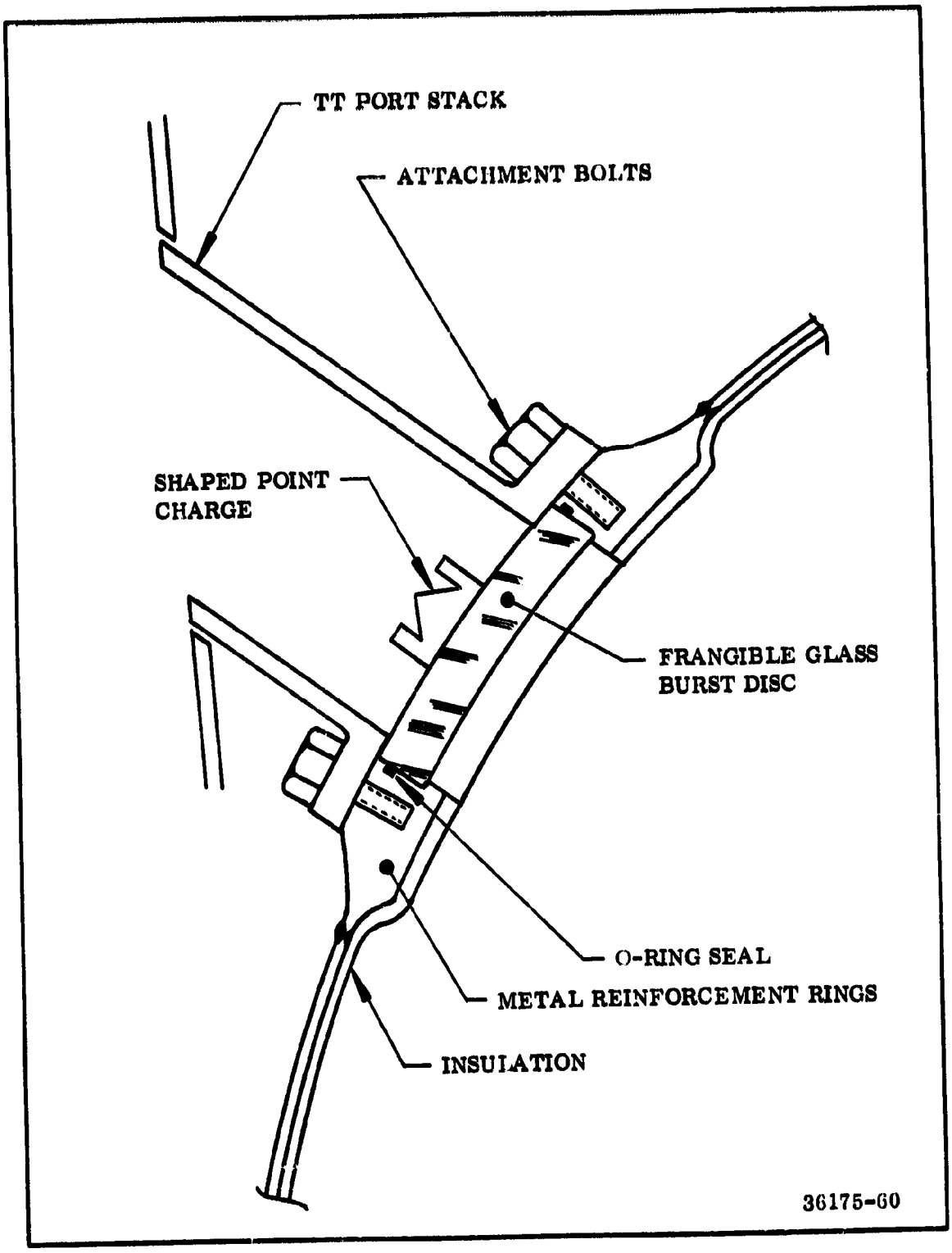

Figure 3-61. Frangible Burst Disc Concept

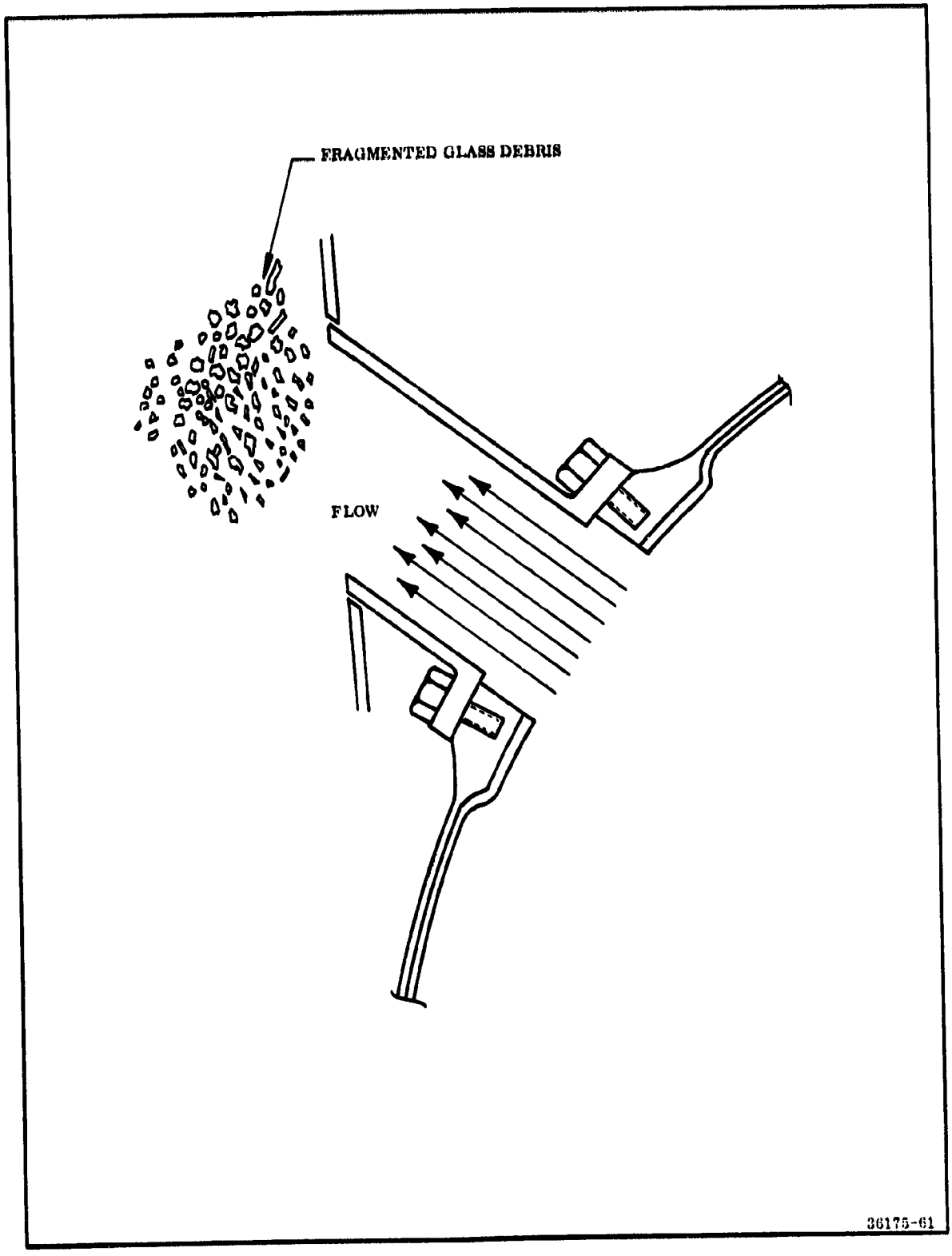

Figure 3-62. Flow Schematic of Frangible Glass Concept

1. The dome adjacent to the port opening was reinforced with a builtup metal collar which in addition to reinforcing the hole cutout, provides a bolt ring onto which the the TT stacks can be bolted.

2. The TT stacks were assumed to protude through the interstage structure but are not rigidly attached to it. Any movement of the TT stacks due to dome rotation would be accommodated by clearance between the stack and the interstage structure.

A brief design description of each concept follows.

Cut Dome Concept (Figure 3-59) - This design concept is similar to the one presently employed in the TITAN IIIC motor program. The dome reinforcement and coverplate are integral and placed in the dome by three dimensional machining or welding (where possible). The TT stacks are bolted to the reinforcement. A shaped charge is placed around the outside circumference of the dome plate. The port is activated (Figure 3-60) by firing the shaped charge through the insulation and the metal dome. The cut plate is ejected through the TT stack and the port flows gas. The hot gas is in direct contact with the cut metal edge because of the nature of the charge cut. This design concept is probably not capable of surviving a full term low pressure firing without a great deal of meltback in the metal.

Ductile Bubble Concept (Figure 3-56) - This design is really an extention of the cut dome plate concept. The reinforcement ring and bubble dome are machined integrally and welded into the dome. Because of its small radius of curvature, the bubble dome can be much thinner than the plate in the cut dome plate concept. A hard type (erosion resistant) insulation ring can be installed around the reinforcement ring, providing the capability to endure, thus insuring relatively long-term operation times.

The system is activated by firing a cross pattern shaped charge which cuts the bubble into quadrants. The material selected for the bubble application must be capable of being bent back against the stack wall without frangible fracture. Many materials are capable of this requirement, including the HY-140 steels. After cutting the dome, the port is allowed to flow without any direct contact between the gas flow and the reinforcement ring.

Frangible Burst Disc Concept (Figure 3-61) - In this concept the dome is again reinforced with a metal ring, but a hole is left in the center of the reinforcement ring. A glass pressure barrier is placed in the port during motor operation. The barrier is a dish-shaped design which utilizes polycrystalline glass as a structural and frangible material. By applying unique processing methods, the part is prestressed during manufacture. The prestress consists of high compressive stresses at both outer surfaces, and tension stresses at midthickness. These residual stresses are beneficial in utilization of the frangible pressure barrier concept and are

responsible for excellent mechanical properties. A 30,000 psi modulus of rupture tensile strength is a reasonable design value. Any externally applied load must overcome the residual compressive stress to produce high enough tension at the surface to cause rupture. Further, by introducing a discontinuity in the prestressed outer surface the part will experience complete disintegration. Fracture proceeds throughout the part at approximately the speed of sound in the medium.

At the loaded edge, the glass disc is completely encased in a rubber boot to provide a soft support foundation to help insure an evenly distributed support load.

The system is activated by firing a conical shaped charge into the center of the burst disc, which disintegrates the disc into extremely small particles of glass which are ejected through the port.

Table 3-30 is a summary list of the advantages and disadvantages of each concept. The ductile bubble dome concept was selected for the baseline design primarily because it does not release debris that might impact the orbiter and cause damage.

TABLE 3-30

COMPARISON OF VARIOUS TT CONCEPTS

Concept	Advantages	Disadvantages
Cut dome plate	1. No pressure seal required 2. General concept has been demonstrated on Titan program 3. Tested during normal hydrotest	1. Large energy release in case 2. Large cutting charge required 3. Metal disc projectile 4. Metal reinforcement is exposed to flow since insulation is cut on same line as metal. Usability questionable if porting is required
Frangible glass disc	1. Almost no energy release to case 2. Minimum energy required to fracture	1. Development effort required 2. Pressure seal required 3. Solid glass debris 4. Separate proof test required for glass plate 5. Metal reinforcement is exposed to flow. Usability without rework not possible. Rework capability not probable 6. Possibility of damage prior to firing
Ductile bubble	1. Applicable to all designs 2. No hard debris to consider 3. Metal dome can be protected during operation giving good chance of reusability without rework when TT porting is required 4. Light cutting charge required 5. Small energy release in case upon firing 6. Tested during normal hydrotest	1. New concept. Not yet proven 2. Only feasible with relatively ductile materials such as HY-140. 3. Pressure seal required 4. Not tested during normal hydrotest

3.4.2.2.2.3 Thrust Termination Ordnance Design

Explosive Transfer System and Cutting Charge - There are two TT stacks on each SRM. When thrust termination is required, it will be a function of the TT ordnance system to cut the ductile dome which is bolted to the reinforcement ring inside the TT stacks. This cutting can be conveniently accomplished by the use of crossed linear shaped charges. A 100 gr/ft aluminum sheathed RDX linear shaped charge will cut through the dome, but will not completely penetrate the internal insulation. Each TT port will have a single crossed linear shaped charge to cut the port hole into four quadrants (Figure 3-58). Each crossed shaped charge will be initiated in three places.

The porting shaped charges will be mounted in a shock absorbing plastic material supported by a metal shell which will be rigidly attached to the port domes. The charge support structure will hold the shaped charge at the required standoff and orientation to the port dome. See Figure 3-63 .

The TT transfer system will function as follows: There will be a S & A device mounted on the forward dome of each motor. A fire current applied to the device in the armed condition will initiate two detonators which in turn will initiate two 2.5 gr/ft RDX confined explosive leads. These leads are connected to a manifold which is also mounted on the head end of the motor. The manifold will contain a 10 gr/ft RDX explosive train formed in a loop so that it can be initiated at both ends by the redundant leads from the S & A device. From the manifold, three 2.5 gr/ft confined explosive leads will originate at each side of the manifold. Two of the leads will initiate the explosive shaped charge in the stack on each end of the cross.

Safety and Arming Device - The S & A device used for the TT system is the same device used for the motor ignition system except it is modified to initiate an explosive train. This modification requires the replacement of the squibs with 1 amp, 1 w rated detonators of the same physical dimensions. This detonator has been qualified on the Titan IIIC TT device. Figure 3-64 shows the S & A device-to-manifold interface.

The S & A devices are essentially identical to those used on the Titan IIIC in form, fit, and function, and are recommended because of cost savings and increased reliability.

Explosive Lines - The explosive lines will be of confined mild detonating fuse. Detonating fuse core loadings of 2.5 gr/ft of RDX have been demonstrated reliable in many systems. The confined core consists of a core of explosive with a lead sheath. A solid plastic sheath is extruded over the lead and then five to seven layers of nylon are braided over the plastic sheath. Each end of the explosive lead terminates in an end primer and attachment fitting.

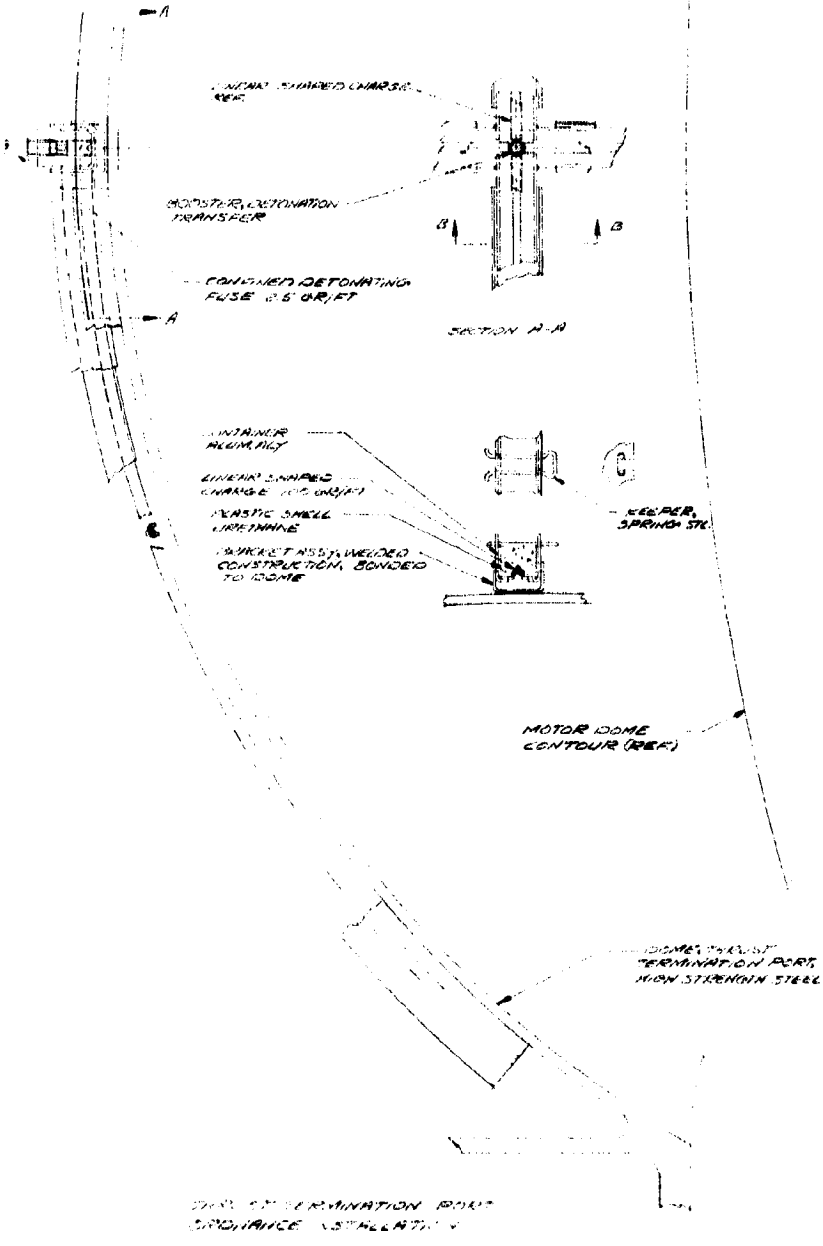

Figure 3-63. Thrust Termination Layout, Port Removal

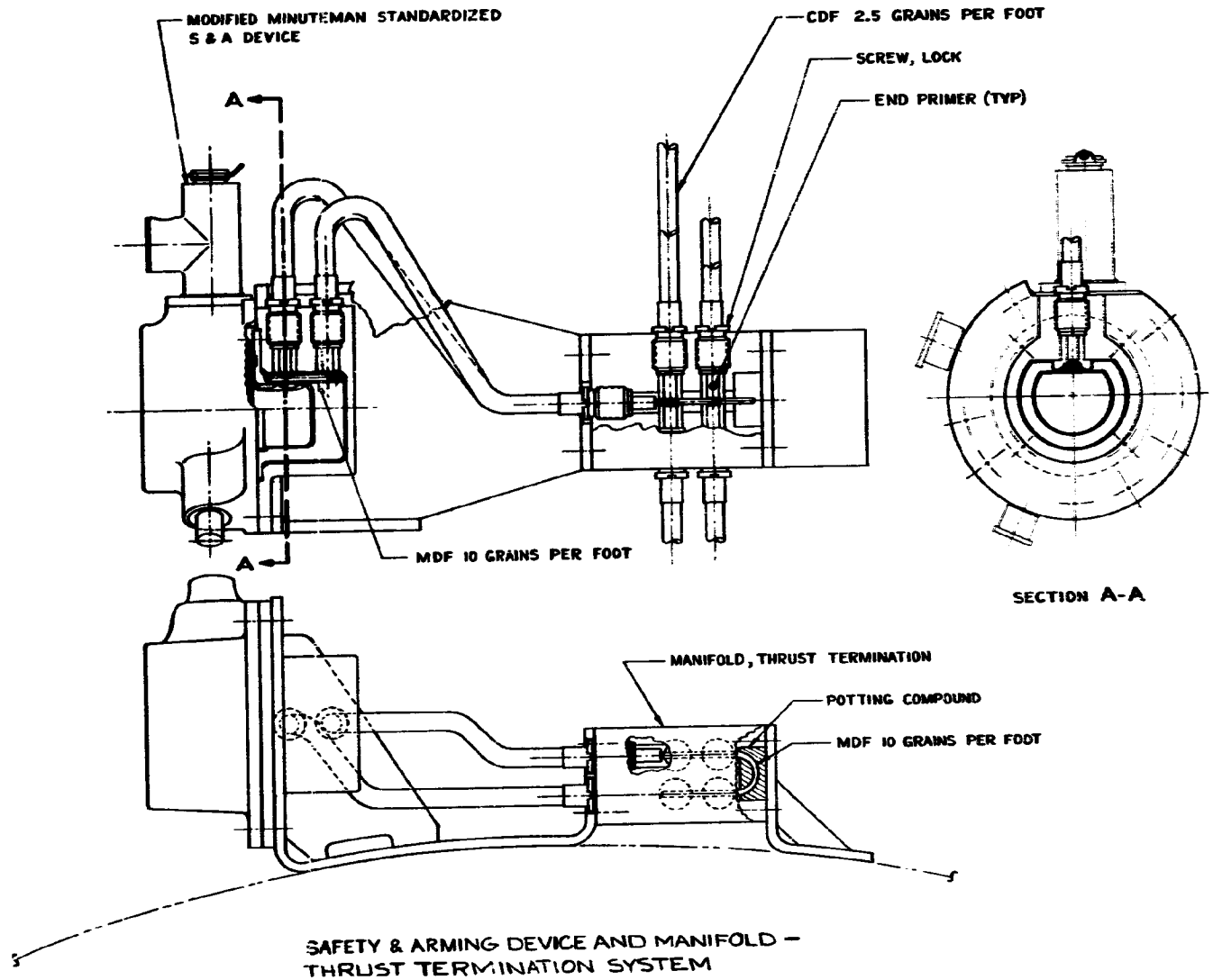

Figure 3-64. Thrust Termination Manifold Layout

End Primer - The end primer and attachment fitting consists of a steel booster cup with a pressed explosive charge. The next step in the explosive train is a conical charge pressed into a metal housing. This charge makes the diameter transition between the charge in the cup and the small diameter charge in the detonating cord which provides reliable detonation in either direction. The cup covers both main charge and conical charge and fits over a steel housing to which the cup is welded for a strong, moisture-proof seal. The housing slips over the cover on the detonating cord. The internal surface of the housing is threaded to provide good mechanical contact to the cord cover. The housing is bonded and mechanically swaged onto the detonating cord, providing an extremely tight grip on the detonating cord cover. This design provides a reliable end primer capable of serving as either a donor or a receptor with a minimum of parts and excellent seal and mechanical strength.

Manifold Design - The manifold proposed for this explosive system (Figure 3-65) will contain a single continuous loop of 10 gr/ft MDF explosive lead which will be initiated on both ends by redundant leads coming from the S & A device. Outgoing explosive leads from the manifold have end primer receptor charges which butt up against the looped lead charge in the manifold.

Shaped Charges - Aluminum sheathed RDX shaped charges are the baseline selection for the TT system. A charge loading of 100 gr/ft of RDX is specified. This is the charge weight that will penetrate the dome but not the internal insulator. Figures 3-66 and 3-67 show the optimum standoff and penetration as a function of charge loading for an aluminum sheath RDX linear shaped charge. Final selection of charge loading cannot be made until penetration tests have been conducted on pressurized bottles made of the same material as the motor dome.

There will be attachment bracketry permanently attached to the dome for installation of the shaped charges. During final assembly of the TT system, the charge assembly can be placed on the port and bolted or clipped to the bracketry. The assembly is then completed by screwing the initiating leads into the fittings on the charge assembly and lockwiring them in place (Figure 3-58). The detonation and penetration sequence for the LSC are shown in the figure.

Fabrication Techniques - The explosive components (ie, linear shaped charges, end primers, explosive leads, confined detonating cords, and manifold lead charges) will be procured from outside sources and assembled by Thiokol.

The TT system will be designed so that all explosive leads, manifolds, and the S & A device may be installed at the Wasatch Division before shipment. The large cross porting charges will be packaged and shipped separately.

Redundancy is achieved by having two distinct explosive trains initiated by redundant power supplies. The power supplies are arranged so that each fires one initiator on each S & A device (Figure 3-68).

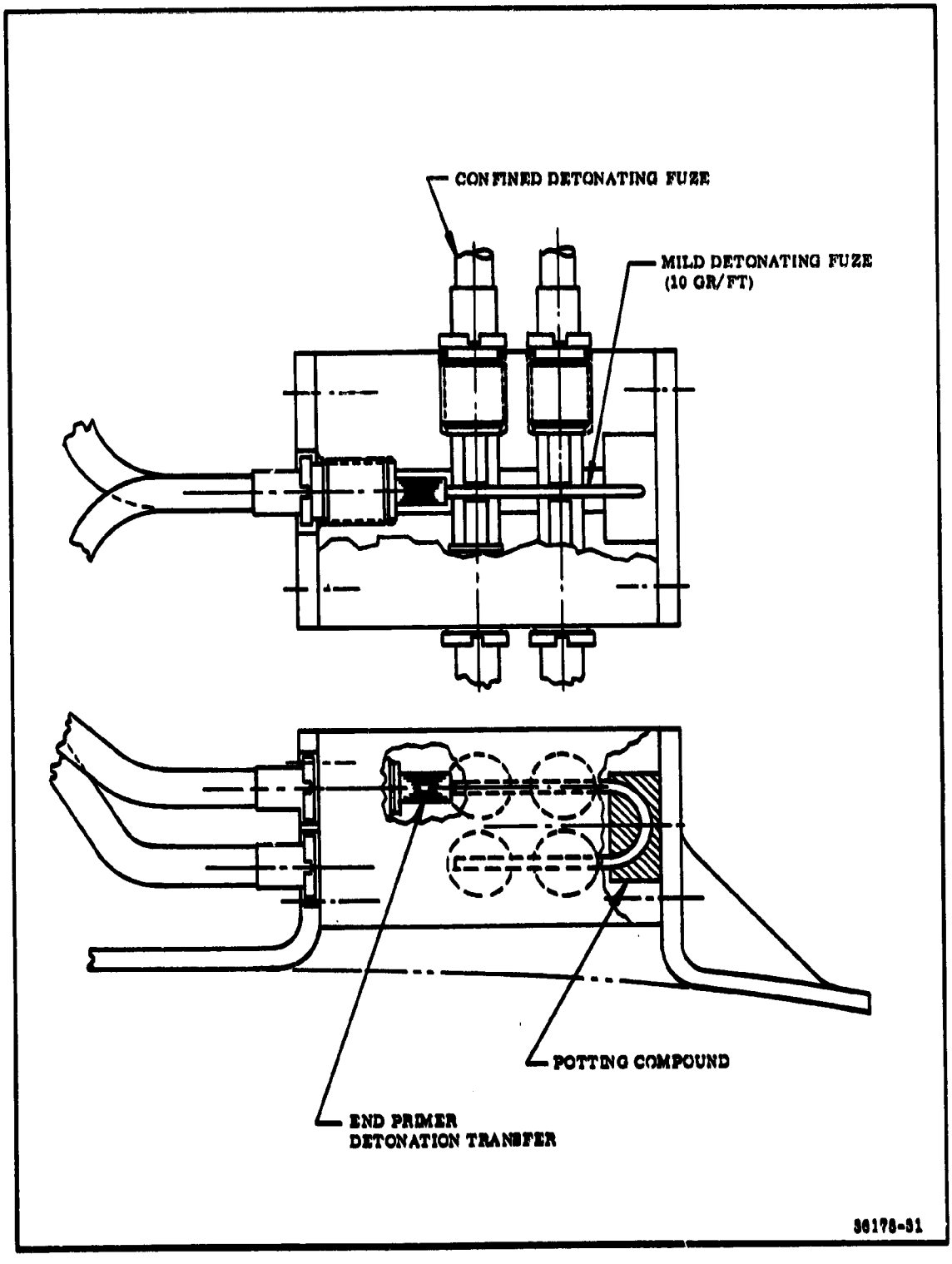

Figure 3-65. Thrust Termination System Manifold

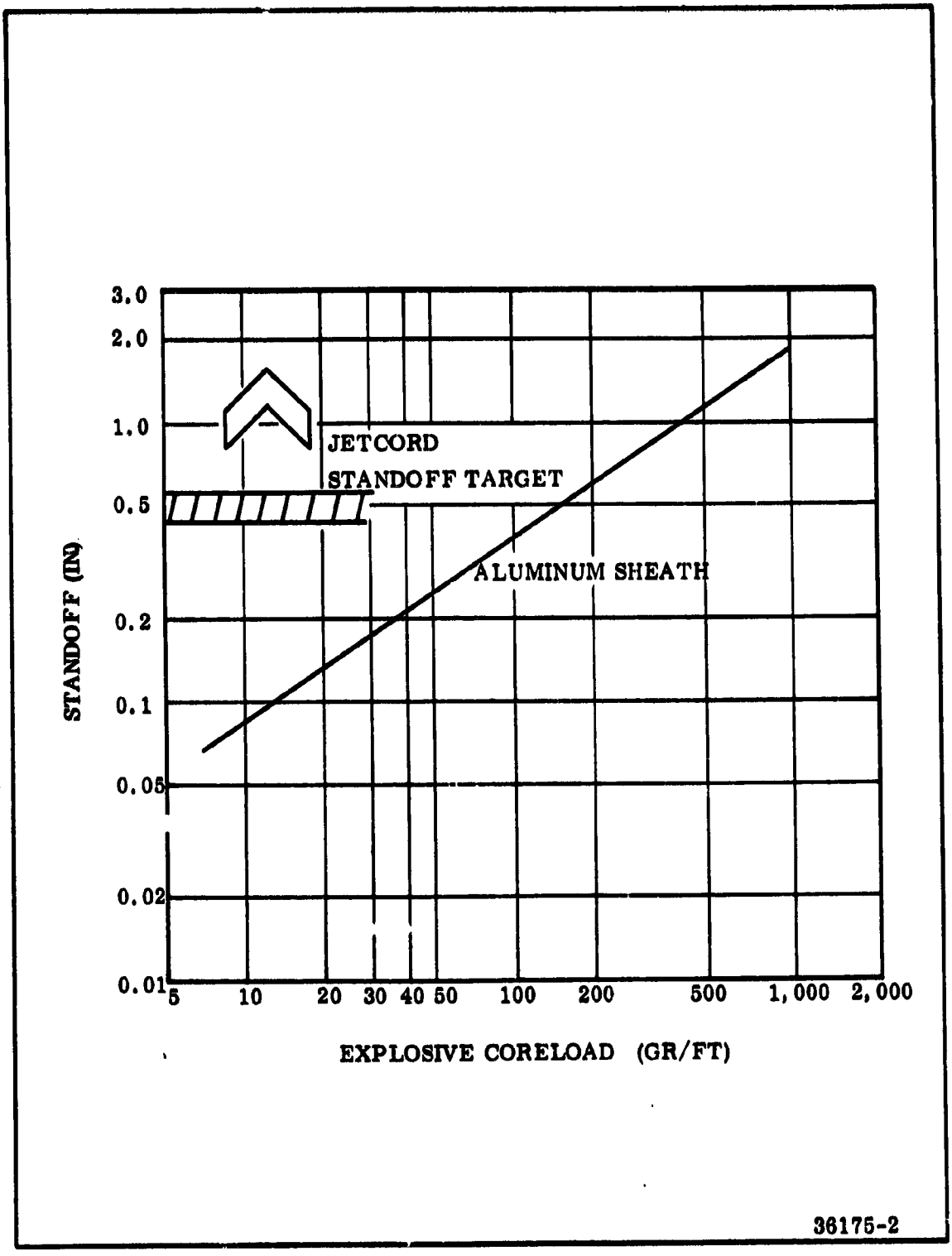

Figure 3-66. Standoff for Optimum Performance (RDX or PETN Explosive)

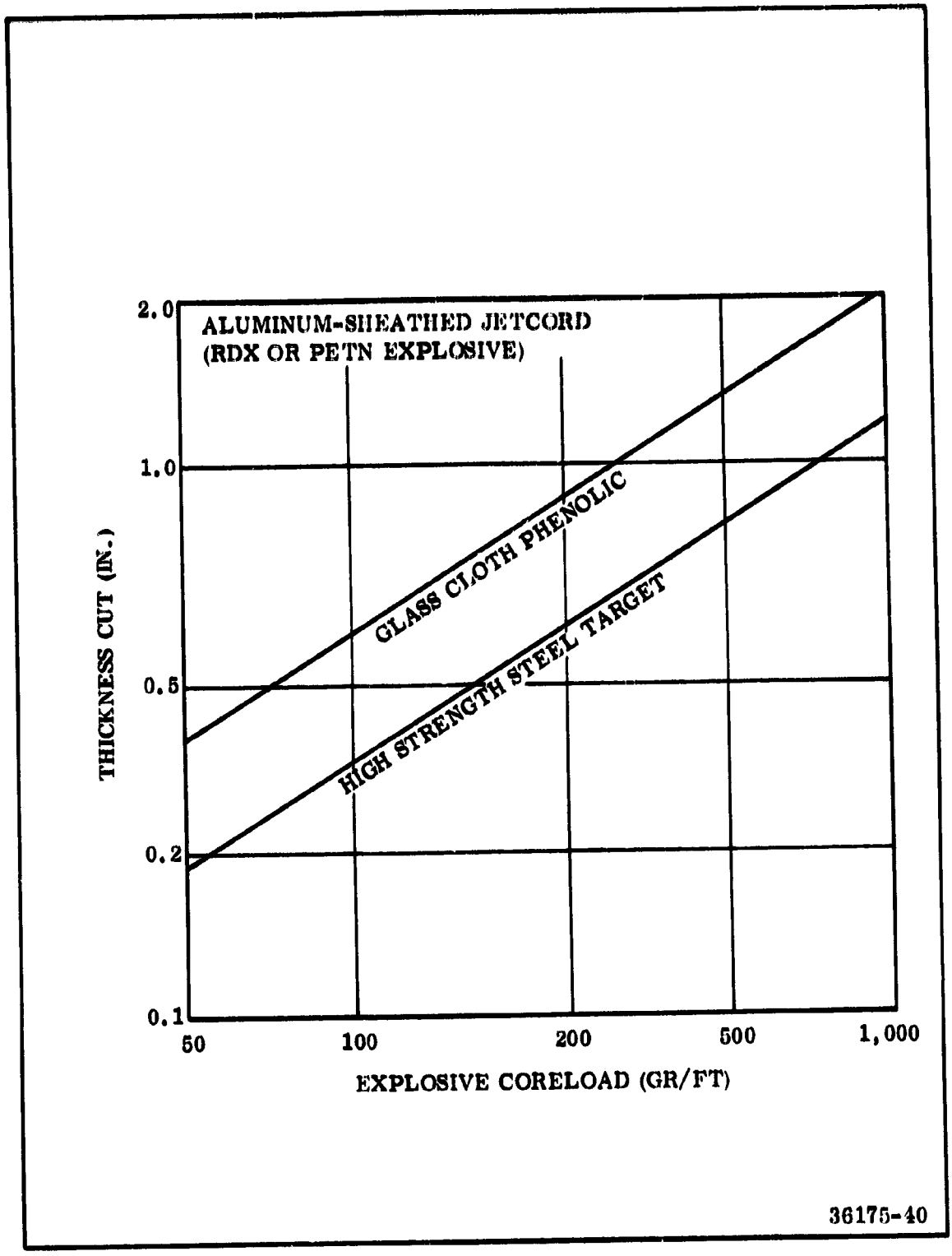

Figure 3-67. Minimum Cutting Performance at Optimum Standoff

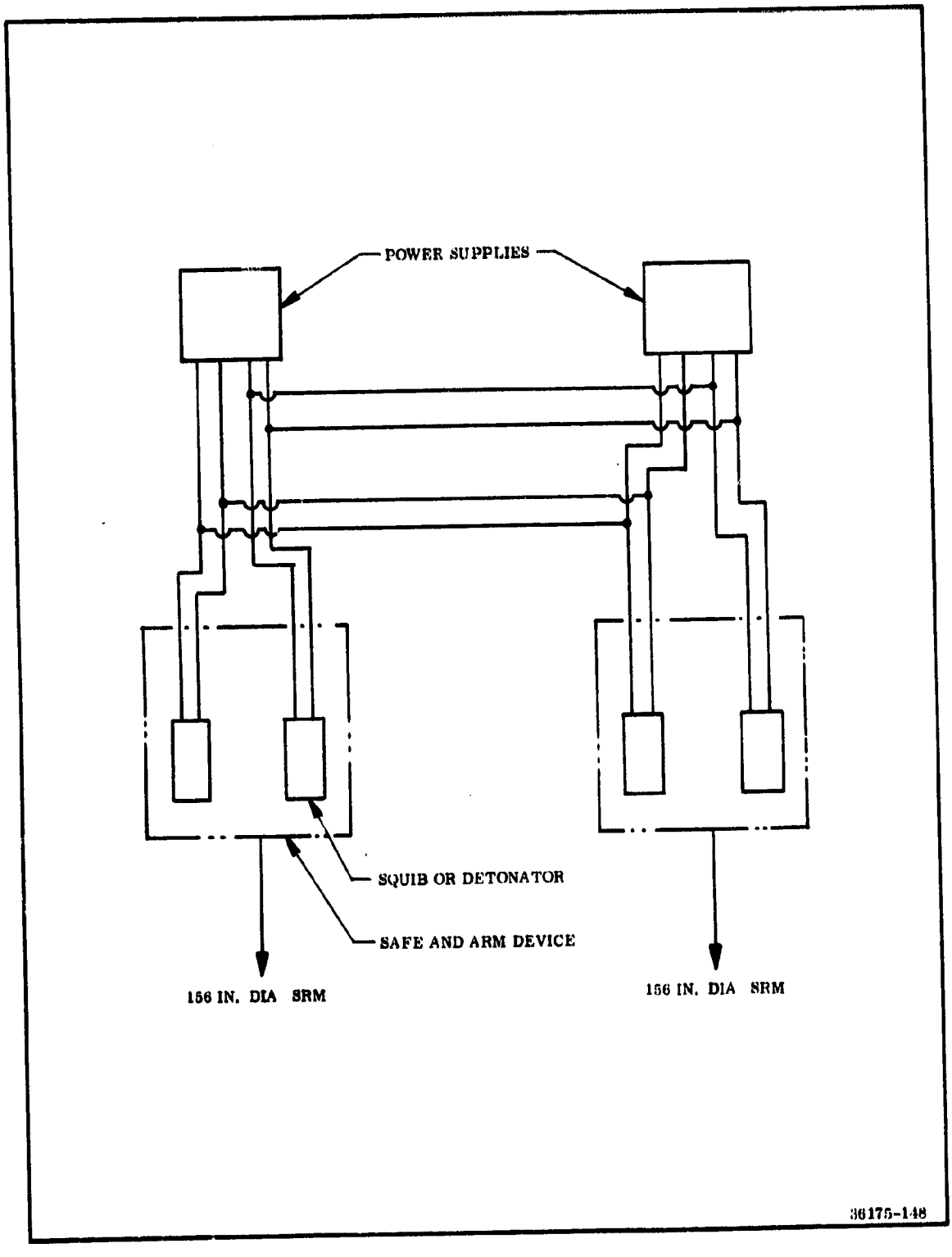

Figure 3-68. Initiation System Ordnance Redundancy for Ignition, Thrust Termination and Destruct

The explosive train is completely redundant. The lack of redundancy in the shaped charge is compensated for by triple initiation (Figure 3-69). Detonation proceeds in both directions along the linear shaped charge from the point of initiation. Therefore, one successful initiation on each system will serve to open the TT port.

3.4.2.2.2.4 Thrust Termination Plume

A characteristic of the headend porting technique of thrust termination is the exhaust plume at the headend of the motor after the ports are cut. The characteristics of this exhaust plume were predicted using the same techniques as used for the analysis of the main nozzle plume at altitude (MOC program). The results of these predictions are shown in Figures 3-70 and 3-71. Figure 3-71 shows the maximum exhaust plume that could be produced by exhausting all of the gases through one TT port with an average chamber pressure of about 850 psia. Using two ports, these conditions would be reduced to the plume shown in Figure 3-70 within about 0.5 sec. This occurs because the additional port area reduces motor chamber pressure to about 100 psia. The TT exhaust plume opposes the missile velocity causing a smaller plume than that exiting from the motor's nozzle.

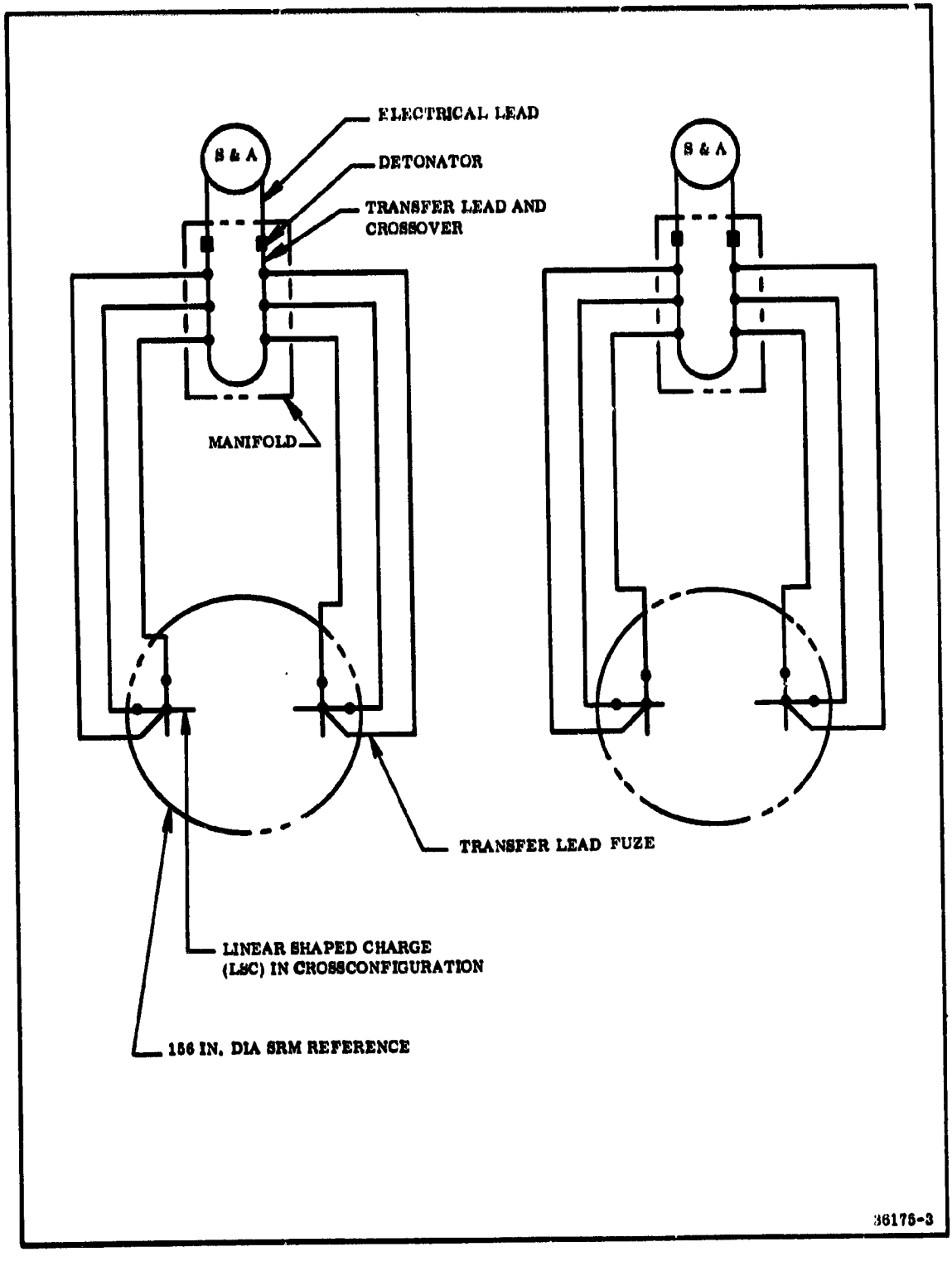

Figure 3-69. Thrust Termination System, Redundant Impulse Transfer

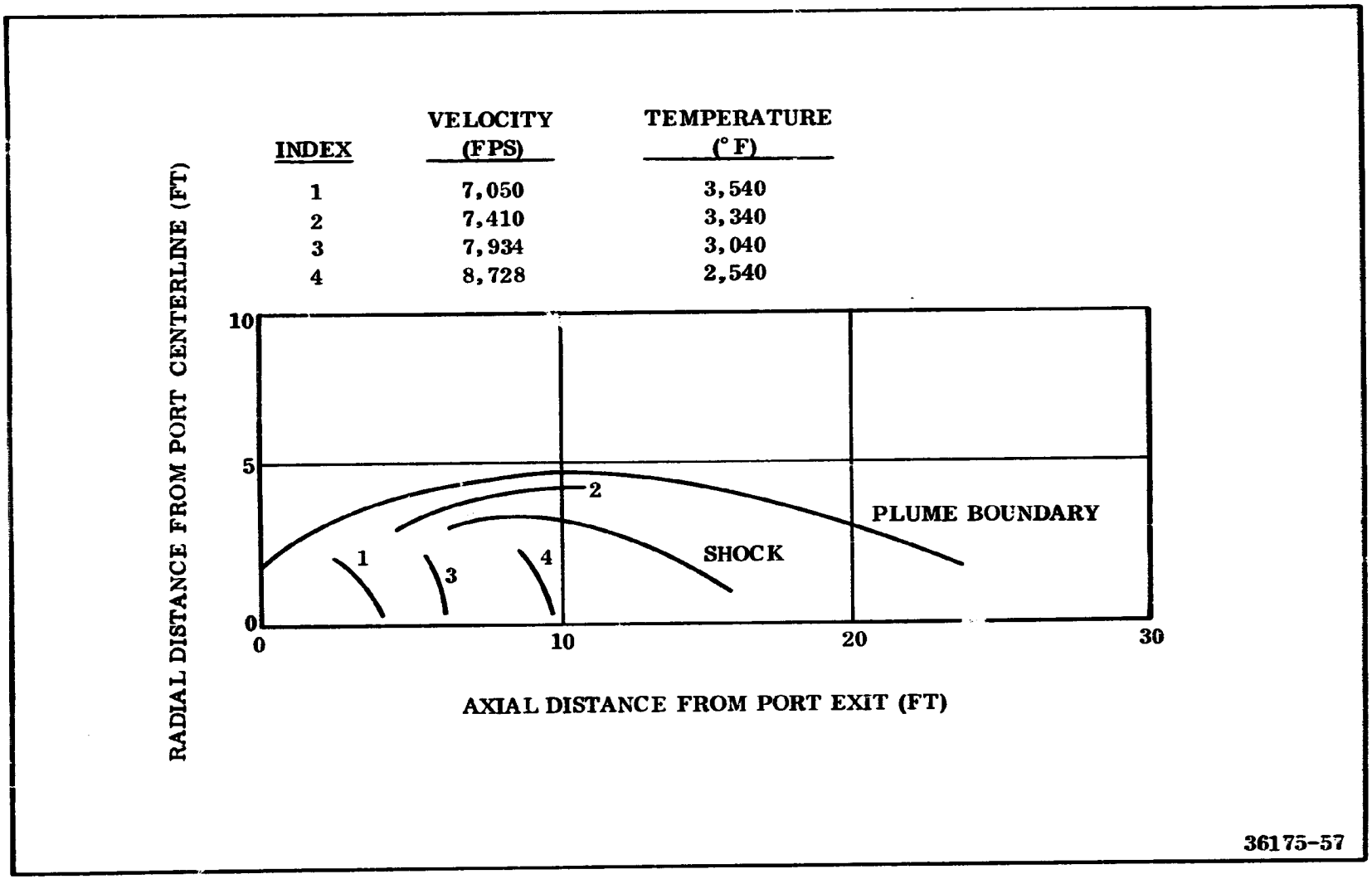

Figure 3-70. Thrust Termination Port Exhaust Plume at 100,000 Foot Altitude Using Two Exhaust Ports at T = 0.5 Sec

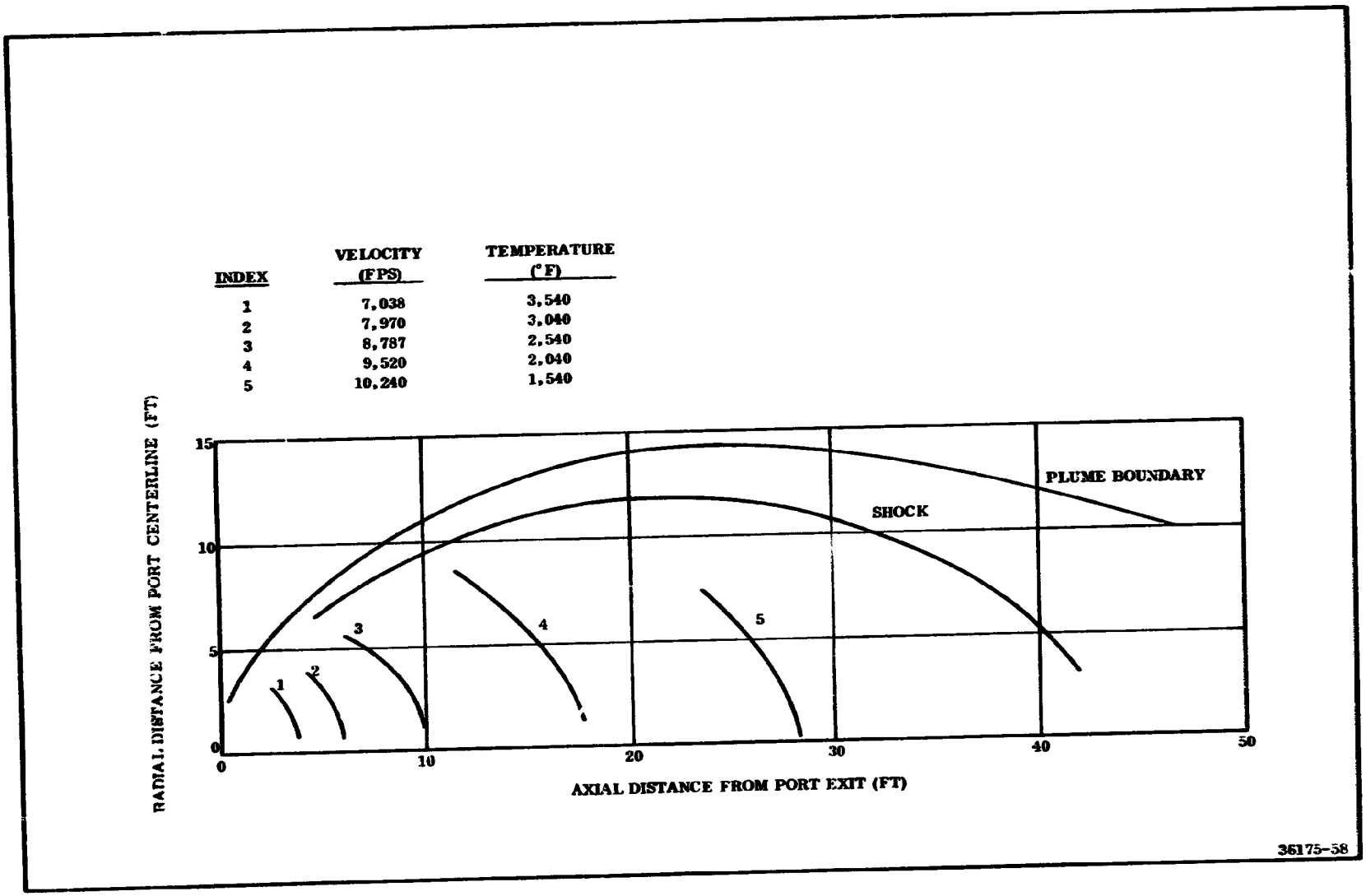

Figure 3-71. Thrust Termination Port Exhaust Plume at 100,000 Foot Altitude Using One Exhaust Port at T = Zero

3.4.2.2.2.5 Destruct System

Range safety procedures may require a destruct system on each SRM and if so designated such a system can be adapted to the Space Shuttle motors. A description of the destruct system design is presented herein.

The destruct system on each SRM will be initiated by the detonators in an explosive train S & A device. This device will be identical to the thrust termination S & A device except that the firing connectors will be keyed differently to avoid accidental switching of firing lines during final assembly.

There will be two parallel, 250 gr/ft RDX aluminum sheathed linear shaped charges in the SRM raceway. The charges will be located on the cylindrical section of each segment.

The shaped charges will be connected to the S & A device and to each other by explosive leads. These explosive leads will be identical in design to those developed for the thrust termination system. There will be an explosive crossover between the charges at each motor segment. Figure 3-72 is a schematic layout of the destruct system and Figure 3-73 shows details of the crossover detonation transfer lead and LSC connections.

Mounting clips will be provided in the raceway for the shaped charges. The shaped charges will be shipped separately from the motor segments. The safety and arming devices and explosive leads will be installed before shipment. The shaped charges will be assembled to the motor at the launch site, as shown in Figure 3-74.

The shaped charges will be designed to cut through the case and approximately half-way through the internal case insulation so that an inadvertent firing of the destruct system on an unignited motor would not result in ignition of the motor propellant. This system will provide destruct capability at low as well as high motor pressures. Destruct system design parameters are presented below.

Parameters	Requirement
Redundancy requirements	Two complete systems side by side, with redundancy between, either of which is capable of SRM destruct.
Destruct time after signal is received at S & A device	0.006 sec (max)

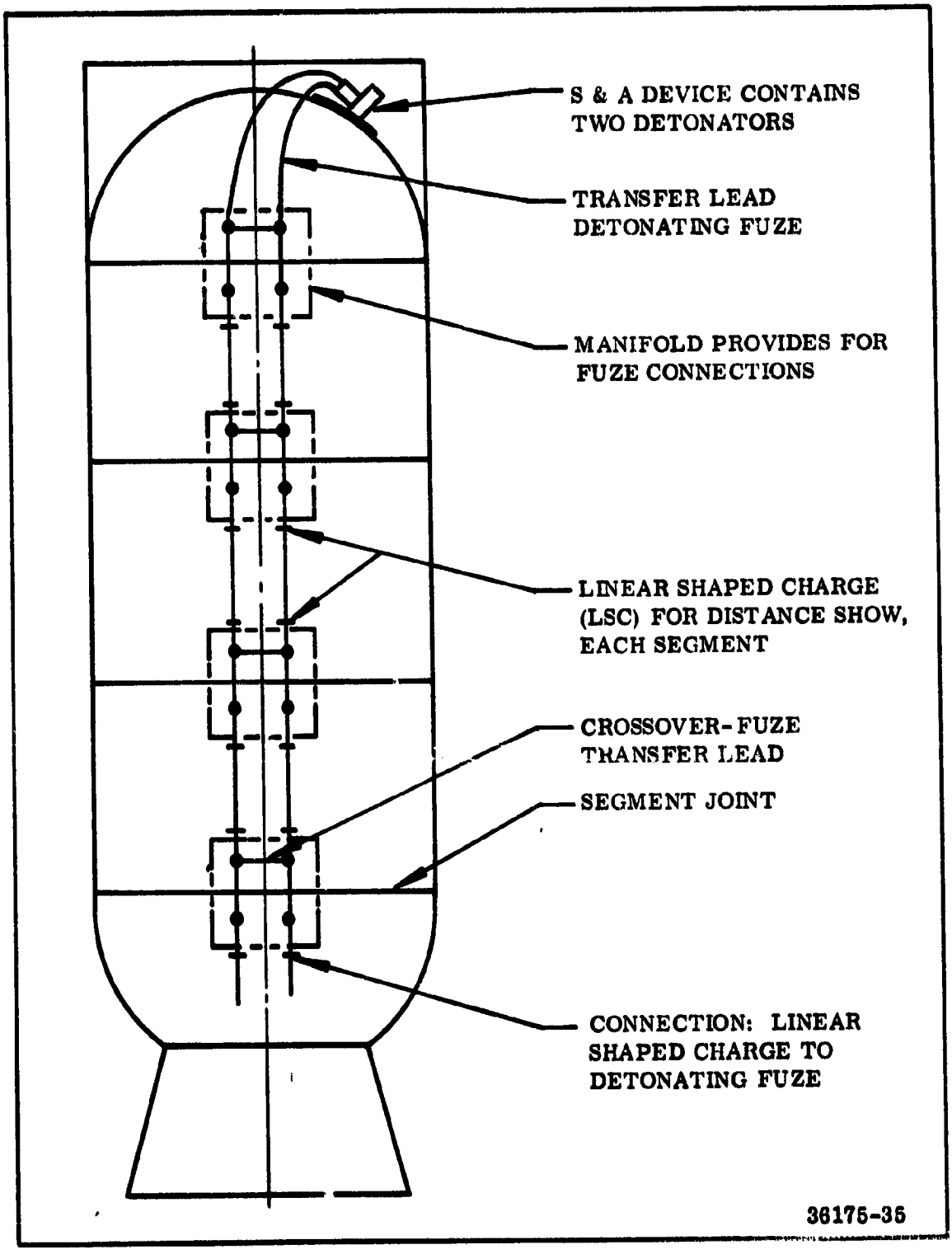

Figure 3-72. Destruct System, Redundant Impulse Transfer

FOLDOUT FRAME /

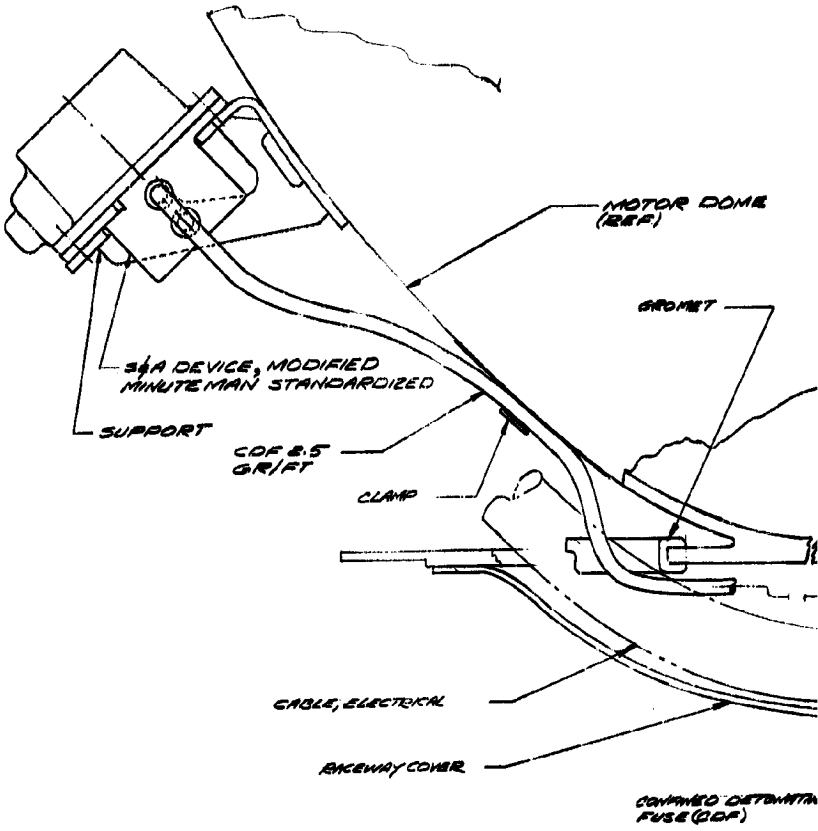

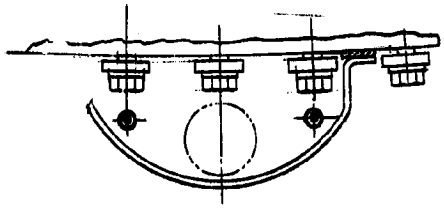

SECTION C-C

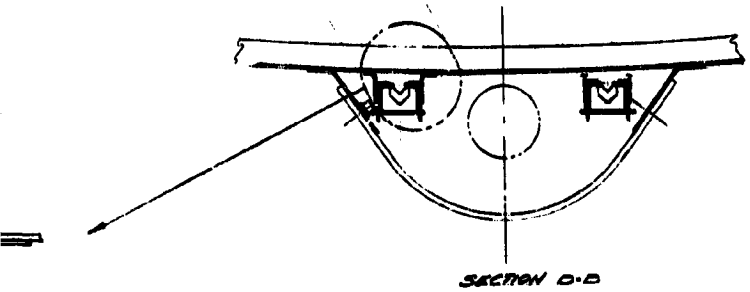

SECTION D-D

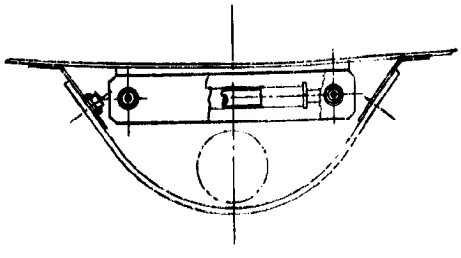

SECTION B-B

DESTRUCT SYSTEM
156 IN DIA SPACE SHUTTLE MOTOR
1-26-98

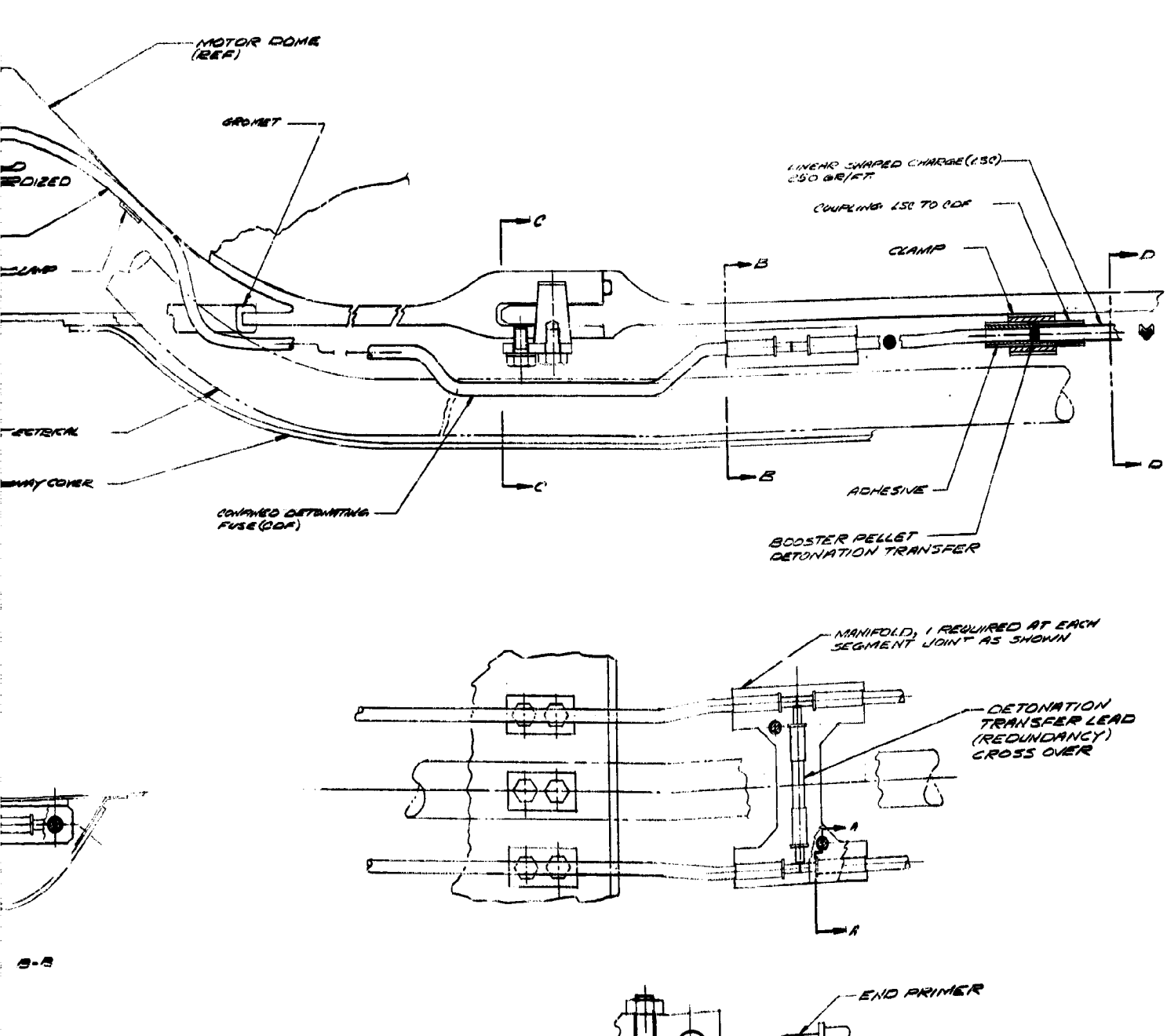

Figure 3-73. Destruct System Layout

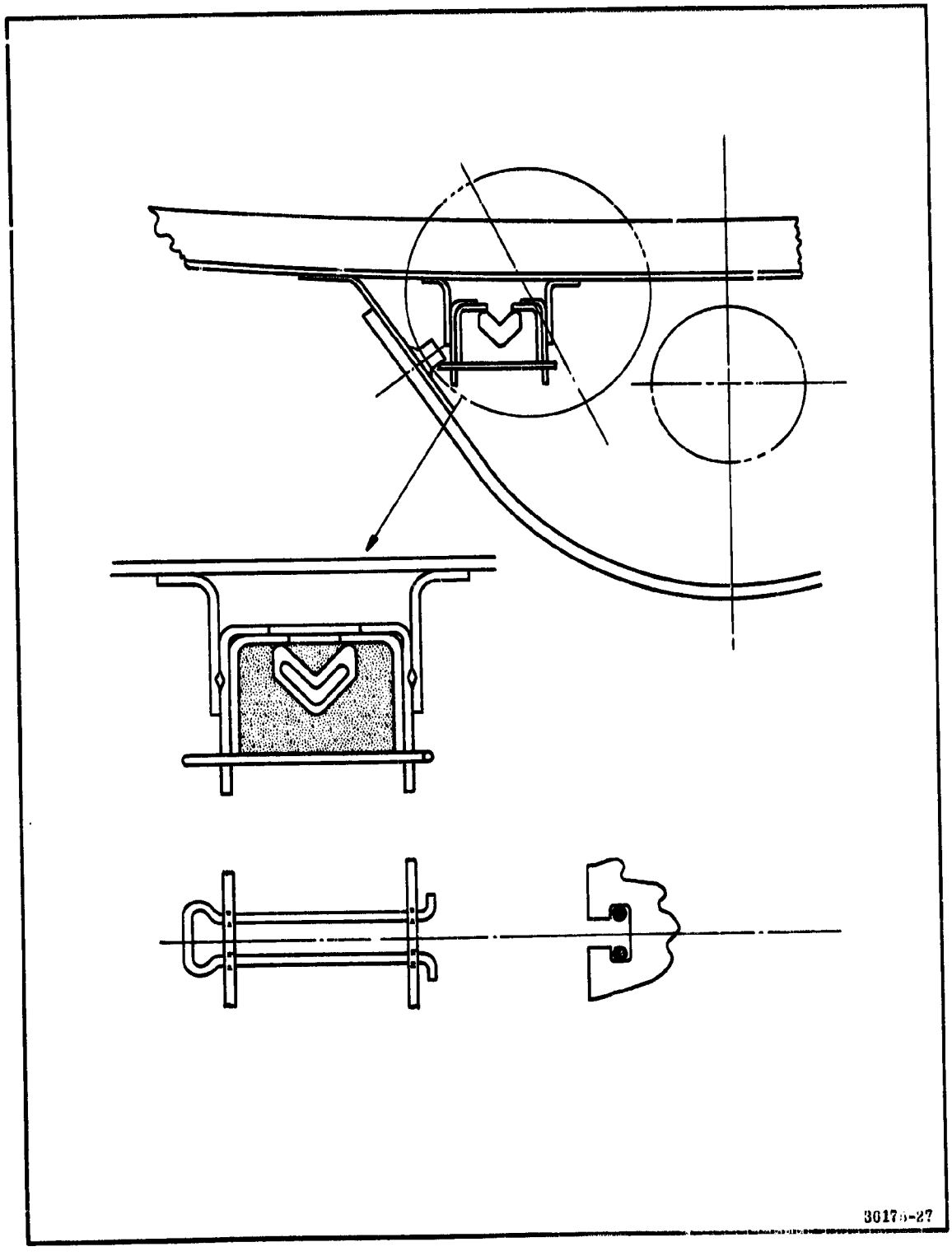

Figure 3-74. Destruct System Installation

Parameters	Requirement
Depth of cut	Through case and approximately half-way through internal case insulation.
Charge standoff	0.44 in.
Charge sheath material	Aluminum
Charge explosive material	RDX
Approximate length of charge (each side by side charge)	85 ft
Number of crossovers	One at each segment joint.

The ignition delay of the detonator is 200 to 300 microseconds. The linear shaped charges and explosive leads have a total length of about 1,020 in. At a detonation velocity of 6,500 meters/second (RDX), the time to detonate the complete charge from the S & A device to aft segment is less than six milliseconds.

The charges will penetrate through the case cylindrical sections in two parallel cuts.

The explosive components will be procured from an explosive component manufacturer and assembled at Thiokol.

The destruct system (except the shaped charges) will be assembled to the segments at the Wasatch Division. Final assembly of the charges into the raceway will take place at the launch site. The destruct system brackets, S & A device, LSC, and crossovers can be installed at the launch site with ease on the reclaimed motor cases if required.

3.4.2.2.3 Electrical and Electronic Systems

Power for the TVC system will be supplied from the ground electrical systems before launch and from the onboard battery system after launch. Remote switching capability between the ground and airborne power will be provided with control from the ground.

Other electronic and electrical subsystems required will be:

1. TVC distribution box
2. HPU control system
3. TVC power
4. Staging rocket ignition
5. Thrust termination and destruct

The same reliability requirements applicable to the baseline electronics and electrical subsystems also apply to the optional subsystems.

The nozzle actuation and staging rockets are discussed in a separate section. This section describes the destruct system and thrust termination.

During countdown and until the ordnance is armed, the simulator resistors and igniter S & A devices are monitored for unsafe voltage levels. The stray voltage detectors indicate excessive voltage by an electrically open condition on their output leads. Stray voltage detection (SVD) monitor circuits will be designed to detect current levels in excess of 500 milliamperes (ma) in the primer circuits. Detection is denoted by the removal of power from the ground checkout devices monitoring the state of the SVD circuit.

Separate voltage regulators are used for the enable/disable circuit and the igniter stray voltage detector. The latter circuit will be supplied with ground power during checkout and is inoperative during flight. The power supply voltage to the SRM enable/disable circuit is supplied by the ordnance battery.

The instrumented parameters directly associated with the box will be provided with circuit protection resistors within the unit, and final signal conditioning will be accomplished in the Flight Instrumentation Enclosure. These parameters are the "enable" indication, the "disable" indication, and the ignition currents (2).

The destruct system destructs the SRM case upon receipt of command from the the Space Shuttle Orbiter. These functions are accomplished by rupturing the motor case through detonation of linear shaped charges mounted on the SRM.

Safe and arming functions are accomplished by a mechanical S & A device with integral simulator resistors which allow continuous circuit monitoring for stray voltage.

Orbiter command signals for ignition command, destruct, malfunction detection enable and disable, and staging motor ignition are received and distributed by the ordnance distribution box. Power for the malfunction detection system (MDS) is supplied by the airborne ordnance battery.

Destruct subsystem design requirements will be satisfied by using qualified components. Destruct subsystem components which satisfy the requirements of the Space Shuttle are:

1. S & A device
2. Destruct charges
3. Transfer charges
4. Destruct raceway
5. Ordnance battery
6. Ordnance distribution box

The capability must be provided to arm the thrust termination or destruct explosive packages either by mechanical or electrical techniques and determination of the arm or disarm status must be possible by simple external inspection. Arming by solenoid or other electrical means will be accomplished prior to missile first motion. This incorporates a capability to permit electrical disarming from a remote location and a means of mechanically disarming at the missile. A system incorporating both arm and disarm capability also will provide a means of remotely indicating the arm or disarm status.

The SRM segment of the command destruct system will interface electrically with the Space Shuttle through the forward staging connectors. The command destruct electrical signal from the Orbiter will be routed through the ordnance distribution box to the destruct S & A which will detonate the destruct charges.

In accordance with design requirements, an electrical system for inflight disarming of the thrust termination and destruct systems will be provided. To provide the disarming function, an additional circuit will be designed and incorporated in the ordnance distribution box. The circuit will utilize the disable command signal to transfer ordnance battery power to the thrust termination and destruct units safe circuitry.

The ordnance distribution box provides the switching circuitry for firing the staging motors. Both the staging command and staging power are derived from the Space Shuttle vehicle.

In addition to performing the sensing and logic functions to provide malfunction detection, the ordnance distribution box performs a general distribution and control function on all ordnance power and command signals between the SRM and the Space Shuttle vehicle. Particular functions include monitoring the fire command circuits for hazardous currents during prelaunch conditions, distributing vehicle monitor power and Space Shuttle signals, and supplying flight instrumentation input signals. Both the firing and monitoring circuits are redundant. Solid-state active and switching elements are used throughout with the exception of relays which drive status-indicating lights for ground prelaunch monitoring.

The enclosure, which is the major design item, is a one piece aluminum casting. The enclosure provides a rigid assembly for the printed circuit boards and SCR's. The overall unit is approximately 13.9 by 17.0 by 8.5 in. and it weighs less than 50 lb. Discrete components will be mounted directly to the printed circuit boards in a planar arrangement. No connectors will be used in the circuit board assemblies. The harness breakout wires are terminated in crimp-pin connectors which are soldered directly to the circuit boards for improved reliability. The SCR's and power resistors will be mounted on the floor or walls of the enclosure.

3.4.2.3 Stage Components

The design of the structure required to mate the solid motors to the Space Shuttle vehicle and to support the assembled vehicle on the launch pad is presented in this section. Also included is a discussion of staging dynamics and load transmission to the Space Shuttle vehicle during separation of the SRM Stage. Electrical and electronic equipment requirements and interfaces have been discussed previously and therefore are not repeated in this section.

3.4.2.3.1 Introduction

The SRM staging structure was evaluated as a subsystem including (1) attachment structure, (2) nose cone, and (3) aft skirt. There is an interaction between component designs dependent upon the definition or selection of primary attachment locations and configurations.

Location of the primary attach structure in the aft end provides the advantages of deleting the need for a structural nose cone and reduced case launch and flight loadings. The aft skirt must withstand the predominant pad holddown loads and, consequently, is structurally capable of transmitting the thrust loads. However, discussions with prime contractors indicated that the aft attach configuration placed severe penalties on the HO tank design. Since case loads for the forward attach configuration are not significantly greater than horizontal static firing loads and can be readily accommodated in the design of the case segment joints, the forward attach configuration was selected for the baseline. In addition, the design was constrained to implement the distribution of attach structure loads within the nose cone and aft skirt (as opposed to the pressure vessel).

The loads definition for this study has, unfortunately, been rather general. It began with inhouse assumptions (from prior prime contractor data) as to vehicle configuration, acceleration, wind, and control requirements. Data later furnished by The Boeing Co were, in general, more severe than original assumptions and representative of load requirements later obtained through discussions with other vehicle contractors. The Boeing data (Tables 3-31 and 3-32) were input to the Thiokol NASTRAN model of the SRM Stage to establish component or element maximum structural loadings, response, and design requirements.

The baseline SRM Stage structure subsystem designs provide for the details requisite to (1) thrust vector control, (2) thrust termination, (3) staging, (4) recovery and refurbishment, (5) malfunction detection, and (6) electrical and ordnance subsystem components. To compensate for the lack of some fine details and refinements, the structure has been conservatively sized to assure credible costing.

TABLE 3-31

SRM STAGE TIEDOWN LOADS
(2-156 In. SRM's)
(The Boeing Company)

Load Condition	Limit Loads A (KIPS)	B (KIPS)	C (KIPS)	D (KIPS)
1. 1.0g Static	-1220	-1220	-1220	-1220
2. Ground Wind Producing Positive Pitch (Relative to Orbiter)	-871	-1569	-871	-1569
3. Ground Wind Producing Negative Pitch (Relative to Orbiter)	-1569	-871	-1569	-871
4. Full Orbiter Thrust, Zero SRM Thrust	-2842	+1245	-2842	+1245
5. Full Orbiter Thrust, Full SRM Thrust	-1673	+2414	-1673	+2414
6. Full Orbiter Thrust, Full Right SRM Thrust, Zero Left SRM Thrust	-2645	+1043	-1476	+2217
7. Full Orbiter Thrust, Full Left SRM Thrust, Zero Right SRM Thrust	-1476	+2217	-2645	+1048

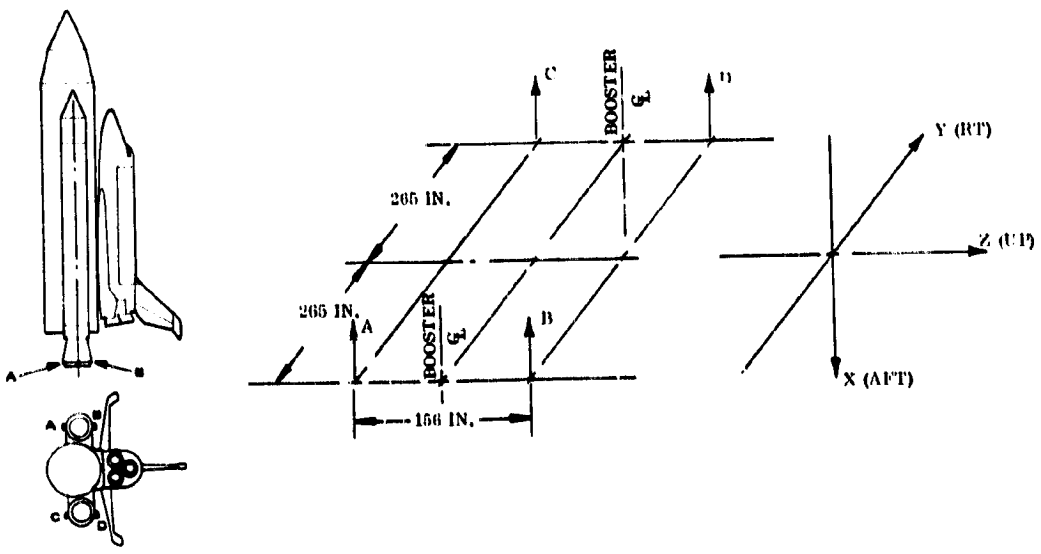

TABLE 3-32

SRM STAGE ATTACHMENT LOADS
(2-156 In. Parallel Burn SRM's)

Load Condition	Limit Loads				
	Forward Attach Fittings			Aft Attach Fittings	
	F_x (KIPS)	F_y (KIPS)	F_z (KIPS)	F_y (KIPS)	F_z (KIPS)
1. Thrust Buildup	-219	-16	-253	+16	-102
2. Launch Release (-)	-593	-43	-121	+43	-115
3. Launch Release (+)	-596	-43	-71	+43	-85
4. 3.0g Boost	-1613	-116	-20	+116	-23

Forward Fitting at Station 985
Aft Fitting at Station 2235

3.4.2.3.2 Stage Structure

3.4.2.3.2.1 Nose Cone

The baseline design selected for the forward structure is a structural nose cone concept, a schematic view of which is shown in Figure 3-75 . The main thrust load is reacted through struts into the main thrust clevis (Figure 3-76) which is bolted to a ring near the apex of the nose cone. The load is then transferred to longitudinal I-beam stringers back into a kick ring at the motor skirt interface. Two circumferential stiffening rings are joined to the longitudinal stringers to enhance the buckling capability.

A thin skin is attached to the outside of the structure for aerodynamic purposes.

The nose cone tip is a spun part attached to the main load ring. Several sway brackets (Figure 3-77) are attached to the kick ring.

The forward thrust structure provides aerodynamic fairing for the front end of the SRM and transfers the thrust load from the SRM to the HO tank. The thrust transfer occurs in such a manner that no deleterious concentrated loads nor bending moments are induced into the SRM case. In addition to the main thrust loads, the forward sway and roll loads are taken by the structure. Compatibility with the forward thrust skirt of the motor is required.

The two major forward thrust structure designs considered were:

1. A single point thrust pickup on a structural skirt extension with an aerodynamic nose cone.

2. A structural nose cone which doubles as an aerodynamic fairing and transmits the SRM thrust to the HO tank by two main struts attached to brackets near the apex of the cone.

Figures 3-78 and 3-75 are sketches of the two designs. Preliminary design studies for each concept indicate that typical weights would be 5,500 and 4,000 lb for the two designs, the structural nose cone concept being the lighter. Following is a list of the advantages and disadvantages of each design.

Structural Nose Cone

Advantages

1. Better distribution of axial load into SRM skirt.

2. Lighter weight, due to dual usage of cone structure and shorter overall length.

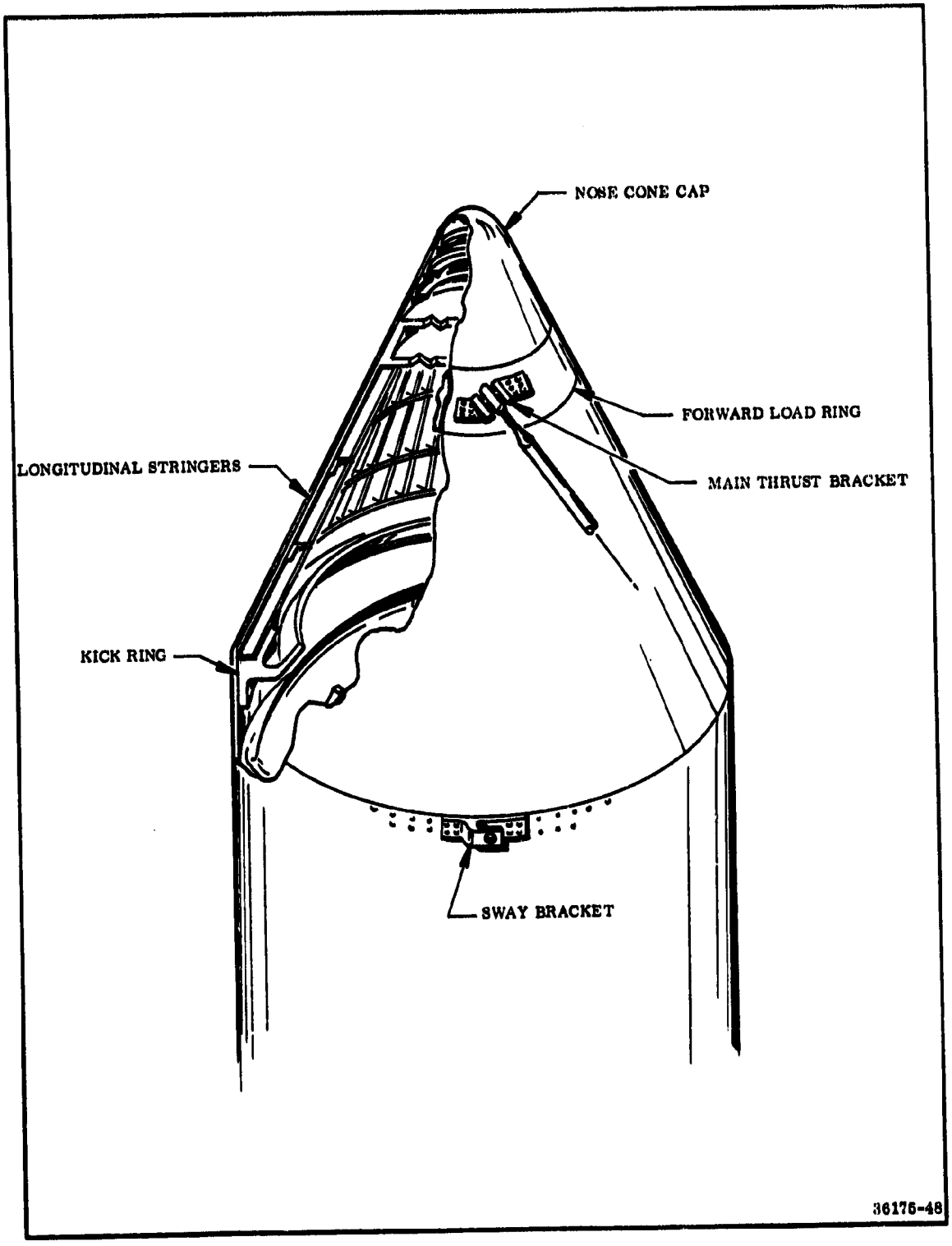

Figure 3-75. Forward Nose Cone

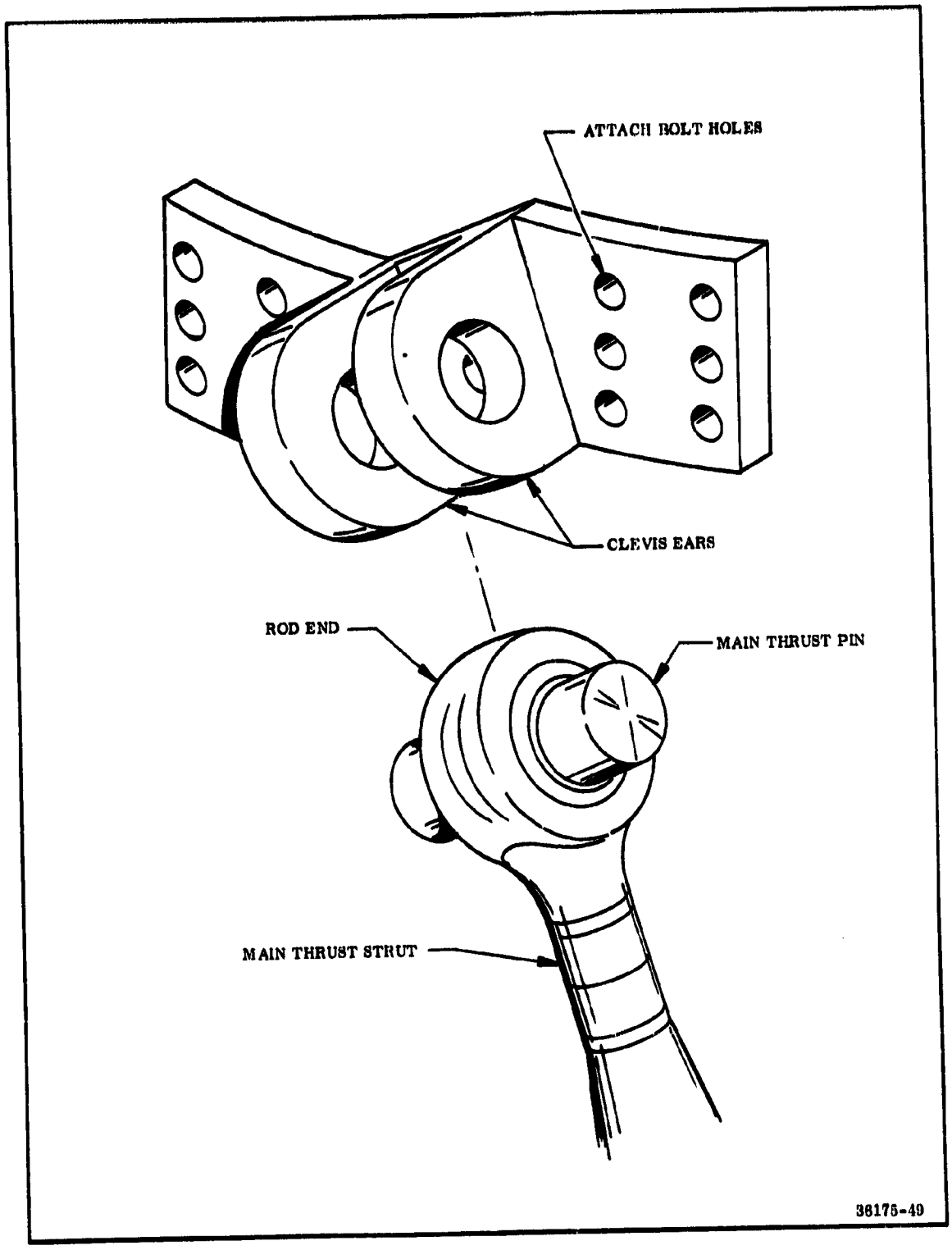

Figure 3-76. Main Thrust Clevis

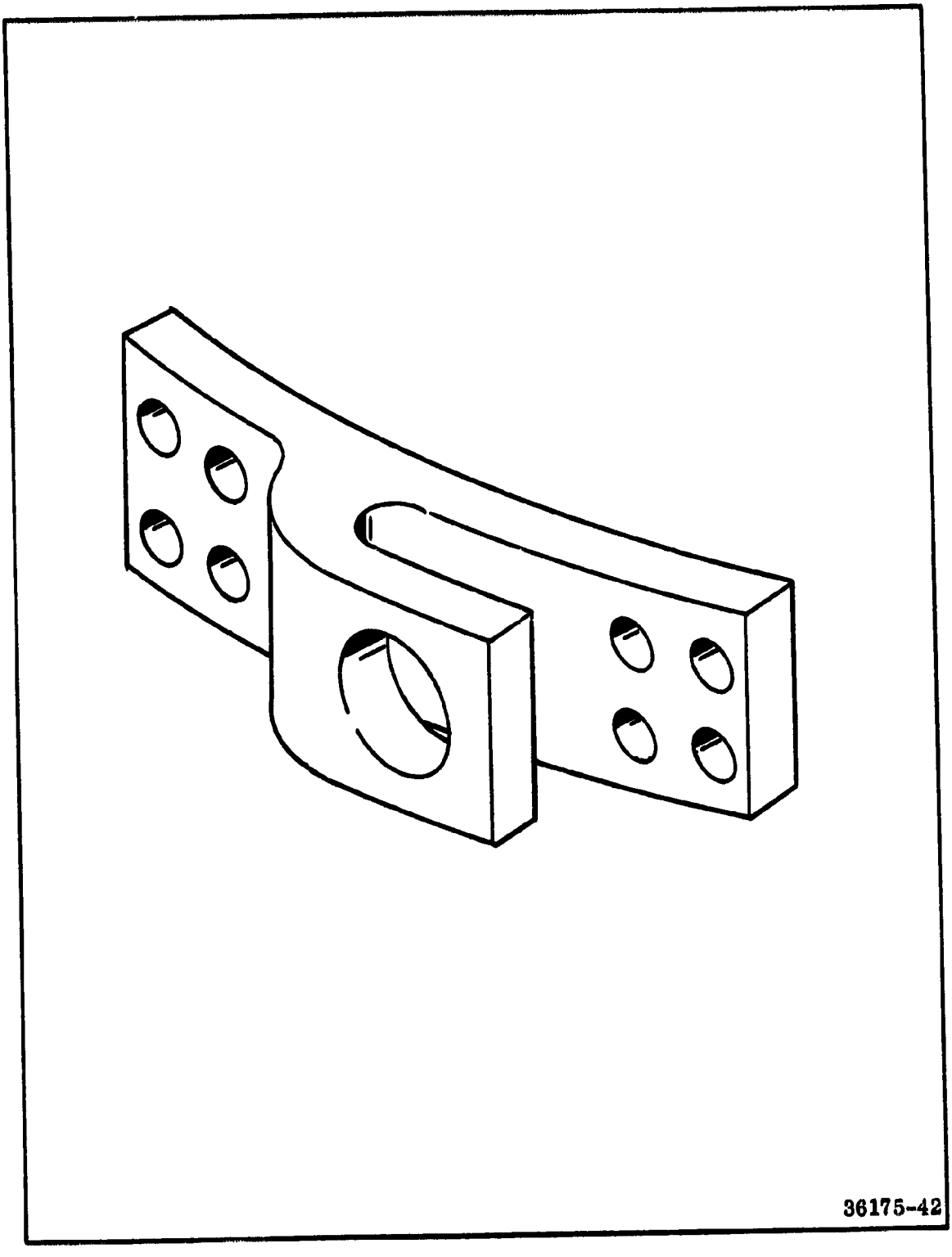

Figure 3-77. Typical Sway Bar and Roll Bar Bracket

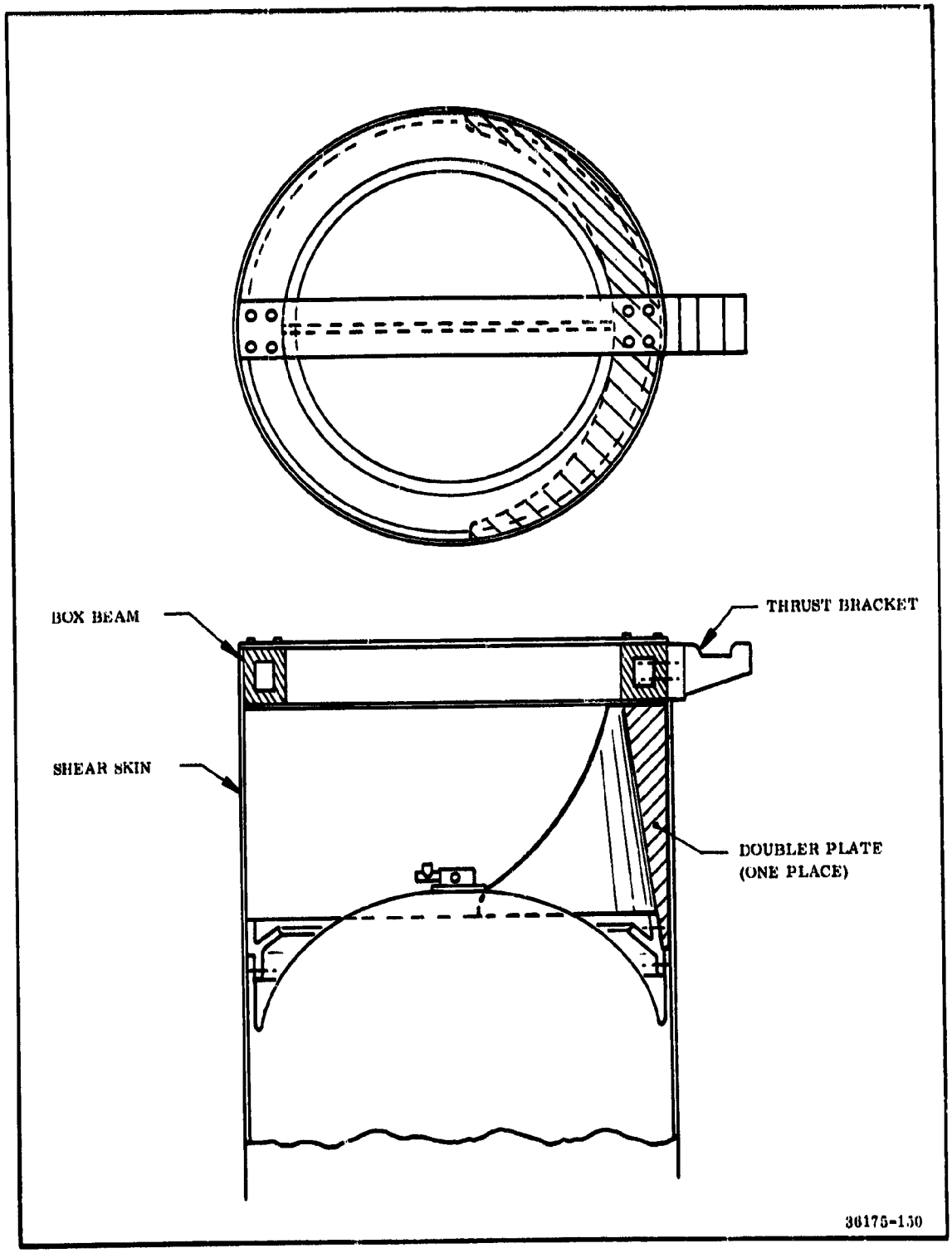

Figure 3-78. Single Point Forward Thrust Skirt

3. Less bending moment in motor case due to axial component of thrust being taken out near motor centerline.

4. Only one interface with motor.

5. More conventional - aircraft type structure; no tapered doubler plate. No large diameter torsional sections required.

Disadvantages

1. Two-point separation of main thrust struts.

2. Thrust termination ports must protrude through more complicated structure.

Single Point Thrust Pickup

Advantages

1. One separation point for main thrust connection.

2. No forward roll or sway bars required.

Disadvantages

1. Induced large additional bending moment in case due to axial thrust component being taken far from motor centerline.

2. Higher circumferential loading transmitted to SRM thrust skirt.

3. Two interfaces, with component interchangeability, will be required - thrust skirt to motor and thrust skirt to nose cone.

All major components used in the baseline forward nose cone and thrust adapter design are 6061-T6 aluminum. The alloy is readily obtained and can be formed and welded easily. Most fabrication shops have ample experience with the material. It has adequate strength in the T6 condition to accommodate efficient design practices.

There are, however, many aluminum alloys which afford essentially the same advantages as 6061 which could be easily substituted.

All fasteners would be standard aircraft type.

The general type of construction (frame, skin stringer) is quite standard in the aircraft industry and represents no significant departure from current fabrication technology.

The nose cone tip will be spun to shape from aluminum plate. The main load ring will be a machined forging or casting.

The longitudinal stringers will be standard I-beam shapes, cut to length and welded forward and aft to the main load ring and the aft kick ring, respectively. Two standard "U" sections will be rolled into circumferential rings and welded to the stringer columns for stiffening.

An aerodynamic skin will be riveted to the outside of the entire frame assembly. The skin will consist of rolled plate with a doubler plate at the skin (seams).

The main thrust bracket and the sway bracket will be machined from 4130 castings or forgings and heat treated to 180,000 psi minimum ultimate strength. They will be bolted to the appropriate rings.

3.4.2.3.2.2 Aft Support Skirt

The baseline design of the aft support skirt is shown in Figure 3-79. The entire assembly is bolted to the aft thrust skirt of the SRM motor at the upper box ring. This ring serves a dual function. It provides a double surface on which to mate the motor and aft structure and provides a stiff frame for aft sway and roll bracket mounting. If TVC is required, the nozzle actuator will also be mounted on this frame.

The entire compression and tensile axial skirt loads enter the structure at two places shown as the holddown and support points. The load carrying capability of these two points is provided by large doubler plates which begin as a very heavy section (approximately 12 in. wide) at the base and spread out at 30 deg (per side) as the thickness decreases. This is required to distribute the axial load.

The compressive axial loading is taken in bearing at the end of the doubler plate, while ports are provided in the doubler for holddown hooks to grip the skirt and react the tensile (thrust) loading.

An "L" frame is provided at the aft end of the skirt to maintain the circularity of the section during loading.

A relatively thin aft fairing skin circumvents the doubler plates and "L" frame. This skin will provide both aerodynamic protection and transverse (shear) load carrying capability.

The center ring is at approximately the midpoint of the aft structure. Shown as a T-section, this ring serves to further distribute the load from the doubler plates,

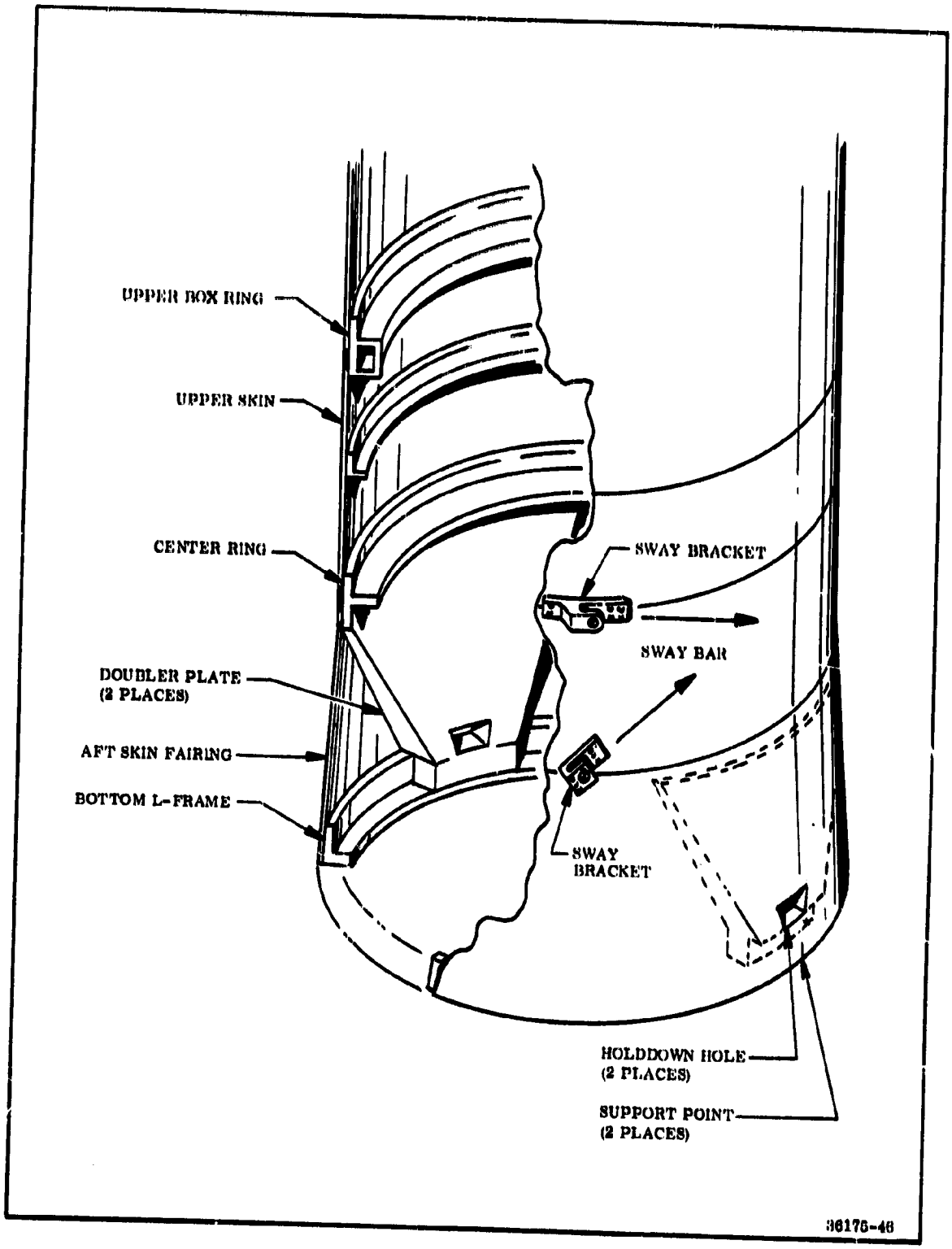

Figure 3-79. Aft Support Skirt

connects the doubler plates and aft skin to the upper skin, and provides a stiff frame for additional sway bar brackets required for staging purposes.

The upper skin is much heavier than the aft fairing since it is a primary load carrying member. The support loads from the doubler plates are transmitted through this skin to the upper box ring and aft skirt of the SRM.

The general nature of the design allows for a fairly conventional approach to fabrication. All mechanical joints will be made with standard type aircraft fasteners. A minimum of welding is required, although welding (spot or seam) will be permitted in constructing the basic skin and frame sections, if required.

The aft support skirt must support the entire weight of the orbiter, HO tank and SRM assembly in the prelaunch condition on the launch pad. In addition, it is required to hold the assembly on the pad in the post-ignition condition.

After the assembly of the complete shuttle unit, all of the weight of the entire assembly including the orbiter, HO tank (loaded), and SRM's must be supported at two points on the aft skirt of each SRM (four points total). In addition, the assembly can be subjected to a ground wind in any direction. This overturning moment contributes additional loads to the load points in the worst condition in addition to the basic compressive load due to weight.

The most severe design condition will occur upon ignition of the orbiter but prior to SRM ignition. At this time the support points must be capable of reacting: (1) the total assembly weight minus orbiter thrust; (2) the overturning moment of the orbiter thrust which acts offline with the support centerline; and (3) an overturning moment due to maximum launch wind loads. A preliminary estimate of these loads was presented earlier in Table 3-31.

Only one general kind of aft skirt assembly presently is being considered. The requirements dictate that the load must enter at two support points. From these points, the load must be spread out through heavy members to an acceptable level before it enters the aft motor case thrust skirt. The heavy structure that serves to spread the load can be fabricated from either tapered plate material as shown in Figure 3-79 or from tubular columns as shown in Figure 3-80.

All major components used in the baseline aft skirt design are 6061-T6 aluminum.

All fasteners would be standard aircraft type.

Except for the size of some of the components, the design of the aft support skirt is conventional and lends itself to standard fabrication procedures. Typical fabrication techniques for each component are as follows.

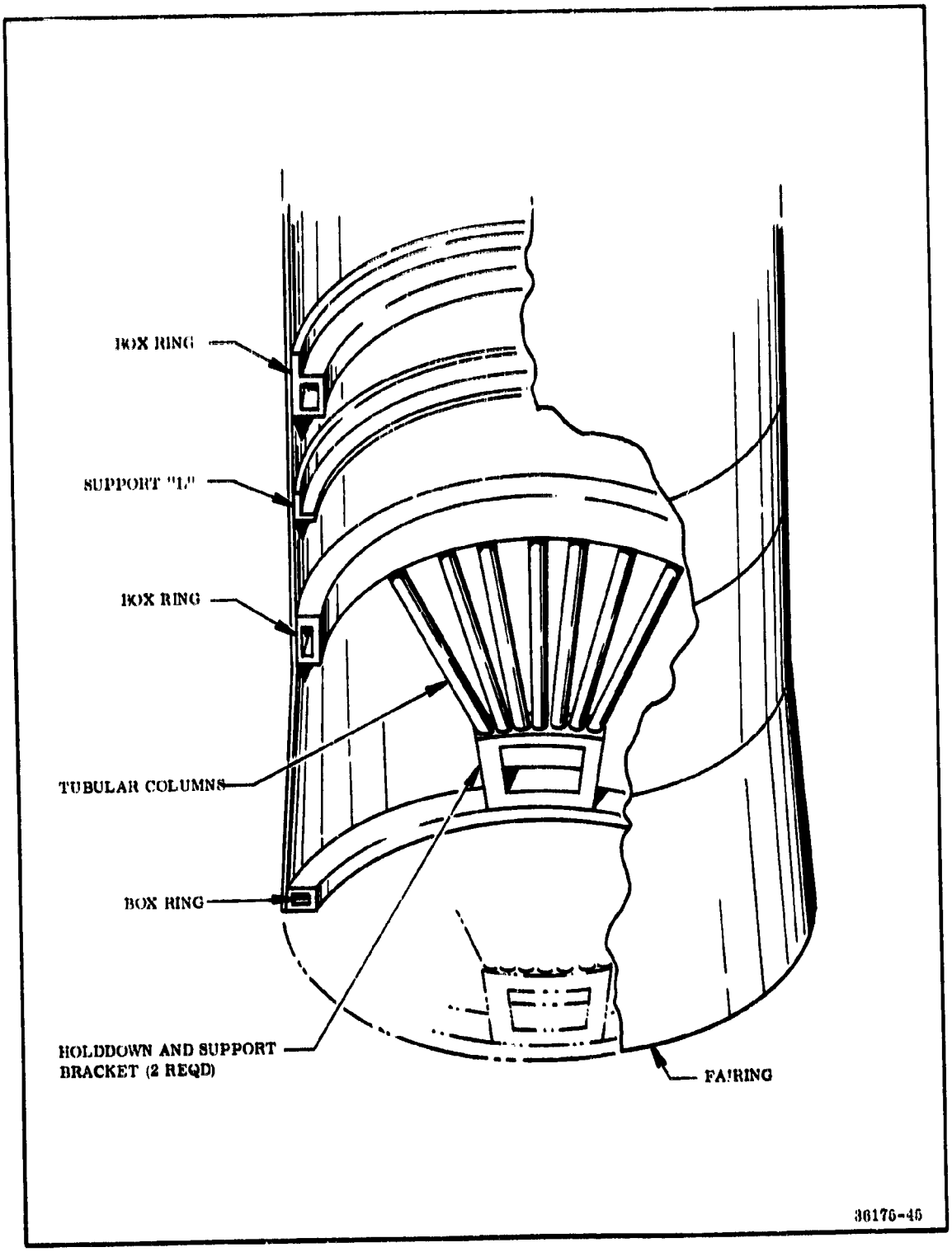

Figure 3-80. Aft Support Skirt Tubular Column Design

The heavy, tapered doubler plates will be rolled to a cylindrical shape from plate material equal in thickness to the maximum required. The doubler shapes will then be cut from the plate, and the contour machined. (The procedure could be reversed, and the contour machined when the plate is flat and then rolled or pressed to shape, either hot or cold.)

The bottom "L" frame will be either a welded section or extruded. The same is true of the upper box ring or the center "T" frame. In large production quantities, it would probably prove economically desirable to procure extrusion dies and extrude the sections.

Both the upper skin and aft skin fairing will be rolled aluminum plate. One or more longitudinal doubler strips are permissible if the sections are segmented.

All connections will be made with standard aircraft connectors (bolts, rivets and special application fasteners).

Interchangeability will only be required at the interface between the aft skirt and the case. The fit of subcomponents within the aft skirt can be built upon a fit at assembly basis and interchangeability will not be required.

3.4.2.3.2.3 Stage Attach Structure

Following the general SRM approach to design and analysis, the stage attach structure is relatively simple and straightforward. A structure of column elements has been selected, because it is analytically predictable, has design flexibility, and can be fabricated easily using available standards. The SRM Stage with the four fixed but adjustable attach points is presented in Figure 3-81. The primary axial loads are transmitted through the tensile elements of the forward frame structures. The aft attachment is not constrained in the axial direction. Details of the elements and components are found in Figures 3-82 and 3-83.

The illustrated design was analyzed for the loads presented in Tables 3-31 and 3-32 using the NASTRAN S3291A computer code. The column or rod elements were so sized that limit stresses were 60 ksi or less. Thus, many relatively low cost, readily available steels are applicable.

The columns or rods will be composed of solid end tubes fitted with rod or clevis ends and ball joints. The tubes will be rolled and welded in standard sizes, and high strength tube ends will be machined from bar stock. All but the main thrust element rod ends will be standard high strength parts. The main thrust rod and the clevis ends will be machined to requirements.

The forward attachment fittings (Figure 3-84) will be machined from forgings and welded to the main thrust elements. They will include the flanges and

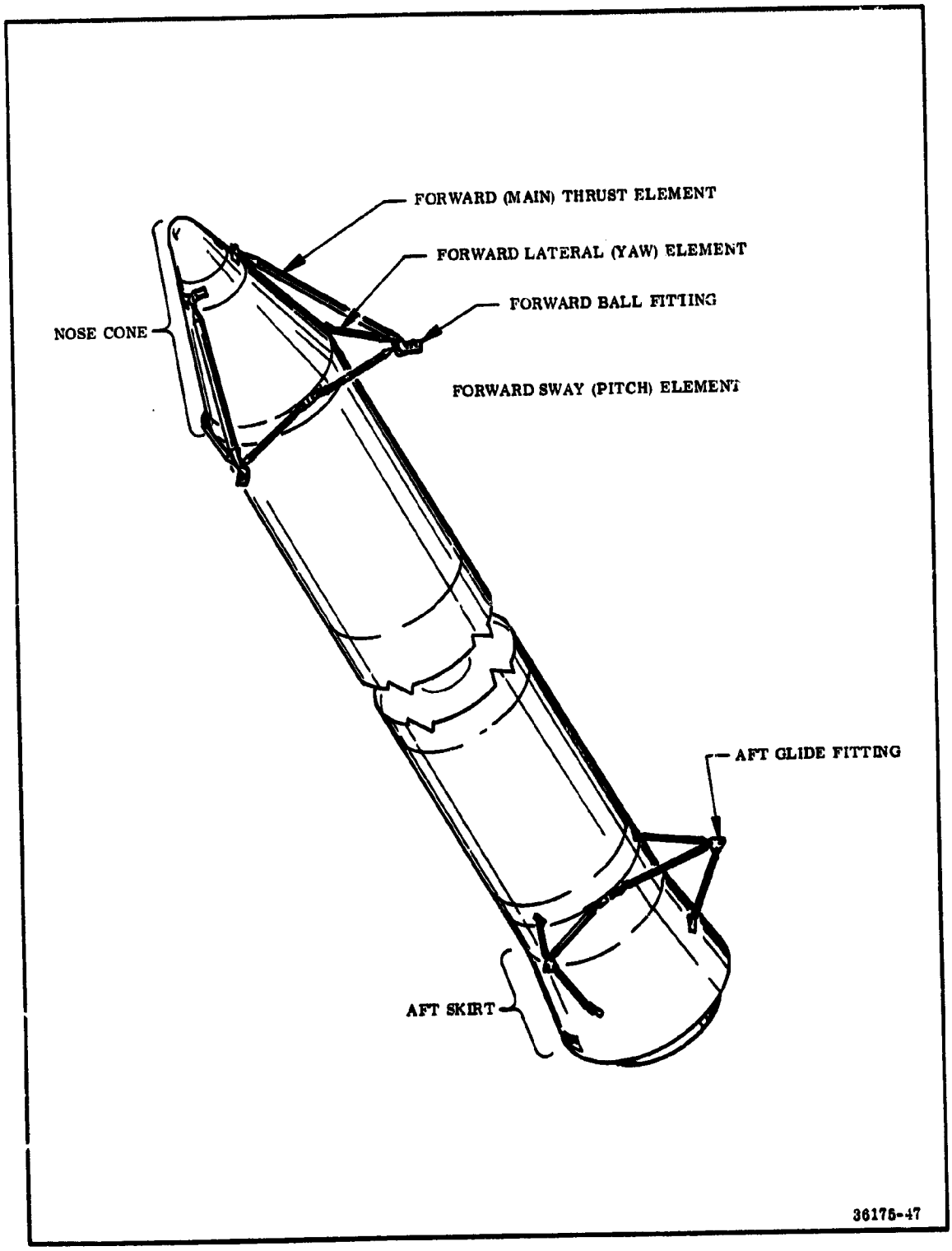

Figure 3-81. SRM Stage Attach Structure

FOLDOUT FRAME

FOLD

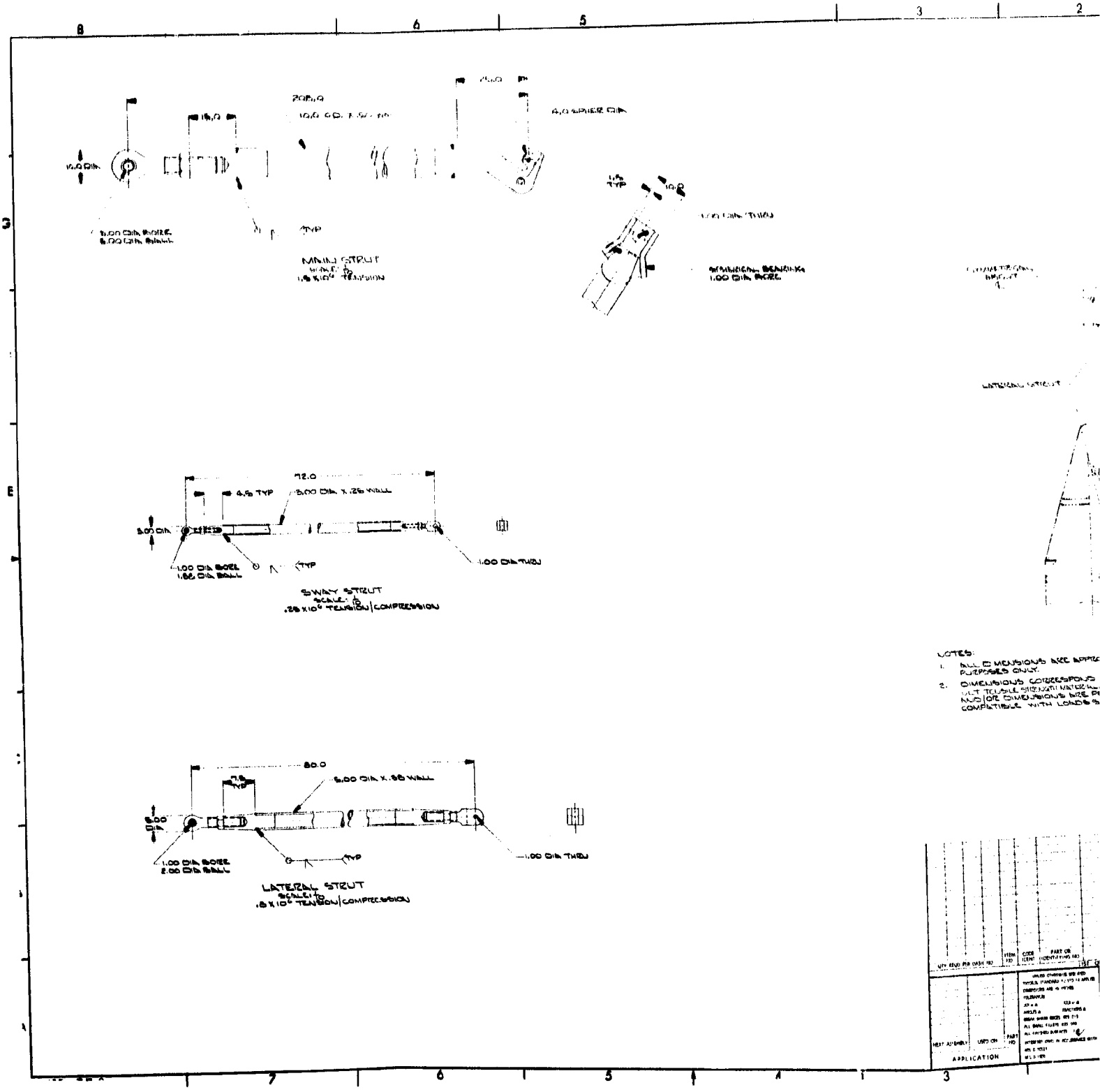

Figure 3-82.

FOLDOUT FRAME

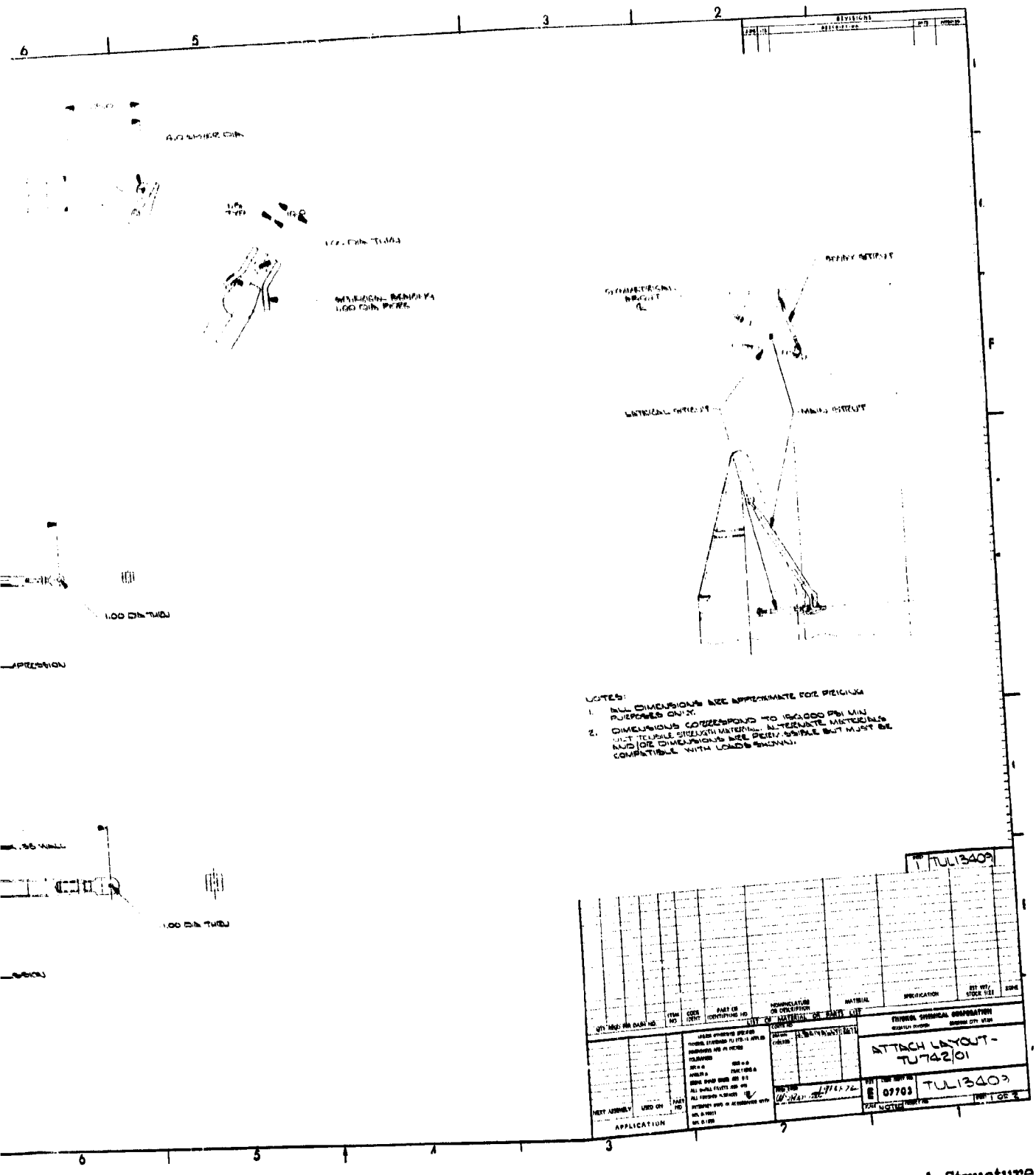

Figure 3-82. Forward Attach Structure

FOLDOUT FRAME 10

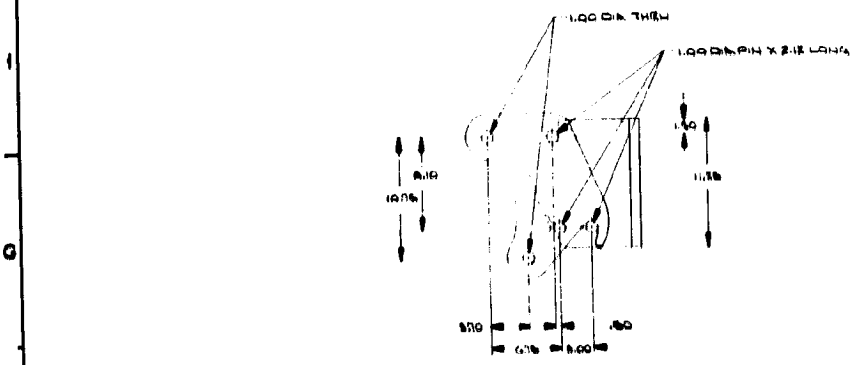

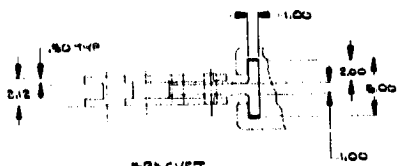

BRACKET
SCALE: 1/2

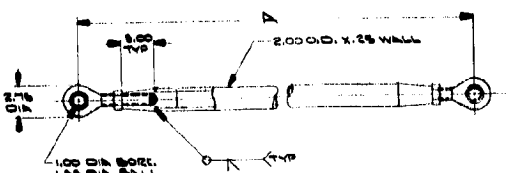

STRUT DETAIL
SEE TAB BLOCK
SCALE: 1/2

	A
LEFT MAIN STRUT	108.0
LEFT LATERAL STRUT	60.0
LEFT SWING STRUT	48.0

} 200,000 LB TENSION/COMPRESSION

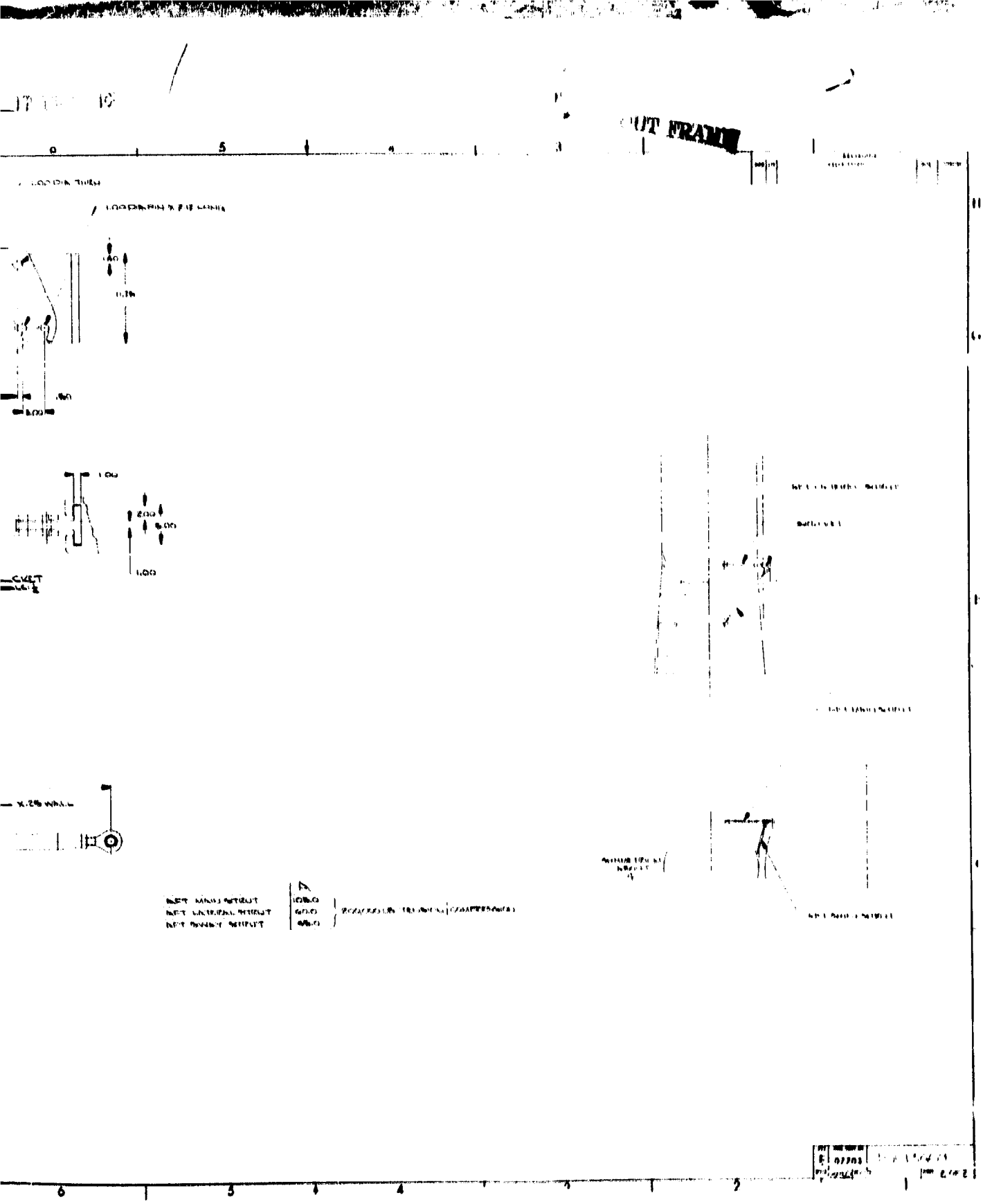

Figure 3-83. Aft Attach Structure

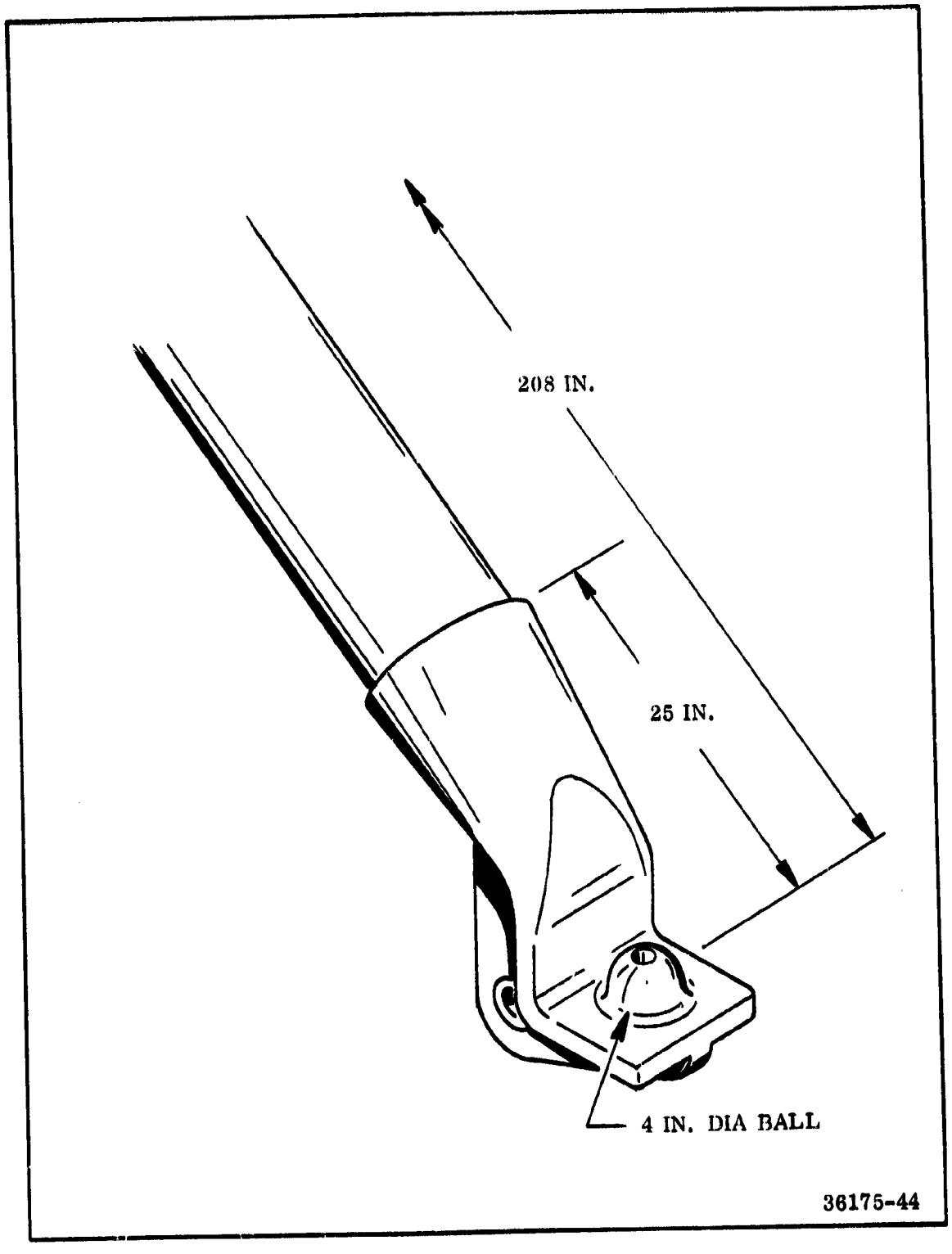

Figure 3-84. Forward Attach Fitting

ball joints to mate the forward stabilizing element clevises. The main ball will interface with the HO tank structure and will include the explosive release bolts.

The aft attachment fittings (Figure 3-85) also will be machined from forgings. The head of the "T" will be the glide that will be contained in a track on the HO tank. The aft lateral element clevis will be double pinned to stabilize or fix the interface dimensions. The fitting will include the ball joints for interface with the thrust and sway elements.

The design requirements for the SRM Stage attach structure are necessarily somewhat general, since a particular vehicle and the associated structural and dimensional interfaces have not been defined. The requirements postulated by Thiokol for the purposes of this study follow.

1. The design will be conservative to assure that any adaptation to future specific requirements will not exceed the predicted costs.

2. The design safety factor will be 1.5 considering the most severe combination of loading for the conditions of launch, flight, staging, and recovery.

3. The attachment structure should be adjustable to compensate for stage assembly tolerances.

4. The design should be compatible with reliable explosive release mechanisms and rocket assisted staging.

5. Localized loads must be transmitted outside of both the SRM and HO tank pressure vessels. Load distributions in the pressure vessels should be reasonably uniform.

While formal trade studies on the stage attach hardware were not developed, the many possible concepts or alternatives were systematically evaluated. This approach led to the baseline selection of the relatively simple, analytically predictable, column element frame structure. The selection is conceptually similar to the Titan IIIC design.

Following are discussions of the more significant elements, parameters, or variables considered.

3.4.2.3.2.3.1 SRM to HO Tank Interface Locations

Vehicle contractors indicate a strong preference for location of the primary attach point at the bulkhead between the Hydrogen and LOX tanks. While advantageous

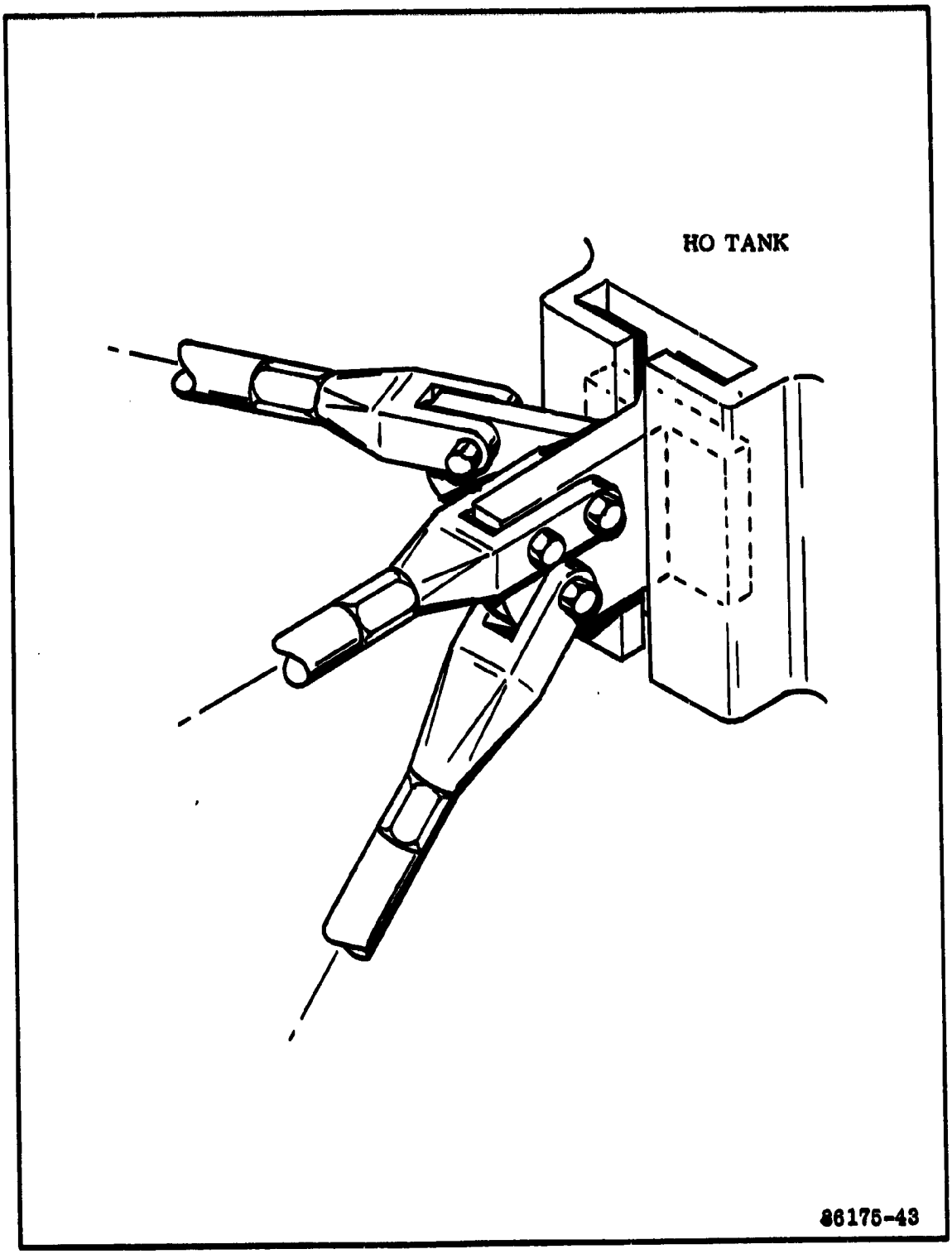

Figure 3-85. Aft Attach Fitting

to the HO tank design, this forward attach point will penalize the SRM design. The forward attach point will require that the case transmit larger bending loads. However, these loads only affect the segment joint design--the design load would be increased by approximately 15 percent.

3.4.2.3.2.3.2 Load Transfer

Column, beam and shear elements and combinations thereof have been considered. A single primary attachment at the tangent point of the SRM and HO tank diameters has been suggested by several vehicle contractors. While apparently simple and attractive, the structure (probably a shear web or truss) required to transfer the load would be relatively complex. This complexity results from the requirement to distribute the loads outside of the SRM case.

The column element frame structure with the major load element (strut) in tension allows the introduction of load high on the nose cone. The nose cone is designed to approach uniform distribution of the load at the case interface. The transverse reactions of the forward and aft stability struts are readily distributed through the attachment ring.

Conceptually the frame structure design is that of the Titan staging structure and has been selected as the baseline for this study.

3.4.2.3.2.3.3 Release Mechanism and Staging Technique

The SRM will be released through an explosive mechanism. While many techniques are practical, a simple explosive bolt has been selected as the baseline. It would be compatible with a ball and socket type joint aligned to transmit the primary load either in shear or compression.

Mechanical aerodynamic staging appears feasible; however, there is some concern as to the difference in release dynamics for the two motors for all vehicle attitudes and maneuvers. Rocket assisted staging should be faster and more consistent of all conditions. In the final analysis, some short term mechanical control or guidance could be desirable.

These considerations resulted in the baseline selection of a compressive ball joint to react the primary load at the forward attach points. The ball will be contained in the socket by an explosive bolt. This bolt will react the SRM burnout (prestaging) tension loads. The aft stabilizing structure attachment will be a glide or roller contained in a track on the HO tank skirt (no vertical constraint).

Two staging techniques have been evaluated. The mechanical staging sequence will initiate with the signal to the explosive bolts. The SRM will slip aft, clearing the ball joint prior to hitting the aft attach fitting stop. Aerodynamic forces (and a

vaulting bar, if required) will force the SRM to pivot about the aft mechanical release mechanism to the required release attitude (30 deg). The rocket assisted staging sequence will begin with the simultaneous initiation of the staging rockets and explosive bolts. The SRM will drop, clearing the ball joint prior to clearing the aft track. The track will be configured to assure the proper initial conditions for the desired staged SRM trajectory.

3.4.2.3.2.3.4 Assembly

The struts of the selected frame structures are, in essence, large turnbuckles. This adjustment feature will allow for assembly tolerances and provide for SRM alignment and limiting strut preloads.

The frame structures must be restrained to the SRM to prevent damage to the orbiter, SRM, and stage structure during staging. Each of the two forward and two aft attach structures will be stable three element frames. The resulting analytical redundancy will be evaluated for the worst combination of coupled and uncoupled elements.

3.4.2.3.3 Staging

Staging of the SRM's in the parallel burn mode requires a smooth separation of the expended motors from the orbiter vehicle, followed by a safe, collision-free trajectory. The relative and absolute motion of the SRM Stage and the aft end of the orbiter vehicle must be considered during the staging sequence to assure that no contact occurs between orbiter vehicle and the staged system. A rigorous and detailed analysis has not been possible, since some items, such as the effects of mutual aerodynamic interference, are beyond the scope of this study; however, within limitations, it has been possible to identify the two methods that appear feasible, which are presented below.

In the first method (Figures 3-86 and 3-87) the SRM forward attachment is mechanically released from the orbiter tank, which allows the SRM, hinged at the aft attachment, to pivot in the yaw plane to an angle of 28 deg. Anticipating small differences in rate of rotation, the SRM's would not be expected to achieve the 28 deg of rotation simultaneously; therefore, when one of them passes the 28 deg position, an explosive charge would be actuated at each aft attachment and both of the expended SRM's would be released from the orbiter tank. There is redundancy in the aft release mechanism provided through a mechanical release of the aft attachment when the SRM's have reached a rotation angle of 30 deg. Simultaneous release of the SRM's will produce a smoother and cleaner staging operation, as smaller unbalanced forces will be transmitted to the orbiter vehicle, resulting in requirement for less control correction in the yaw plane. This method is similar to the mechanical release system proposed by the McDonnell Douglas Astronautics Company.

Time zero in the staging sequence occurs when the SRM thrust has decayed to 75,000 lbf. At this time, the forward attachment is released, allowing the SRM's to shift aft to a position where the aft end is hinged and the forward end is free. In the hinged position an initial force of 86,400 lbf acts forward and parallel to the orbiter's centerline. This force imparts an acceleration of 0.57 g's to the SRM relative to the orbiter flight path.

The acceleration of the orbiter is sufficient to initiate an outward rotation of the SRM. As the SRM rotates, aerodynamic forces will contribute to the outward angular acceleration until the SRM reaches its point of release. After final release, each SRM assumes its individual trajectory away from the orbiter vehicle.

From initial release and during the rotational sequence, the SRM residual thrust continues to decay until at the time of final release it has reached approximately 10,000 lbf. The forward differential acceleration at the aft attachment increases in response to the SRM thrust decay, aerodynamic forces and realignment of the thrust vector as the SRM rotates outboard. The maximum reactions

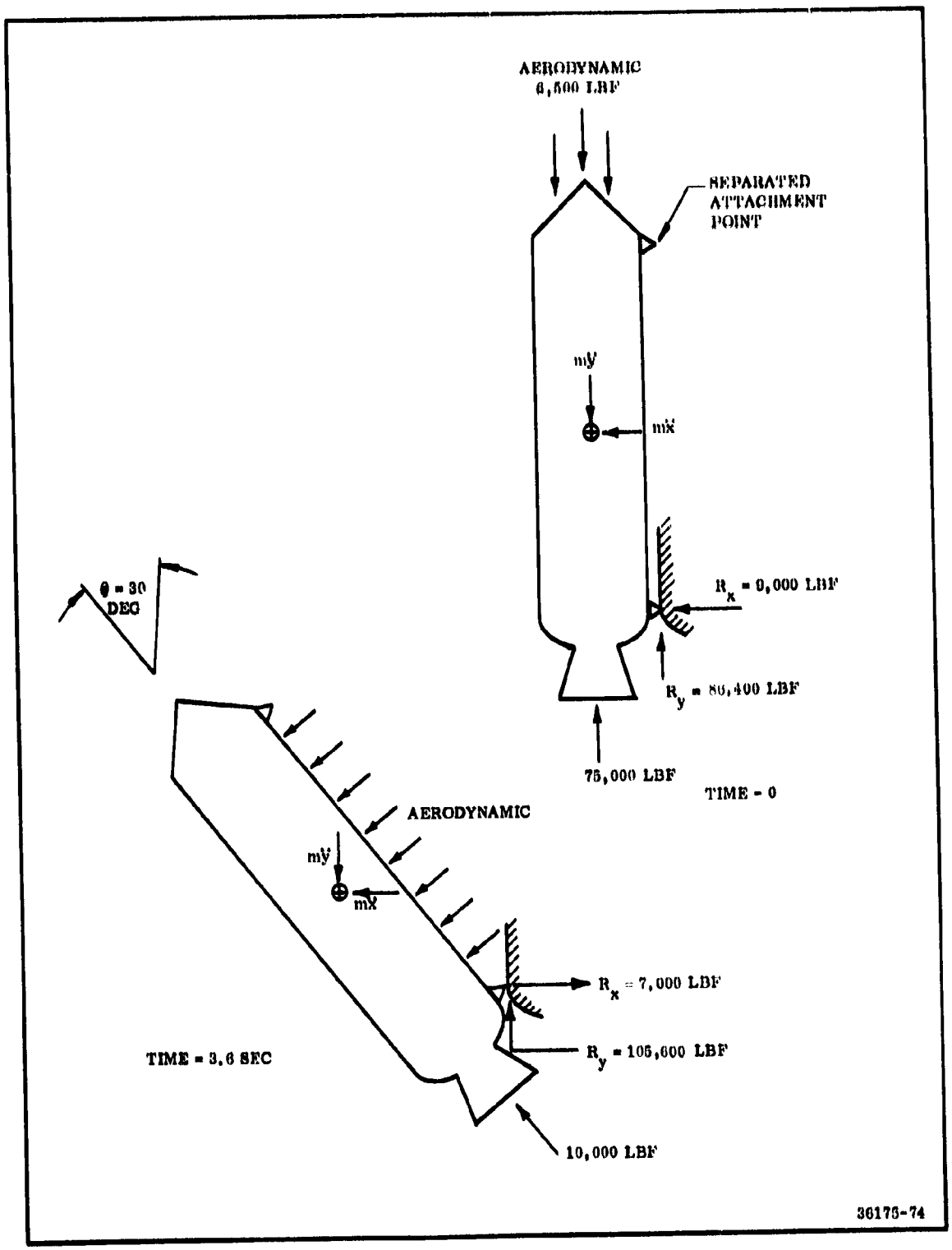

Figure 3-86. SRM Staging Forces Diagram

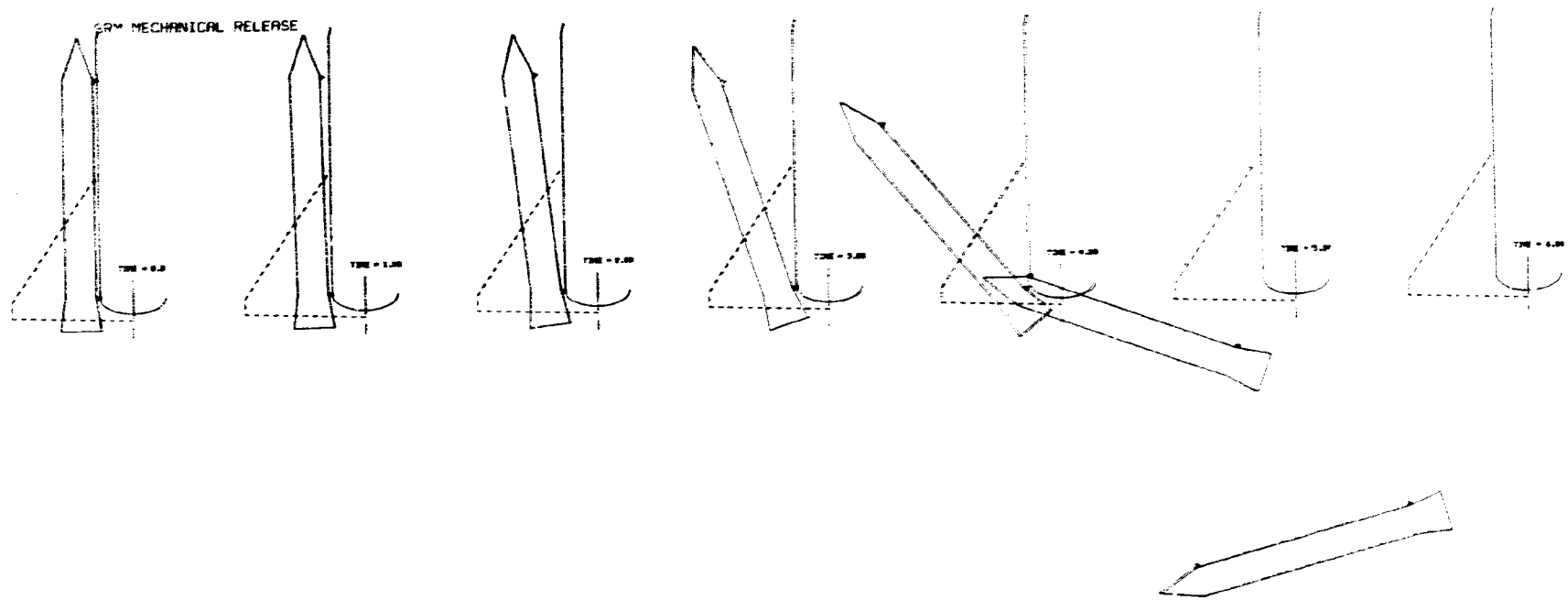

Figure 3-87. SRM Staging Positional Sequence Diagram

calculated for the connection during the staging sequence are 118,000 lbf forward and 14,000 lbf laterally at 11 deg rotation angle.

In the staging sequence where release at the aft attachment is effected in the redundant mode (mechanical release at θ = 30 deg), there will be an instantaneous change in the connector reaction force equal to 105,000 lbf. As the release is mechanical, it is not probable that the two SRM's will release at the identical time instant; therefore, the force imbalance imposed on the orbiter vehicle would cause its rotation toward the first released SRM. The release of the second SRM would remove the force imbalance, but the motion induced on the orbiter would represent a yaw error and might require correction by the orbiter controls.

The predicted forces and accelerations at initial and final stages of separations are shown in Figure 3-86 . It is shown by simulation that, in this case, successful staging will occur. This method of separation does not represent a hazard to the crew nor will it cause such damage to the SRM's that recovery and refurbishment would be impaired. The trajectories of the SRM's during the staging sequence are shown schematically in Figure 3-87.

The alternate staging method employs a rack of solid propellant staging motors attached to the forward and aft ends of the SRM's and provides redundancy to the mechanical staging mechanism. In this staging concept, the SRM's may be released simultaneously without inducing asymmetric disturbance in the orbiter vehicle.

This method provides for the SRM's to be translated laterally and downward from the orbiter vehicle in a stable manner until they have cleared the collision envelope. At time zero of the staging sequence, the separation motors are ignited; the SRM is released at the head end and the aft end moves back along a guide rail. This restriction of lateral motion at the aft end insures that the forward end will rotate outward into the airstream. The direction of travel of the aft end of the SRM is controlled by the guide rail to impart the desired orientation of the velocity vector which complements the velocity imparted by the thrust forces from the staging motors.

It is considered imperative that the individual motors of the forward rack have greater thrust than those of the aft rack so that rotation begins and the aerodynamic forces on the SRM augment the other forces toward increased separation distance. To accomplish this, the forward rack of staging motors will have a high initial thrust with a regressive thrust trace and the aft staging motors will have a low initial thrust with a progressive thrust trace.

The staging motor system should safely stage each SRM if one of the eight individual motors should fail to ignite. This requires that the initial thrust of only

three forward motors be greater than the initial thrust of all four aft motors to assure that the resultant force would cause the forward end of the SRM to rotate laterally and down. In case only three of the aft staging motors operate properly, the initial thrust must be sufficiently high to assure that the aft end of the SRM translates laterally and down to clear the orbiter HO tank and the orbiter wing.

The staging motors will be designed with identical hardware except that the fore and aft attachment fixtures will not be interchangeable. Manufacturing tooling will be designed to prevent interchanging propellant grains between the forward and aft motors.

The size of the staging motors was based upon staging dynamics at 160,000 ft using a simulation which neglected aerodynamic interactions between the SRM and the orbiter. The assumed altitude is the highest shown in data obtained from the vehicle contractors. It represents the lowest aerodynamic forces and thus demonstrates the case for which physical separation will require the longest period of time. The study of effects resulting from orbiter maneuvering at the time of release is beyond the scope of present study effort; these effects must be studied in detail to adequately characterize the separation motors.

A sketch of the staging motors is shown on Figure 3-88. Expected thrust-time history is shown in Figure 3-89 .

The separation sequence is shown schematically for the normal and the two failure modes (where either a headend or aft end motor failed to operate) in Figure 3-90 .

The selection of the staging mechanism is based upon cost, redundancy, reliability, ease of staging, and crew safety. The mechanical system is the simplest to design and the least expensive, requiring only the successful release of the headend connection.

The alternate method results in increased system weight by addition of the separation motors. The system will provide a smooth separation and has comparable, or greater, reliability and increased crew safety relative to the mechanical release system.

The simplicity and relative reliability of the purely mechanical system makes it the system selected for the parallel burn baseline design.

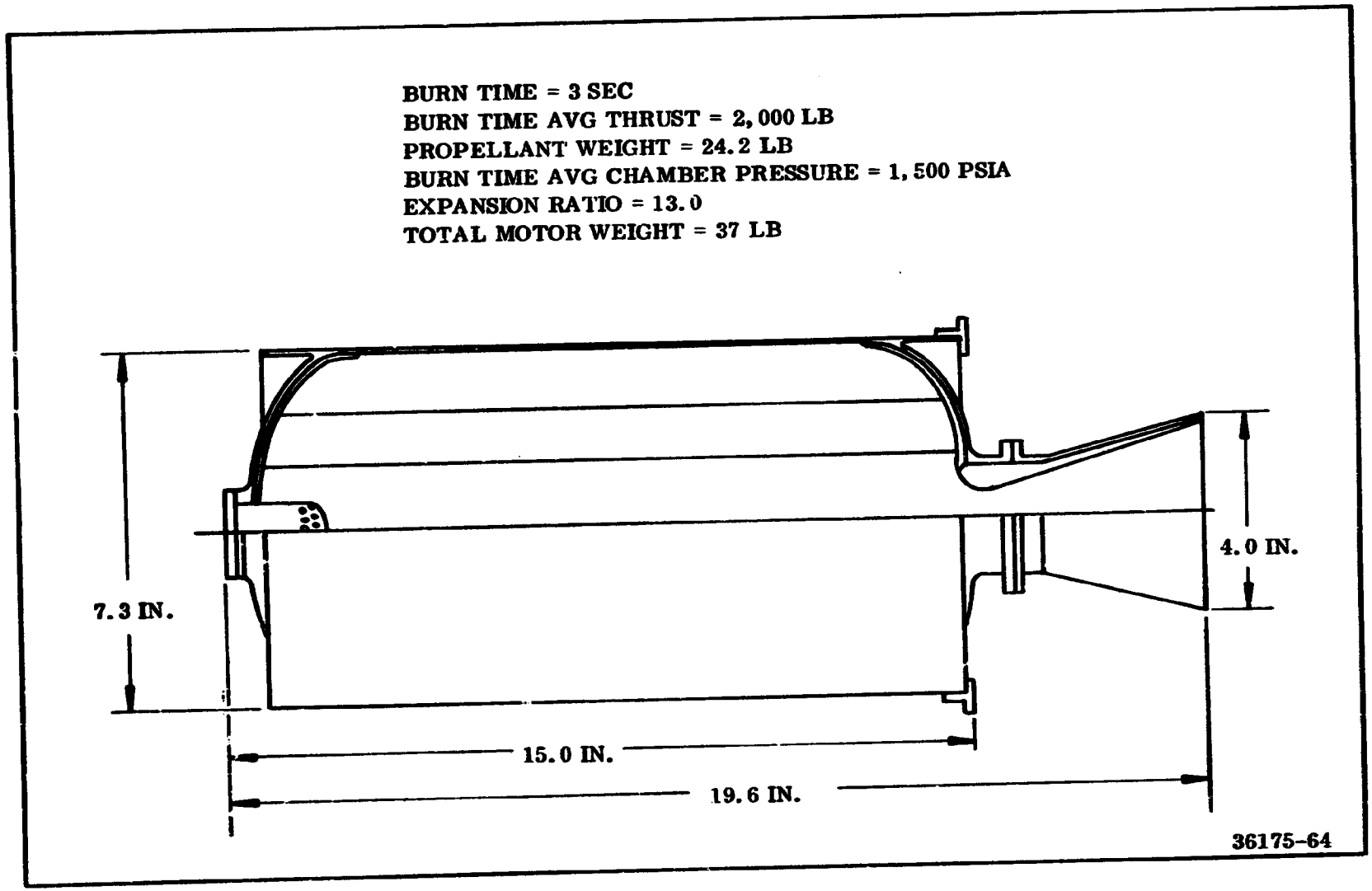

Figure 3-88. SRM Staging Motor

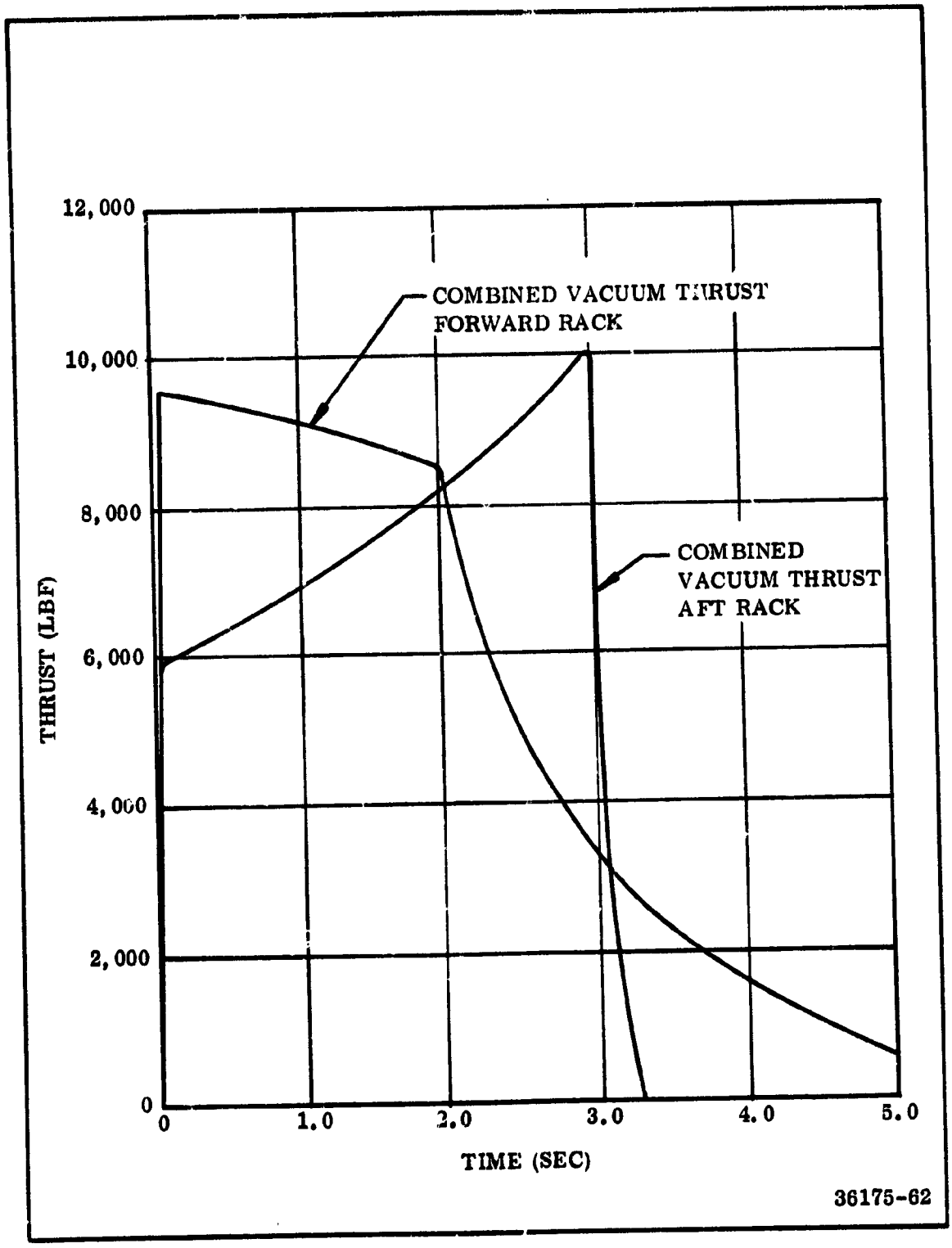

Figure 3-89. Operational Characteristics of SRM Staging Motors

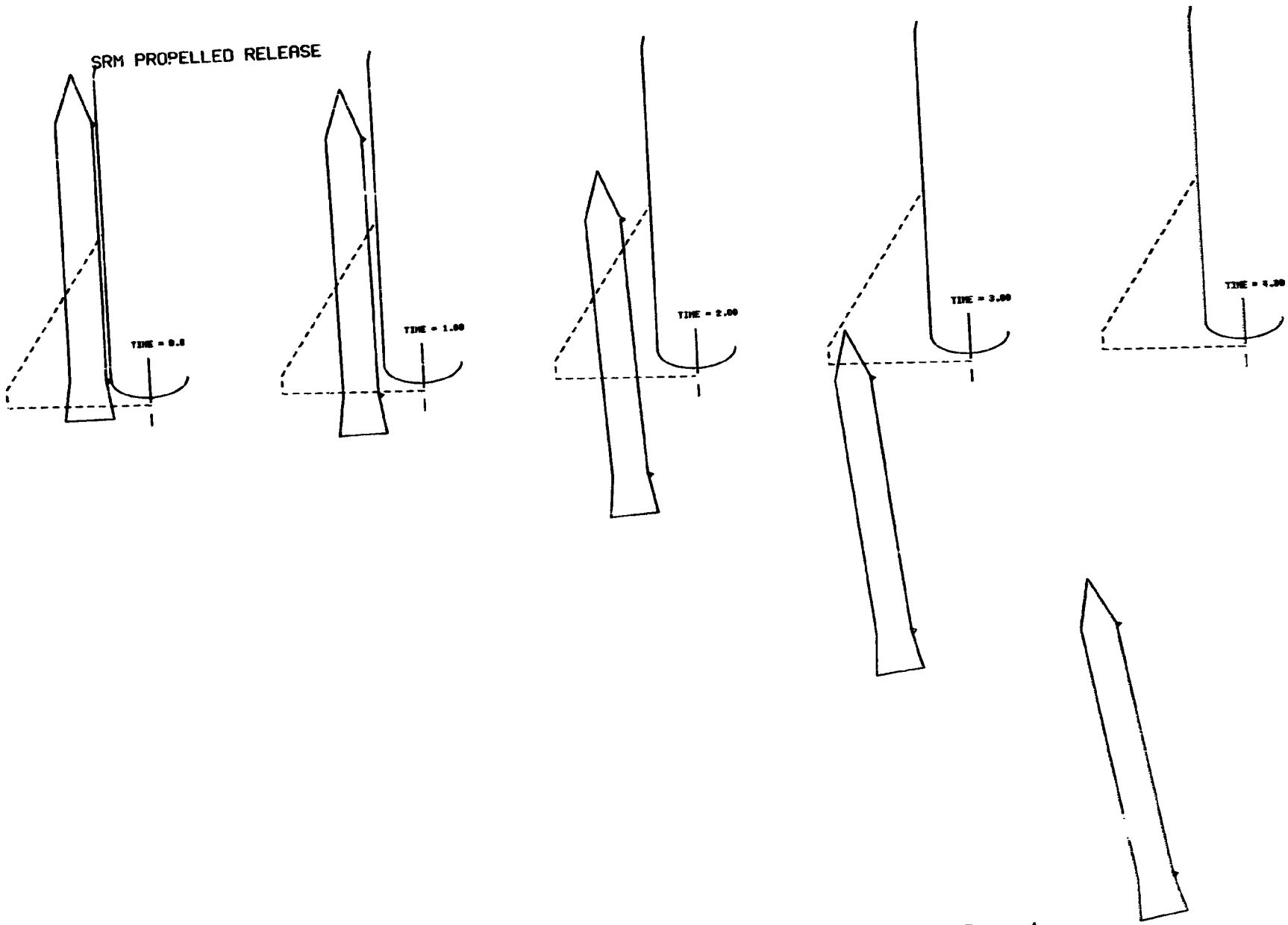

Figure 3-90. SRM Staging Positional Sequence Diagram, Alternate Concept

3.4.2.4 Mass Properties

Weight, center of gravity, and moment of inertia data are presented in detail in Appendix B, "Mass Properties Report." Table 3-33 summarizes weight data for the SRM Stage with all options included.

3.4.2.5 SRM Stage and SRM Contract End Item (CI) Specifications

Preliminary contract end item (CI) specifications have been prepared for the baseline SRM Stage and SRM and are contained in Appendix C.

3.4.2.6 Drawings, Bill of Materials, and Preliminary ICD's

A preliminary design package has been prepared, consisting of drawings, bills of materials, and preliminary ICD's. This information is presented in Appendix D.

TABLE 3-33

SRM 156 INCH
MASS PROPERTIES SUMMARY

	Weight (lb)
Case	102,724
Insulation	11,906
Liner	1,278
Igniter	571
Nozzle	11,862
Raceway	171
Thrust Vector Control	2,154
Thrust Termination	661
Propellant	1,214,327
Motor Assembly	1,345,654
Nose Cone	9,269
Aft Skirt	12,112
Stage Attach Provision	5,177
Instrumentation	552
Destruct System	211
Staging Motors	296
Recovery System	11,133
Total	1,384,404
Total Stage (2 Motors)	2,768,808

3.4.3 156 Inch SRM Stage Series Burn Configuration

The 156 in. SRM Stage for the series burn configuration is very similar to the parallel stage. The main differences are:

1. The stage is larger. It consists of three 156 in. motors with 1.5 million lb of propellant in each.
2. The physical arrangement is that the SRM's are clustered and mounted behind the HO tank.
3. The stage hardware configuration is consistent with the tandem physical arrangement.
4. The series burn requires TVC on the baseline motor.

3.4.3.1 Basic Motor

The motor design for the 156 in. series configuration is very similar to the motor for the 156 in. parallel configuration. The grain design is a center perforate with radial slots at the segment joints. The propellant is TP-H1011, identical to the propellant in the 156 in. parallel. The motor contains 1.5 million lb of propellant.

As shown on Figure 3-91, the case is longer and consists of four cylindrical center segments instead of three. The insulation and liner are similar to the parallel motors.

The performance of the series burn 156 in. SRM Stage is shown below. Discussions on the TVC system, the staging hardware, and a weight summary are presented later in this section.

FOLDOUT FRAME

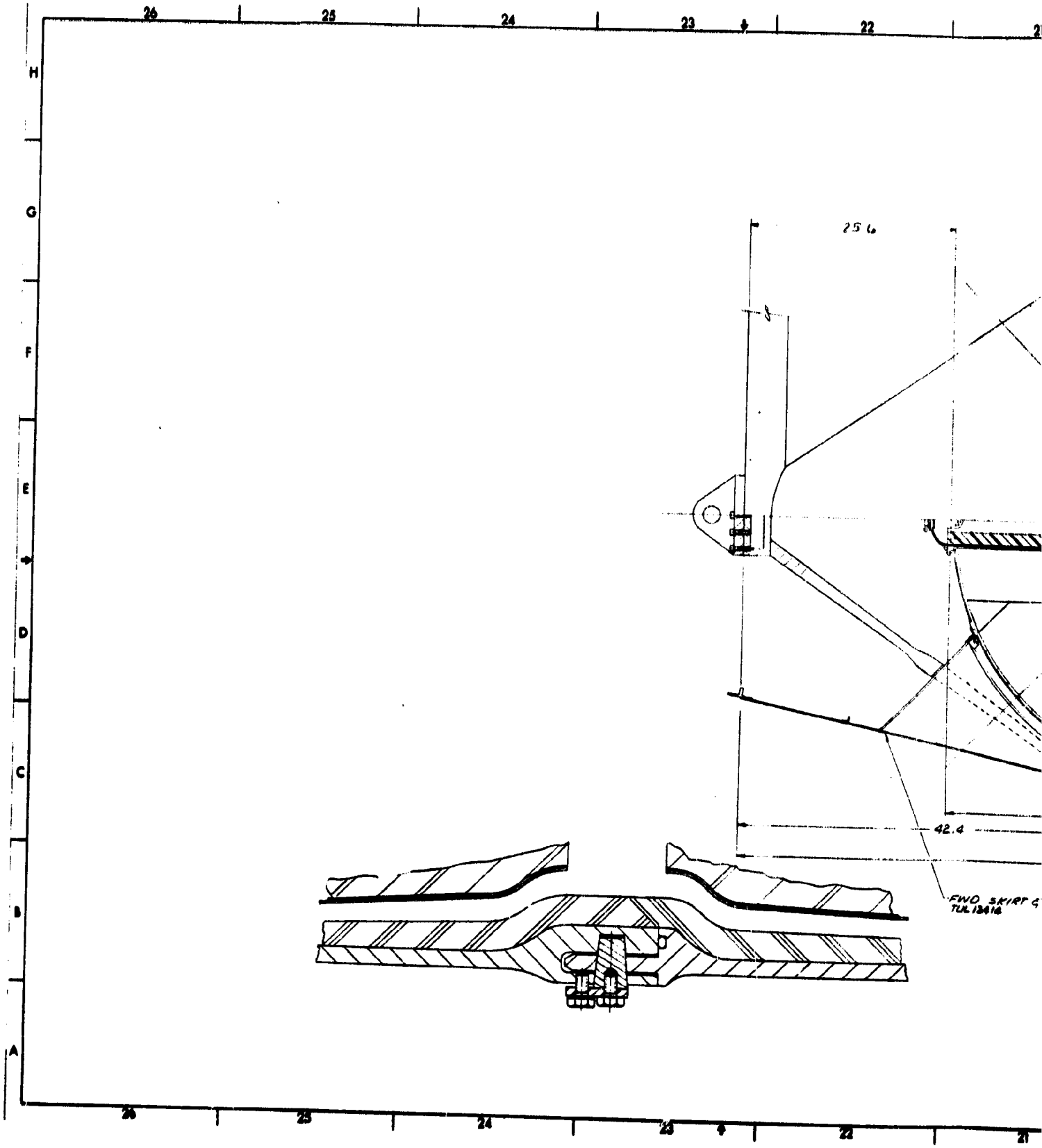

FOLDOUT FRAME 2

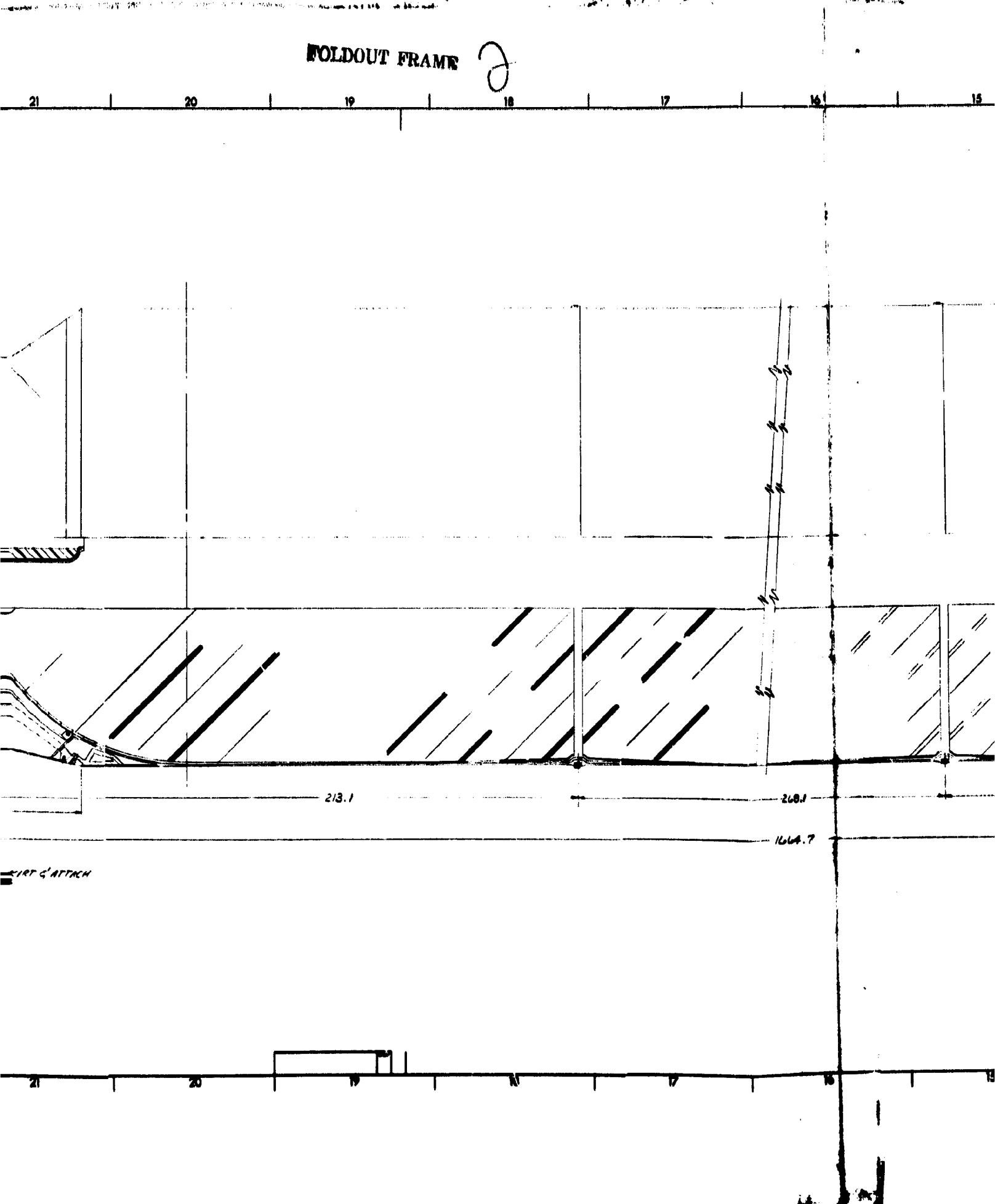

FOLDOUT FRAME 3

FOLDOUT FRAME 4

FOLDOUT FRAME

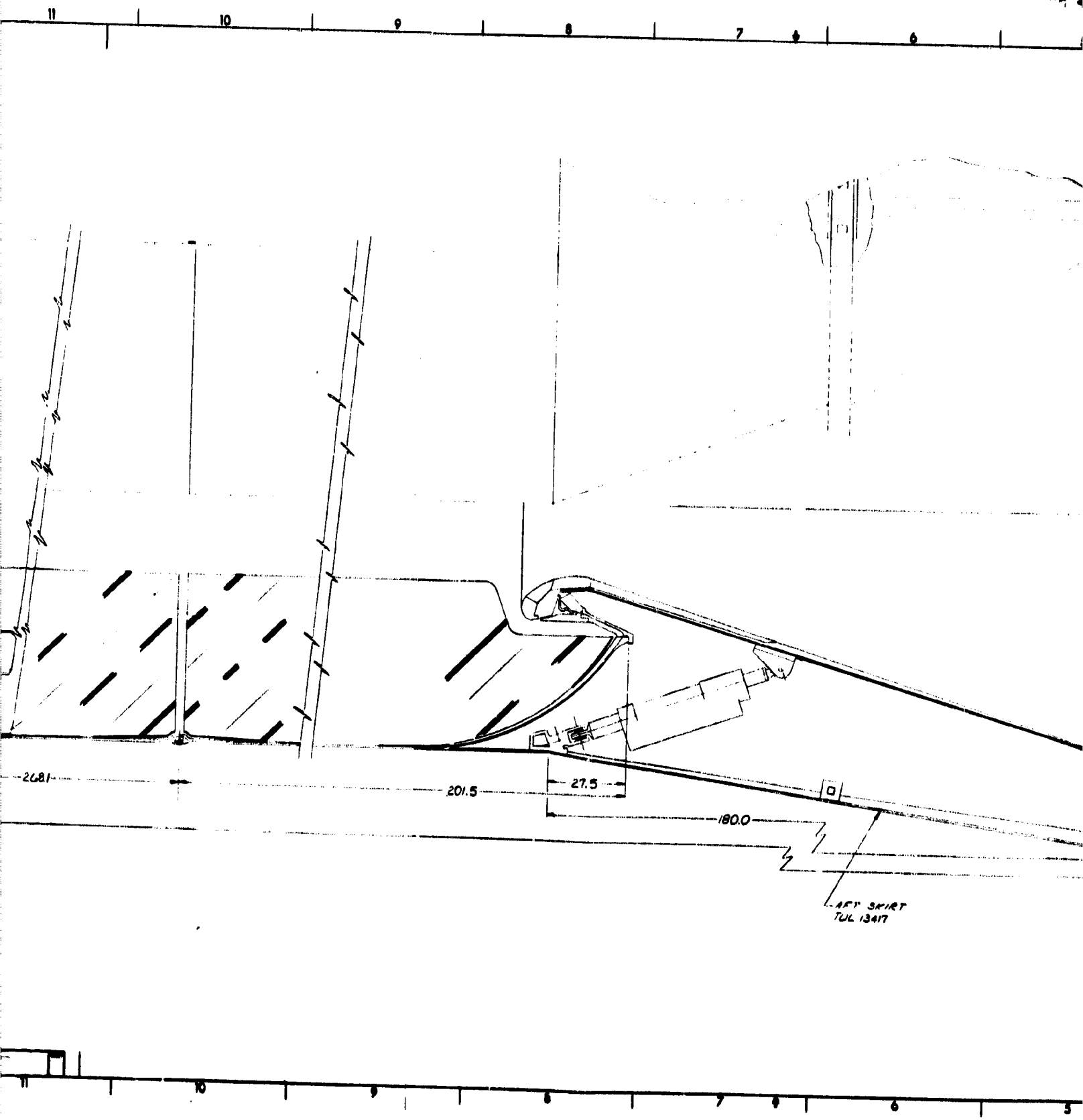

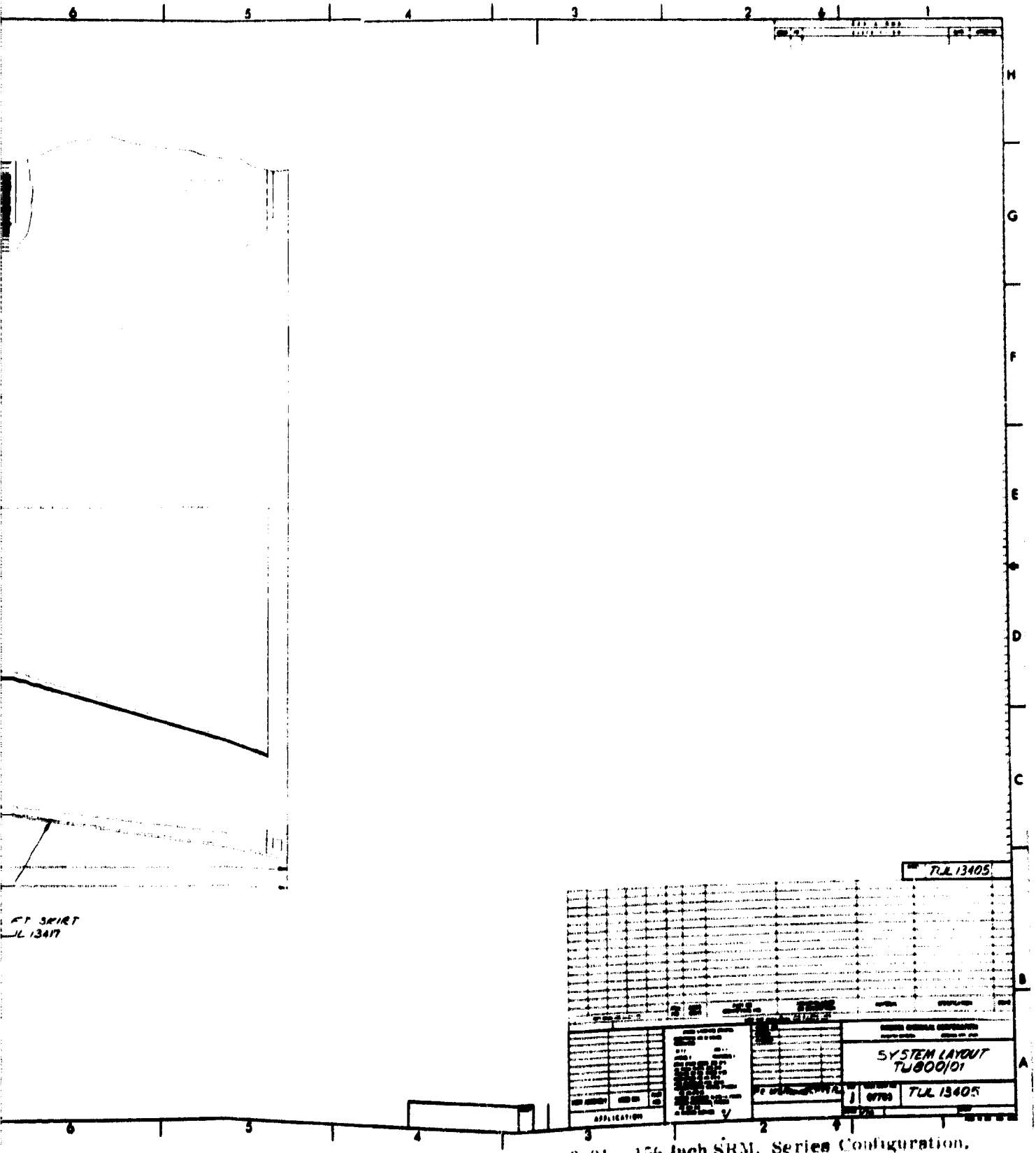

Figure 3-91. 156 Inch SRM. Series Configuration.

Performance Summary
156 Inch SRM, Series Burn Configuration

PERFORMANCE:

Thrust, avg, vac (lbf)	2,970,000
Burn time (sec)	135
Operating pressure (psia) avg	830
MEOP	1,000
Specific impulse, vac (sec)	267.2

WEIGHT:

Propellant weight (lb)	1,500,000
Total motor weight (lb)	1,654,000
Motor mass fraction	0.906
Total stage weight (lb)	1,670,000
Stage mass fraction	0.894

3.4.3.1.1 Grain Design and Performance

The grain design for the series motor is the same as that of the baseline design of the 156 in. parallel booster system except for the forward segment. Here, a cylindrical port (CP) configuration is substituted for the four slot-slotted tube configuration of the parallel system grain design. This results in a more neutral performance. The cylindrical perforated port diameter is 55.6 in. and the web thickness is 49.6 inches.

The 156 in. baseline motor design for the series system will exhibit almost the same degree of flexibility in burn time as does the baseline 156 in. design for the parallel booster system. Within the framework of the design and propellant system, the burn time can vary between 125 and 176 sec. Modifying the grain design by reducing the web thickness can reduce the burn time to 113 sec with a corresponding increase in grain length of 5.6 percent.

These burn time flexibility limits (for no grain design modifications) and the limits for operation at the minimum obtainable chamber pressure, as well as operation at the nominal pressure, are listed below.

Burn Time Flexibility, 156 In. Series System

Motor designation	TU-800
Nominal burn time (sec)	135
Nominal avg chamber pressure (psia)	930
Max burn time for operation at nominal chamber pressure (sec)	166
Max burn time for operation at minimum chamber pressure, imposed by motor design (sec)	176 at 622 psia
Min burn time available with no grain design modification (sec)	120

The flexibility in ballistic modification of this design is the same as that of the baseline 156 in. parallel design. The analysis of ballistic modification presented earlier in the discussion of the parallel design summarizes the capabilities of this design as well.

The analysis described previously in the section of tailoff performance of the parallel system is relevant to this design. However, the magnitude of the thrust levels (between the parallel design and this one) are different and thus only the normalized thrust differential data, shown in Figure 3-11, are directly applicable to this design. The thrust differentials shown on the other figures in that section would need to be scaled up by the ratio of: thrust at web time, series design/ thrust at web time, parallel design.

3.4.3.1.2 Propellant

The propellant used in this design is the same as that of the baseline parallel system, 156 in. motor. Propellant composition and properties were tabulated previously in the parallel motor design description.

3.4.3.1.3 Case

The case for the 156 in. series burn SRM will be of the same general configuration as that used for the 156 in. parallel motor. Case construction will differ only in that the series baseline will have four center segments and the baseline design inclusion of a movable nozzle will cause minor differences in the aft dome opening. Case design safety factors and material parameters previously set forth apply to this design as well.

3.4.3.1.4 Insulation

The insulation design approach, materials, and fabrication for the 156 in. series system is identical to that of the baseline 156 in. parallel design.

3.4.3.1.5 Liner

The liner material and application on the 156 in. series motor is identical to that of the 156 in. parallel baseline system.

3.4.3.1.6 TVC System

3.4.3.1.6.1 TVC Nozzle

The nozzle for the baseline series burn SRM Stage is a partially submerged, omniaxial movable, state-of-the-art design providing ±5 deg thrust vector control capability. Its size, configuration, gimbaling mechanism and materials are typical of those of the 156-9 nozzle successfully demonstrated on a 156 in. diameter SRM static tested by Thiokol in 1967.

The gimbaling mechanism is a forward pivoted flexible bearing consisting of alternate laminae of metallic and elastomeric shims integrally bonded to and between forward and aft end rings. The end rings in turn interface with the nozzle movable and fixed sections to form the complete assembly.

The nozzle is tailored to the performance requirements of the SRM. It incorporates all possible features to assure a low cost, highly reliable assembly. Because of its proposed use in a manrated system, somewhat higher margins of safety have been applied to ablative materials, structures and proof test levels than are generally used in SRM nozzle design for missile systems.

The divergent cone has a 17.5 deg half angle and is 159 in. long from throat to exit plane. The required structural and ablative material thicknesses at the exit result in an OD of 152 in., well within the motor diameter. When vectored 5 deg, the OD of the cone moves outward to a diameter of 184 in. in the vector plane. An aerodynamic and structural skirt protects the nozzle from external aerodynamic loads.

The nozzle design is shown in Figure 3-92. Criteria employed in making the design and dimensional characteristics of the nozzle are listed in Table 3-34 .

The ablative, insulative, and structural materials selected for the nozzle and the metallic and elastomeric materials in the flexible bearing assembly are the same as those for the 156 in. parallel burn SRM nozzle and flexible bearing assembly and they were selected for the same reasons. Fabrication and assembly methods are also identical to those of the parallel burn SRM movable nozzle. The same analyses were conducted to insure design and performance integrity of the final configuration.

Erosion and char profiles resulting from the analyses are shown in Figure 3-93. Mass properties of the design are listed in Table 3-35 . Analysis of the flexible bearing torque values are given in Table 3-36 .

3.4.3.1.6.2 Actuation System

The TVC actuators for this booster configuration are identical to those for the 156 in. parallel burn except for size as shown in Table 3-37 .

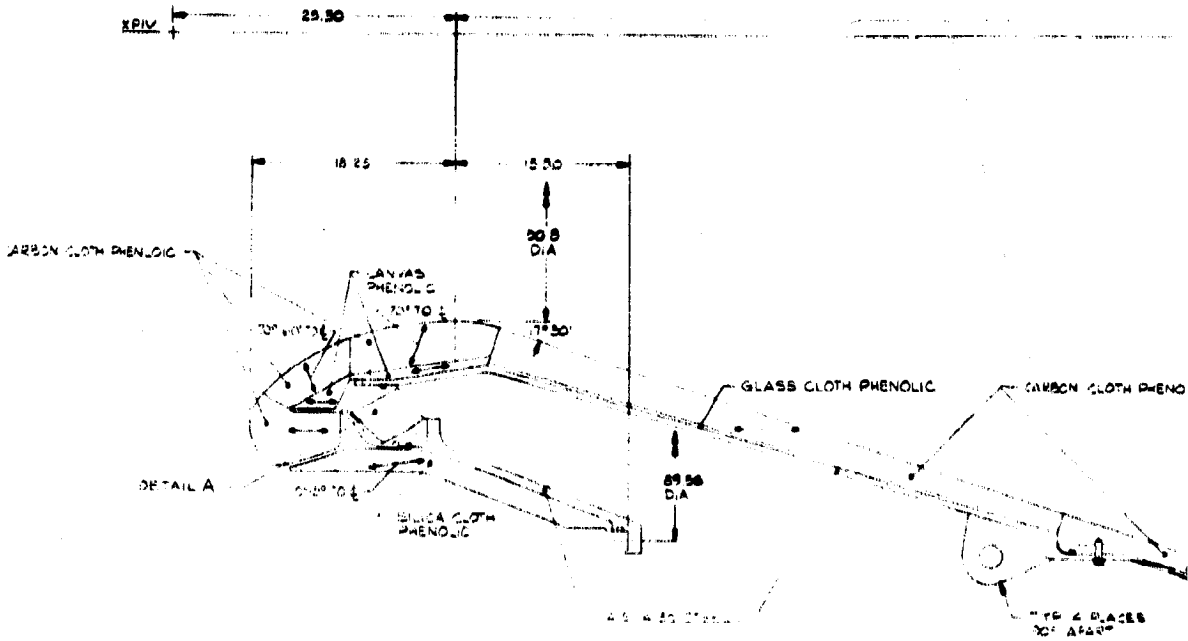
XPIV
29.50
18.25
15.50
20.8 DIA
CARBON CLOTH PHENOLIC
CANVAS PHENOLIC
GLASS CLOTH PHENOLIC
CARBON CLOTH PHENO
DETAIL A
69.56 DIA
SILICA CLOTH PHENOLIC
AISI 4130 STEEL
TYP 4 PLACES

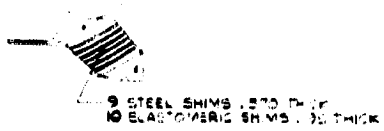
9 STEEL SHIMS
10 ELASTOMERIC SHIMS

DETAIL A

FOLDOUT FRAME 2

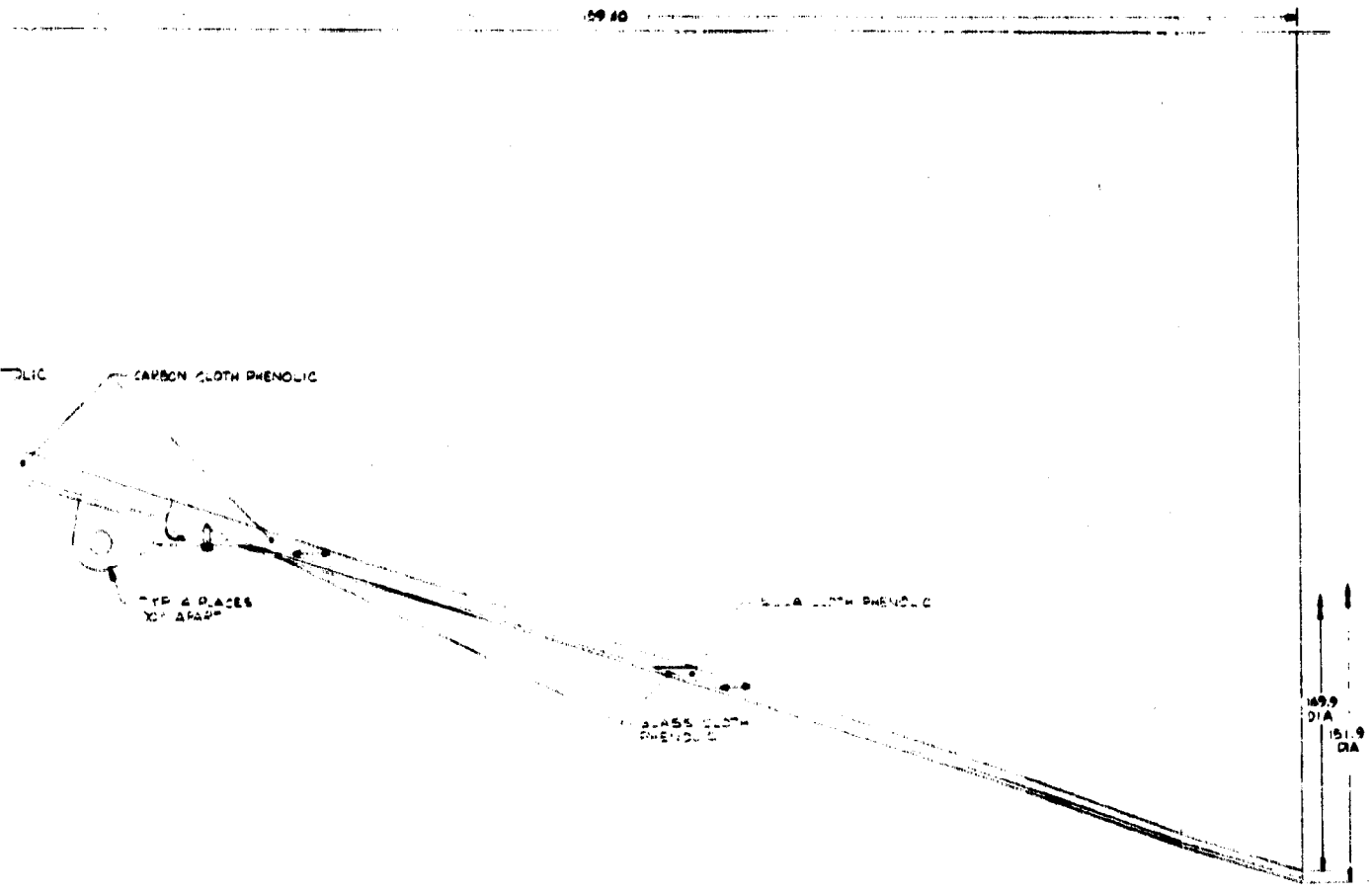

FIG. 3-2. SRM

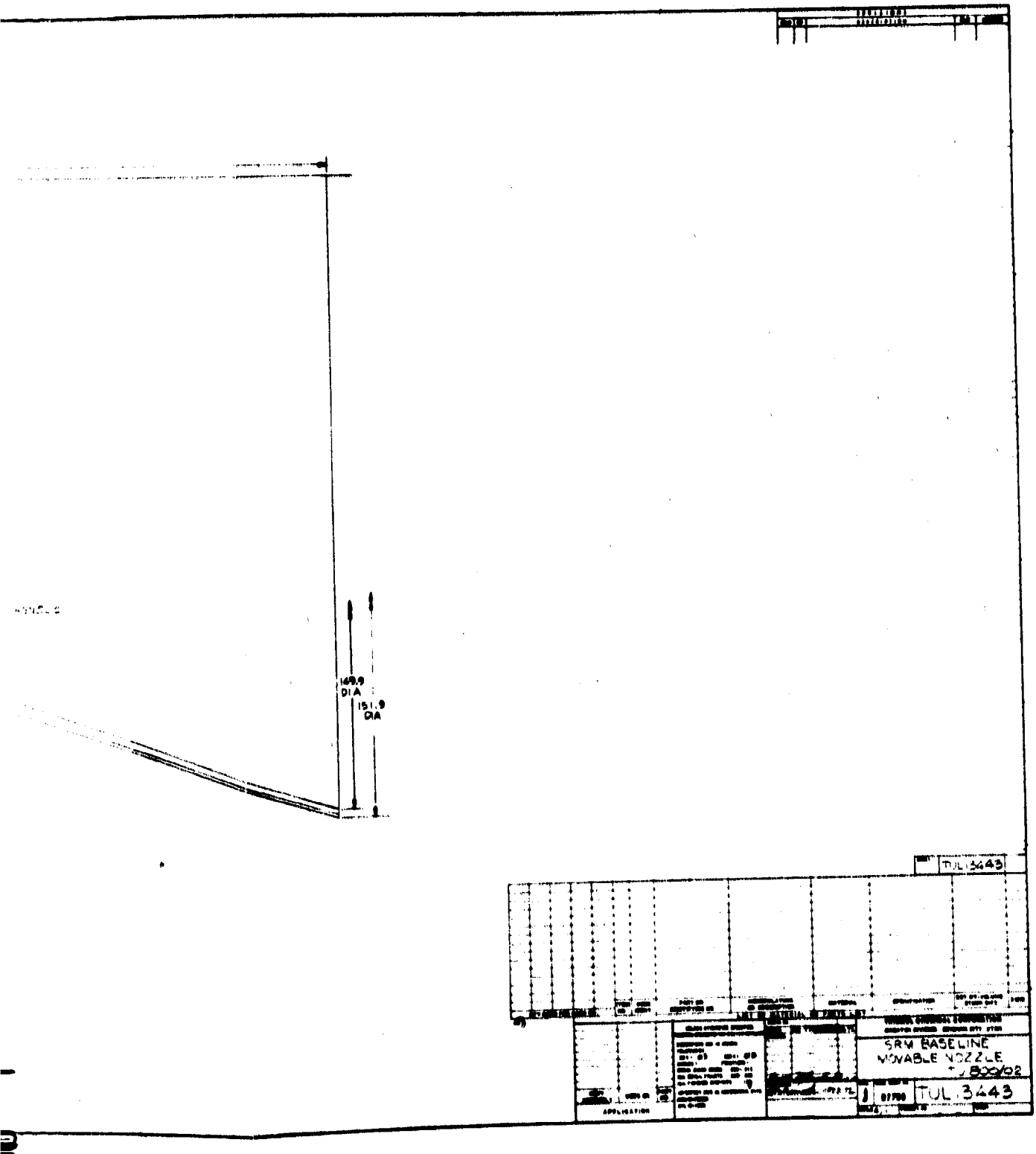

Figure 3-2. SRM Baseline Movable Nozzle, Series Configuration

TABLE 3-34

NOZZLE CHARACTERISTICS DESIGN CRITERIA

Throat diameter, initial (in.)	50.8
Throat area, initial (sq in.)	2,026
Exit diameter, initial (in.)	149.9
Exit area, initial (sq in.)	17,647
Expansion ratio, initial	8.7:1
Exit cone half angle (deg)	17.5
Submergence (%)*	10
TVC capability (deg)	± 5
TVC slew rate (deg/sec)	5
Pressure, avg (psia)	830
MEOP (psia)	1,000
Safety factors	
Ablatives	2.0
Structure	1.4
Proof pressure test, flex seal	1.2 x MEOP
Nozzle weight (lb)	12,763

*Submergence, % = $\frac{\text{Length, Throat to Flange}}{\text{Length, Throat to Exit}}$ x 100

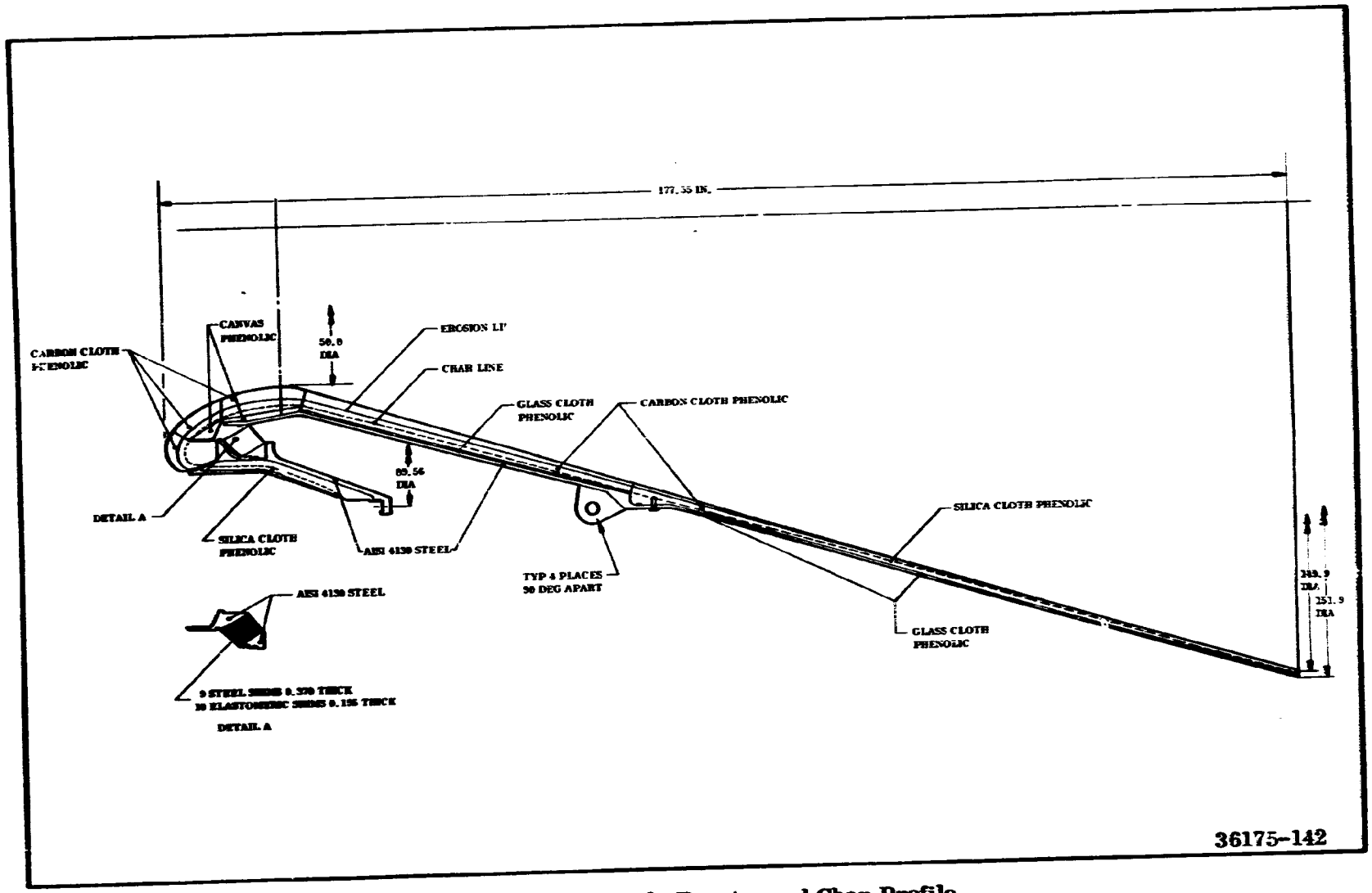

Figure 3-93. Nozzle Erosion and Char Profile

TABLE 3-35

MASS PROPERTIES DATA
SRM BASELINE NOZZLE, SERIES BURN

	WEIGHT (LBS)	CENTER OF GRAVITY LONG.	LAT.	VERT.	MOMENT OF INERTIA PITCH	ROLL	YAW
TOTAL NOZZLE ASSEMBLY	12763.585	121.473	100.000	100.000	8897.118	5323.015	8897.118
FIXED PART ASSEMBLY	2756.624	88.164	100.000	100.000	503.391	934.269	503.391
FLEXSEAL ATTACH STEEL	326.452	80.684	100.000	100.000	44.711	85.305	44.711
STEEL	1620.744	92.962	100.000	100.000	300.594	565.747	300.594
SILICA CLOTH PHENOLIC	806.239	84.973	100.000	100.000	146.768	274.056	146.768
RUBBER O RINGS	3.310	90.707	100.000	100.000	0.652	1.121	0.652
MOVABLE PART ASSEMBLY	10006.761	130.512	100.000	100.000	7576.772	4388.726	7576.772
NOSE CARBON CLOTH PHEN.	401.616	70.237	100.000	100.000	55.012	109.204	55.012
BACKUP CARBON CLOTH PHEN.	228.494	71.826	100.000	100.000	22.844	45.291	22.844
THROAT CARBON CLOTH PHEN.	411.572	81.474	100.000	100.000	35.229	68.128	35.229
CANVAS CLOTH PHENOLIC	65.976	73.085	100.000	100.000	7.426	14.811	7.426
THROAT CANVAS CLOTH PHEN.	95.356	81.527	100.000	100.000	9.367	18.260	9.367
FLEXSEAL ATTACH STEEL	508.385	75.537	100.000	100.000	57.816	114.549	57.816
FLEXSEAL	674.707	78.731	100.000	100.000	83.876	167.219	83.876
RUBBER SEAL V-44	33.873	76.983	100.000	100.000	4.602	9.171	4.602
EXIT CONE CARBON CLOTH	1419.733	112.595	100.000	100.000	254.101	377.785	254.101
EXIT GLASS CLOTH PHENOLIC	232.761	114.936	100.000	100.000	45.518	65.207	45.518
EXIT CONE STEEL	2675.522	116.193	100.000	100.000	681.162	860.586	651.162
STEEL ACTUATOR BRACKET	18.940	133.596	100.000	100.000	4.223	8.416	4.223
EXIT CARBON CLOTH PHEN.	947.575	141.171	100.000	100.000	292.484	508.495	292.484
EXIT GLASS CLOTH PHEN.	969.377	155.934	100.000	100.000	604.155	798.652	604.155
BACKUP GLASS CLOTH PHEN.	50.570	152.957	100.000	100.000	12.926	25.418	12.926
EXIT SILICA CLOTH PHEN.	1208.548	213.117	100.000	100.000	674.623	1192.125	674.623
RUBBER O RINGS	3.161	114.699	100.000	100.000	1.184	1.104	1.184

TABLE 3-36

FLEXIBLE BEARING NOZZLE ACTUATION TORQUE

Component	Torque (million in.-lb)
Internal aerodynamic	1.47
Offset	0.47
Bearing spring (5 deg vector)	1.09
Bearing boot spring (5 deg vector)	0.05
Gravity (considered only for horizontal static test)	0.77
Total	3.85

With the Space Shuttle vehicle mounted nonsymmetrical to the cg of the three booster motors, large roll moments are induced into the vehicle if all three solid rocket motors nozzles are vectored the same amount in the yaw plane. This can be avoided by differential movement of the nozzles. Assuming the required vehicle side force is equivalent to a 5 deg vector angle, the total required side force from the stage is 78,000 lb ($2.97 \times 10^6 \times \sin 5 \text{ deg} \times 3 = 78,000$). To induce this side force and not induce a roll moment, it is necessary that the vehicle roll moment and yaw moments as shown in the equations on Figure 3-94 both be satisfied. This can be accomplished if Nozzles 1 and 2 supply the majority of the required yaw side force while Nozzle 3 supplies just enough side force to null the induced vehicle roll rates due to Nozzles 1 and 2. Since the total vehicle cg location is below the centerline of Motors 1 and 2, the required side force from Motor 3 is additive to the side force of Motors 1 and 2. If however, the vehicle cg was located above the centerline of Motors 1 and 2, the side force of Motor 3 would subtract. As the vehicle cg location moves from the booster cg location, the TVC nozzle angle to supply the required vehicle side force increases.

For the required vehicle side force of 78,000 lb, the TVC nozzle deflection of Motors 1 and 2 must be increased from 5 deg to slightly greater than 6 deg. The third nozzle TVC requirements would be reduced to approximately 4 deg.

From a commonality standpoint, each of the three nozzles would be sized for 6 deg deflection. Nozzles 1 and 2 would each receive identical guidance commands while Nozzle 3 would receive a reduced command in order to null the roll rate.

The TVC control system for this booster configuration is identical to that of the 156 in. parallel burn configuration.

The HPU subsystems for this SRM are identical to those selected for the 156 in. parallel burn optional SRM configuration.

3.4.3.2 Stage Structure

The general philosophy followed in the design of the series stage structure was to design a structure that would transmit the thrust and provide support as well as serve to tie the three motors together. This would alleviate any requirement for joining structure on the pressurized case wall.

The aft support structure is shown on Figure 3-95 and is essentially a shell and ring construction with tapered doublers utilized to distribute the concentrated support and holddown loads. The three tapered conical skirts intercept at three planes where makeup joints are provided so that the overall assembly can be shipped as three separate subcomponents.

TABLE 3-37

TVC ACTUATOR REQUIREMENTS
156 INCH SERIES BURN

TVC angle (deg)	5
TVC slew rate (deg/sec)	5
Load (lb)	50,000
Area (sq in.)	17.3
Stroke (in.)	$\pm$6.4
Supply pressure (psi)	4,000
Flow rate (gpm)	33.0
Max pump horsepower	77.0
Redundancy	Active/standby

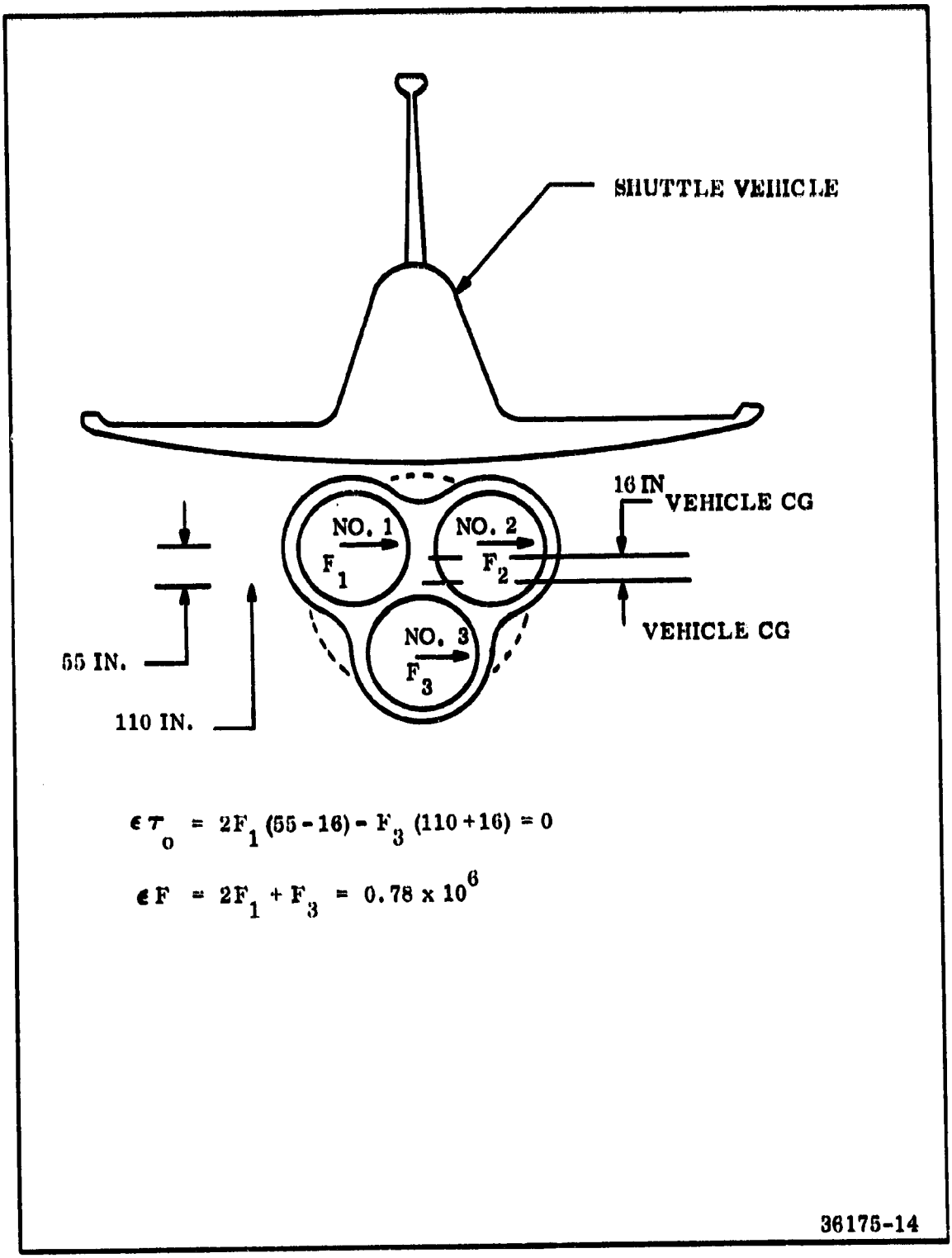

Figure 3-94. Thrust Vectoring Induced Roll Moment Schematic

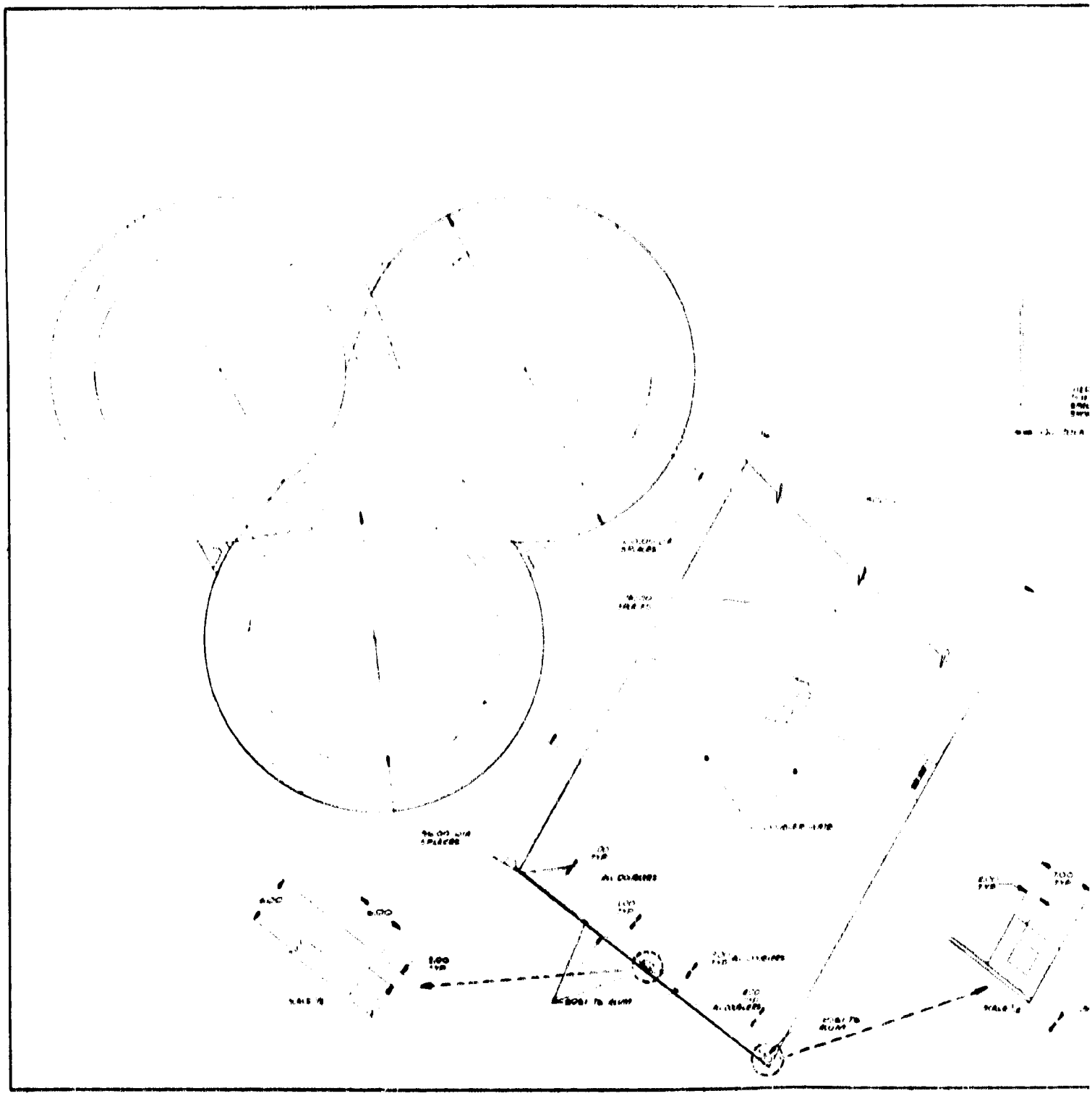

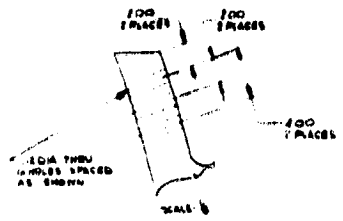

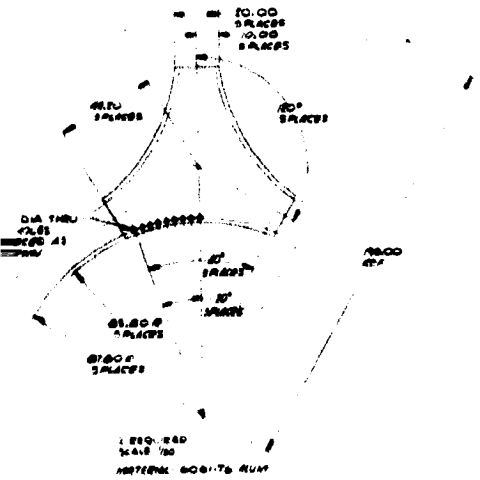

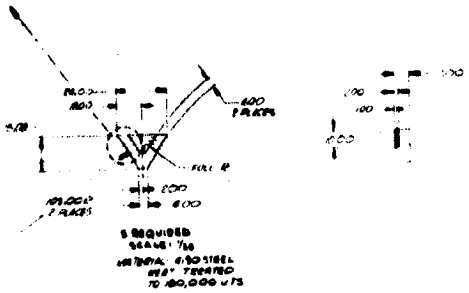

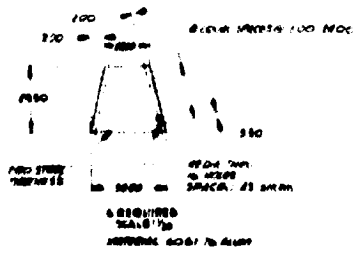

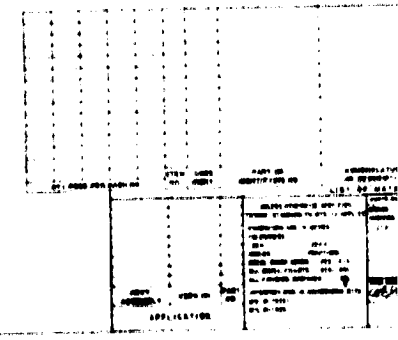

FOLDOUT FRAME 2

FOLDOUT FRAME 3

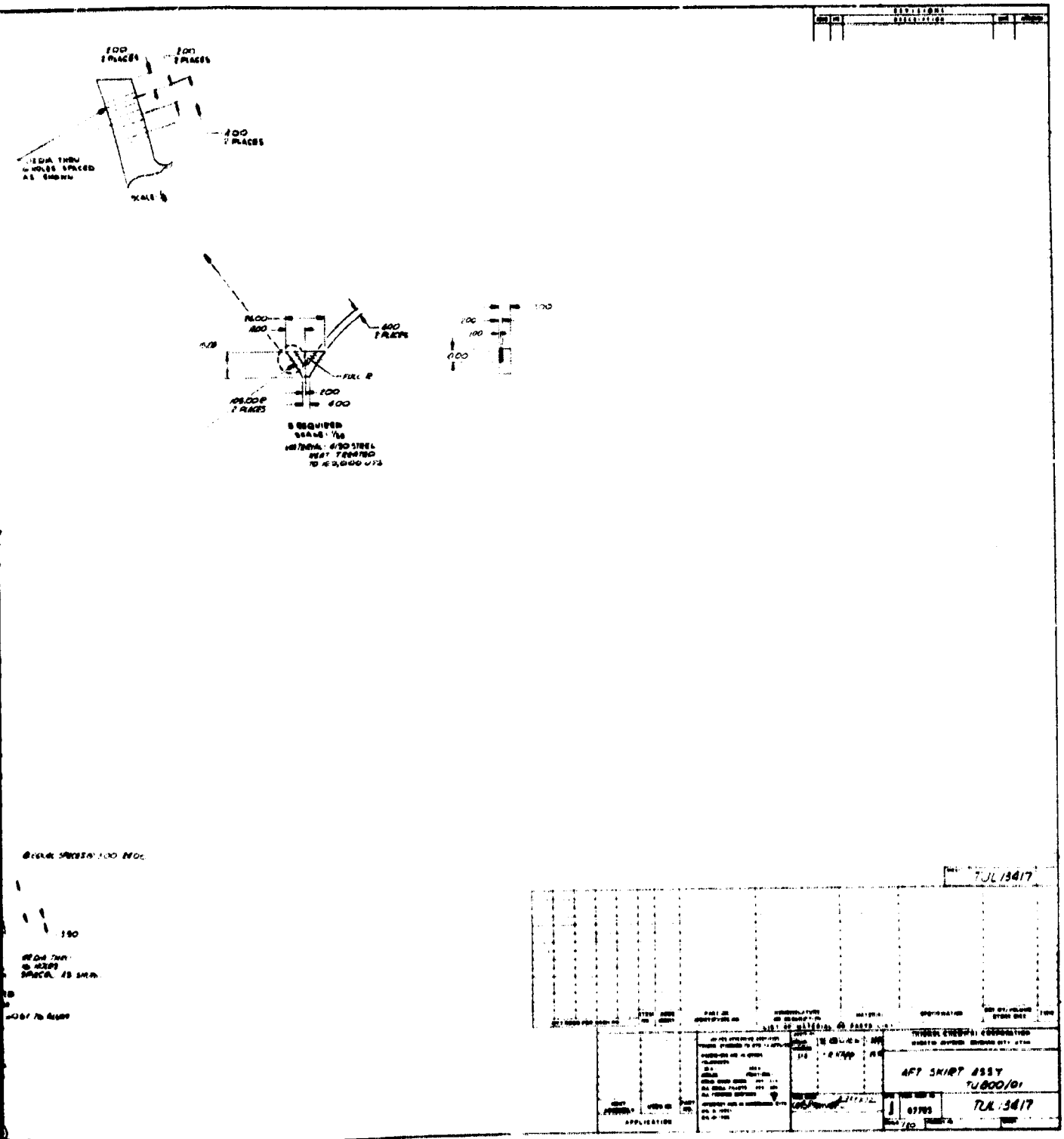

Figure 3-5. Aft Skirt Assembly

3-23

The structure will support the Orbiter-SRM assembly at six points, and provide holddown capability at three points. The aft structure consists of 6061-T6 aluminum throughout except for the three holddown brackets.

The aft connection of the motors is accomplished by bolting the main circular rings together by using doubler plates.

The forward support structure is shown on Figure 3-96 and is comprised of three conical shells (one at the head end of each motor). At the apex of each thrust cone is a clevis. The three clevises are fastened together by a triangular, box beam frame thus tying the motors together at the forward end. The thrust points for the orbiter assembly are the three clevises at the apex of the thrust cones.

Thrust termination ports protrude through the thrust cone with circular reinforcement rings required around the cutouts.

3.4.3.3 Mass Properties

The mass properties data for the series configuration is shown in detail in Appendix B. Weights are summarized in Table 3-38.

FOLDOUT FIG. M3

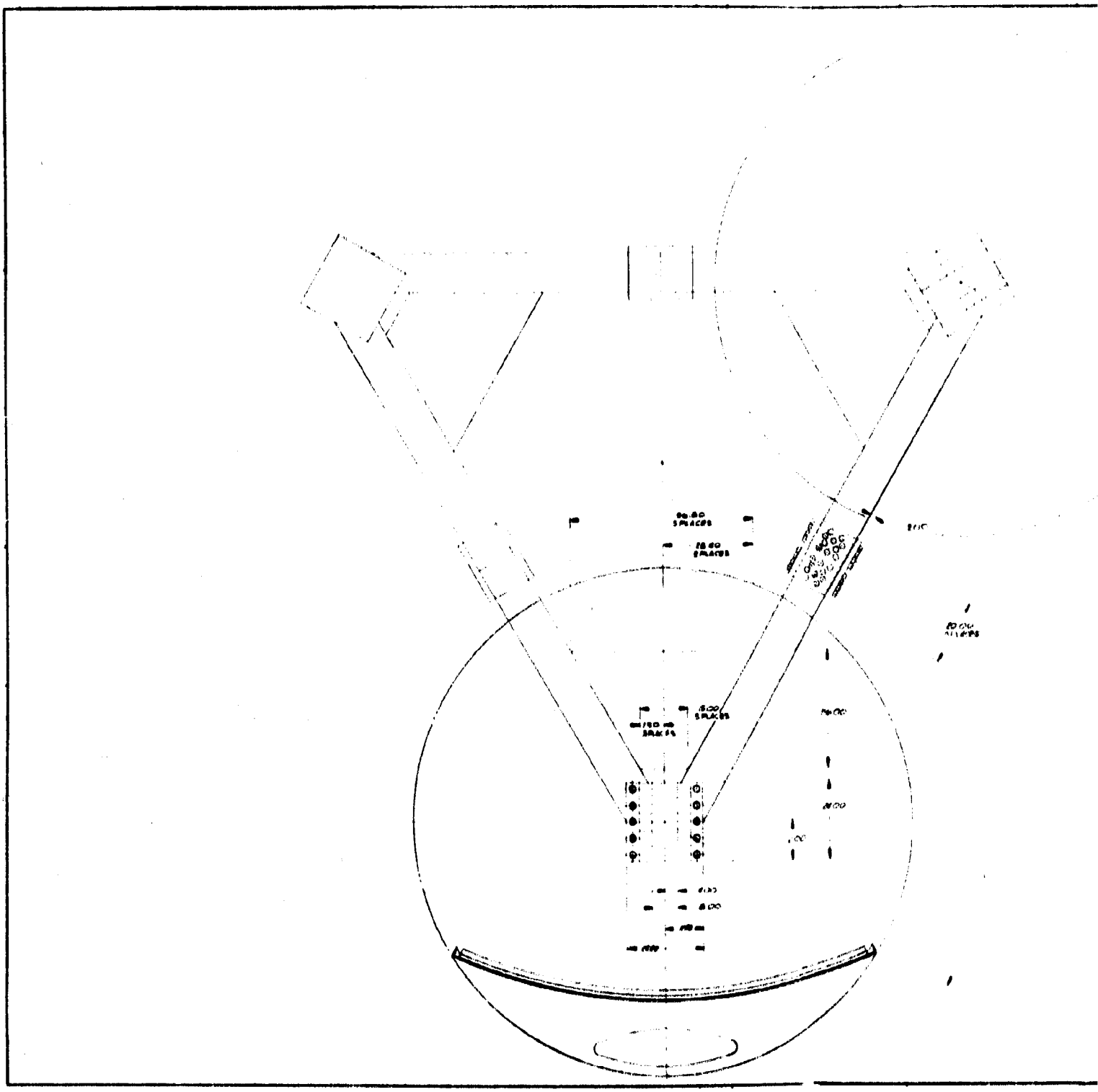

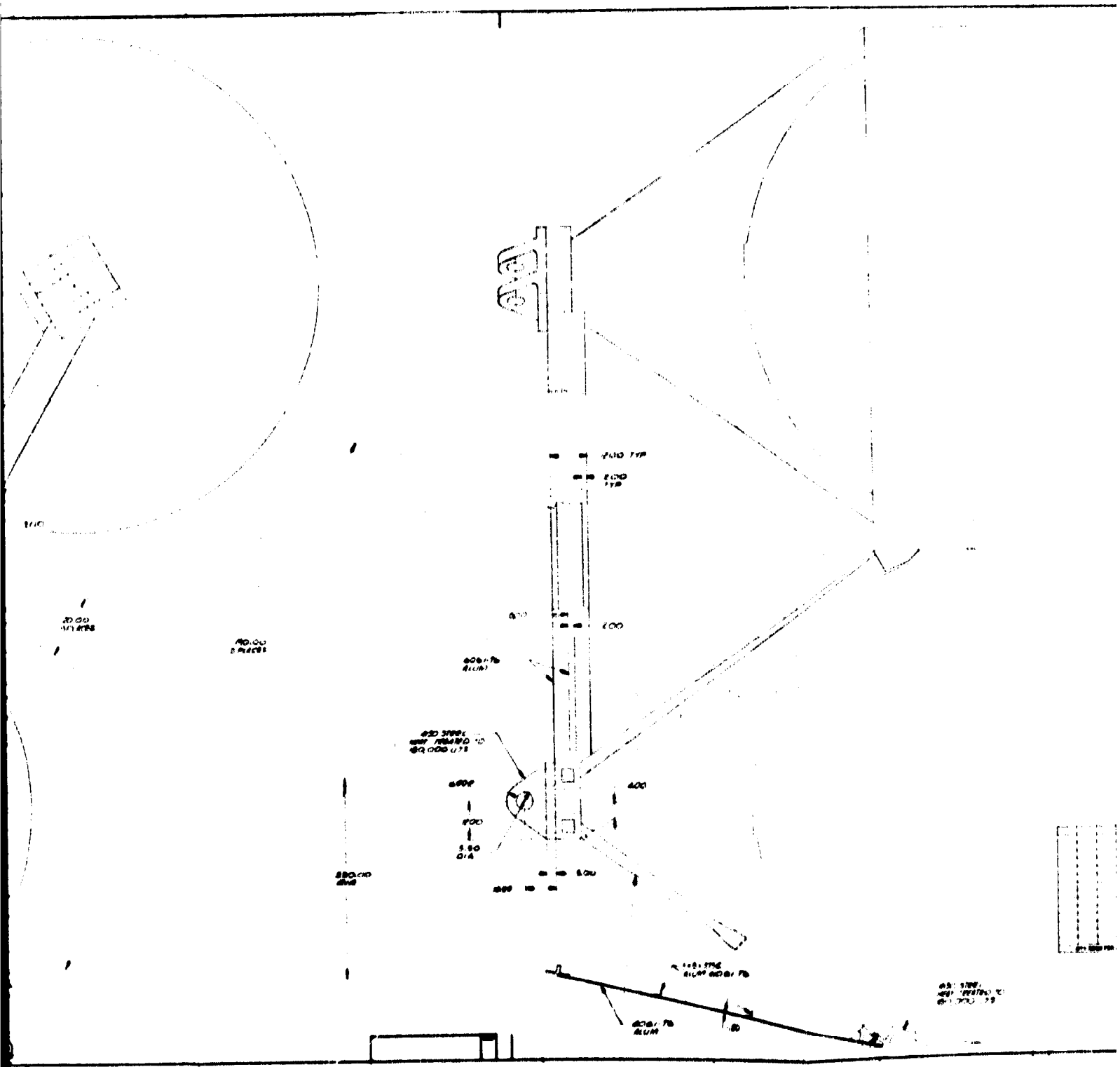

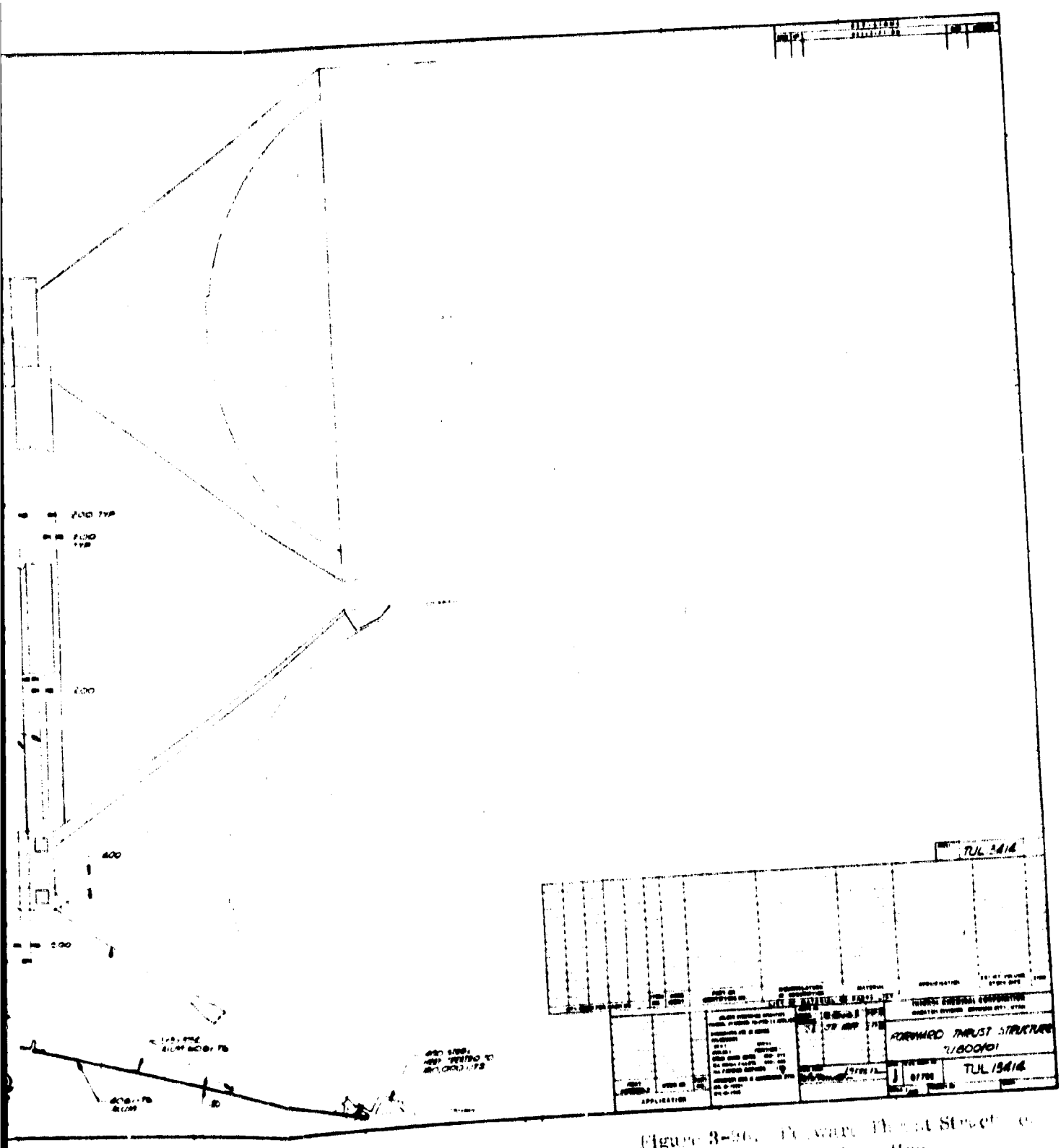

Figure 3-36. Forward Thrust Structure Strut Configuration

TABLE 3-38

MASS PROPERTIES SUMMARY
156 INCH SERIES BURN

Description	Current Weight (lb)
Case	123,244
Insulation	13,150
Liner	1,554
Igniter	660
Nozzle	12,724
Raceway	213
Thrust Vector Control	2,260
Propellant	1,500,625
Motor Assembly	1,654,430
Motor Assembly (3 each)	4,963,290
Forward Thrust Structure	34,806
Aft Skirt	31,216
Instrumentation	1,656
Total Stage	5,030,968

3.4.4 120 In. SRM Stage Parallel Configuration

The 120 in. SRM Stage parallel burn configuration is similar to the parallel 156 in. stage in most respects. The main difference is that the stage consists of four 120 in. motors, each containing 566,100 lb of propellant.

3.4.4.1 Basic Motor

The 120 in. motors are similar in design features to the 120 in. motor presently in production and the 156 in. motors presented in Section 3.0. The main difference from the existing 120 in. motors is the TVC system. A flexible bearing nozzle with a 6 deg cant and a 5 deg vector angle was assumed.

The motor layout is shown in Figure 3-97. The case is 120 in. in diameter and has seven center segments in addition to the forward and aft dome segments.

The grain design is a cylindrical perforate with a star in the head end. A radial slot is located at each case segment joint. To control the surface area, one side of each slot is inhibited. The port in the cylindrical segment is tapered to provide a longer tailoff on the thrust trace. This grain design was selected to maintain similarity with the existing Titan IIIC 120 in. SRM.

The performance of the SRM stage is shown on Table 3-39.

3.4.4.1.1 Grain Design and Performance

The grain design for the 120 in. motor is a modification of the 156 in. parallel system design. This design consists of a seven segment cylindrical perforation (CP) configuration. The center segments have identical configurations with tapered port cavities that produce a sliver at web burnout and result in a gradual thrust decay during tailoff. The forward segment grain configuration incorporates an 8-slot tube design to produce the slightly regressive thrust-time performance.

Figure 3-98 presents the thrust-time and pressure-time performances of this motor. The propellant grain dimensions are as follows.

Cylindrical perforated port diameter (tapered)	42.5 to 52.5 in.
Port to throat (end of segment)	1.56

Considerations involved in the discussion of the burning time flexibility of the 120 in. motor design are similar to those of both 156 in. motor designs (parallel and series systems). The burning time can range between 100 and 205 sec without grain design modifications.

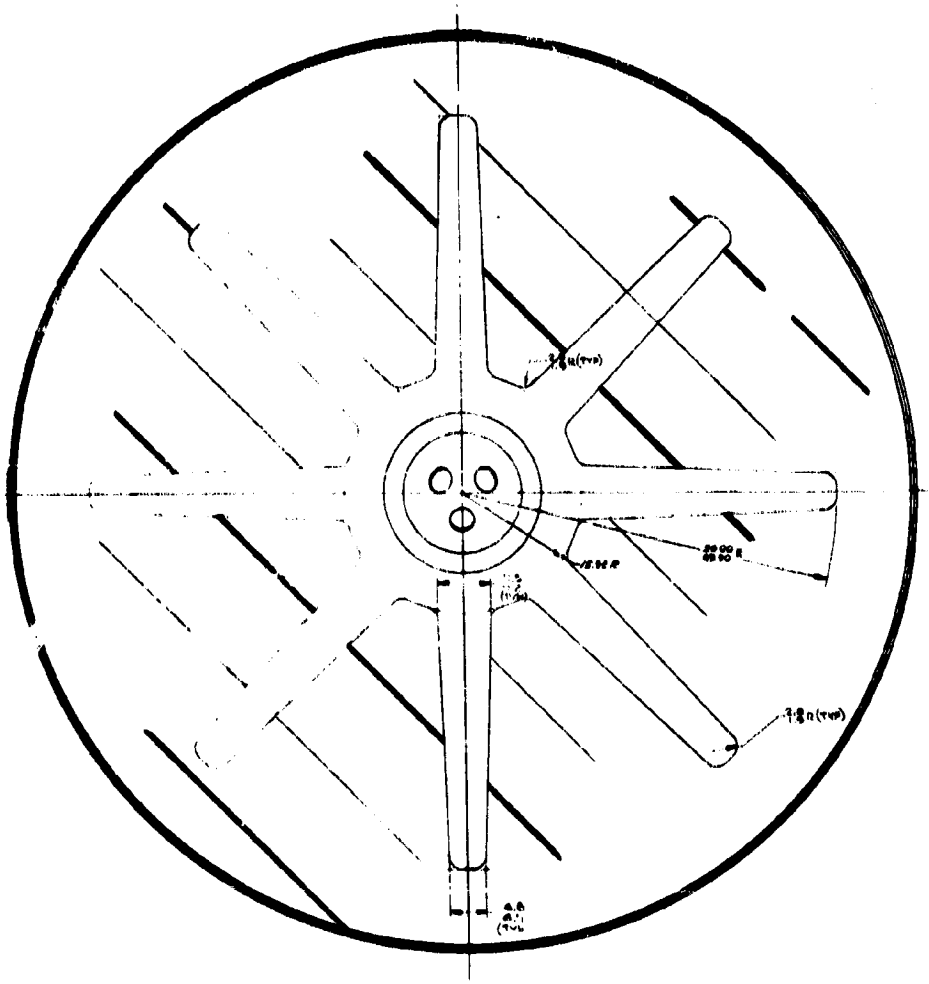

SECTION A-A

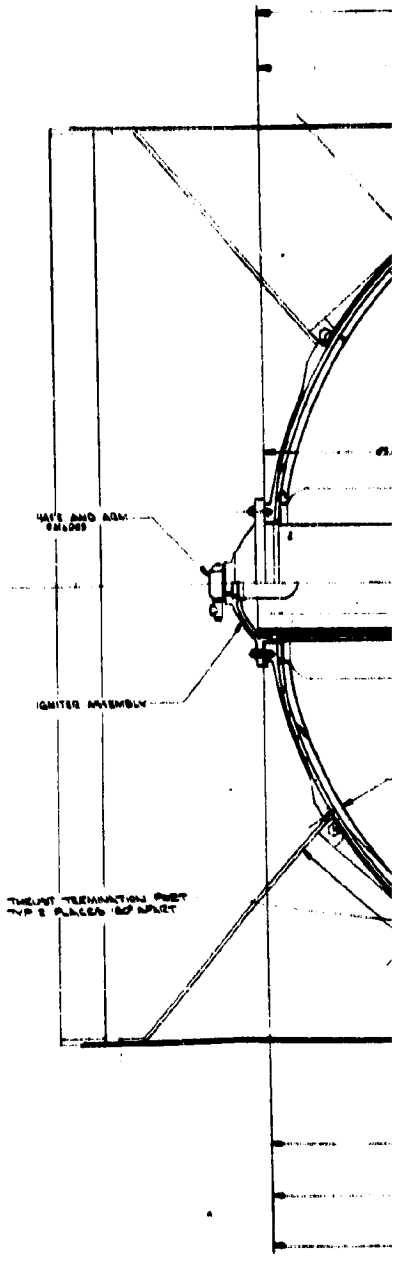

FOLDOUT FRAME 2

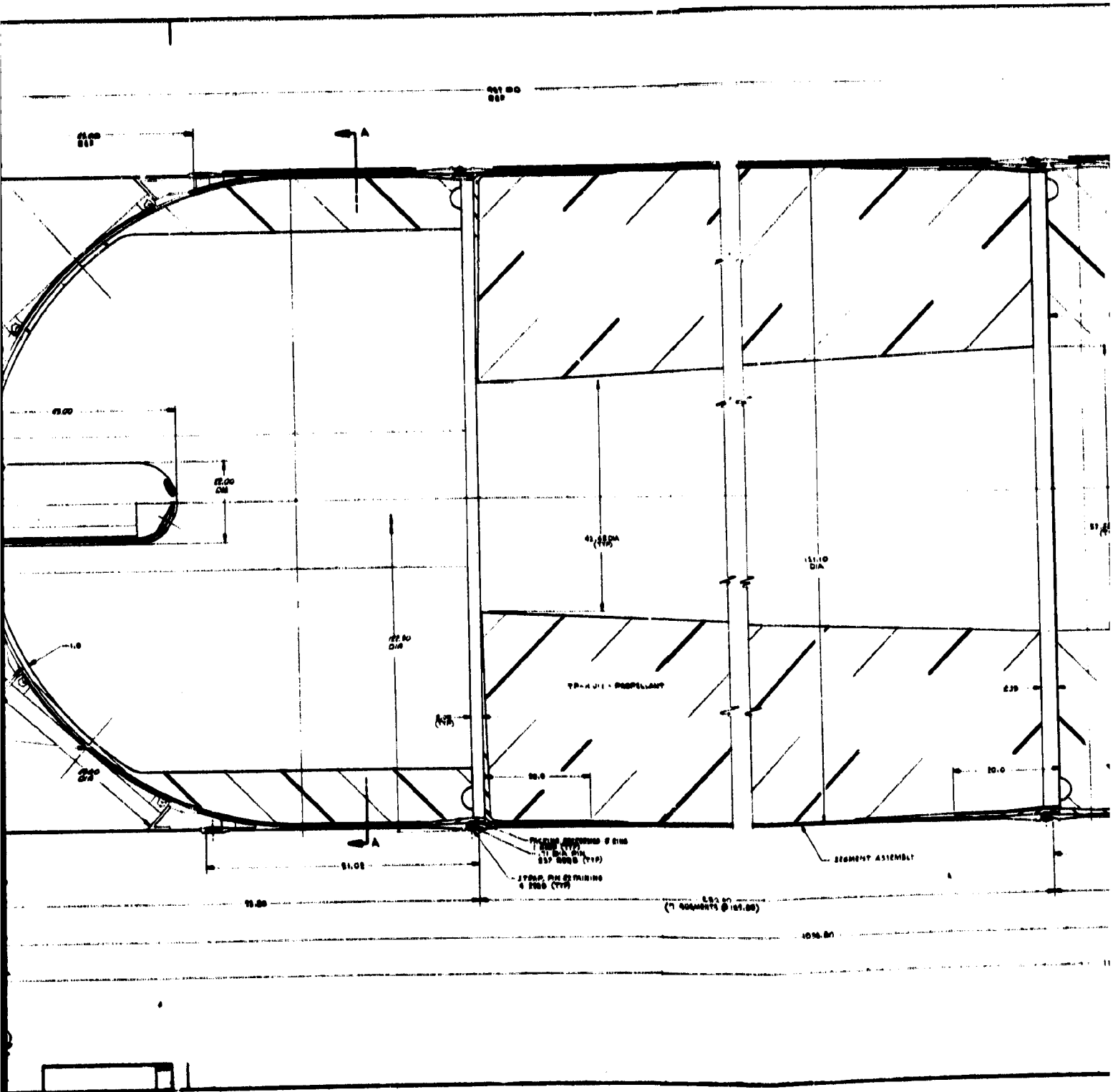

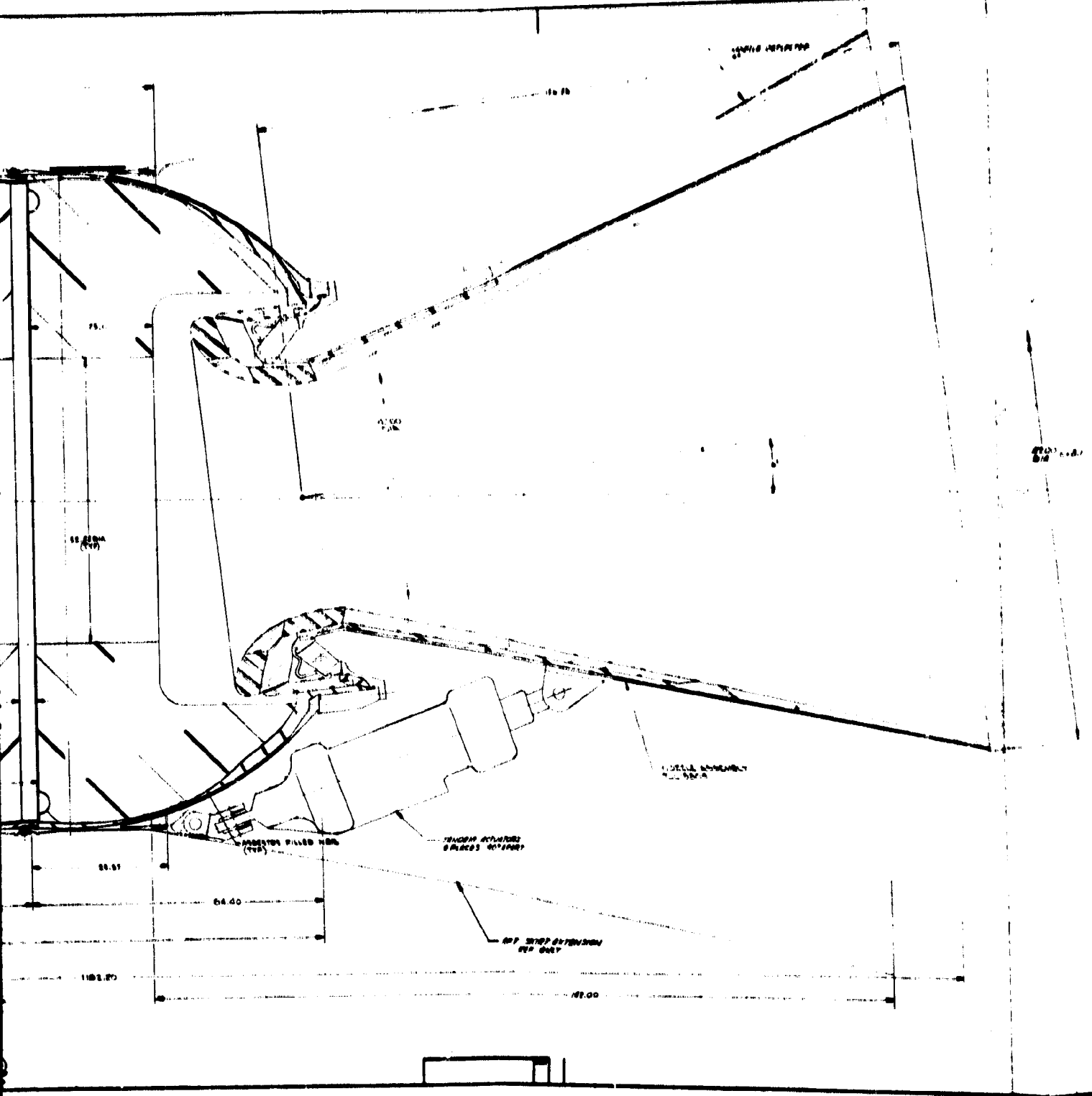

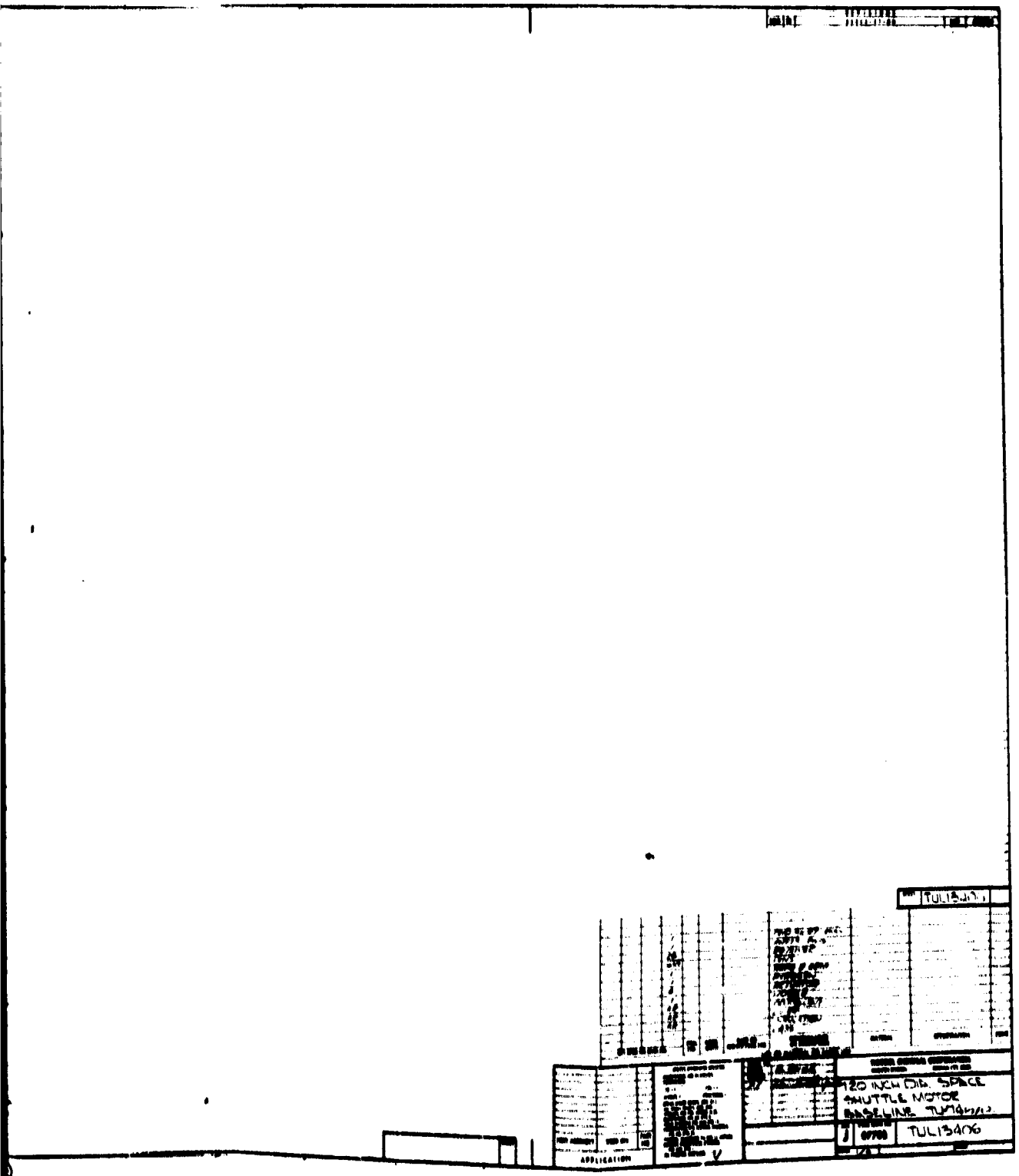

Figure 3-97. 12-1 SRM P allel Co figuratio

TABLE 3-39

PERFORMANCE SUMMARY
120 INCH SRM PARALLEL BURN CONFIGURATION

Parallel--Four Per Launch Vehicle

Performance	Average Vacuum Thrust (lb)	1,407,000
	Burn Time (sec)	112
	Average Operating Pressure (psia)	665
	MEOP (psia)	800
	Specific Impulse Vacuum (sec)	270
Weight	Propellant Weight (lbm)	566,100
	Total Motor Weight (lbm)	634,830
	Motor Mass Fraction	0.892
	Total Stage Weight (lbm)	642,241
	Stage Mass Fraction	0.8814

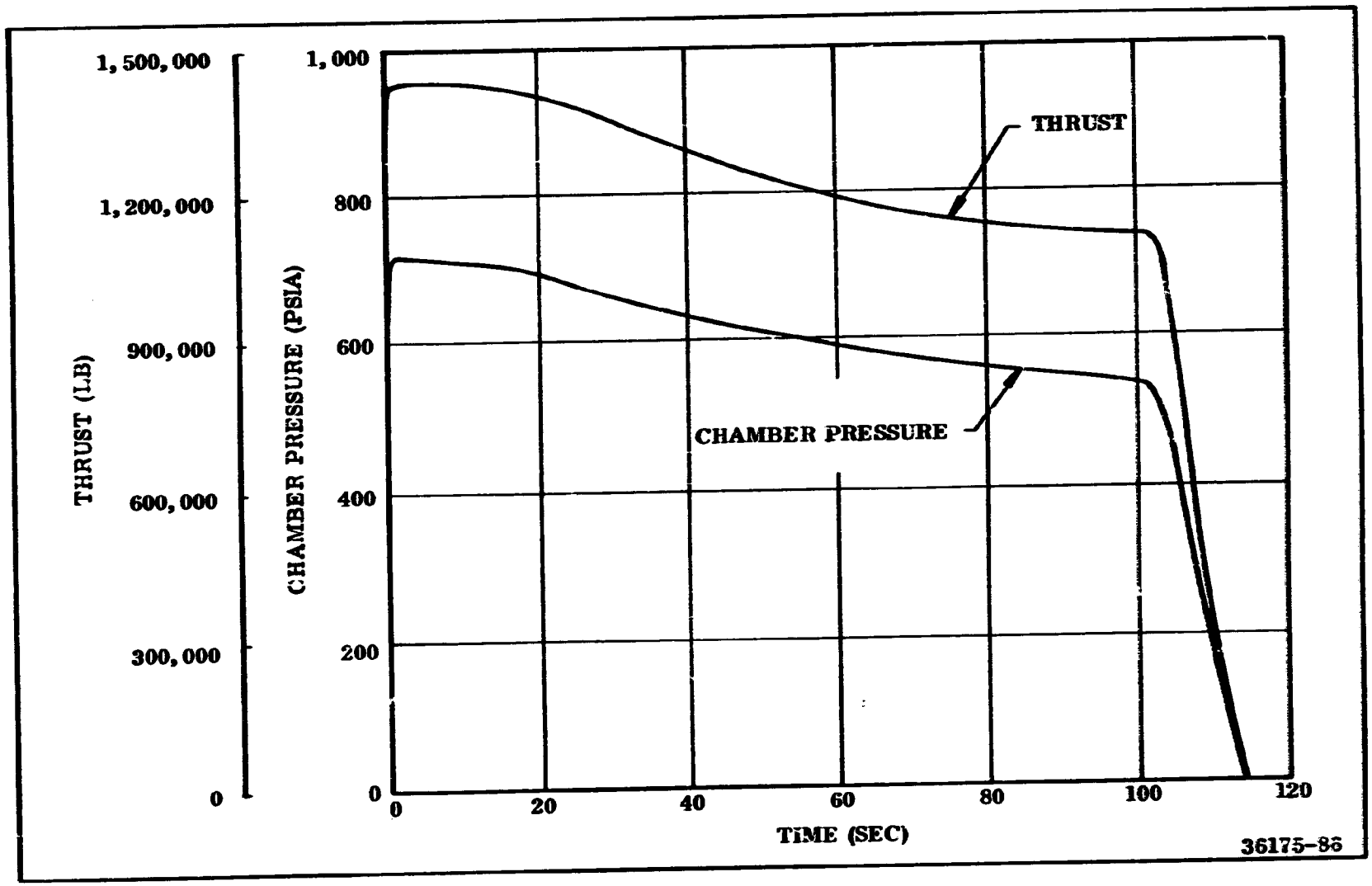

Figure 3-98. 120 In. SRM Motor Thrust-Pressure Curves

3.4.4.1.2 Propellant

The propellant used for this design is the same as that of the baseline parallel system, 156 in. motor. Propellant composition and properties are presented in the parallel motor design description (see 3.4.2.1.2).

3.4.4.1.3 Case

The case for the 120 in. parallel burn SRM will be of the same general configuration as that used for the 156 in. parallel motor. Case construction will differ only in that the 120 in. parallel baseline will have seven center segments and the baseline design inclusion of a canted nozzle will cause minor differences in the aft dome opening. Case design safety factors and material parameters set forth in 3.4.2.1.3 apply to this section as well.

3.4.4.1.4 Insulation

The insulation for the 120 in. diameter motor is identical in design approach, materials, and fabrication to that of the 156 in. parallel baseline system.

3.4.4.1.5 Liner

The liner on the 120 in. diameter motor is UF-2121, the same as that used on the parallel baseline 156 in. diameter system. The liner will be applied using sling lining equipment.

3.4.4.1.6 Nozzle

The nozzle for this booster configuration is a submerged, omniaxial flexible bearing movable nozzle, essentially the same as that of the 156 in. parallel burn SRM, except somewhat smaller in size. It is mounted off-center on the hemispherical dome so that a 6 deg cant is obtained. This provision is to assist in aligning the resultant thrust vector through the center of gravity of the flight configuration assembly. All criteria relative to materials, analysis, fabrication and assembly are the same.

3.4.4.1.7 Actuation System

The TVC Actuator for this booster configuration is identical to that used for the 156 in. parallel burn with the exception of size as shown in Table 3-40. The total number of actuators required is doubled, due to the increased number of solid rocket motors.

The TVC Control System for this booster configuration is identical to that used for the 156 in. parallel burn, except that twice as many control units are required due to the increased number of solid rocket motors.

TABLE 3-40

TVC ACTUATOR REQUIREMENTS
120 INCH PARALLEL BURN

TVC Angle (deg)	5
TVC Slew Rate (deg/sec)	5
Load	21,000
Area (sq in.)	7.0
Supply Pressure (psi)	4,000
Flow Rate (gpm)	15
Maximum Pump Horsepower	35
Redundancy	Active/Standby

The design of the actuation system for the 120 in. SRM will he similar to that of the series 156 in. SRM, but, considerably smaller in power. The redundancy and consequent reliability will be identical to that provided in the series 156 in. SRM to insure that all requirements for a manrated vehicle will be met.

The predicted torque for the 120 in. SRM is 1.26×10^6 in.-lb. The hydraulic power unit for the 120 in. motor movable nozzle would require approximately 35 hp. These values are well within the present state-of-the-art for TVC actuation systems. The existing production unit for the First Stage Poseidon has a capability of 27 hp. This HPU is composed of a solid propellant warm gas generator, turbine, gearbox and a fixed displacement hydraulic pump.

Increasing the pump output pressure from 3,100 to 4,000 psi in the present Poseidon HPU would result in a change of horsepower from the present 27 to the required 35. Minor modifications would be required in the turbine emission and gas generator configuration in order to drive the higher horsepower pump. A schematic of the present Poseidon HPU is shown in Figure 3-99.

Hydraulic power units utilizing liquid fuel gas generators have also been designed and produced in the horsepower range required for the 120 in. motor. Figure 3-100 shows a pictorial representation of the emergency power unit currently employed on the F-15 aircraft, which is built by Sundstrand.

Note that the shaft is rated at 30 hp which is very near the 35 hp required for the 120 in. motor. It is anticipated that minor modifications would be required in order to obtain the power necessary for the 120 in. motor application.

The 35 hp requirement for the 120 in. motor is a very conservative value and in all likelihood may be reduced in a detail design. This would be more in line with the two systems described above. The use of currently qualified hydraulic power units would be extremely advantageous from both cost and development time standpoints.

3.4.4.2 Stage Structure

The stage structure for the 120 in. SRM parallel motor will be designed to the same general philosophy as that used for the 156 in. parallel baseline motor, except that the stage will consist of four motors rather than two.

The motors will be staged by dropping one from each side, similar to the manner described for the 156 in. parallel configuration. When the first two clear the orbiter, the second two would be released.

3.4.4.3 Mass Properties

Weight data for the 120 in. SRM stage is shown on Table 3-41.

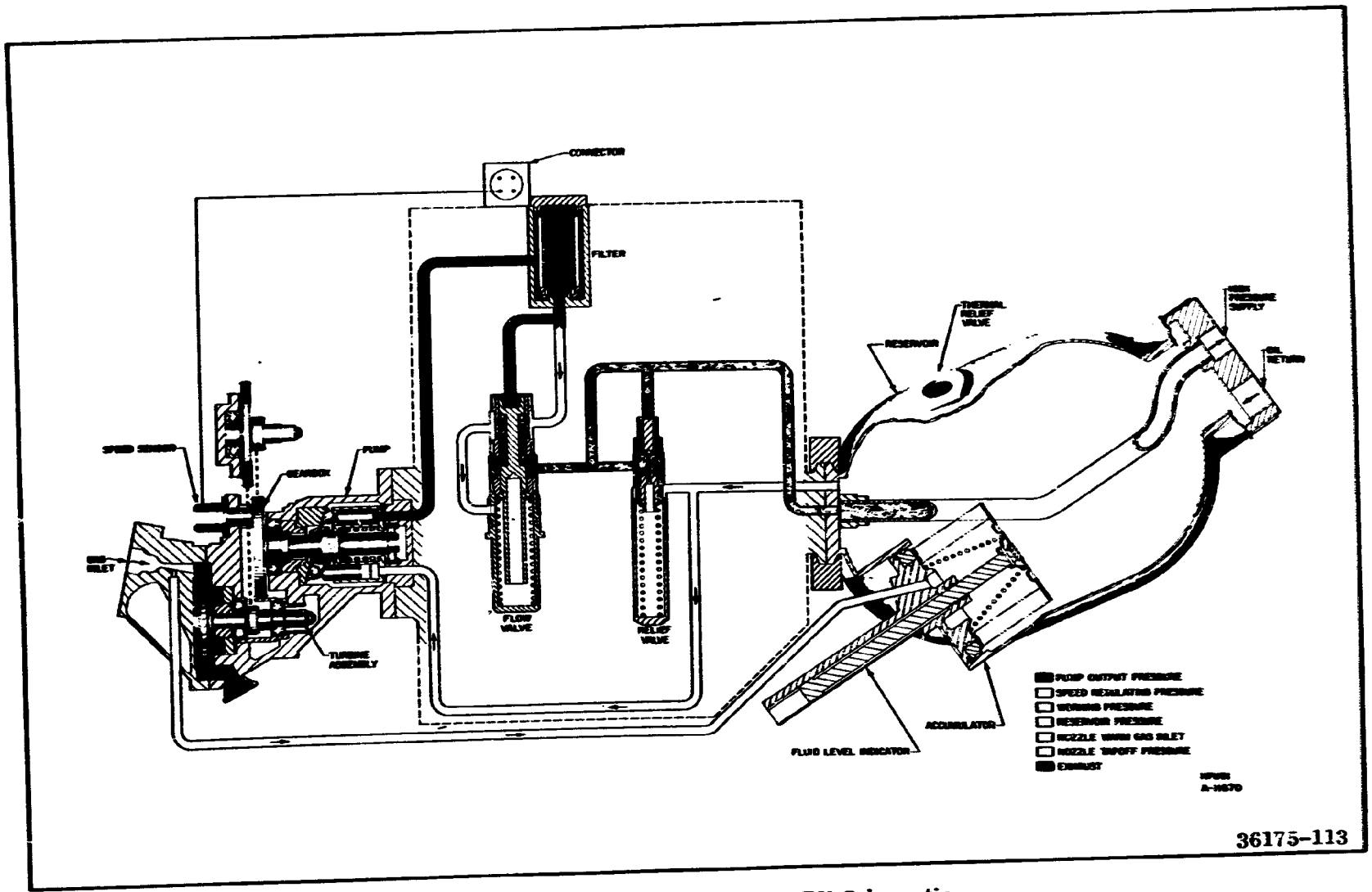

Figure 3-99. Stage I Poseidon HPU Schematic

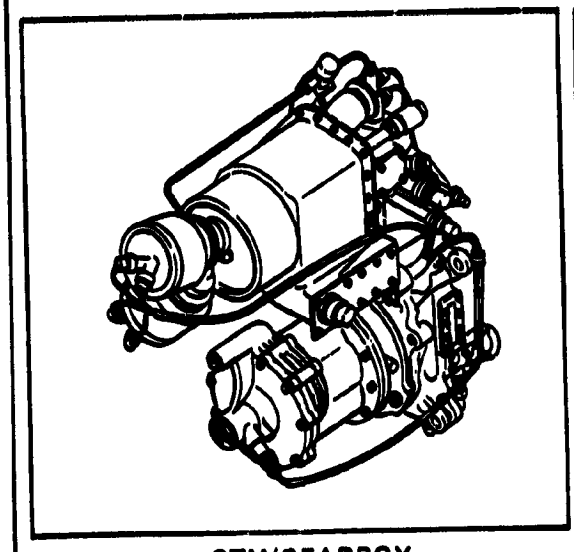

GTM/GEARBOX

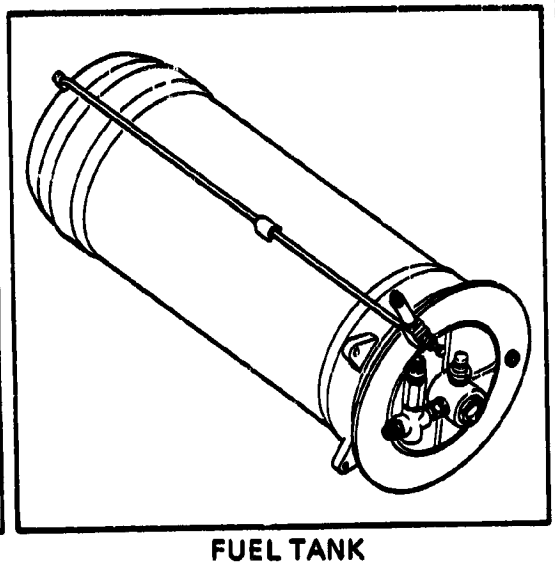

FUEL TANK

DRIVEN ACCESSORY . . . . . 2.4 $in.^3$/rev. Hydraulic Pump

RATED OUTPUT . . . . . 30 SHP @ 1892 RPM

TURBINE
- Type . . . . . Axial Flow Impulse
- Diameter . . . . . 3.49 inches
- Nominal Operating Speed . . . . . 100,000 RPM

ELECTRICAL POWER REQUIREMENTS
- Momentary (3 sec.) . . . . . 18.0 amps
- Continuous . . . . . 3.0 amps

36175-116

Figure 3-100. Liquid Fueled APU

TABLE 3-41

MASS PROPERTIES SUMMARY
120 INCH SRM, PARALLEL BURN

Description	Current Weight (lb)
Case	49,353
Insulation	8,439
Liner	755
Igniter	372
Nozzle	7,121
Raceway	151
Thrust Vector Control	2,029
Thrust Termination	510
Propellant	566,100
Motor Assembly	634,830
Nose Cone	2,095
Aft Skirt	2,804
Stage Attach Provision	2,124
Instrumentation	225
Destruct System	162
Total Stage (4 motors)	2,568,964

3.4.5 260 In. SRM Stage Series Burn Configuration

The 260 in. stage for the series burn configuration is very similar to the 156 in. series stage except that a single 260 in. diameter motor is used instead of the cluster of three 156 in. motors. From a performance point of view this provides a somewhat more efficient stage; however, the logistics problems associated with the large motor need to be evaluated in greater detail than was possible during the scope of this study.

3.4.5.1 Basic Motor

The motor design for the 260 in. SRM stage is in many respects similar to the 156 in. motor for the series configuration. The main difference is that the motor is monolithic. The motor could be built using the same segmenting techniques as those used for 156 in. motors; however, at 260 in., even the segments cannot be shipped by air or rail and must be transported by water. Consequently, the main reason for segmenting (i.e., transportation problems) is not alleviated by segmenting, and all 260 in. motors to date have been monolithic.

The 260 in. SRM stage is shown in Figure 3-101. Performance data are shown in Table 3-42.

3.4.5.1.1 Grain Design and Performance

The grain design for the 260 in. motor will consist of a five-pointed star. This design produces a slightly regressive thrust performance with a tailoff of about 15 sec duration. A design and performance summary of this motor was presented in Table 3-43. The star configuration was selected to enable the design of a highly loaded (volumetric loading greater than 0.80) motor within the constraints of the Minuteman propellant burn rate capability.

The star configuration severely restricts the range of thrust-time ballistic tailoring that can be accomplished. The shape of the thrust-time performance is predetermined and only minor tailoring of the trace can be accomplished.

The 260 in. baseline motor design for the series system will exhibit almost the same degree of flexibility in burntime as does the baseline 156 in. design for the parallel booster system. Within the framework of the design and propellant system, the burntime can vary between 110 and 160 sec.

3.4.5.1.2 Case

The general design of the 260 in. steel case will be much the same as the design for the 156 in. parallel case. The shape of the forward and aft segment domes will be the same as those used for the smaller motors. The cylindrical section of the case will not be segmented but will be rolled and welded plates and

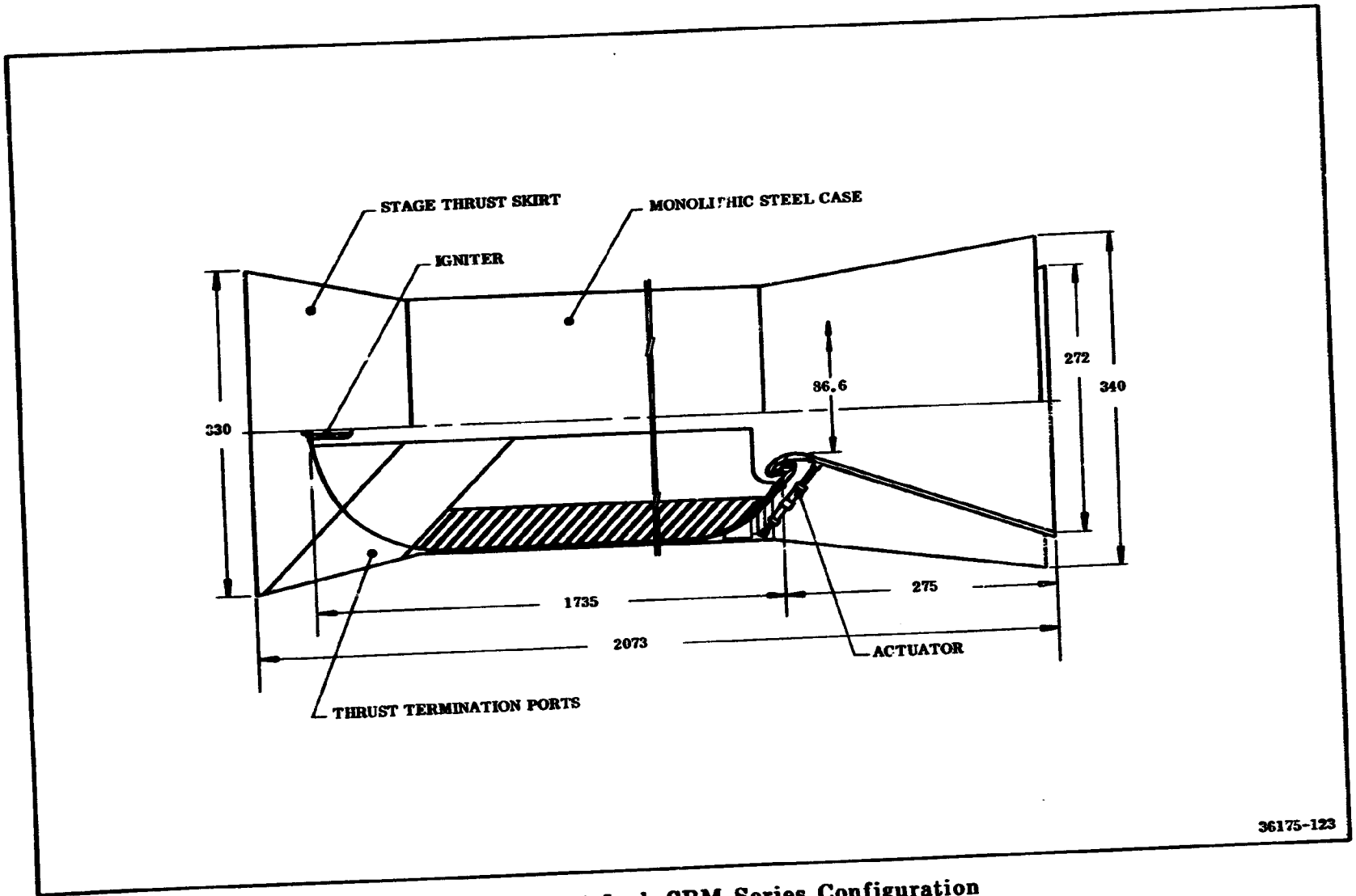

Figure 3-101. 260 Inch SRM Series Configuration

TABLE 3-42

PERFORMANCE SUMMARY
260 INCH SRM, SERIES BURN

Series--One Per Launch Vehicle

Performance	
Average Vacuum Thrust (lb)	8,920,000
Burn Time (sec)	135
Average Operating Pressure (psia)	830
MEOP (psia)	1,000
Vacuum Specific Impulse (sec)	267
Weight	
Propellant Weight (lb)	4,500,000
Total Motor Weight (lb)	4,972,000
Motor Mass Fraction	0.905
Total Stage Weight (lb)	5,023,000
Stage Mass Fraction	0.896

TABLE 3-43

MOTOR DESIGN SUMMARY
260 INCH SRM, SERIES BURN

MEOP = 1,000 psia

Ballistics	
Delivered Vacuum Specific Impulse (lbf-sec/lbm)	267
Total Time (sec)	137
Web Time (sec)	135
Average Vacuum Thrust (million lb)	8.92
Average Chamber Pressure (psia)	830
Propellant Burn Rate at 830 psia (in./sec)	0.345
Average Nozzle Expansion Ratio	8.5
Average Nozzle Throat Diameter (in.)	86.6
Propellant Grain Design Characteristics	
Grain Configuration	5 Point Star
Initial Port to Throat	1.70
Volumetric Loading	0.81
Regressivity (thrust at web time/maximum thrust)	0.886

incorporate longitudinal weld seams. Maximum weld efficiencies of 90 percent will be assumed for the design and the entire plate will be thicker than required to account for the reduction of strength in weld areas. Maximum weld mismatches of 0.060 in. can be tolerated. The case material will be 200 grade 18 percent nickel vacuum arc remelt, maraging steel. This material selection is based upon the demonstrated successful fabrication of 260 in. motor cases using this material.

3.4.5.1.3 Insulation Design

The internal insulation design approach used in the 260 in. motor is identical to that used in the 156 in. parallel baseline motor with the exception that during fabrication the case will be sealed and used as an autoclave.

3.4.5.1.4 Liner

The same UF-2121 liner material used in the 156 in. parallel baseline system will be used in the 260 in. series motor.

3.4.5.1.5 TVC System

All technology and fabrication capability for the production of 260 in. diameter motor nozzles are in existence and have been successfully demonstrated. Two full scale (89.1 in. throat diameter) fixed nozzles have been successfully tested on 260 in. diameter motors.[1,2] In addition, the full scale TVC element recommended in a NASA study for the 260 in. motor nozzle has been fabricated and successfully bench tested at the identical loading and through the same vectoring duty cycle as it would be subjected to in an actual 260 in. test firing.[3] Thus all that remains to be accomplished to demonstrate a 260 in. TVC nozzle in a test firing is the relatively simple step of combining these successfully developed components.

The TVC actuator for this booster configuration is similar to the actuator used for the 156 in. parallel burn. The actuator specific data are shown in Table 3-44. Due to its large size and flow rate, the TVC actuator will require an additional hydraulic power stage. The servoactuator would consist of a primary and secondary actuator. The secondary actuator will house the required pilot servovalves and failure detecting logic. The primary actuator will consist of the power ram, engage

---

[1]260 In. Diameter Motor Feasibility Demonstration Program. Final Report. NASA CR 72125. Contract NAS3-6284. Aerojet-General Corp., April 1966.

[2]260-SL-3 Motor Nozzle and Exit Cone Design, Fabrication and Assembly. Final Phase Report. NASA CR-72283. Contract NAS3-7998. Aerojet-General Corp., June 1967.

[3]Design, Fabrication, and Test of Omnidirectional Flexible Seals for Thrust Vector Control of Large Solid Rocket Motors. Final Report. NASA CR-72889. Contract NAS3-12049. Aerojet-General Corp., June 1971.

TABLE 3-44

TVC ACTUATOR REQUIREMENTS
260 INCH SRM, SERIES BURN

TVC Angle (deg)	5
TVC Slew Rate (deg/sec)	5
Load (lb)	140,000
Area (sq in.)	47
Supply Pressure (psi)	4,000
Flow Rate (gpm)	150
Max Pump Horsepower	350
Redundancy	Active/Standby

valves and mechanical input four-way hydraulic valve. Four additional LVDT's for secondary actuator feedback are required as shown in Figure 3-102.

The control system for this booster configuration is similar to that used for the 156 in. parallel burn. Four additional LVDT's for the secondary actuator are required together with their increased power supply requirements. Only one control unit is required for this configuration.

The TVC actuation system power supply design for the series 260 in. SRM will be similar to that of the series 156 in. SRM, the major difference being the increase in size. Reliability and redundancy will be identical to that of the series 156 in. SRM (primary and secondary actuation and control systems). This approach will provide for multiple failure and redundancy necessary for manrated conditions. The forecasted torque for the 260 in. flexible bearing nozzle is 12.5×10^6 in.-lb. Hydraulic power will be provided by a 350 hp monopropellant turbine driven pump.

The HPU for the 260 in. SRM will consist of a hydrazine gas generator with its associated tankage, controls and hot gas line supplying hot gas to a turbine driven hydraulic power unit. A schematic of the HPU is shown in Figure 3-103.

As shown (Figure 3-103), the nitrogen gas pressurization of the hydrazine storage tank will provide fuel to the gas generator. The hot decomposition gases from the generator will rotate the axial flow impulse turbine which, in turn, will provide the power to the fuel pump to increase the injection pressure into the gas generator. The output of the gas generator is regulated by a flow control valve, which is modulated by the controller which senses the turbine speed, to maintain a constant speed.

The controller will be a solid stage, modular construction, electronic design using existing circuits which have been developed and flight qualified for aircraft HPU. The fuel control valve will be similar in design to those used in electro-hydraulic servocontrol system. The portions of the valve in contact with the hydrazine will be of corrosion resistant materials that are compatible with hydrazine.

The gas generator is a regenerative type consisting of an insulated chamber (pressure vessel), fuel injector assembly, regenerative tubes, electric glow coil (heater), and a normally-closed thermal switch. This particular design is functionally identical to that developed and qualified for use with the liquid monopropellant ethylene oxide powered Nike Hercules APU. This reaction chamber has been proven an efficient design for operation with hydrazine.

The fuel pump will be a vortex (drag) pump driven by the turbine at turbine speed through a hermetically sealed magnetic coupling. The pump runs on its own bearing which will be lubricated and cooled by the fuel. The vortex design will permit the flow to be varied over a broad range without overheating the fuel.

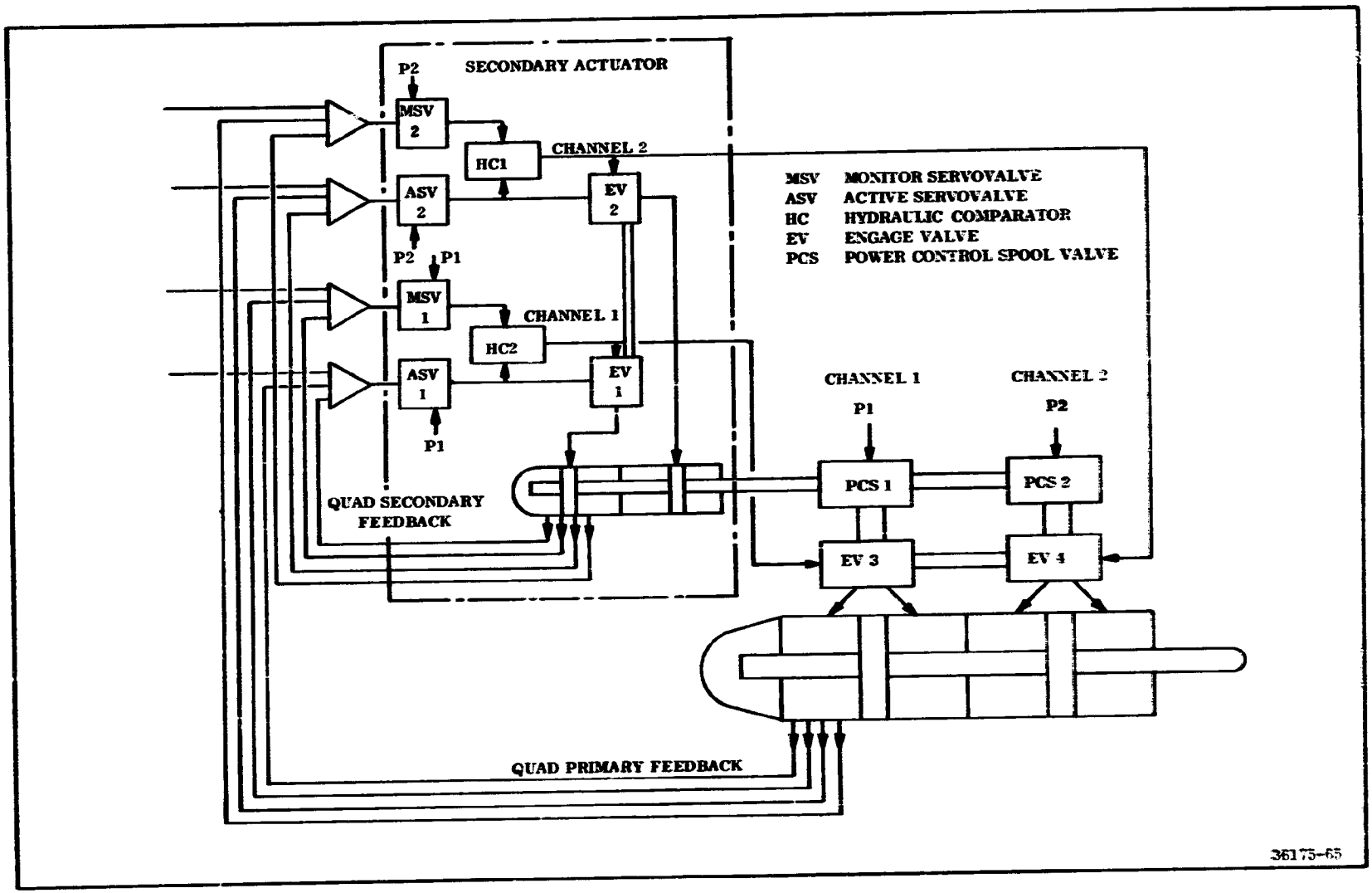

Figure 3-102. TVC Servoactuator System Concept

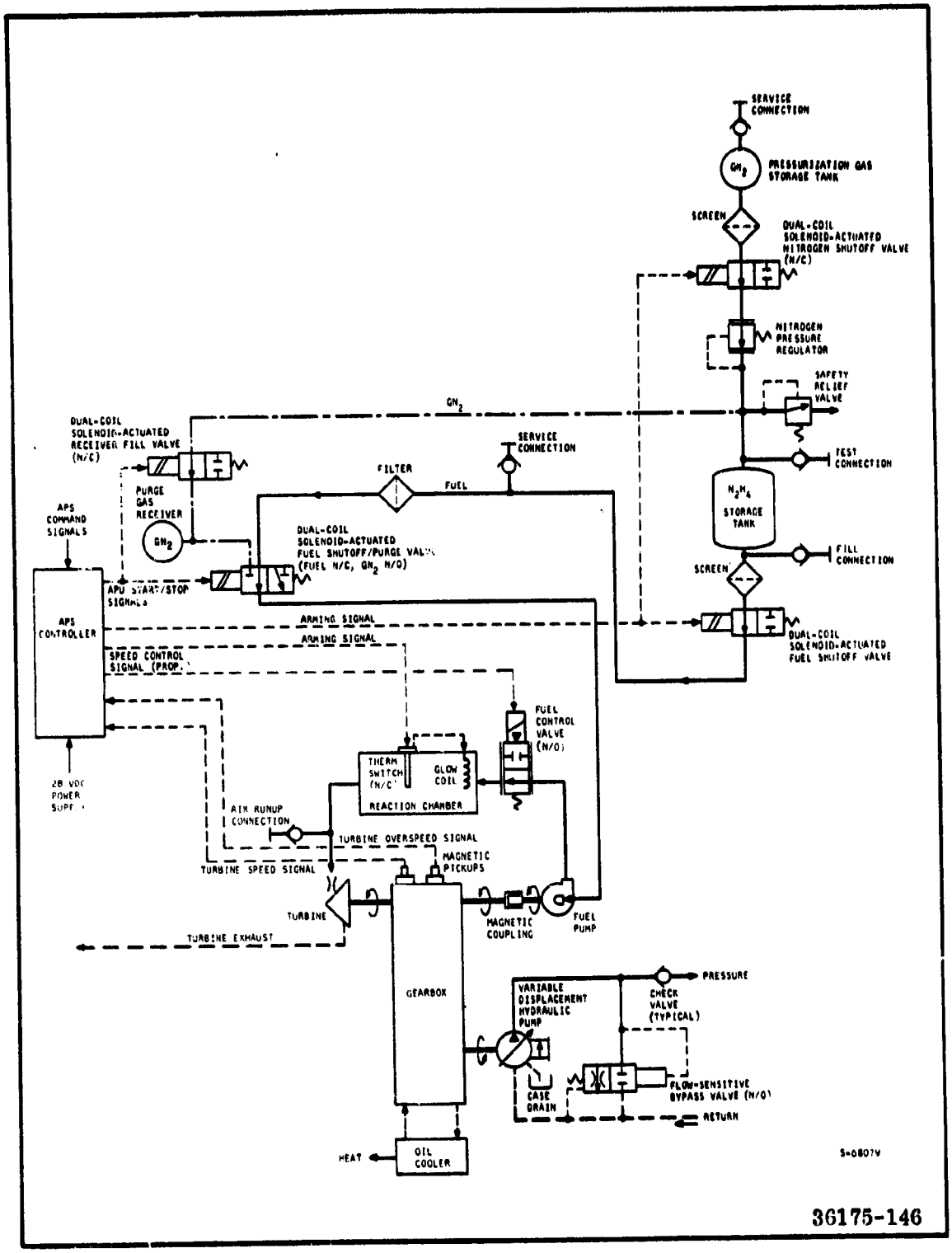

Figure 3-103. Schematic Diagram of 260 Inch HPU

The power unit is composed of the axial flow, impulse turbine, gearbox, fuel pump and the variable displacement hydraulic pump. The turbine is similar to that utilized for the Spartan unit, but because of the increased power requirements, its diameter has been increased and the nozzle arc of admission has been increased from approximately 70 to 100 percent. In addition, a new gearbox based upon a proven design (by AiResearch) replaces the existing Spartan gearbox.

The speed of the turbine-pump combination is maintained constant by an electronic speed control which modulates the hydrazine supply to the gas generator. Use of a variable displacement, axial piston pump (theoretical displacement of 6.0 cu in./revolution), permits efficient matching of generator power to load demand.

The remaining hydraulic subsystem would be similar to that shown in Figure 3-103. The sizing of these components is dependent upon details of the load duty cycle, particularly load spikes, which must be accommodated and which are not yet known for the present application.

3.4.5.1.6 Stage Structure, 260 In. Series

The staging structures for the 260 in. single motor stage will be similar to that used in the 156 in. series configuration. The use of only one motor per stage simplifies the structure required. As in the 156 in. series baseline design, the aft skirt will be designed and used to support the entire vehicle prior to launch, and will be designed for vehicle holddown on the pad.

3.4.5.2 Mass Properties

The weight data for the 260 in. SRM stage are presented in Table 3-45.

TABLE 3-45

MASS PROPERTIES SUMMARY
BASELINE SRM 260 INCH, SERIES BURN

Description	Current Weight (lb)
Case	390,938
Insulation	28,860
Liner	3,525
Igniter	1,985
Nozzle	40,656
Raceway	353
Thrust Vector Control	5,683
Propellant	4,500,000
Forward Thrust Structure	29,000
Aft Skirt	21,100
Instrumentation	900
Total Stage	5,023,000

3.5 SUPPORTING RESEARCH AND TECHNOLOGY

The results of the study of SRM's for a Space Shuttle booster were reviewed to determine the need for a supporting research and technology effort. For the basic SRM Stage no technology deficiencies exist which would prevent the timely design development and operation of SRM's for a Space Shuttle booster.

Recovery of the SRM Stage requires further study and development testing to assure successful implementation of SRM Stage recovery during the Space Shuttle program. Since the potential cost savings associated with SRM Stage recovery are high, recommended technological efforts have been identified and for convenience purposes are presented in Appendix H, SRM Stage Recovery.